REPORT UAG - 44

WORLD DATA CENTER A
for
Solar-Terrestrial Physics

SYNOPTIC MAPS OF SOLAR 9.1 cm MICROWAVE EMISSION FROM JUNE 1962 TO AUGUST 1973

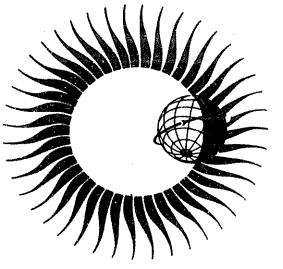

May 1975

WORLD DATA CENTER A

National Academy of Sciences

2101 Constitution Avenue, N.W. Washington, D.C. U.S.A., 20418

World Data Center A consists of the Coordination Office

and seven subcenters:

World Data Center A
Coordination Office
National Academy of Sciences
2101 Constitution Avenue, N.W.
Washington, D.C., U.S.A. 20418
Telephone (202) 389-6478

Glaciology:
World Data Center A:
Glaciology
U.S. Geological Survey
1305 Tacoma Avenue South
Tacoma, Washington, U.S.A. 98402
Telephone (206) 593-6506

Longitude and Latitude
World Data Center A:
Longitude and Latitude
U.S. Naval Observatory
Washington, D.C., U.S.A. 20390
Telephone (202) 254-4023

Meteorology (and Nuclear Radiation):
World Data Center A:
Meteorology
National Climatic Center
Federal Building
Asheville, North Carolina, U.S.A. 28801
Telephone (704) 258-2850

Oceanography:
World Data Center A:
Oceanography
National Oceanic and
Atmospheric Administration
Washington, D.C., U.S.A. 20235
Telephone (202) 634-7249

Rockets and Satellites:
World Data Center A:
Rockets and Satellites
Goddard Space Flight Center
Code 601
Greenbelt, Maryland, U.S.A. 20771
Telephone (301) 982-6695

Seismology, Tsunamis, Gravimetry, Earth Tides, Recent Movements of the Earth's Crust, Magnetic Measurements, Paleomagnetism and Archeomagnetism, Volcanology, Geothermics:
World Data Center A:
Solid-Earth Geophysics
Environmental Data Service, NOAA
Boulder, Colorado, U.S.A. 80302
Telephone (303) 499-1000 Ext. 6311

Solar-Terrestrial Physics (Solar and Interplanetary Phenomena, Ionospheric Phenomena, Geomagnetic Variations, Magnetospheric and Interplanetary Magnetic Phenomena, Flare-Associated Events, Aurora, Cosmic Rays, Airglow):
World Data Center A
for Solar-Terrestrial Physics
Environmental Data Service, NOAA
Boulder, Colorado, U.S.A. 80302
Telephone (303) 499-1000 Ext. 6467

Notes:

(1) World Data Centers conduct international exchange of geophysical observations in accordance with the principles set forth by the International Council of Scientific Unions. WDC-A is established in the United States under the auspices of the National Academy of Sciences.

(2) Communications regarding data interchange matters in general and World Data Center A as a whole should be addressed to: World Data Center A, Coordination Office (see address above).

(3) Inquiries and communications concerning data in specific disciplines should be addressed to the appropriate subcenter listed above.

WORLD DATA CENTER A
for
Solar-Terrestrial Physics

REPORT UAG - 44

SYNOPTIC MAPS OF SOLAR 9.1 cm MICROWAVE EMISSION FROM JUNE 1962 TO AUGUST 1973

by

Werner Graf and Ronald N. Bracewell
Radio Astronomy Institute
Stanford University
Stanford, California 94305 USA

May 1975

Published by World Data Center A for
Solar-Terrestrial Physics, NOAA, Boulder, Colorado
and printed by
U.S. DEPARTMENT OF COMMERCE
NATIONAL OCEANIC AND ATMOSPHERIC ADMINISTRATION
ENVIRONMENTAL DATA SERVICE
Asheville, North Carolina, USA 28801

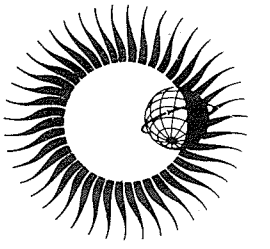

SUBSCRIPTION PRICE: $25.20 a year; $12.00 additional for foreign mailing; single copy price varies.* Checks and money orders should be made payable to the Department of Commerce, NOAA. Remittance and correspondence regarding subscriptions should be sent to the National Climatic Center, Federal Building, Asheville, NC 28801, Attn: Publications.

*PRICE THIS ISSUE $2.55

TABLE OF CONTENTS

SYNOPTIC MAPS OF SOLAR 9.1 cm MICROWAVE EMISSION FROM JUNE 1962 TO AUGUST 1973

by

Werner Graf and Ronald N. Bracewell
Radio Astronomy Institute
Stanford University
Stanford, California 94305 USA

SUMMARY

The distribution of microwave emission over the sun at a wavelength of 9.1 cm was mapped by the Stanford spectroheliograph on nearly every day from June 1962 to August 1973. As these spectroheliograph records form a valuable resource for comparison with other solar and terrestrial data, they have been reduced to a homogeneous format and are now available in the form of numerical printout, contour diagrams, movies, punched cards and 9-track magnetic tape. As a visual guide to the content of the records, this publication presents monthly synoptic maps formed by assembling the meridian data. In addition, the course of development over this 11-year interval is illustrated by a microwave butterfly diagram and by 12 annual average microwave maps.

1. INTRODUCTION

Microwave emission from the sun was first observed by G. C. Southworth in 1942, but it was some years before microwave antennas were designed for mapping the distribution of emission over the sun's disk. When effective temperatures were accurately measured, it became apparent that the emission must originate partly in the chromosphere and partly in the corona. The height of microwave emission, which is difficult to measure, is deducible only from long series of daily observations. Correlation of microwave emission with sunspots and other manifestations of solar activity also requires long runs.

The 9.1 centimeter microwave spectroheliograph at Stanford is fully described in Appendix A. When the telescope came into operation in 1960, it was used for special studies, as reported by G. Swarup in his Ph. D. dissertation of 1961 and subsequent publications. Its angular resolution was very much higher than had been reached by other radiotelescopes operating near the same wavelength and, indeed, even today the Stanford sun maps cannot be duplicated by any other instrument. The regular program of observations was carried out by Joel Deuter (1962-1973) and James Rutherford (1965-1973).

Maps were made at noon nearly every day, displaying a degree of reliability that is not often matched in solar observing, as witnessed by the following table:

Year	Number of Maps	Year	Number of Maps	Year	Number of Maps
1962	157	1966	354	1970	358
1963	280	1967	359	1971	364
1964	329	1968	361	1972	363
1965	350	1969	360	1973	243

As a result of this virtually gap-free performance, requests for maps at the time of eclipses, rocket flights, balloon flights, satellite observations or moon flights could nearly always be met. The maps supplied welcome supportive data and were often published by investigators.

Other kinds of investigation have been made possible that become arduous or impossible when gaps are present in data. In addition, the digital character of the maps makes them computer compatible. The Stanford microwave spectroheliograph is remarkable for being the first radiotelescope (and possibly the first telescope of any kind) in 1961 to produce output automatically in printed form just as it would appear in publication.

Important series of sun maps are also available at millimeter and decimeter wavelengths. The only other microwave solar data extended in time are series of fan beam scans made in Canada and Japan. All these records could now gain in significance by intercomparison with these 9.1 cm synoptic maps.

The present synoptic maps, one per solar rotation, have been prepared to facilitate access to the daily maps for intercomparison with other data. The style of the synoptic maps has been chosen to conform with the *Cartes Synoptiques de la Chromosphère Solaire* of L. and M. L. d'Azambuja, just as was done by M. Waldmeier in his *Heliographic Maps of the Photosphere*. Additional synoptic guides to the daily maps are the annual average maps and the butterfly diagram.

The daily maps were published monthly in *Solar-Geophysical Data*, issued by the same group first in the National Bureau of Standards, then in the Environmental Science Services Administration and lastly in the National Oceanic and Atmospheric Administration. They are now available in various forms including magnetic tape and motion picture film as described in Section 2.

Appendix B reproduces the instructions that were published annually for the use of the daily maps.

Section 3 explains some details, not previously published, regarding the method of interpolation which was used in order to rotate the digital maps. Unless this is done the solar axis turns through $\pm 27°$ over the course of the year. A method of interpolating between consecutive maps is also described. This latter kind of interpolation proved convenient in preparing transparencies to lay over optical pictures taken some hours before the map and was also used to produce artificial maps for missing days, a device that is very convenient for the programmer concerned with certain kinds of computation on long series of maps.

Section 4 compresses the whole run of data in two special ways. One is the butterfly diagram introduced by E. W. Maunder for displaying the latitude drift of sunspot zones; in our case the intensity of microwave activity stands out in an interesting way. We also present average sun maps for each year. These unusual diagrams show what would be recorded if a filtergram were made with an exposure time of one year. Far from being vague blurs, the annual maps have interesting detail, and they are all different.

Finally, Section 5 explains the synoptic maps which form the bulk of the publication.

2. DAILY SUN MAPS

A total of 3,878 9.1-cm spectroheliograms were made at daily intervals between June 1962 and August 1973 at the Stanford Radio Astronomy Institute using the microwave spectroheliograph illustrated in Figure 1. Many others were made at irregular intervals dating back to April 28, 1959.

Description of Instrument (Appendix A). As this instrument is quite unlike any kind of optical spectroheliograph, it is desirable to become familiar with the principle of operation and the instrumental parameters if fine points of interpretation are to be discussed. The definitive description is found in Appendix A.

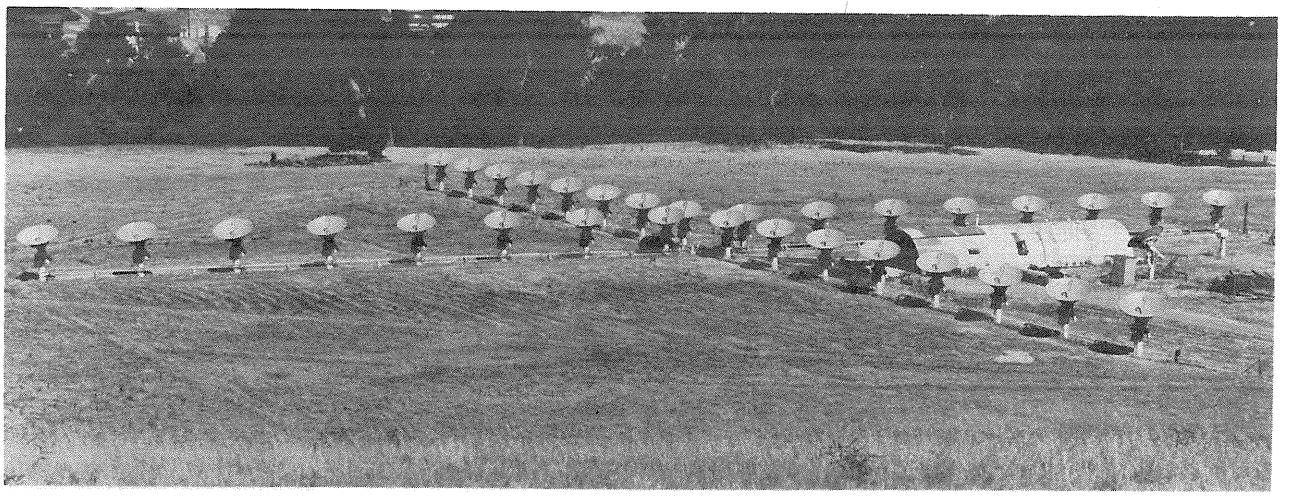

FIG. 1. The Stanford 9.1 cm microwave spectroheliograph in 1958.

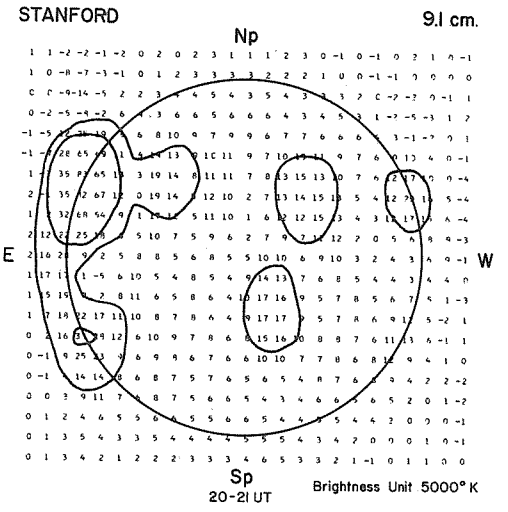

FIG. 2. Example of a 9.1 cm map as published. Contour levels are 50,000 and 100,000 K.

Map Format (Appendix B). Figure 2 shows the sun map for January 3, 1969, in the form in which the series of maps was published monthly in *Solar-Geophysical Data* by the National Oceanic and Atmospheric Administration. The description of these maps is given in Appendix B which explains the digital format and the smoothed contours that act as a visual guide.

Format in Earlier Years. The spacing of map elements is related to angular resolution, which changes with the season. In winter, when the north-south resolution is least, the row spacing may be greater without any loss in information. The method of steering the beam north-south by insertion of phase shifts automatically shifts the beam by an amount that depends on season in precisely the appropriate way.

A modified automatic typewriter was connected to the output of the spectroheliograph so that the row spacing on the typewritten page could be varied in agreement day by day. However, this proved inconvenient for numerical analysis, particularly as computer equipment prints at a fixed row spacing of one-sixth of an inch. Therefore the phase-shifter program was altered daily, starting on 1 January 1964, so that the row and column spacings had the same fixed lattice constants imposed by typewriter and line printer custom. This does not constitute a *square* lattice, but does make the photosphere circular and permits overlays of optical solar data without annoying distortion.

Prior to the introduction of computer-drawn contours, values exceeding a threshold level of 40,000 K were emphasized with underlining (or by dots).

Starting on 1 July 1965 the rotation axis of the sun was made vertical, east was placed on the left, and the unit which had previously varied around 2,000 K was fixed at 5,000 K in subsequent publications.

The 2^s Timing Error. During the quiet solar years 1964-1965 it became apparent that the microwave sun was systematically displaced 0.5' to the east of the expected position. This could be explained by a 2^s error in assumed longitude, but no evidence for such an error has ever been found. Our longitude is based on that of "RATEL 1961", a United States Geological Survey benchmark whose position has been determined twice as follows:

Agency	Date	Method	Position
U.S. Geological Survey	October 1961	Triangulation from second order stations	37° 23' 47.88" N 122° 11' 19.69" W
U.S. Coast & Geodetic Survey	September 1962	Astronomical	37° 23' 50.66" N 122° 11' 21.58" W

Several possible instrumental causes were studied, and it was also suggested that the 2^s difference in travel time between the solar limb and the center of the disk could be responsible, but no explanation could be confirmed. Starting on 3 September 1965, the sun maps were arbitrarily displaced 2^s. The magnitude and sign of the effect may be seen by reference to the annual average maps for years before and after 1966. The shift is one-sixth of the antenna beamwidth.

Missing Data. Dates on which no map was obtained have no dots above the date on the synoptic charts. Refer to Section 3 for a description of the interpolation method used to construct artificial maps for the missing days. Artificial maps are flagged as described below under "Format of Maps on Magnetic Tape".

List of Additional Data. The continuous series of maps begins in 1962, but maps were obtained also in 1959, 1960 and 1961 as follows:

1959 April 28 - May 20; July 25 - August 4; September 4 - October 1; November 3-25.

1960 February 29; March 2, 11, 13-25, 27, 28, 30, 31; April 3-5, 7-15, 17-24, 27-29; May 1, 3-27, 29-31; June 1, 2, 5-7, 9-12, 14-30; July 1, 3, 5-19, 21, 22, 24-29, 31; August 1, 2, 4, 5, 10-12, 14, 16-18, 21-26, 29-31; September 1, 2, 6-8, 12, 20-22, 26-28; October 3, 12-14, 17; November 8-11, 14-18, 21-26, 28-30; December 2, 5-7, 9, 12, 13, 29.

1961 January 3, 4-6, 9-11, 13; February 10-21, 23, 27, 28; March 1-3, 6-10, 13, 14, 17, 20, 22, 24, 27; June 16, 19-22; July 17, 20, 21; August 16, 17, 21-23.

The maps for April, May, June and July 1960 appeared in *Stanford Radio Astronomy Institute Publication Nos. 8, 10, 11, and 12.* Those for May 1960 appeared also in G. Swarup's Ph.D. thesis.

Fan-beam Data. The east-west arm alone was regularly used for obtaining fan-beam scans with a beam width of 2.3 minutes of arc. Starting on July 5, 1958, observations were made daily for several hours before and after the sun map was taken to provide continuous monitoring of flare activity and as an indicator of equipment performance.

Quality of Early Maps. During the period when the reliability of the equipment was being improved the map quality was variable. Undesired effects such as gain variation and baseline drift should be guarded against when individual maps are referred to, especially maps from 1963 and earlier years.

How to Obtain Sun Maps. The primary source of the sun maps is *Solar-Geophysical Data* as published by NOAA and its predecessor organizations, the format being as described in Appendix B. In cases where the quality of reproduction interferes with legibility, both the numerical maps and the contour drawings are on file at Stanford where they may be consulted. Contour maps for special times of day may be constructed as described below in Section 3.

A virtue of digital data is that black-and-white files may be replaced by machine-readable records. Punched cards used in the later years to produce copy for monthly publication have been duplicated for outside users from time-to-time. However, the full collection is bulky and has been transferred to magnetic tape. In addition, the changes in format have been allowed for so that a homogeneous data set now exists on a single 9-track tape covering the whole period from June 1962 through August 1973. The tape is archived at the World Data Center A (WDC-A) for Solar-Terrestrial Physics which can furnish copies at a cost available on request. Copies of the whole tape or of single years may also be obtainable from the authors.

Format of Maps on Magnetic Tape. Each map on the 9-track tape consists of one record of 529 words (= 2116 bytes, 4 bytes per 32-bit word, 2's-complement with the sign bit in the most significant bit). All numbers are integers and each record is arranged in the following way: The first 525 words are the brightness temperature readings of the map with a unit of 1000°K, with 25 words per row. Thus there are 21 rows, starting at the North. The last four numbers are: day (#526), month (#527), year (#528) and a flag (#529). The flag has the following meaning: A map which was obtained by the interpolation procedure described below in Section 3 has a flag equal to zero; if it is a standard map, the flag is greater than or equal to one, and in this case the quantity "flag minus one" indicates the number of rows which had to be edited manually prior to processing by computer, which was necessary on some maps in 1962-63 because of occasional missing rows.

In the period from June 1962 to August 1973 whenever no map was obtained we supplied an interpolated map (see Section 3), with the exception of the interval from 1 February 1963 through 19 March 1963. To facilitate certain kinds of computer analysis, maps during this interval are provided, dated and flagged (with a zero) but the spaces for temperature readings have been filled with zeros.

An EOF (End of File) mark has been placed at the end of each year; thus there are a total of 12 files on a complete tape. The IAU standard solar disk of 15 cm diameter will result from a column spacing of 0.3 inches and rows spaced at 3 per inch as available on line printers.

Movies. A remarkable 16 mm black-and-white movie that compresses 9.5 years of the microwave sun into 10 minutes (at 24 frames per second) has been produced by computer at Sacramento Peak Observatory. A copy is archived at the WDC-A for Solar-Terrestrial Physics. A color-movie also exists for the International Quiet Sun Years 1964-1965.

3. INTERPOLATION

The daily sun maps incorporate a correction for a change in receiver gain during the observation. The gain of the receiver was measured immediately before and after each observation, and the maps were then compensated by assuming that the receiver gain drifted linearly with time.

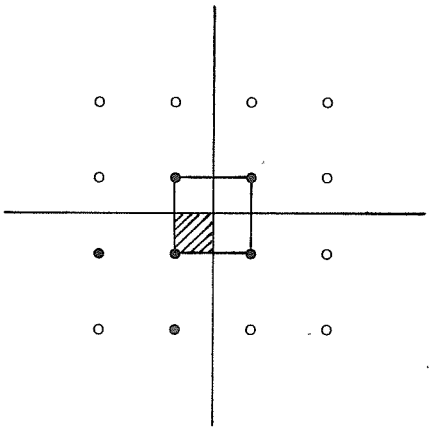

FIG. 3

The rows of the map, as observed, run in a *geographic* east-west direction. To bring the solar rotation axis vertical with North at the top and East on the left, in conformance with the IAU standard, we must rotate the maps through an angle of P degrees, where P denotes the position angle of the northern extremity of the axis of solar rotation (measured eastward from the north point of the disk). To rotate the maps, a six-point bivariate interpolation formula was used, as described on p. 882 of the *Handbook of Mathematical Functions* by M. Abramowitz and I. A. Stegun (Dover, New York). In order to interpolate in the square shown shaded in Figure 3, the six heavy points were used.

For various purposes it was desirable to develop a routine which would permit interpolation between two existing sun maps, i.e., for a point in time where there was no map. This routine was used, for instance, to interpolate maps for the days where no data were obtained; also it permitted generation of maps at 6 hour intervals so that the black-and-white movie mentioned in Section 2 has 4 frames per day.

To interpolate maps in this fashion the sun was assumed to rotate as a solid sphere at a rate of 13.2 heliocentric degrees per day. The 7.25° inclination of the solar axis to the ecliptic may be neglected.

To obtain a map for a time t, intermediate between times t_1 and t_2 for which maps were available, we first used a 4-point (one-dimensional) Lagrangian interpolation formula (p. 879, op. cit.) to get temperature values at the points which would be on the lattice points of the standard map format a time $t-t_1$ later than the first map and a time t_2-t earlier than the second. These two sets of values were then combined in a weighted average using weights $(t_2-t)/(t_2-t_1)$ and $(t-t_1)/(t_2-t_1)$.

Because the S-component of the sun varies only very slowly with time, the interpolated maps have almost the same quality as the original maps. However, if one wants to ascertain the peak brightness temperature of a region on an interpolated map, it should be remembered that the value presented was not actually measured. On the data tapes all interpolated maps are identified as such (see Section 2).

4. BUTTERFLY DIAGRAM AND ANNUAL MAPS

The well-known butterfly diagram of Maunder, which exhibits the latitude zones of sunspot activity, may be adapted to solar microwave emission. In Figure 4 the heliographic latitude ranging between -60° and +60° is plotted against date from 1962 to 1973. Contours of equal brightness temperature show how the activity was spread over two latitude zones, one in the northern and one in the southern hemisphere. As time elapsed, the width of the zones varied and they moved towards the equator.

Within each wing of the butterfly the structure is not uniform but exhibits structure in the form of more or less concentrated outbreaks of activity at intervals of approximately 6 months.

Since the butterfly diagram is ill-proportioned for the display of temporal structure on a time scale much less than 6 months, we have eliminated the fine structure associated with the 27-day recurrence tendency by first taking 54-day running means of the temperatures observed on the central meridian.

Figure 4 represents the view of an observer situated in the equatorial plane of the sun and consequently is neither exactly observable from the earth nor does it precisely represent the dependence of solar-terrestrial influence on geocentric celestial latitude (latitude measured with respect to the ecliptic). For example the two strongest outbreaks in 1967 are shown in Figure 4 as having approximately the same northern heliographic latitude. But the heliocentric latitude of the earlier one was approximately 27° and of the later 14° as measured from the plane of the ecliptic. Thus, to the extent that any particular influence of an active region on the earth depends on its elevation above the plane of the earth's orbit, the butterfly diagram is deceptive. There is another form of the diagram, not presented here, in which the line of zero heliographic latitude is sinusoidal with an amplitude of 7.25° instead of a straight line.

A different way of showing how the activity developed in latitude over the solar cycle is shown in Figures 5*a* to 5*ℓ*. Each of these maps is the average of all the available maps for one whole year. Longitude dependence tends to be smeared out with resulting emphasis on the latitude zones. The perhaps surprising peaks of brightness at the four ends of the two zones are a consequence of two effects: the slowing down of velocity transverse to the line of sight as an active region goes around the limb and the fact that the elevation of the microwave source permits it to be "visible" for some days before and after limb passage. There is no question that the microwave sun possesses these limb concentrations on the average and, indeed, they are quite noticeable when individual maps are sampled at random.

In periods of reduced activity, for example in 1966, the average sun may differ markedly from casual expectation. In the quiet years 1964 and 1965 the limb brightening of the quiet sun is clearly noticeable.

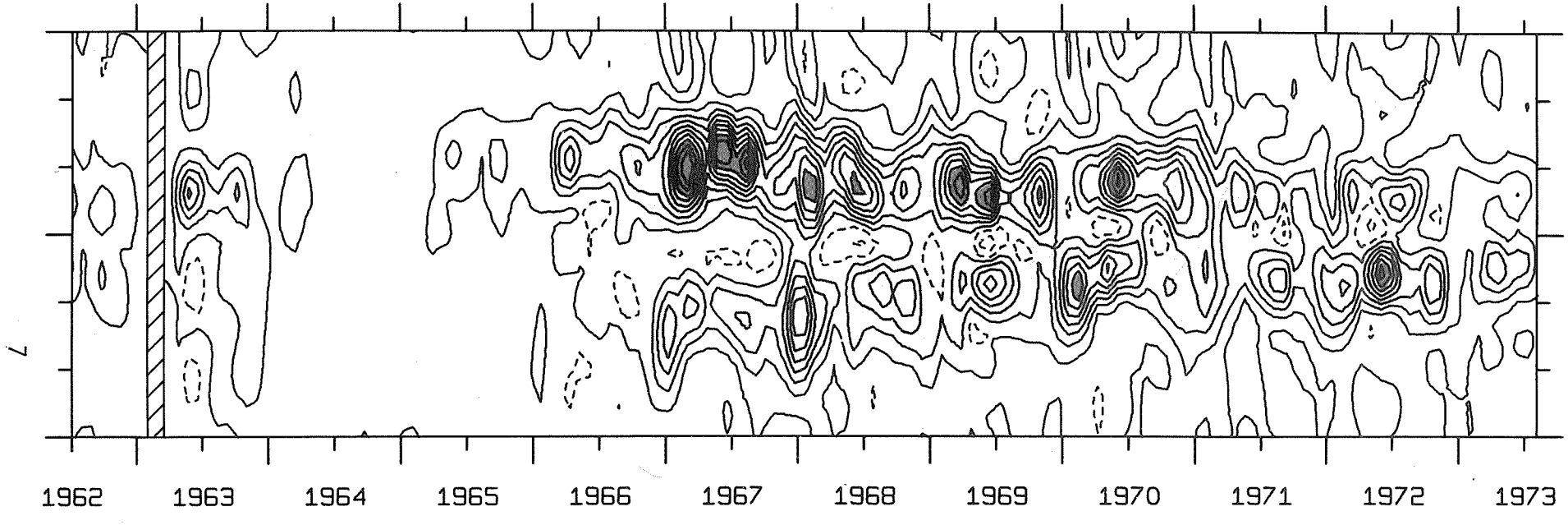

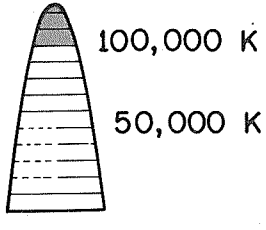

FIG. 4. Butterfly diagram of 9.1 cm microwave emission. The latitude ranges from -60° to +60°.

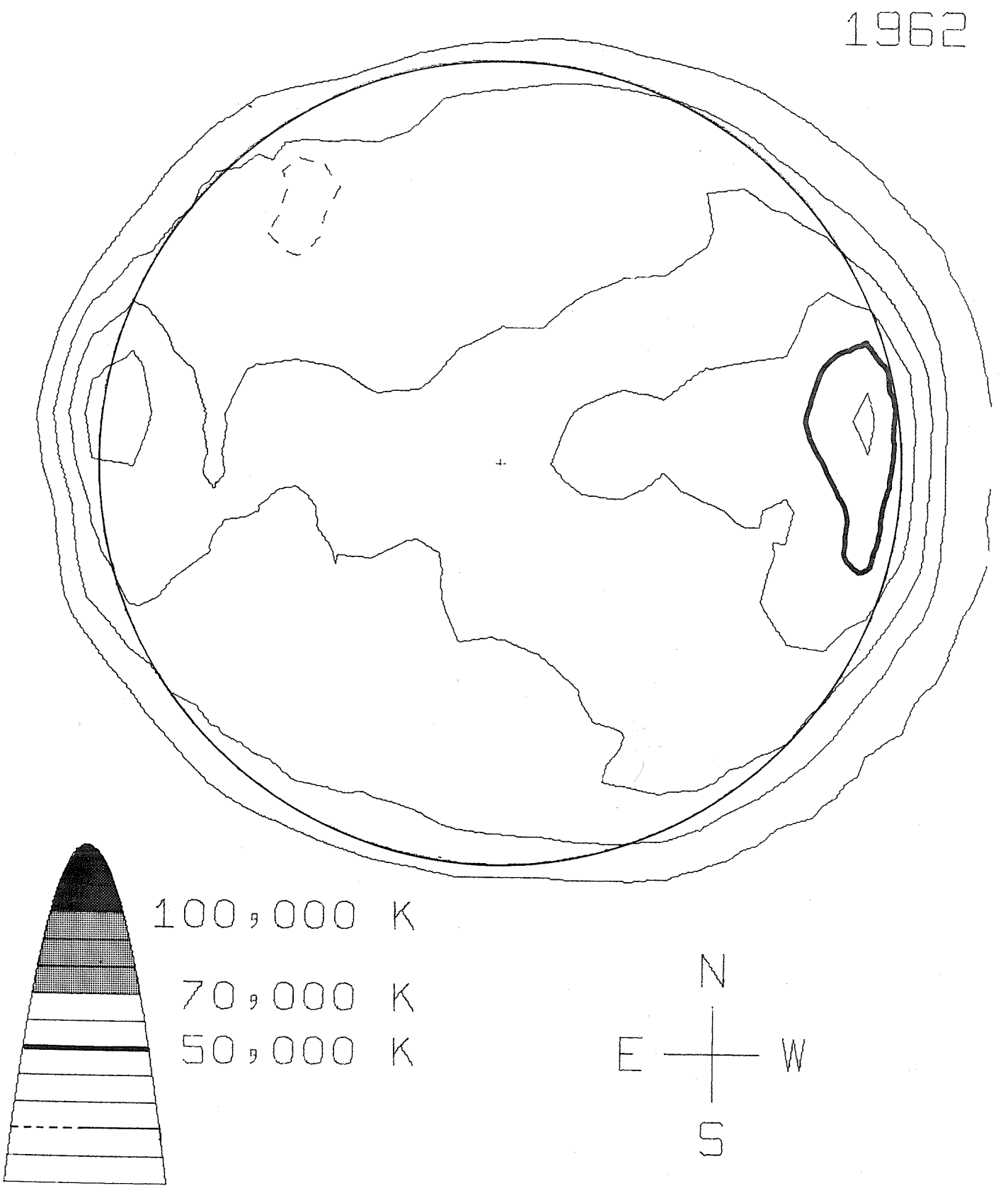

FIG. 5*a*. Yearly average map for 1962.

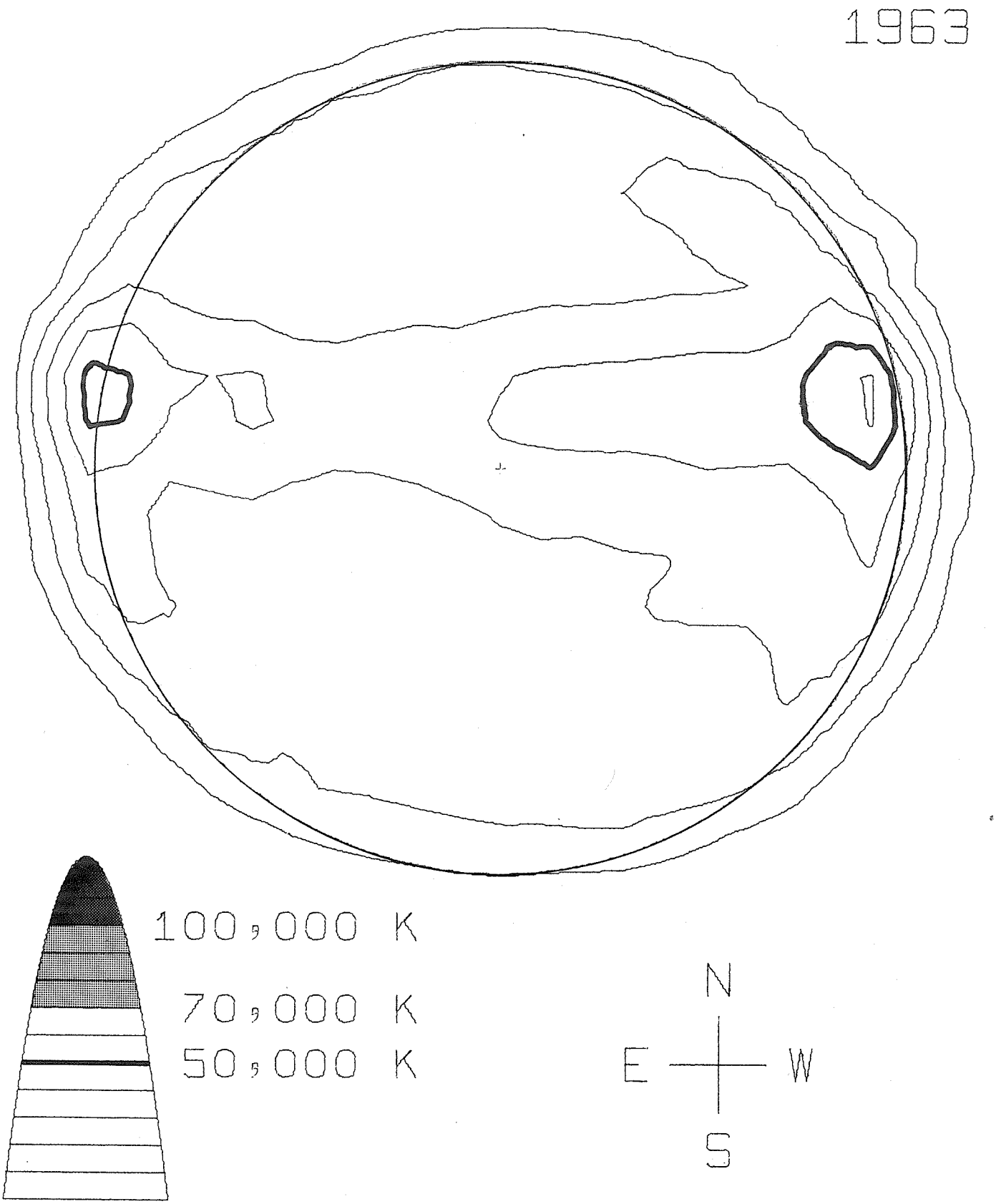

FIG. 5b. Yearly average map for 1963.

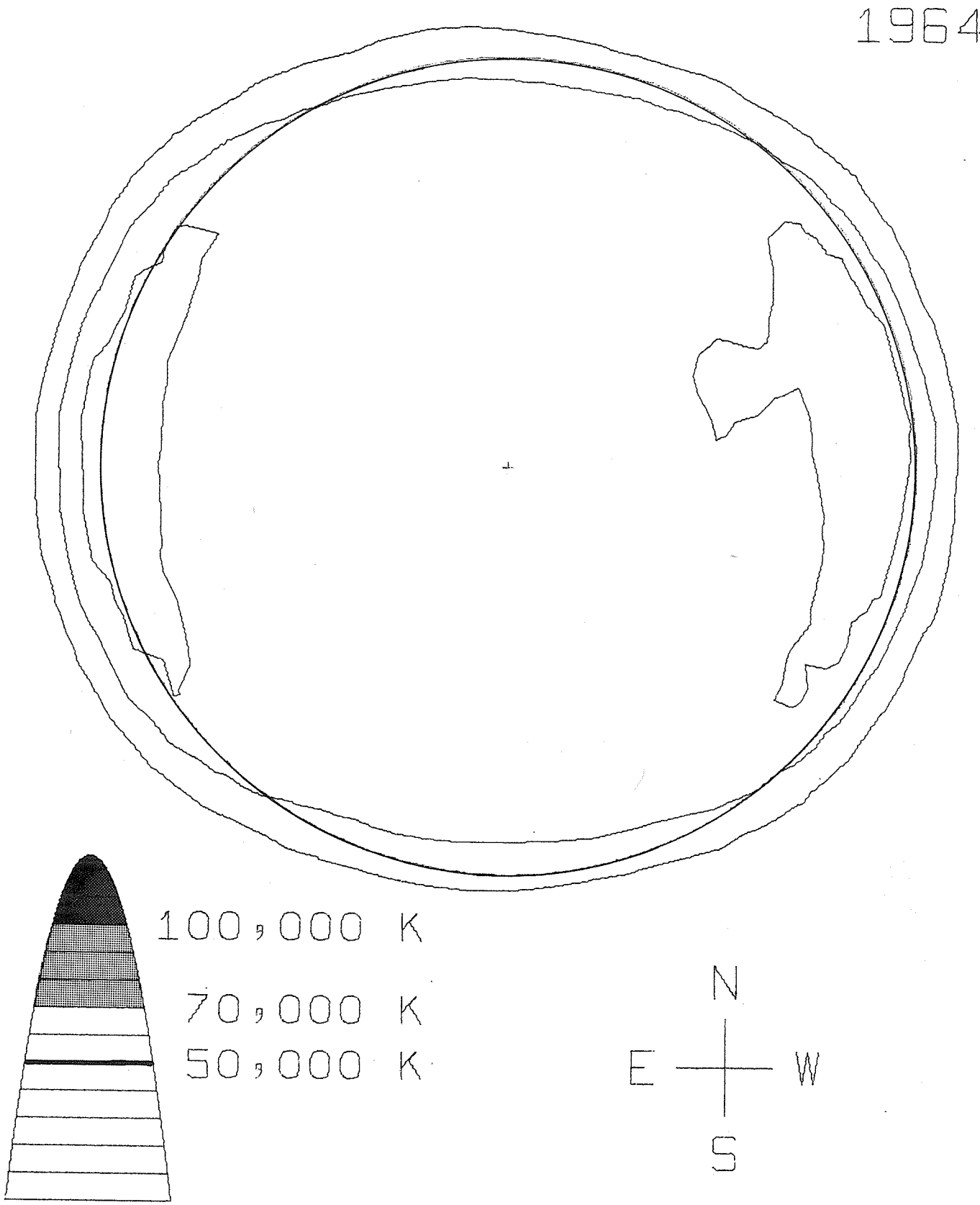

FIG. 5c. Yearly average map for 1964.

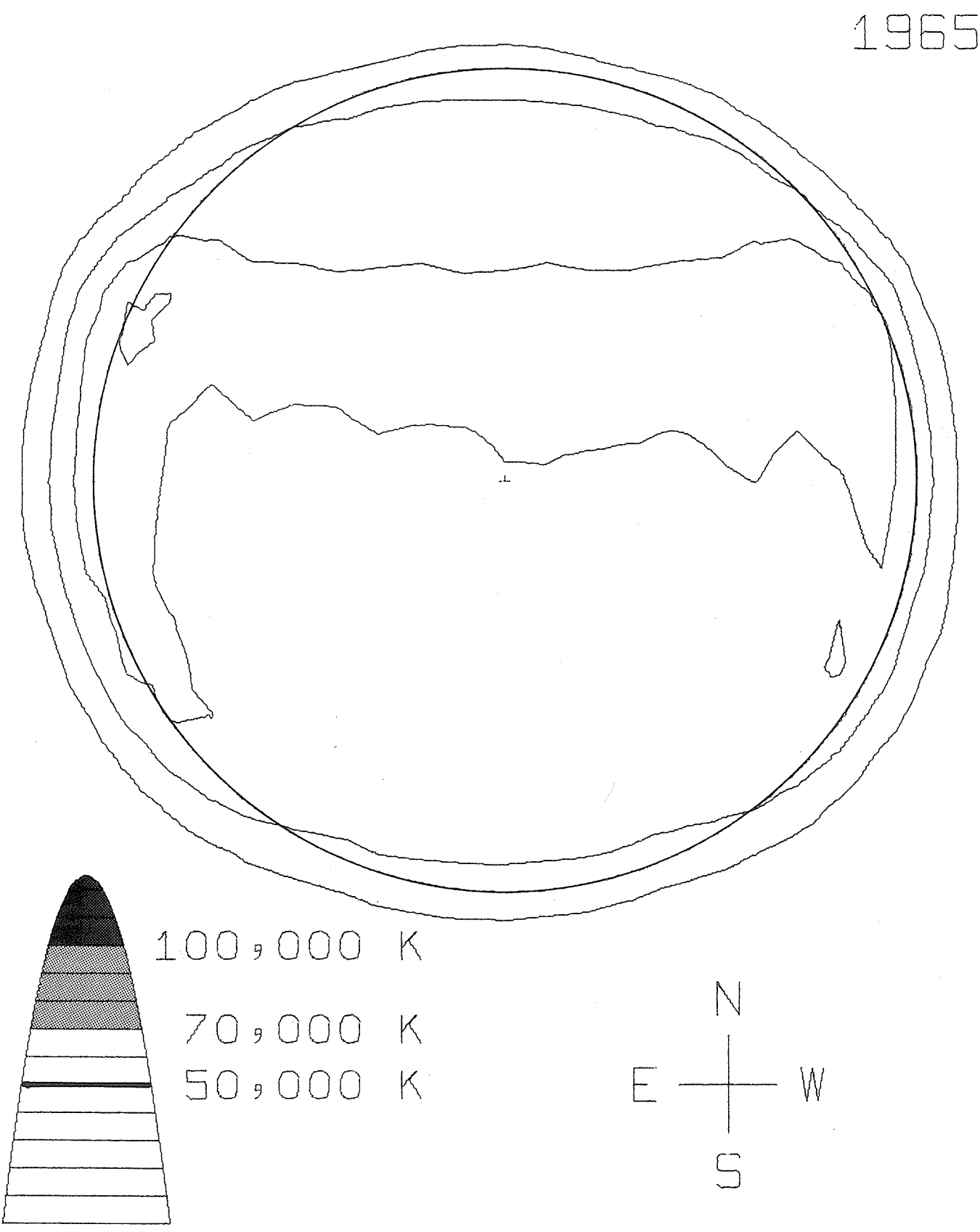

FIG. 5*d*. Yearly average map for 1965.

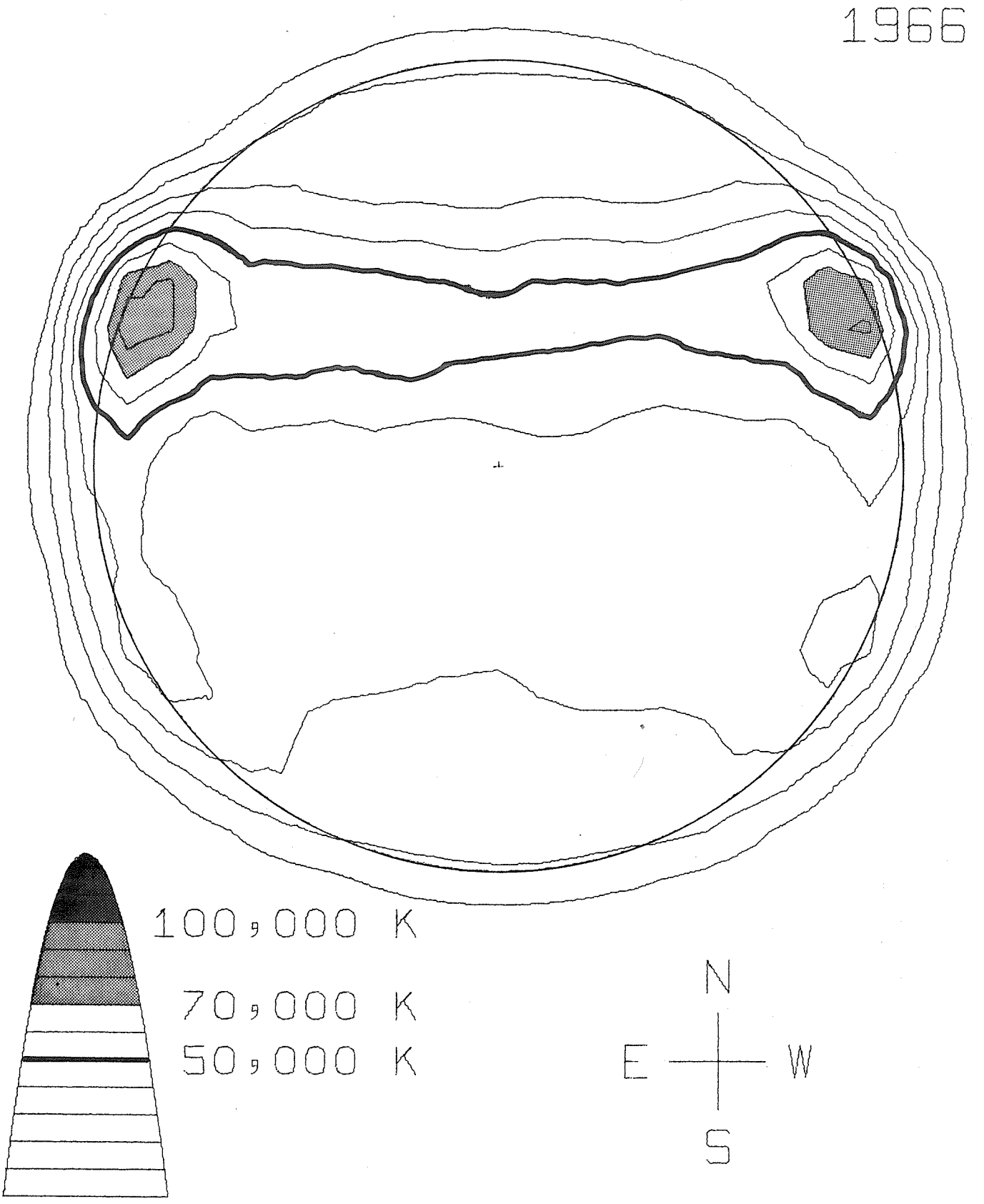

FIG. 5e. Yearly average map for 1966.

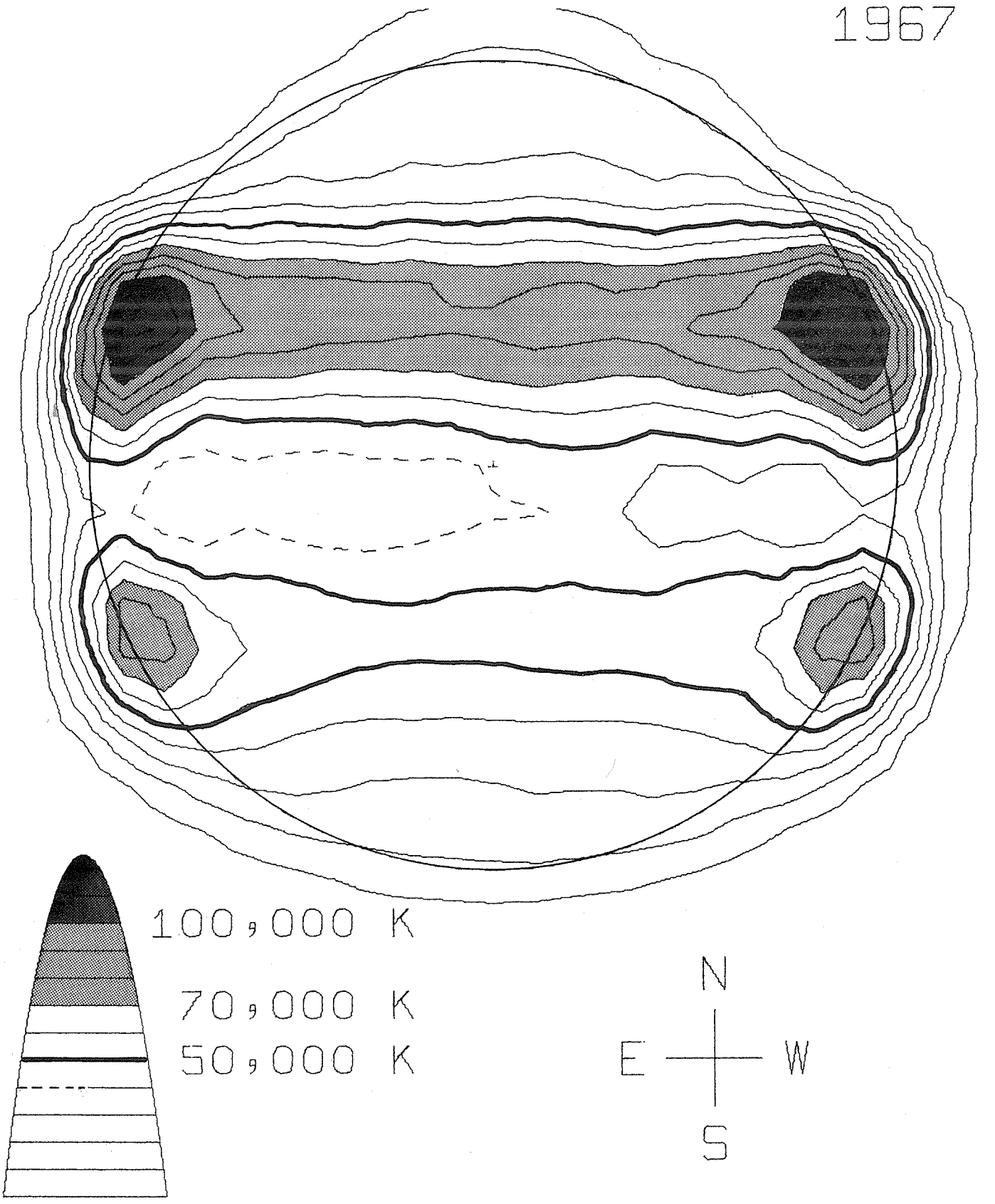

FIG. 5b. Yearly average map for 1967.

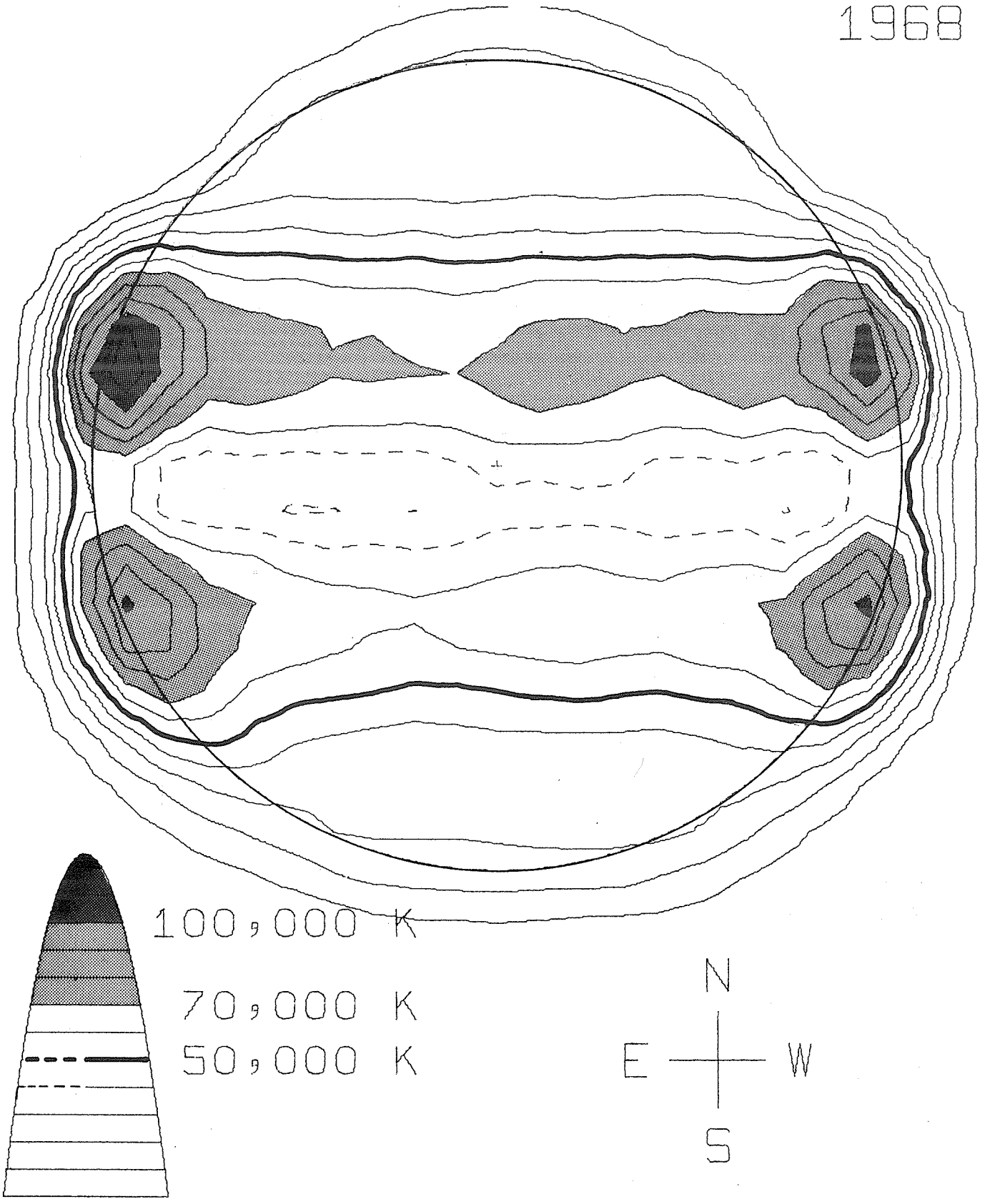

FIG. 5*g*. Yearly average map for 1968.

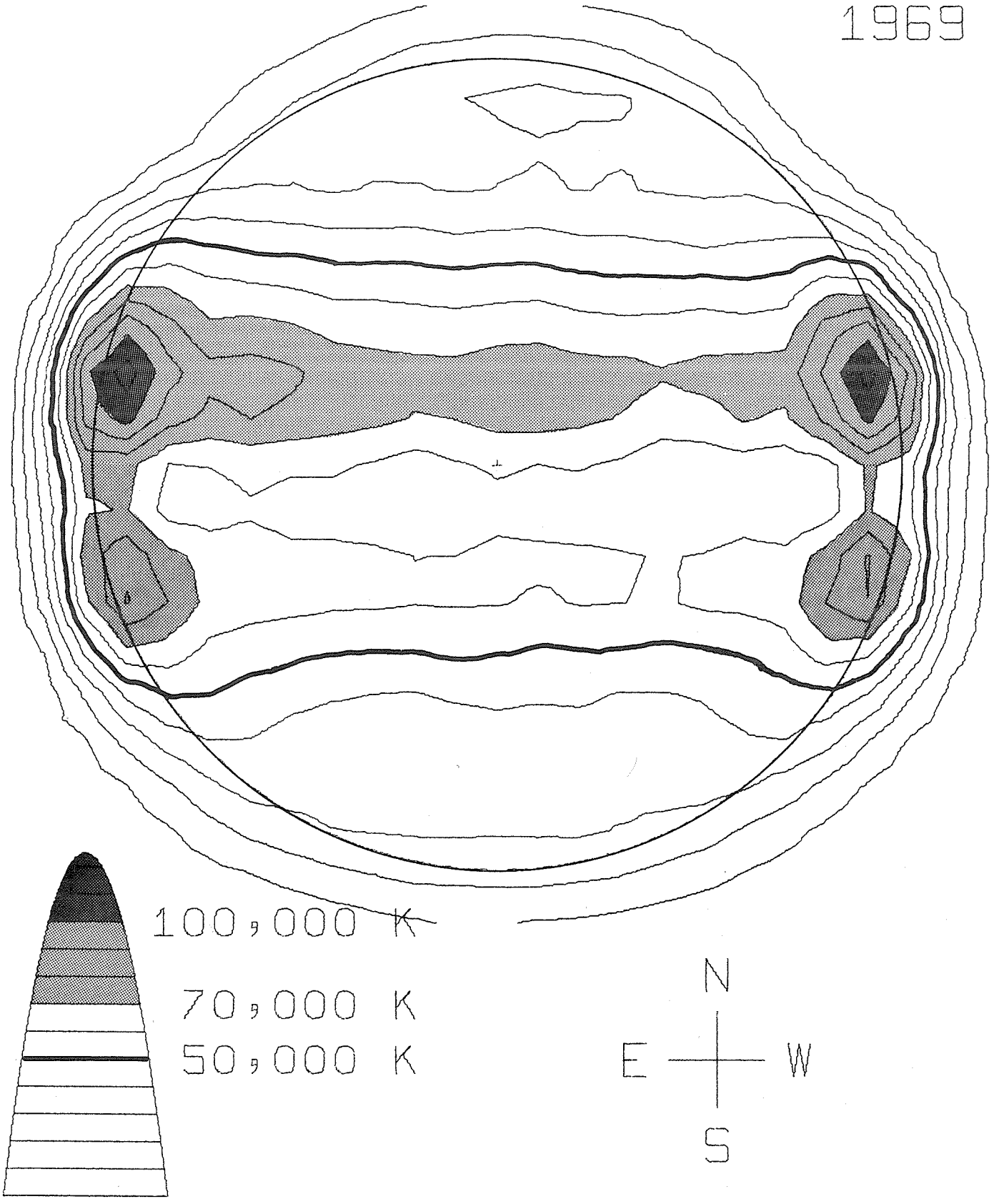

FIG. 5*h*. Yearly average map for 1969.

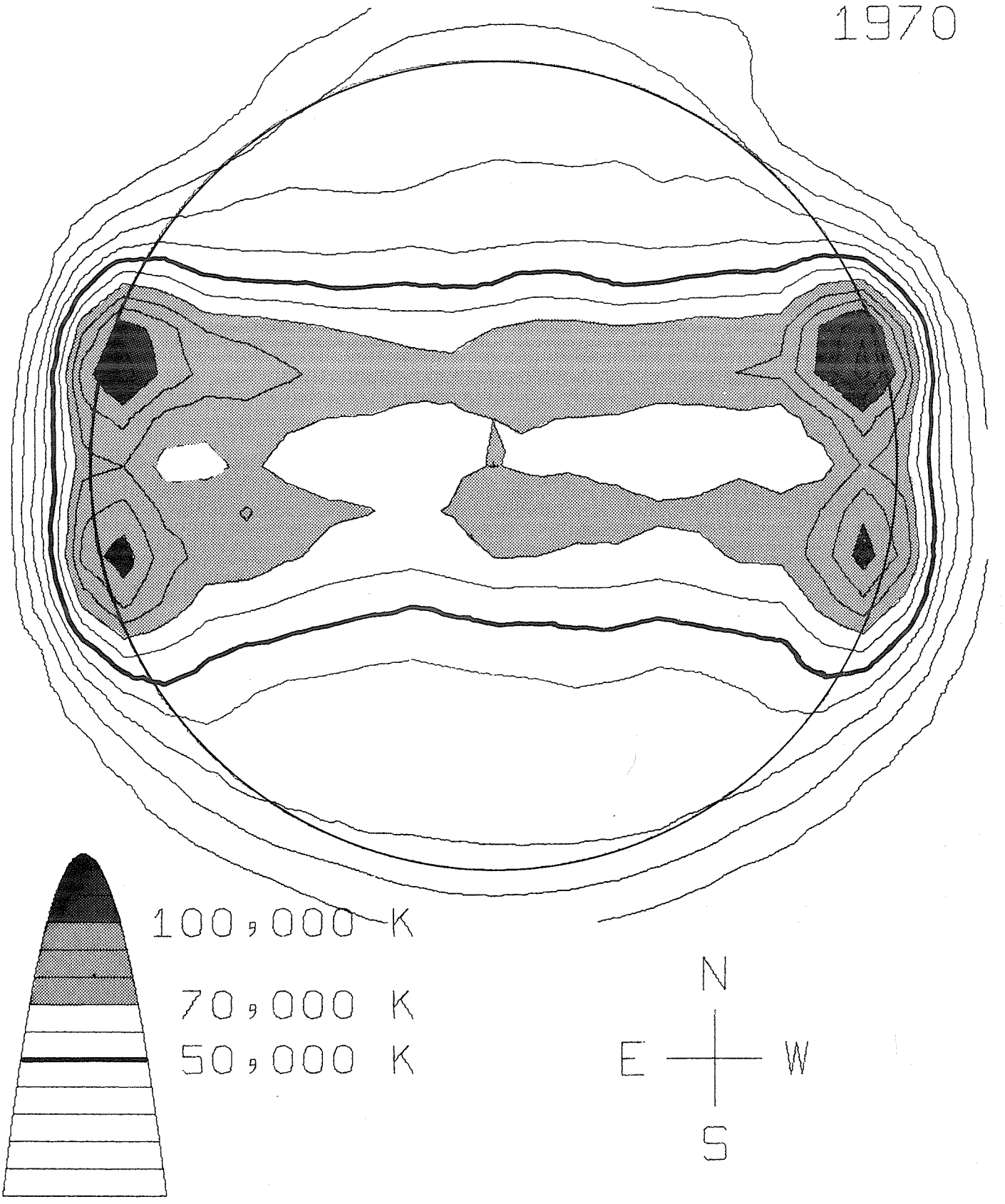

FIG. 5*i*. Yearly average map for 1970.

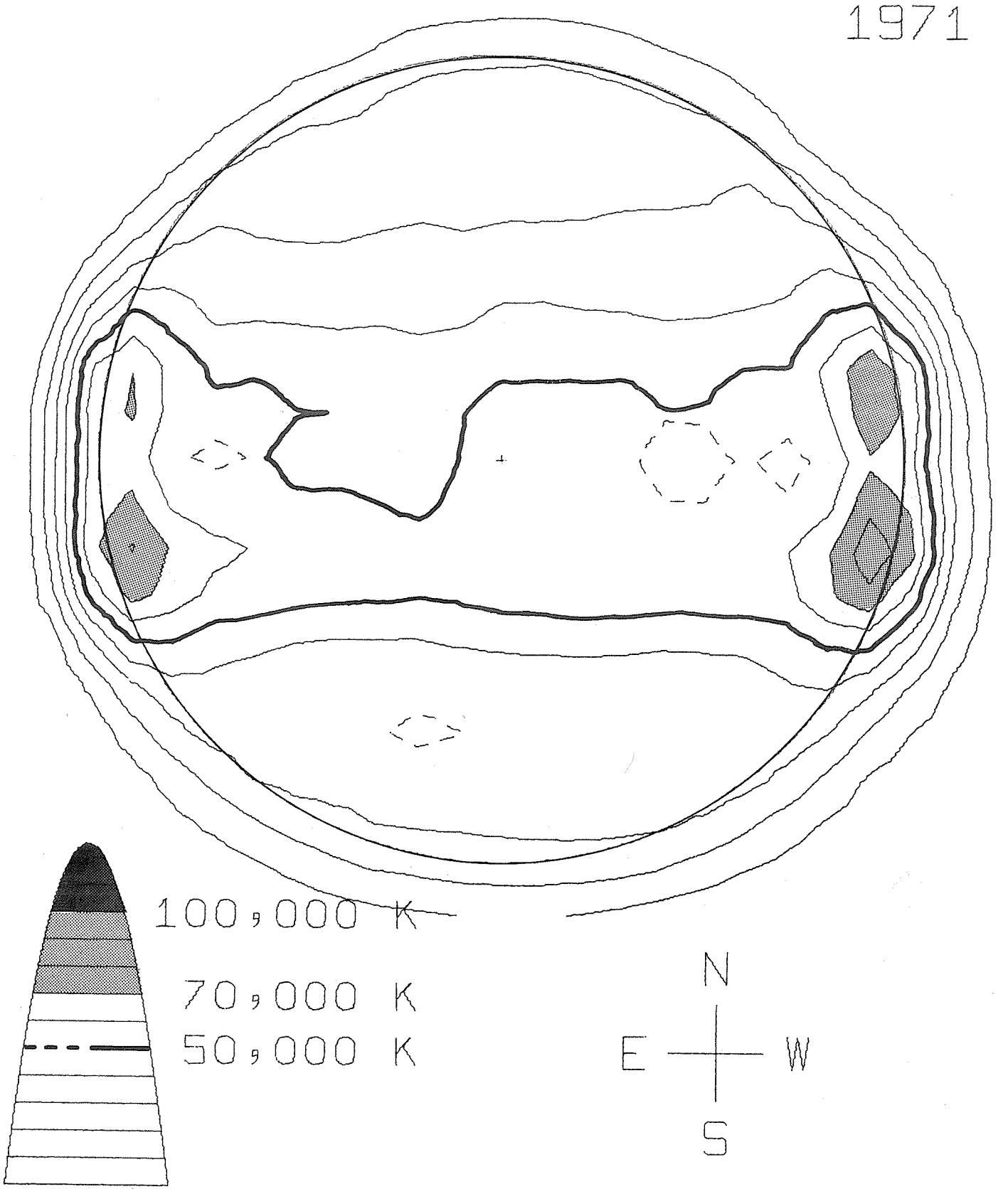

FIG. 5*j*. Yearly average map for 1971.

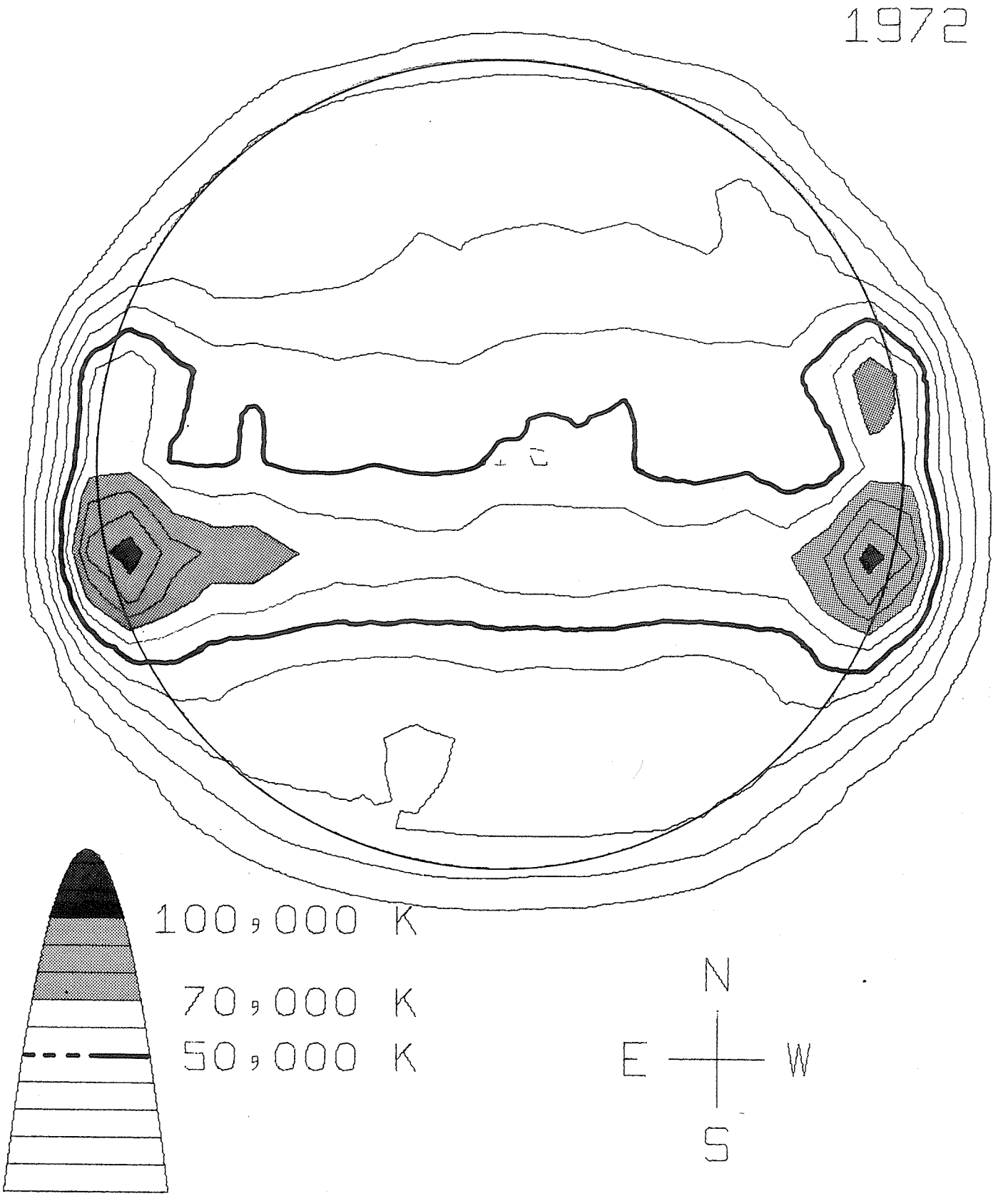

FIG. 5k. Yearly average map for 1972.

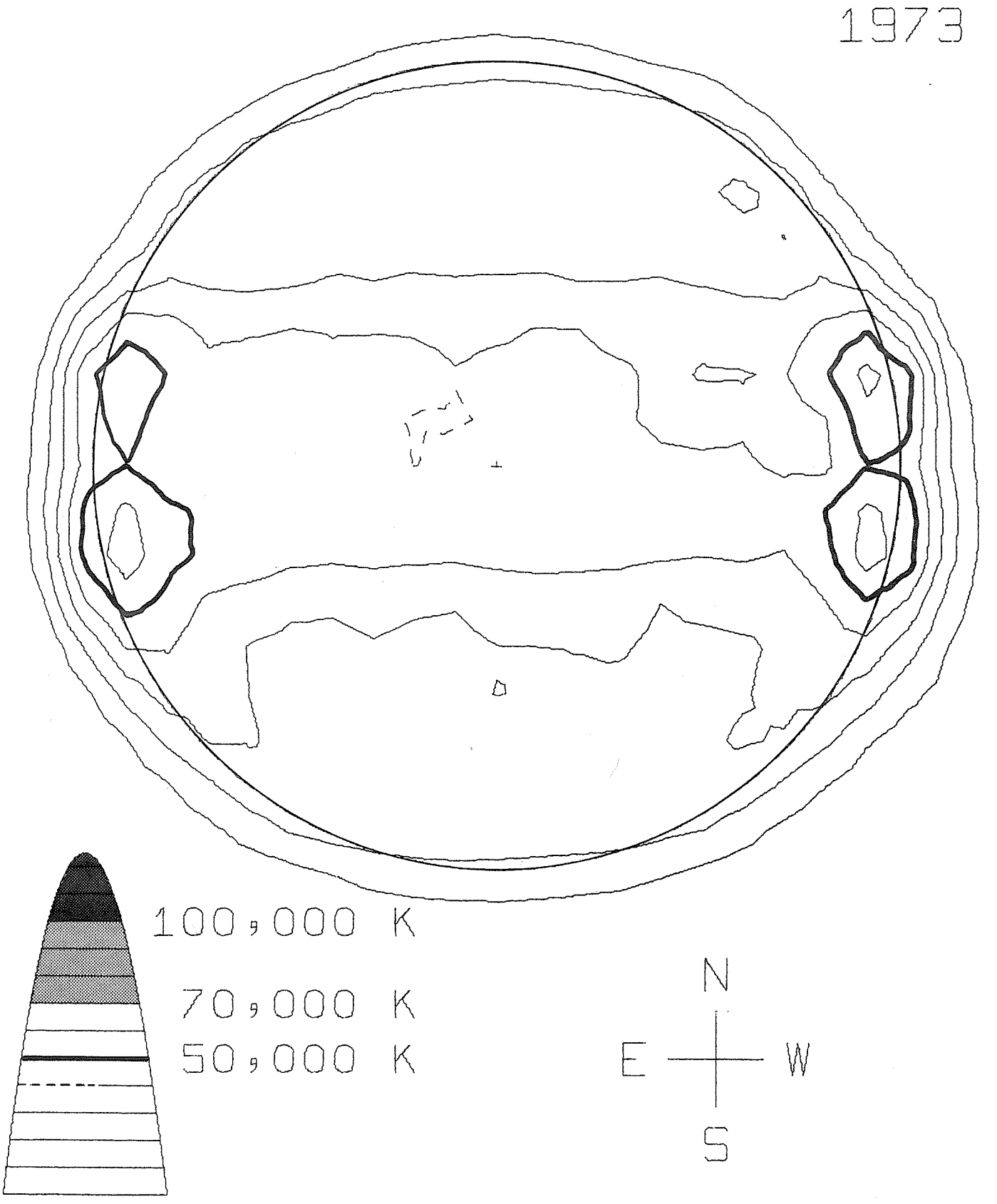

FIG. 5ℓ. Yearly average map for 1973.

5. SYNOPTIC MAPS

As a finding source to the large amount of data (4104 daily sun maps each with 525 data points), we present 151 synoptic maps, one for each Carrington rotation from 1455 to 1605. Each map on the following pages is a contour diagram based on an array of 121 points in longitude and 41 points in latitude.

The central meridian column on the daily maps almost never coincides with a column of the array just mentioned. To construct the array we used the central meridian columns and the two adjacent columns from each daily map. As the sun's rotation rate is approximately two columns per day, one of the outside columns contains information about what will be on the meridian half a day later and the other on what was on the meridian half a day before. Imagine that the central meridian columns of successive maps were placed in a preliminary matrix with a blank column between them. Then the column east of the central meridian column of one map is averaged with the column west of the central meridian column of the next map and the result is placed in the appropriate blank column of the preliminary matrix. This matrix then has 25 rows and 8208 columns. The even finer 41 x 18,121 array needed for the contour program is derived from interpolating at 3° intervals of heliographic latitude and longitude. Cubic spline polynomials were used for interpolation. Each synoptic map is a 121-column segment from this array, the last column of each rotation being the same as the first column of the next rotation.

The scale used is the same as the one introduced by L. and M. L. d'Azambuja: 1 mm corresponds to 1.5 heliocentric degrees in both latitude and longitude.

To indicate L_0, the heliographic longitude of the center of the disk, a dot was placed over each date to mark L_0 at 0000 UT of that date. Since the dot is not really needed for every day, we omit the dot if the map supplied on that day is an interpolated map.

The lowest contour level is 40,000 K, which is slightly above the quiet sun level; other contour levels advance by factors of 2, as shown in Figure 6; above 640,000 K shading is introduced. Dashed lines enclose depressions. Figure 6 also gives the latitude scale.

The contour routine used was adapted to our system from the one used at Sacramento Peak Observatory.

All rotation numbers refer to the Carrington system.

The interpretation of the structure of active regions as shown on the synoptic maps is subject to two points of caution. The first is that by their very nature the maps only refer to the regions as they appeared on the central meridian. For the full detail the daily maps themselves must be consulted. This is in contrast to the maps of d'Azambuja and Waldmeier which refer either to the maximum or to the average development of a feature in the course of its passage across the disk. The second point is that for an isolated strong active region the sidelobe structure of the antenna, described in Appendix A, shows up quite clearly, and it should not be mistaken for additional regions.

ACKNOWLEDGMENTS

Completion of this publication and the solar data set that it describes, while in itself a big piece of work, was only possible by virtue of an even larger job carried out by former students R. S. Colvin, G. Swarup and K. S. Yang and observers J. Deuter and J. S. Rutherford. Construction and initial research with the microwave spectroheliograph was supported by the Air Force Office of Scientific Research, 1956-1962. From 1962 the daily observations were supported by the Central Radio Propagation Laboratory of the National Bureau of Standards, the Environmental Science Services Administration, the Air Force Office of Scientific Research, the Atmospheric Sciences Section of the National Science Foundation, and finally by the National Oceanic and Atmospheric Administration for part of 1973. Research on the data, including the reduction to homogeneous machine-readable form, has been supported by the National Science Foundation under Grant Nos. GA-33000 and DES72-01388. One of the authors (Werner Graf) is also grateful for a visiting fellowship to the Sacramento Peak Observatory of the Air Force Cambridge Research Laboratories and the Joint Institute for Laboratory Astrophysics of the University of Colorado.

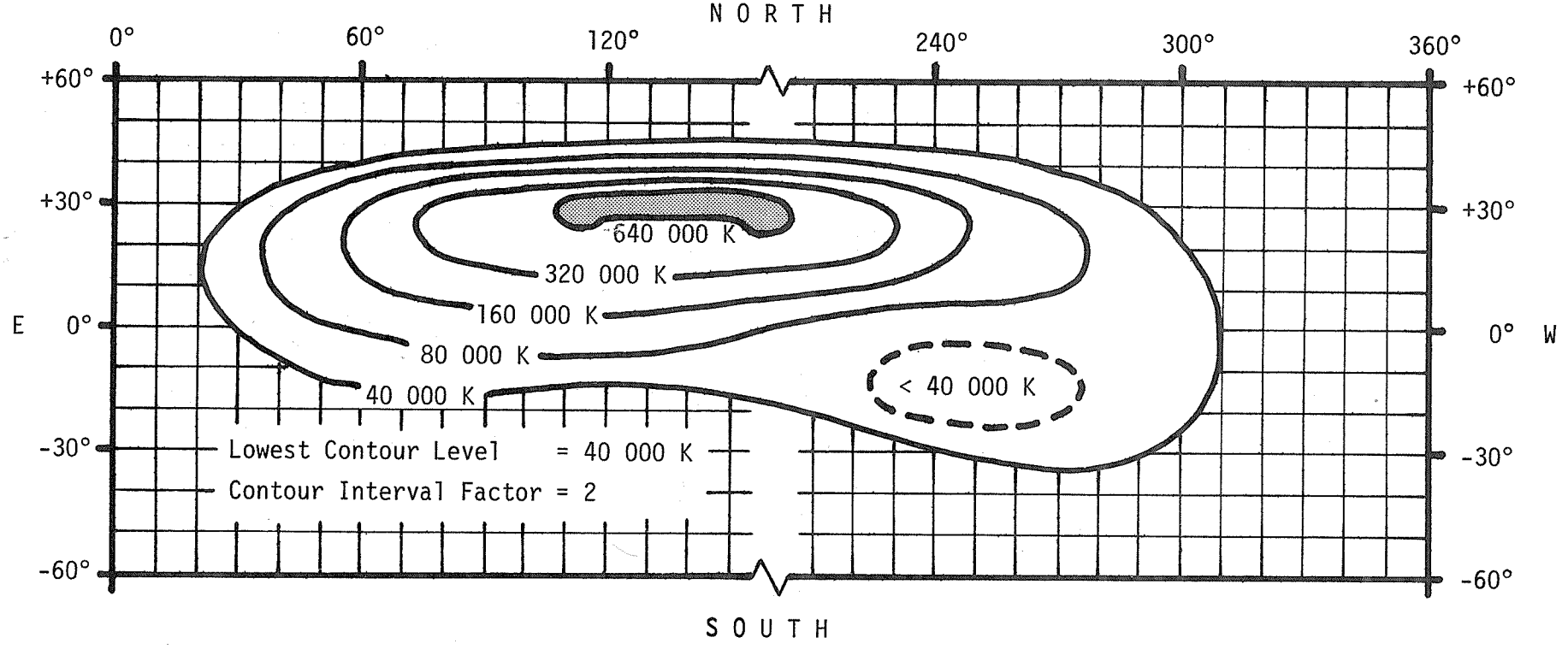

FIG. 6. Schematic synoptic map (not to scale) to show contour levels and the heliographic coordinates. On the actual synoptic maps the longitude of the central meridian of the sun for each day at 0000 UT is marked by a dot on the lower edge of the synoptic maps above the date. To flag the dates of the artificial maps we omit the dot.

ROTATION NUMBER 1455

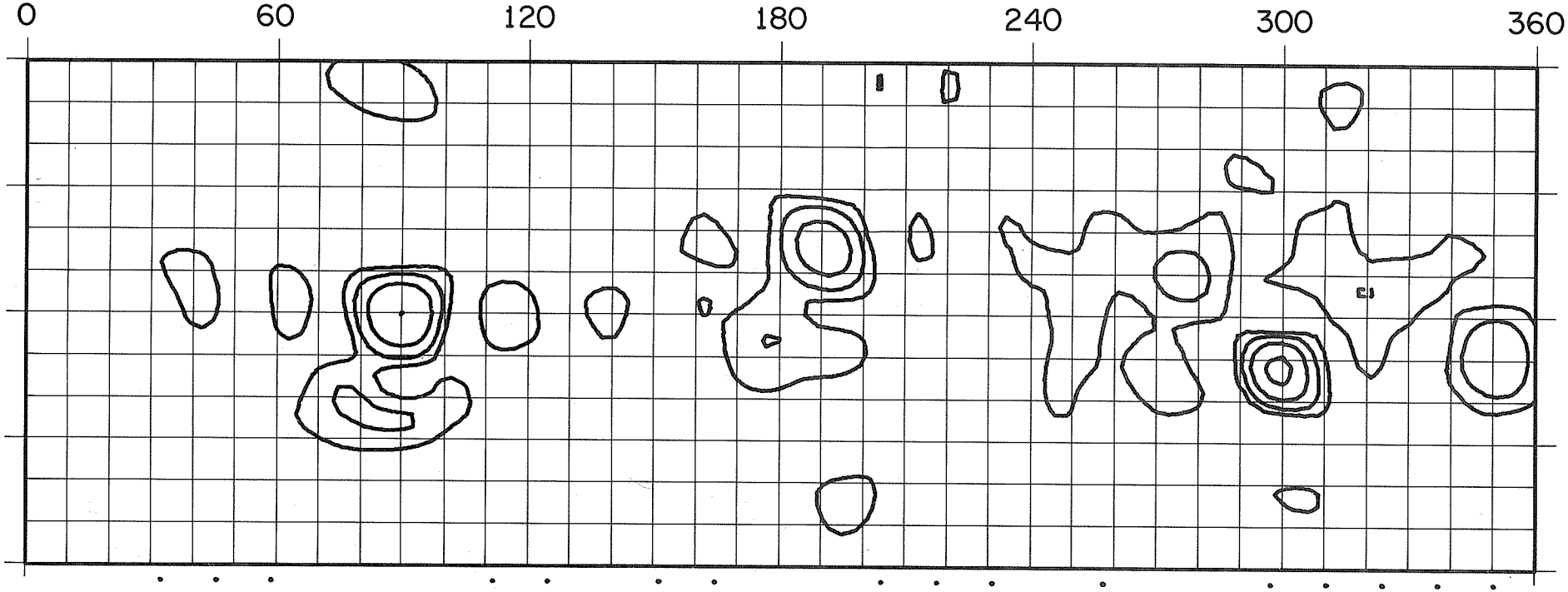

ROTATION NUMBER 1456

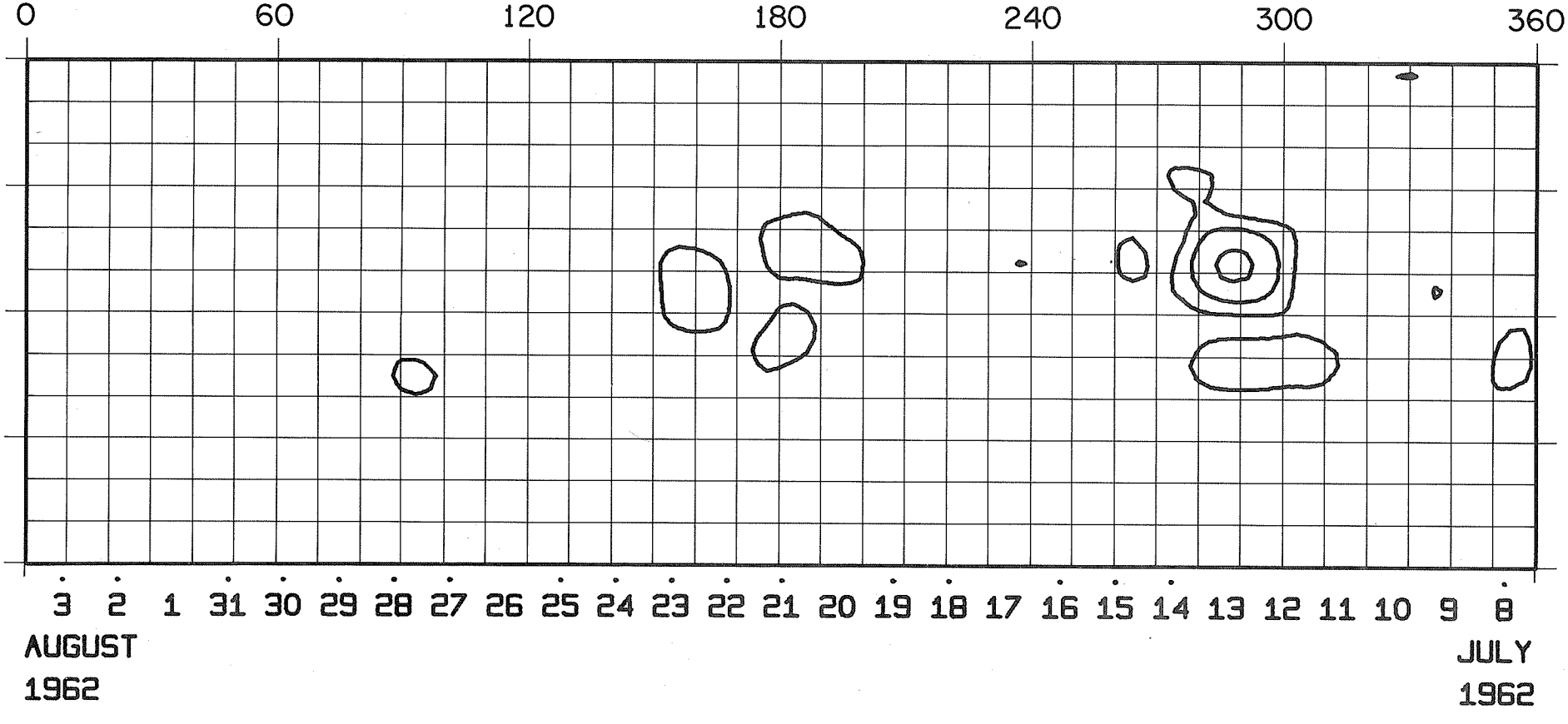

ROTATION NUMBER 1457

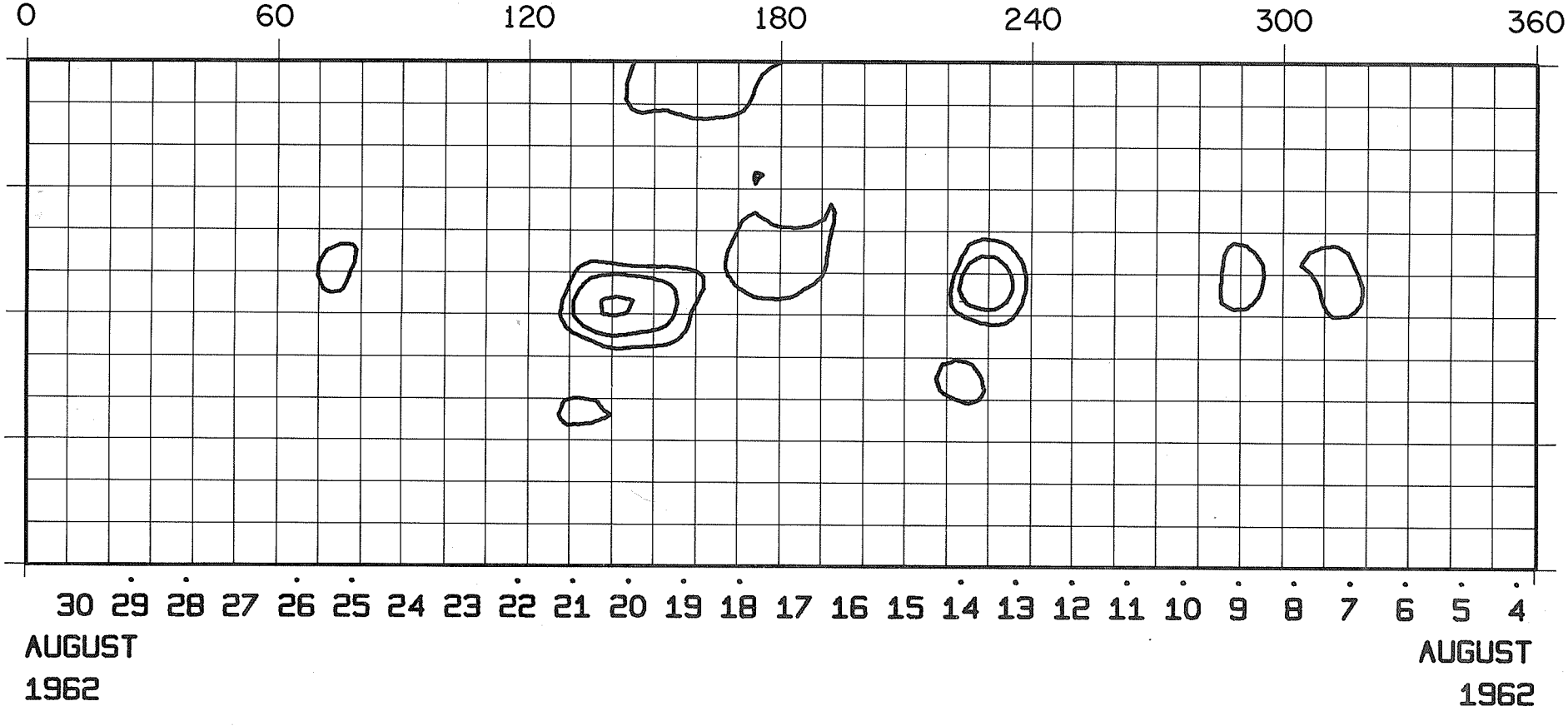

ROTATION NUMBER 1458

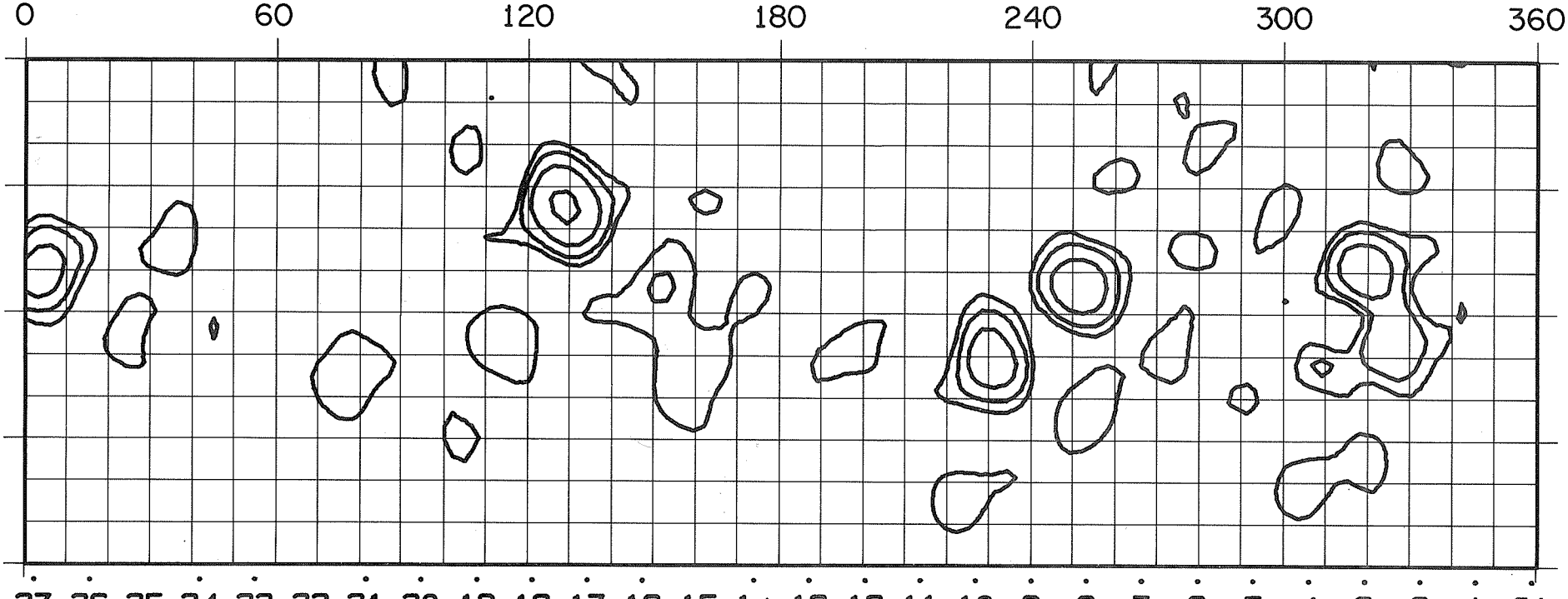

ROTATION NUMBER 1459

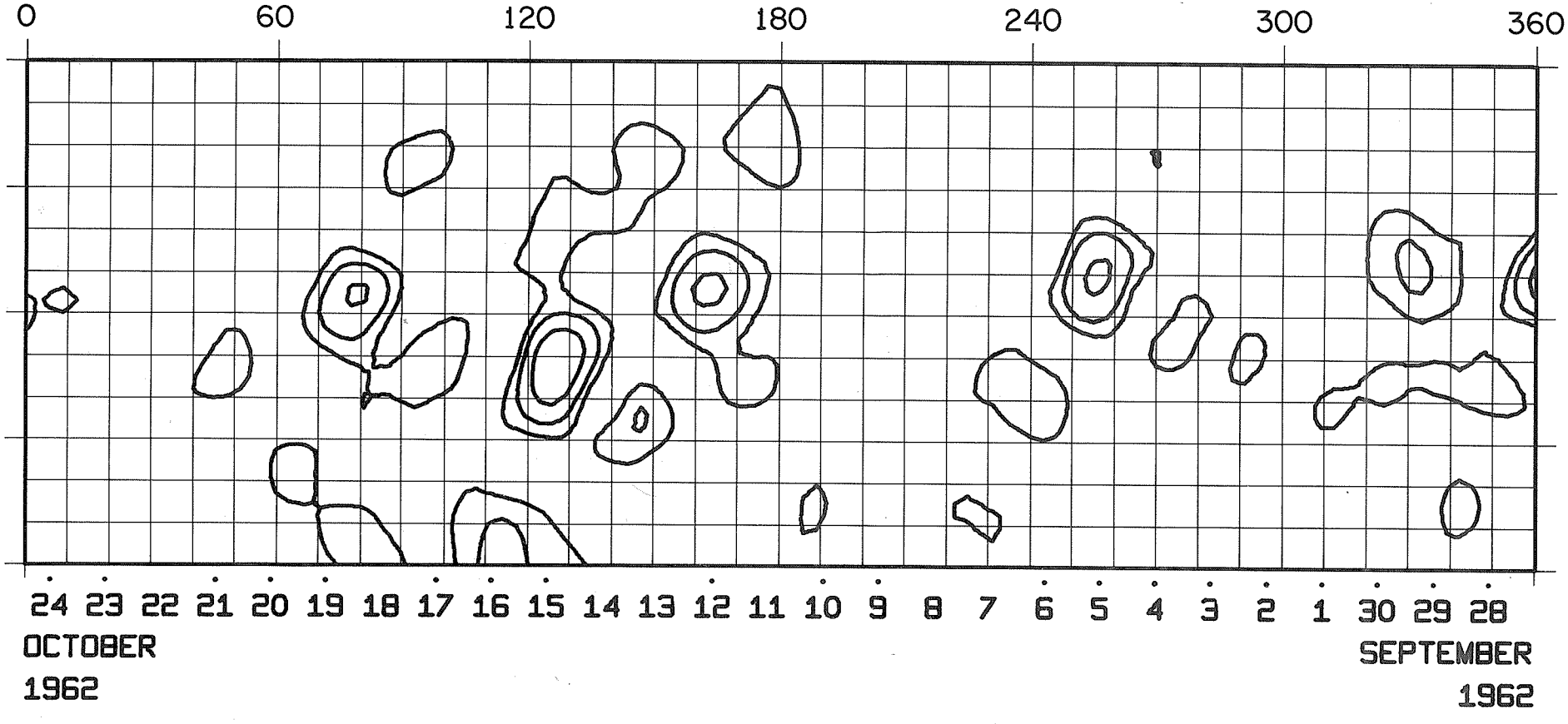

ROTATION NUMBER 1460

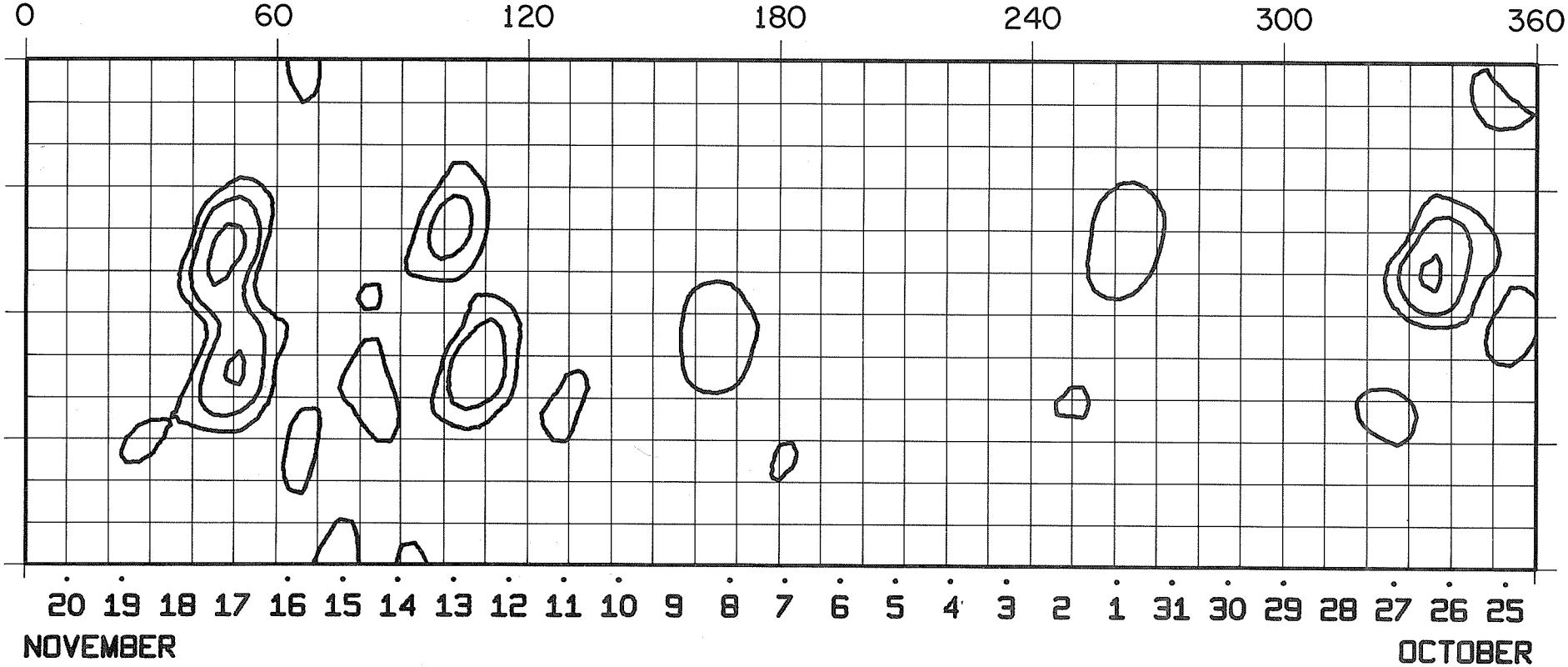

ROTATION NUMBER 1461

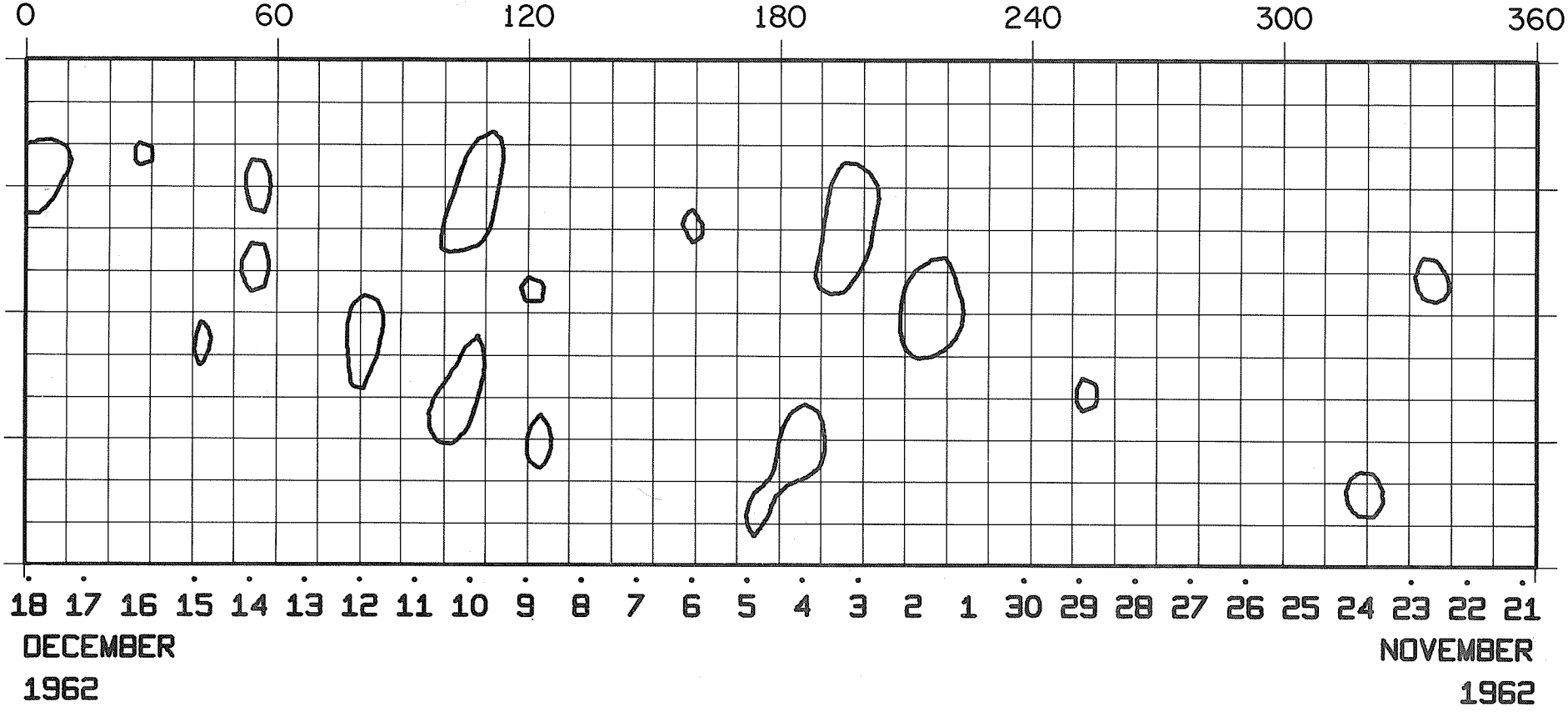

ROTATION NUMBER 1462

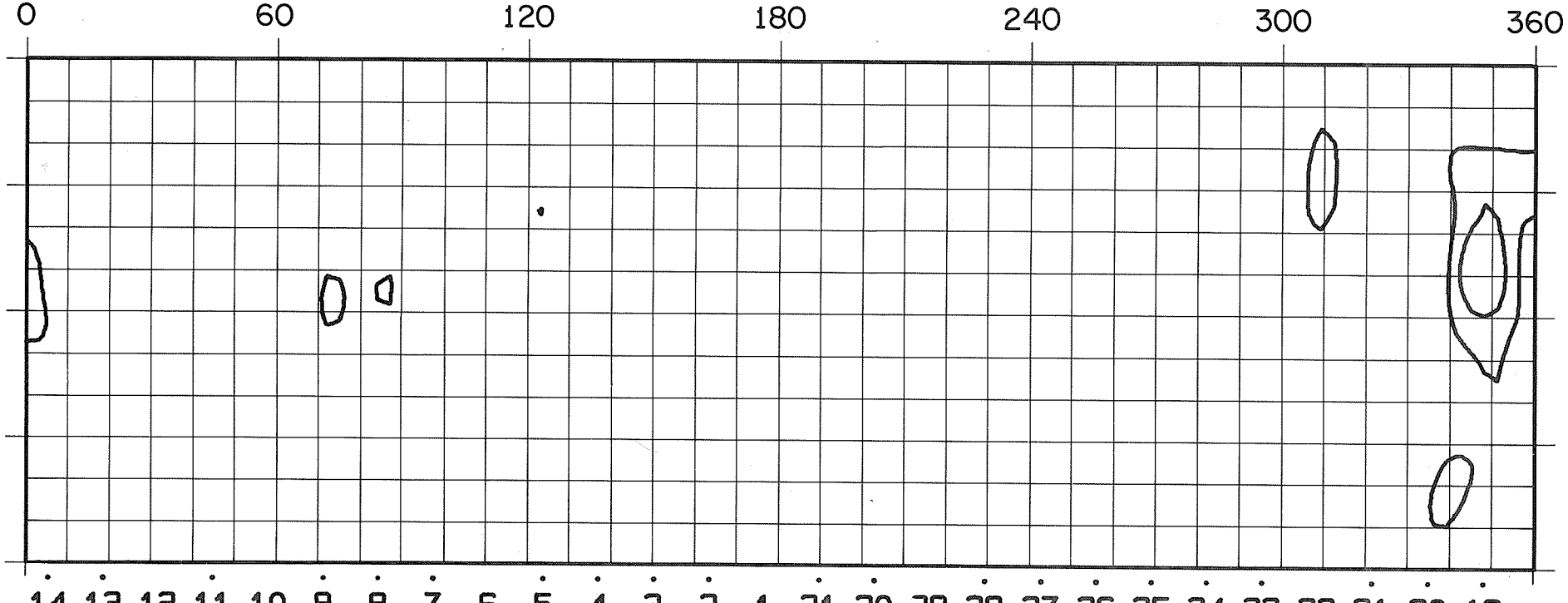

ROTATION NUMBER 1463

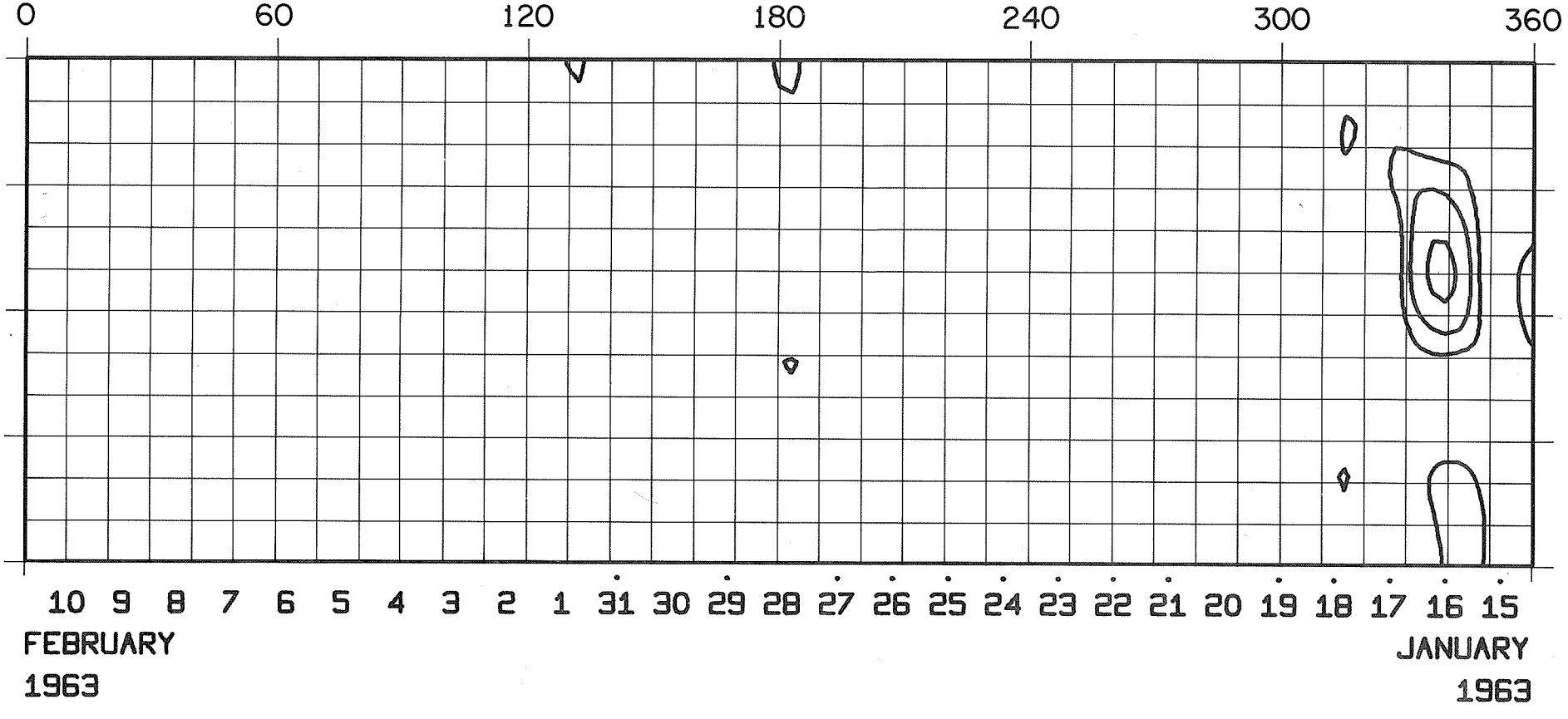

ROTATION NUMBER 1464

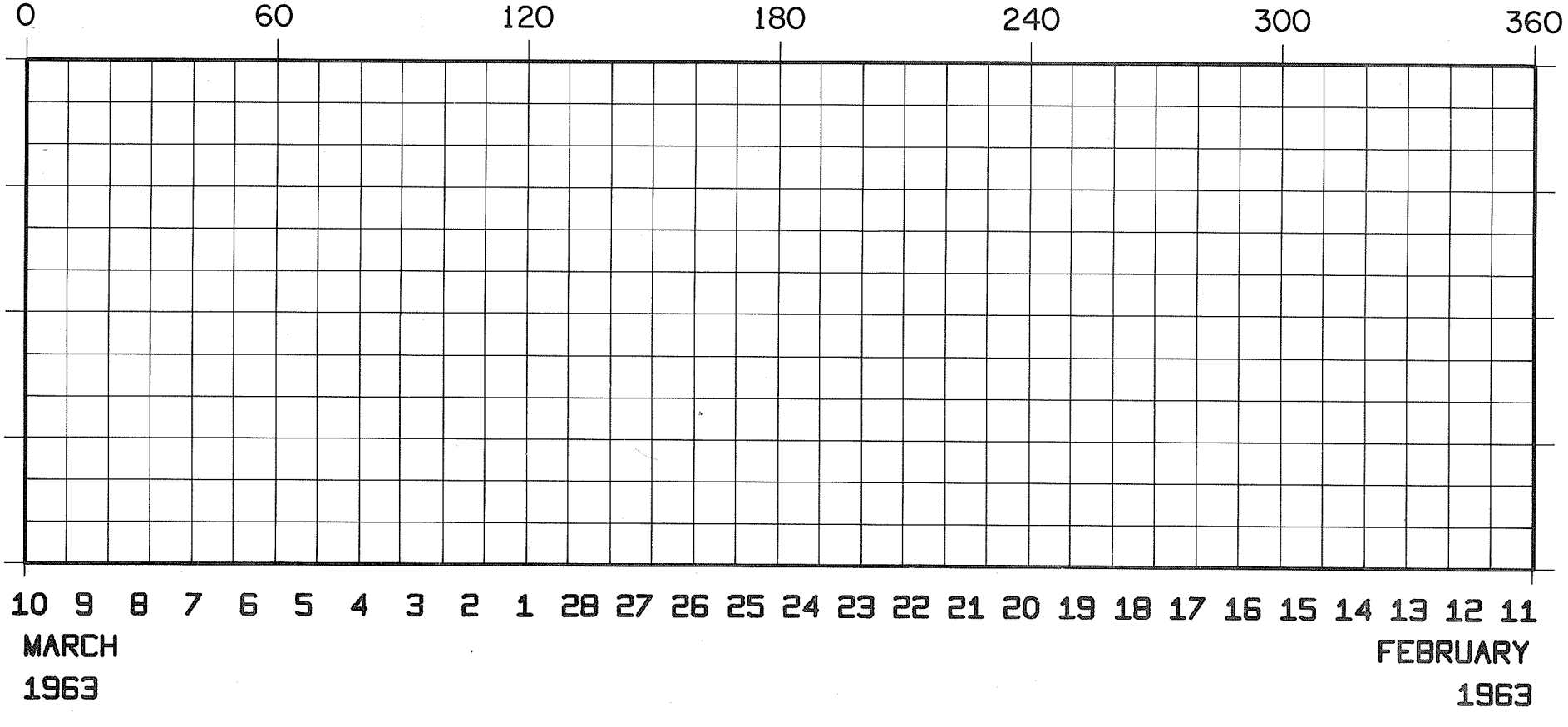

ROTATION NUMBER 1465

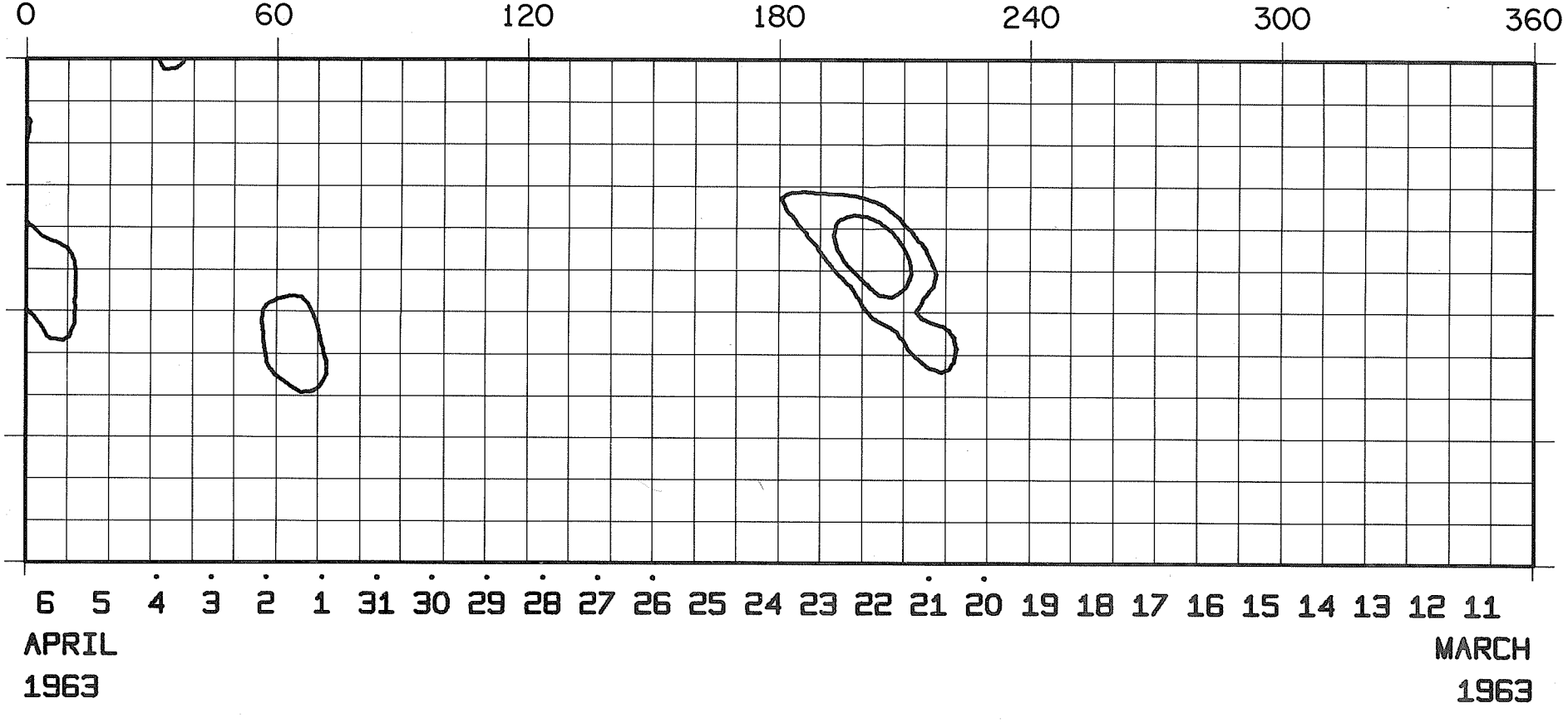

ROTATION NUMBER 1466

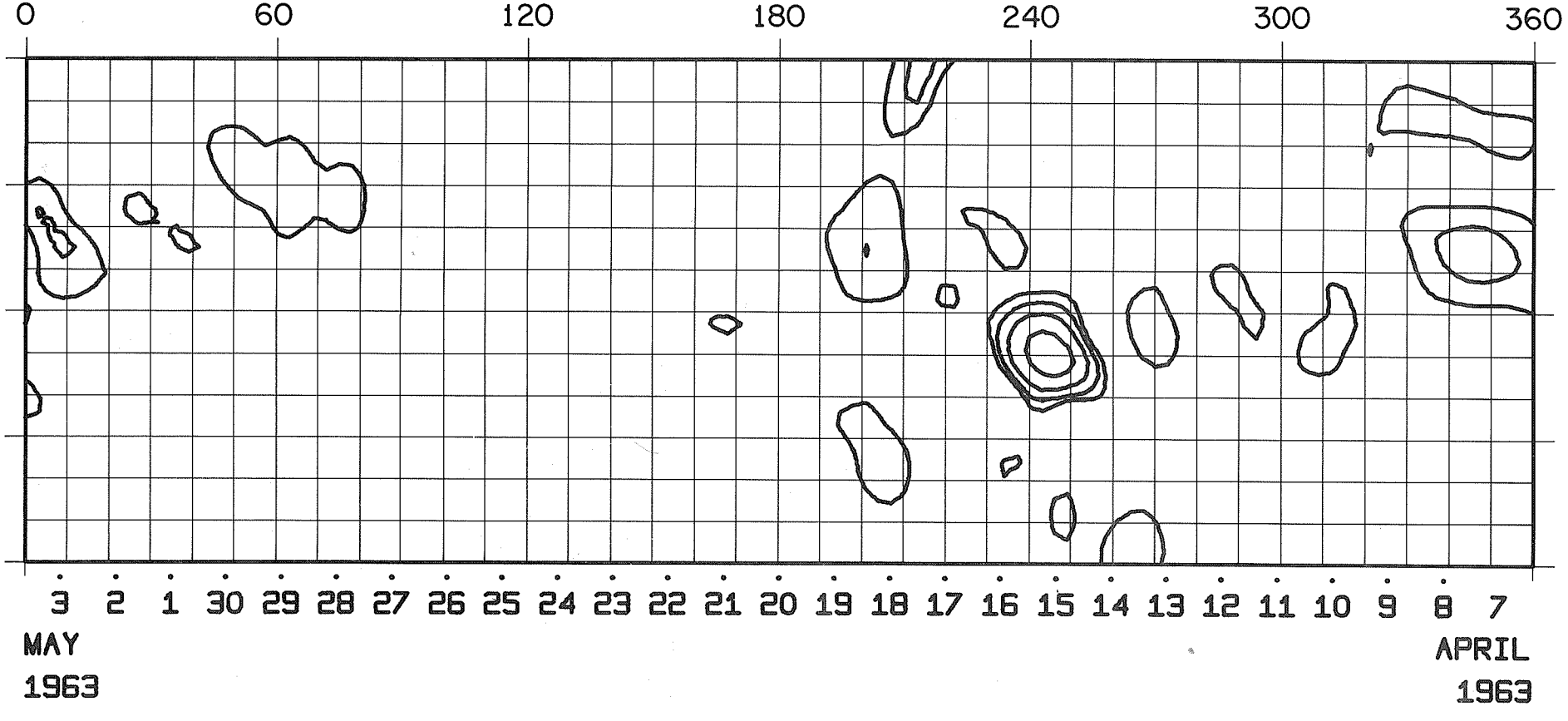

ROTATION NUMBER 1467

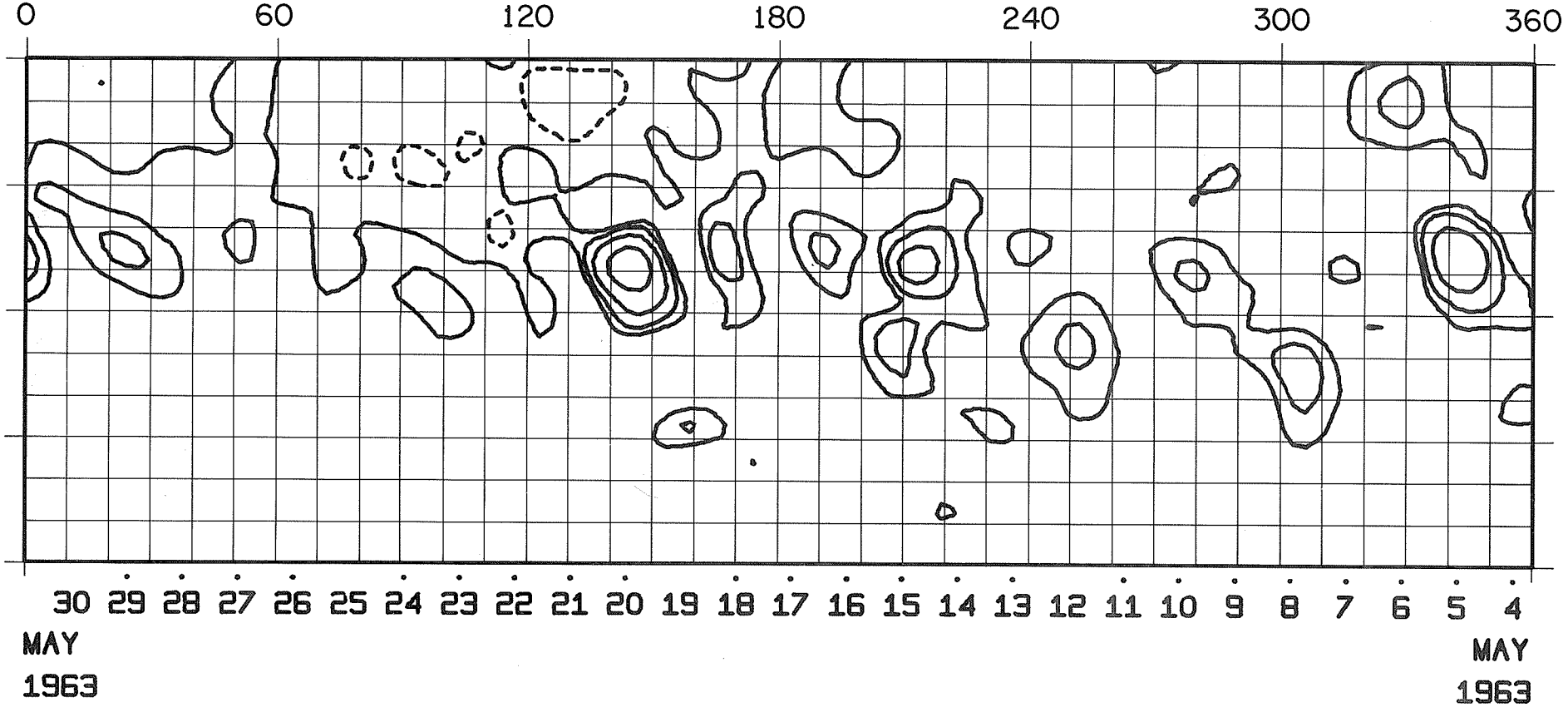

ROTATION NUMBER 1468

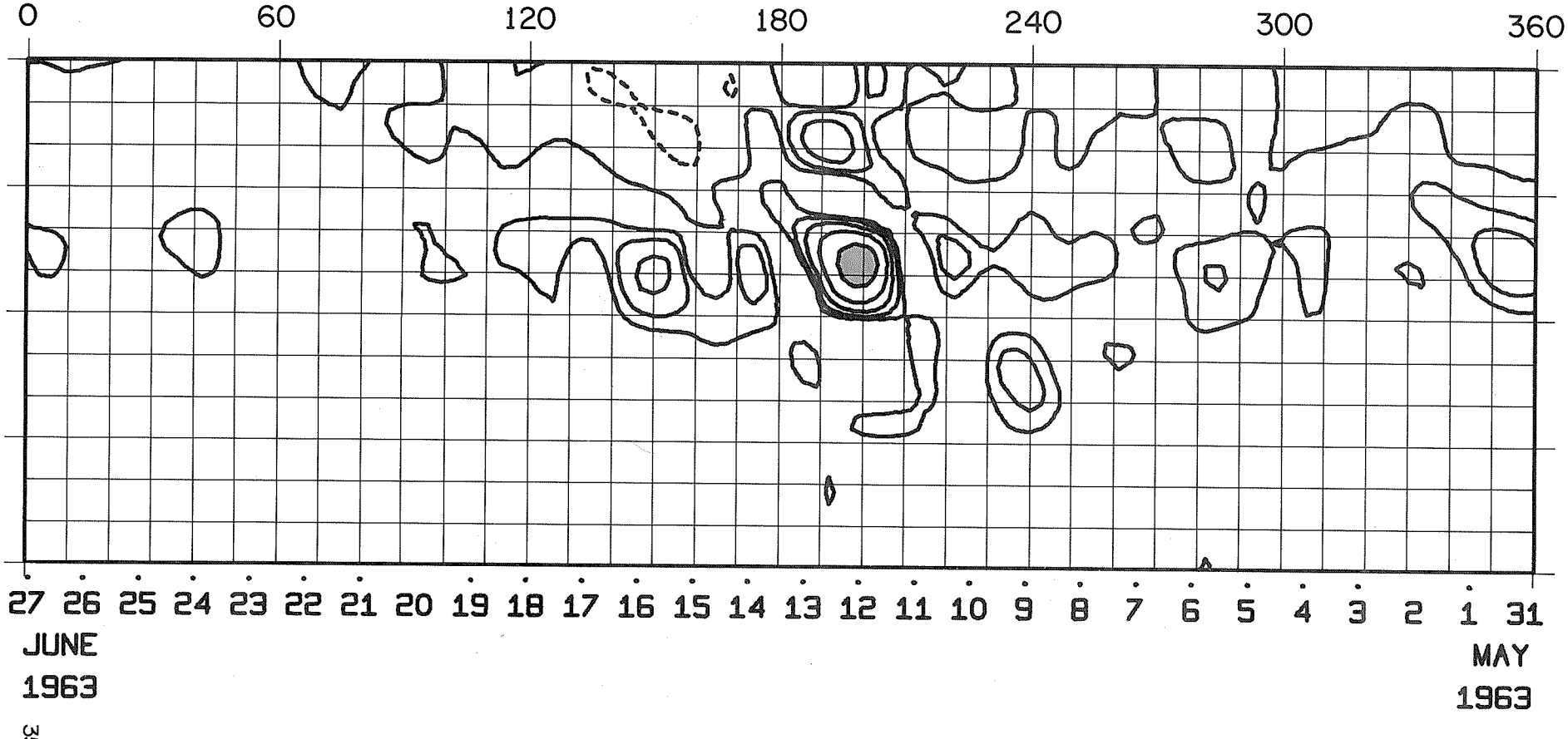

ROTATION NUMBER 1469

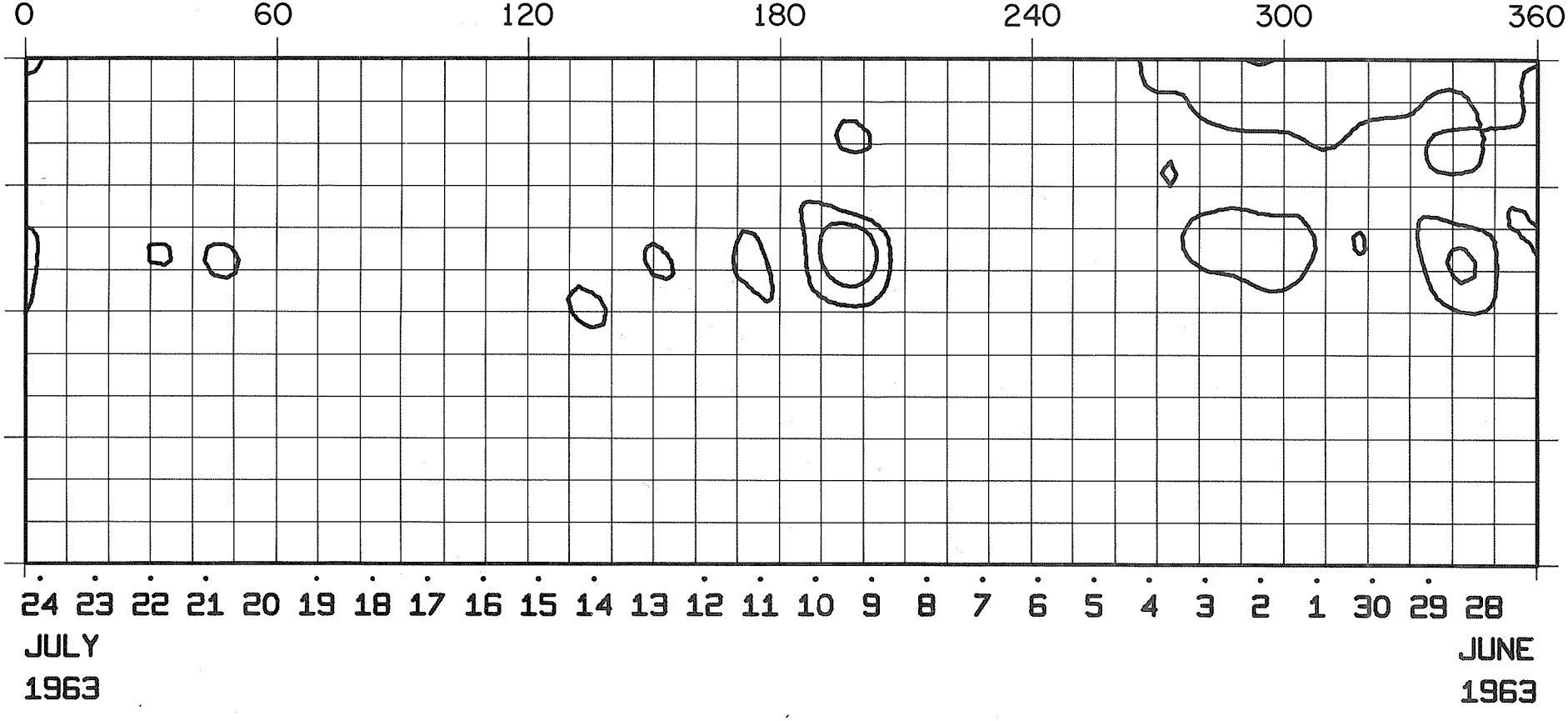

ROTATION NUMBER 1470

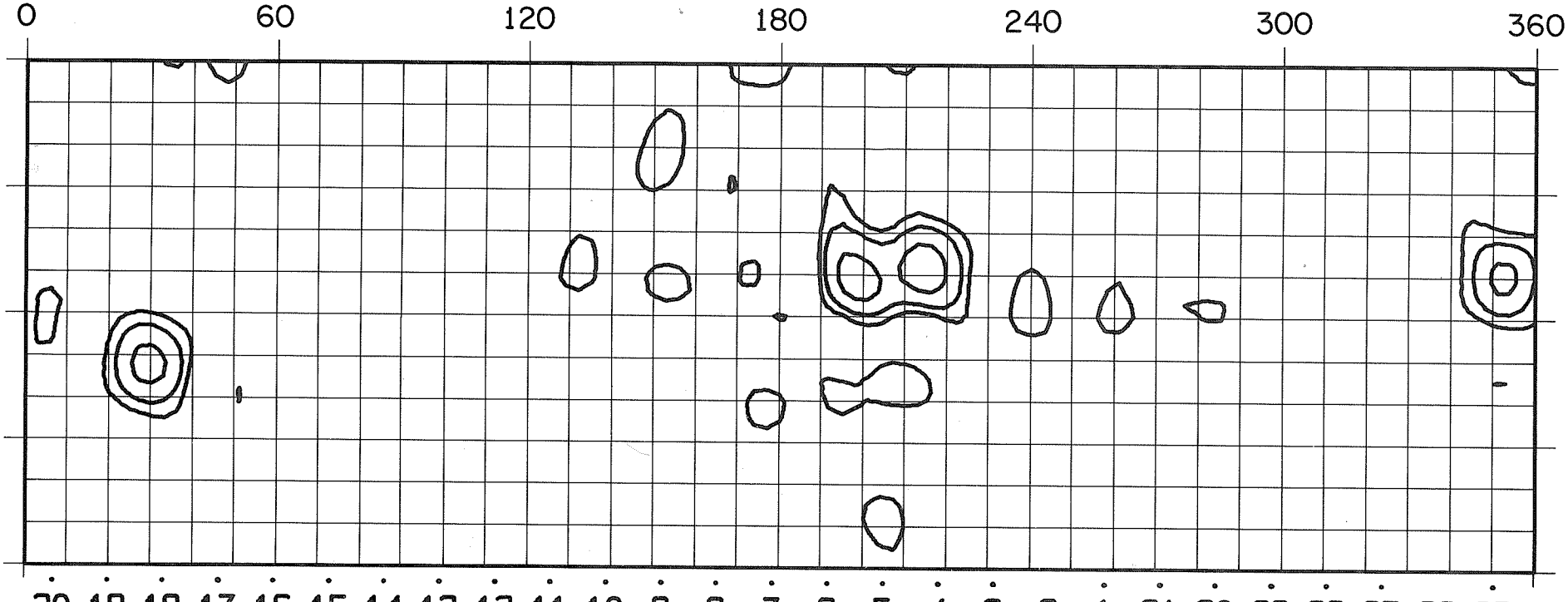

ROTATION NUMBER 1471

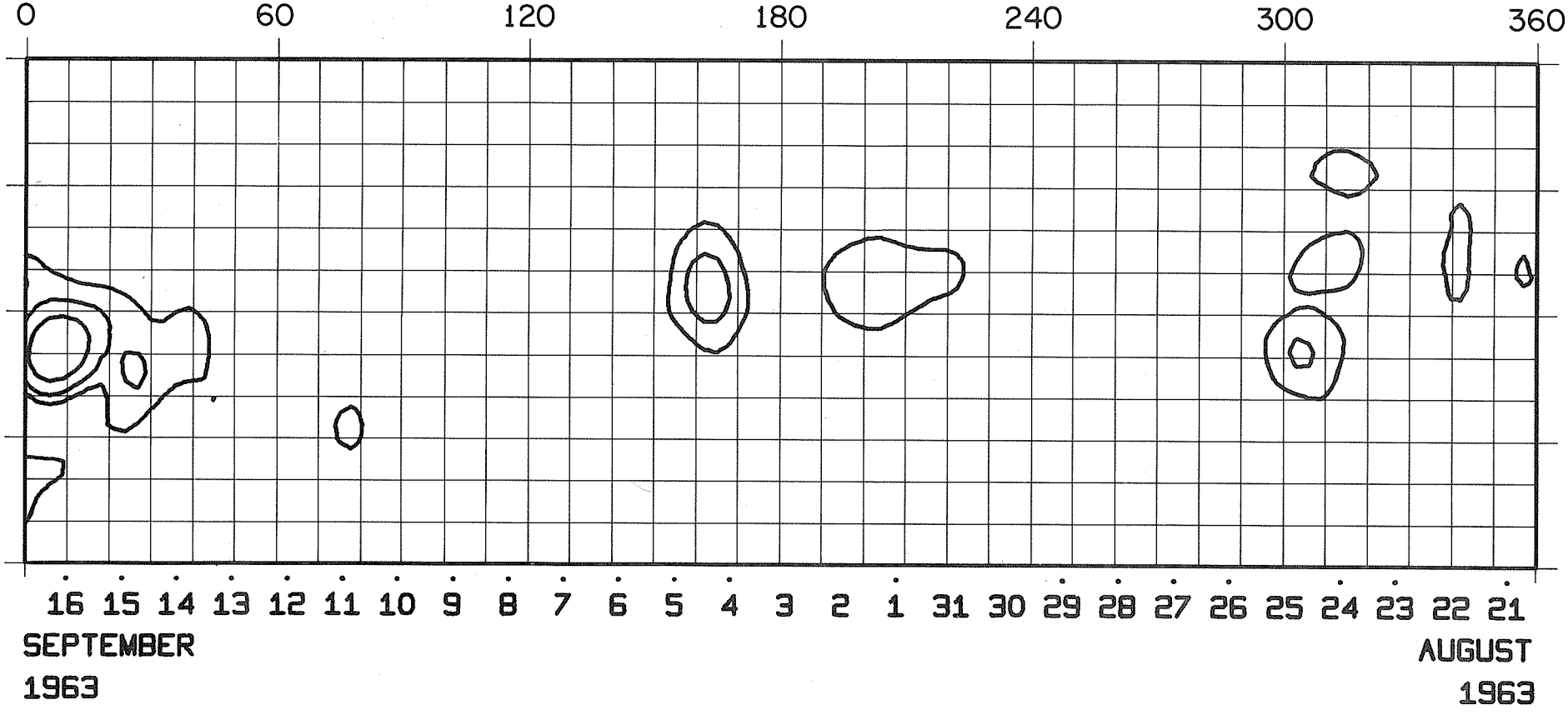

ROTATION NUMBER 1472

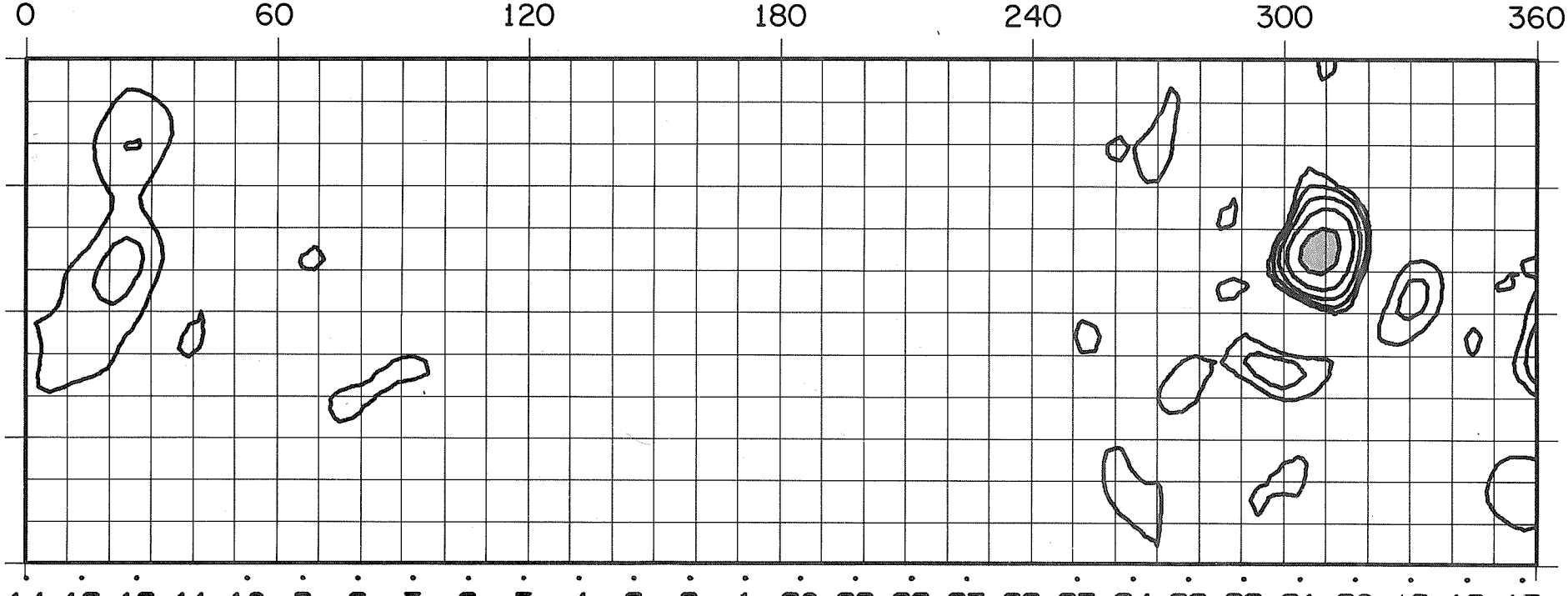

ROTATION NUMBER 1473

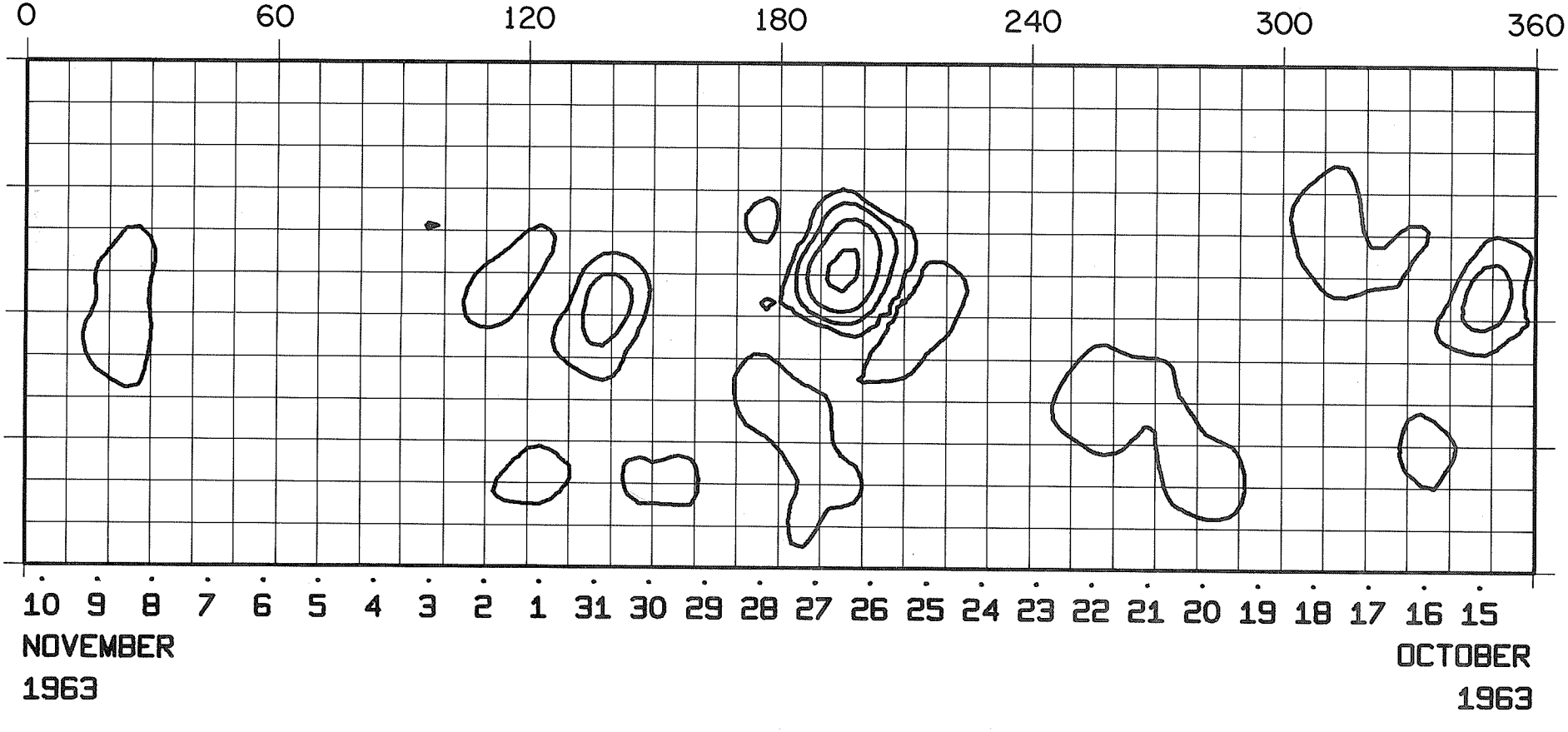

ROTATION NUMBER 1474

ROTATION NUMBER 1475

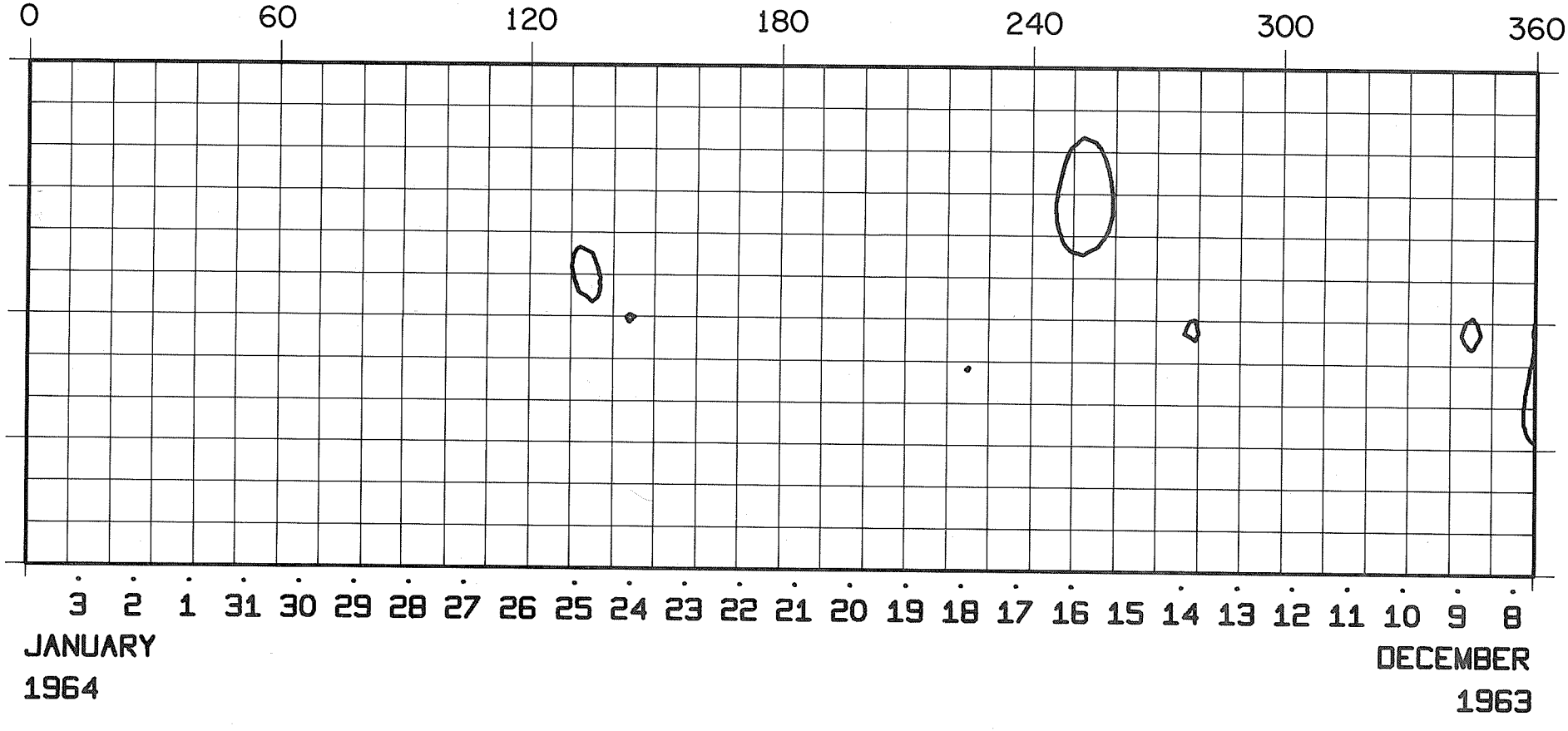

ROTATION NUMBER 1476

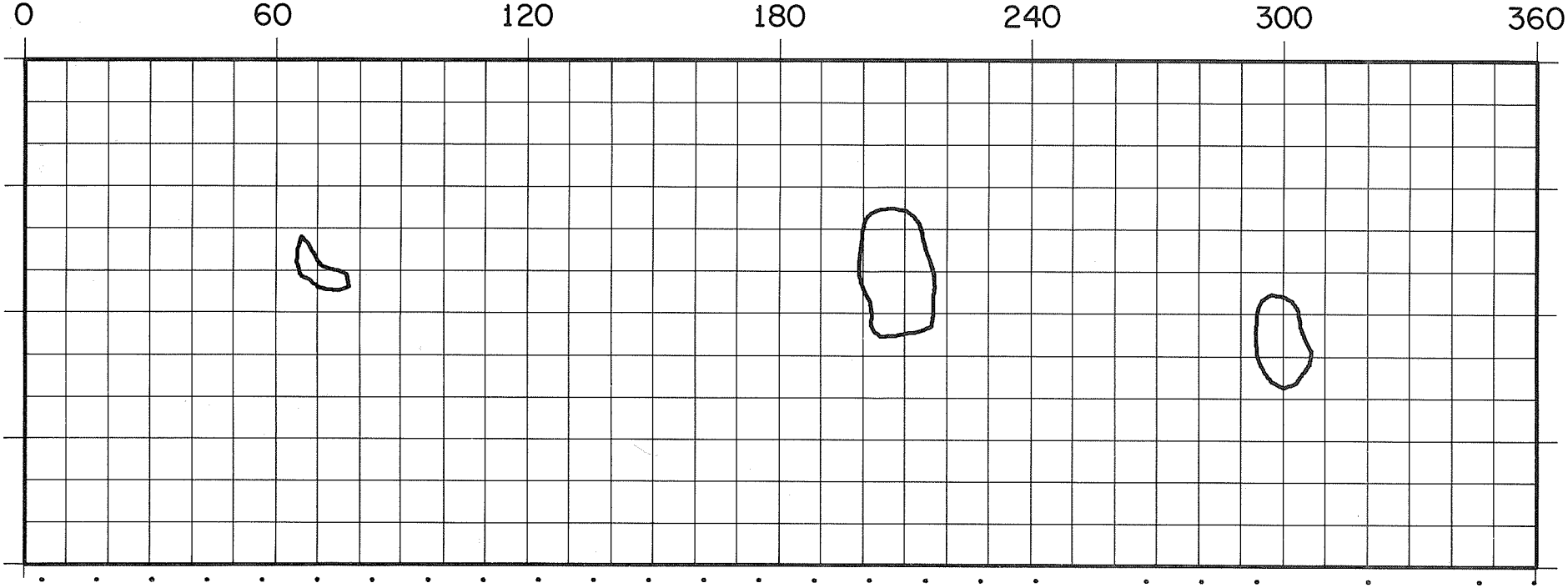

ROTATION NUMBER 1477

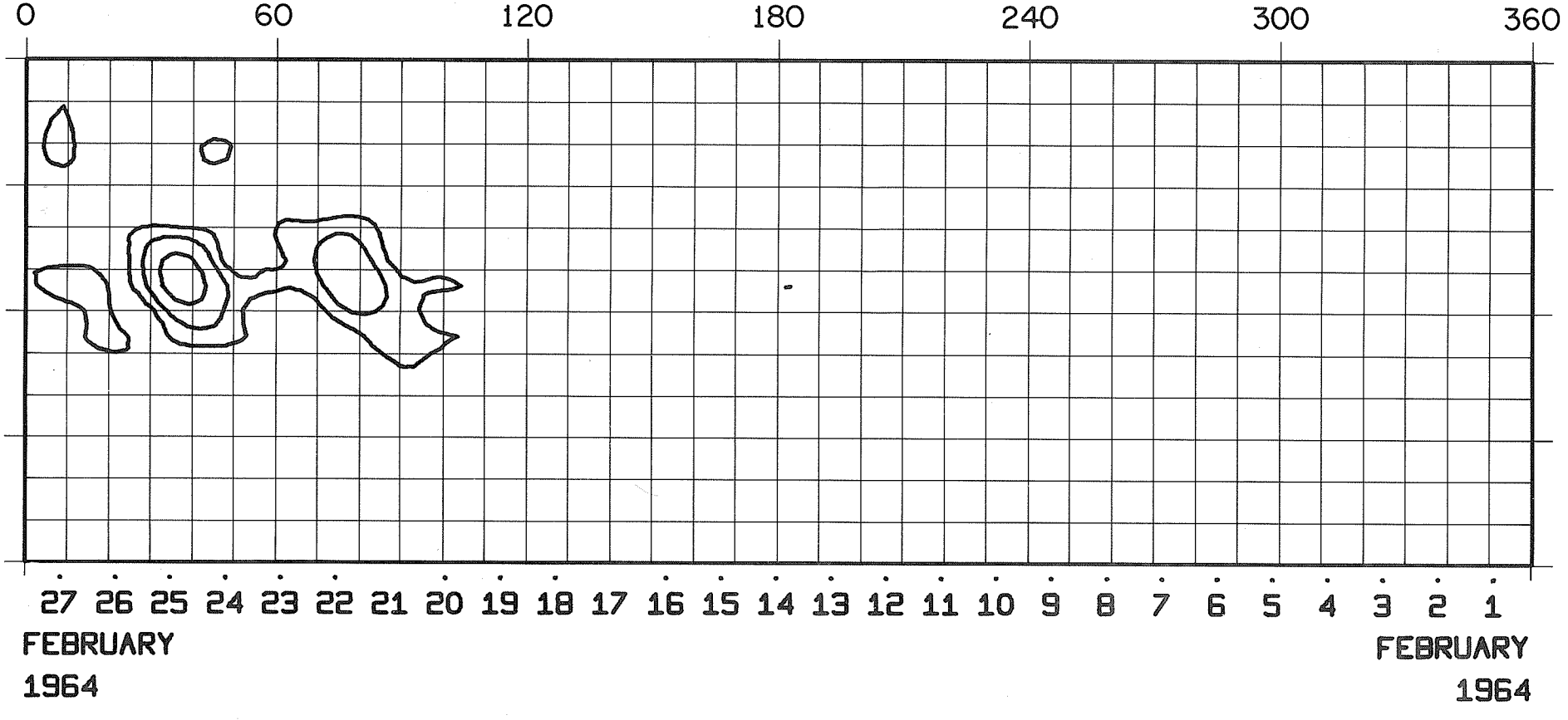

ROTATION NUMBER 1478

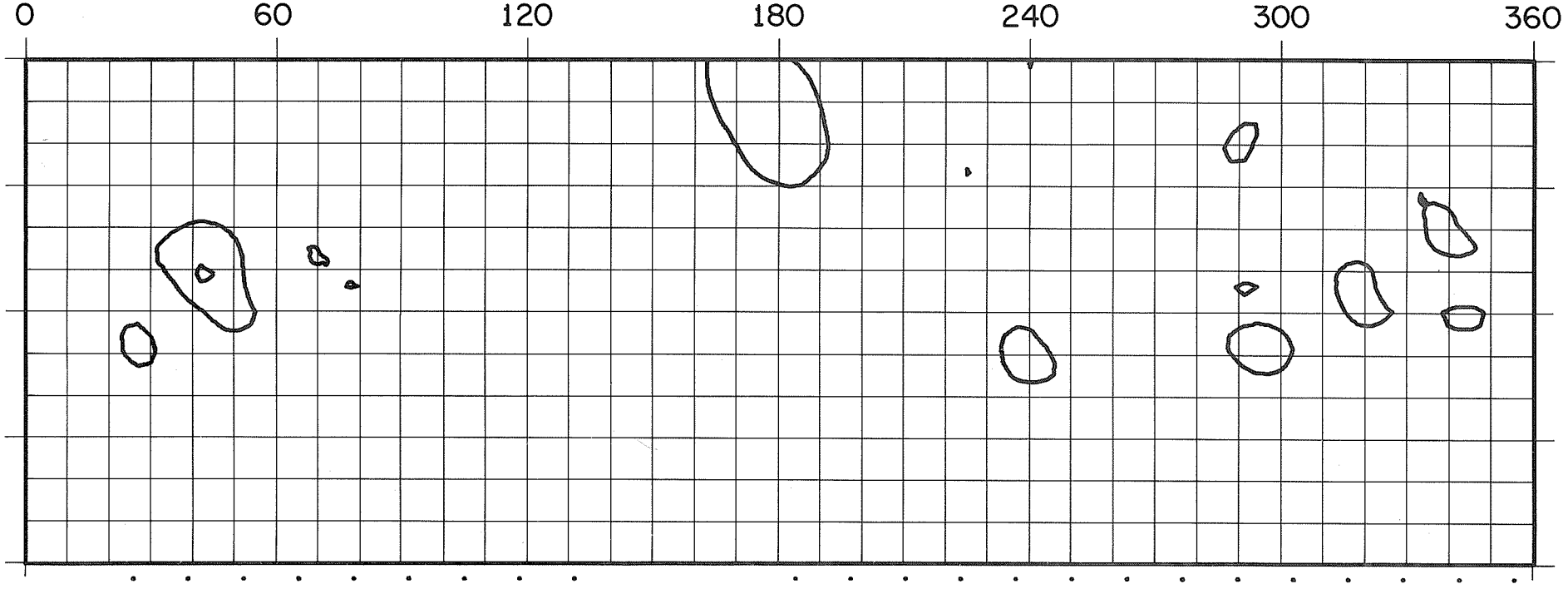

ROTATION NUMBER 1479

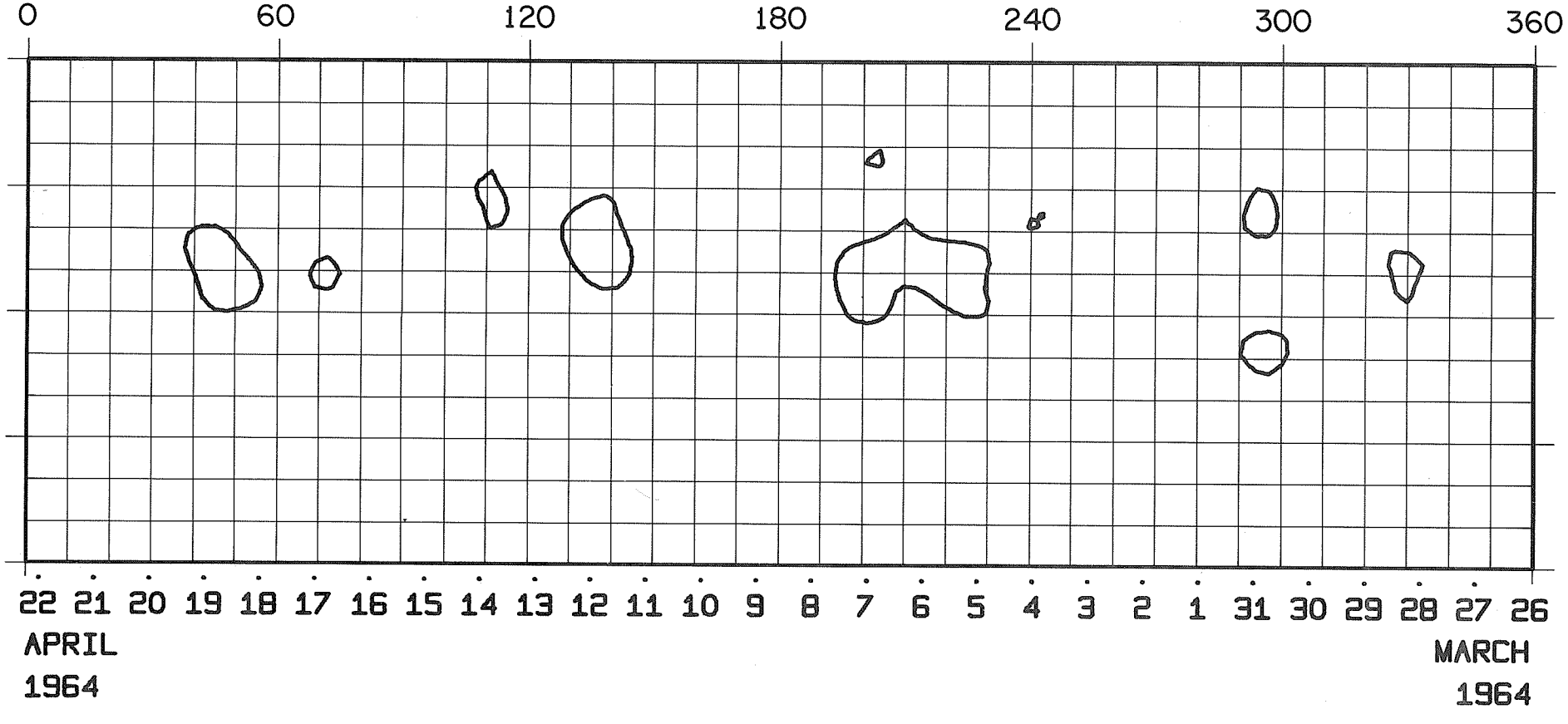

ROTATION NUMBER 1480

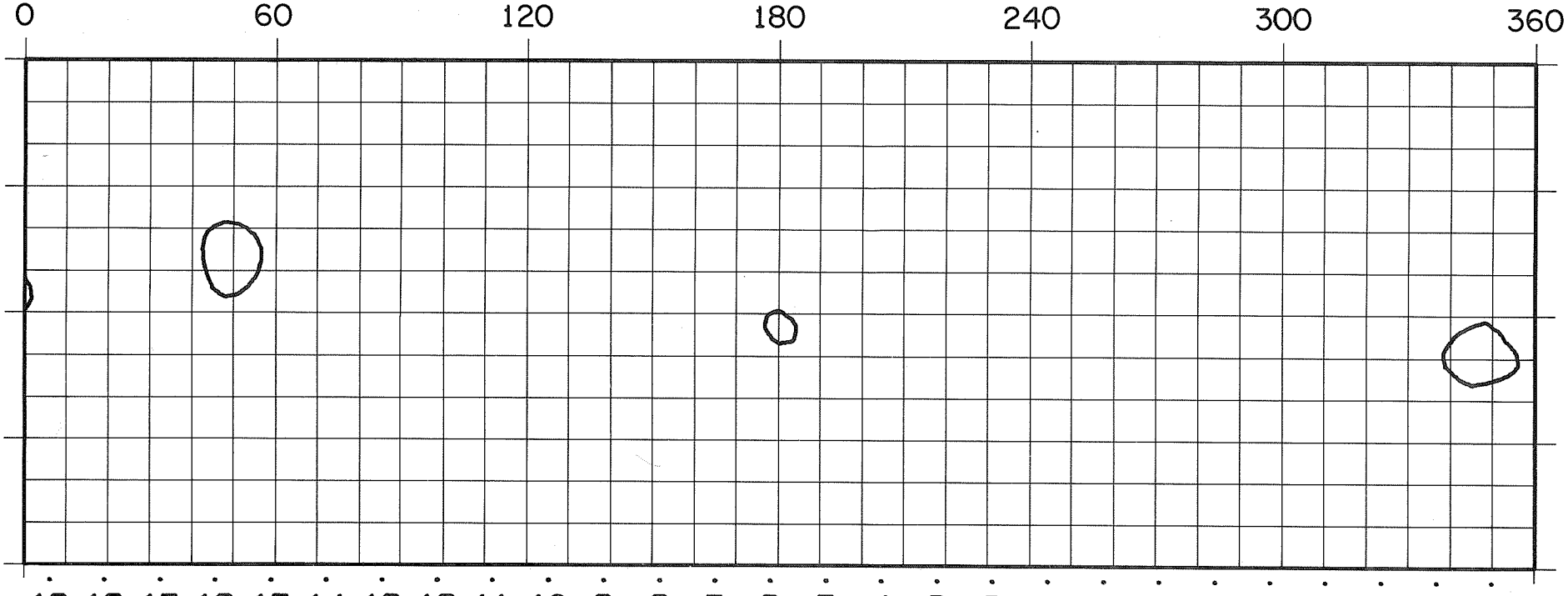

ROTATION NUMBER 1481

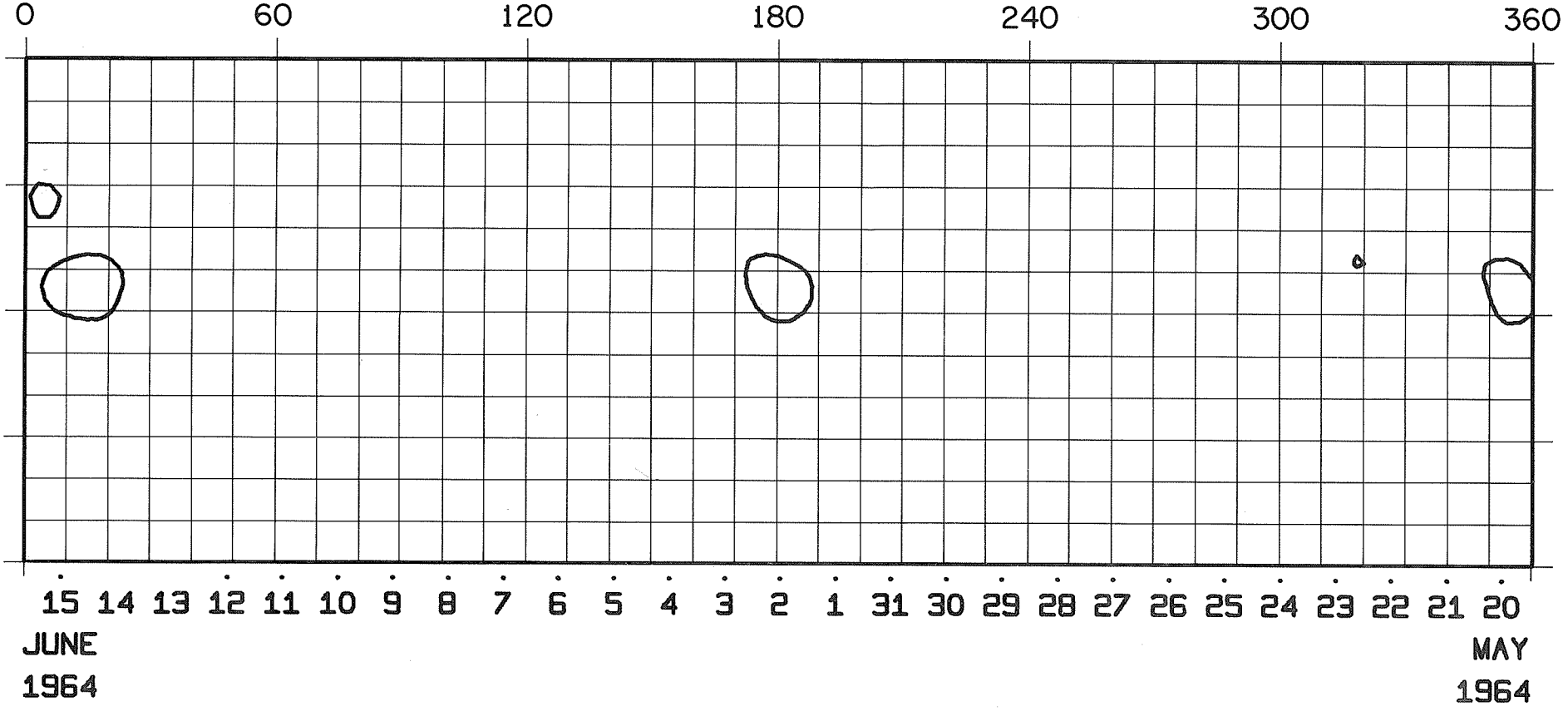

ROTATION NUMBER 1482

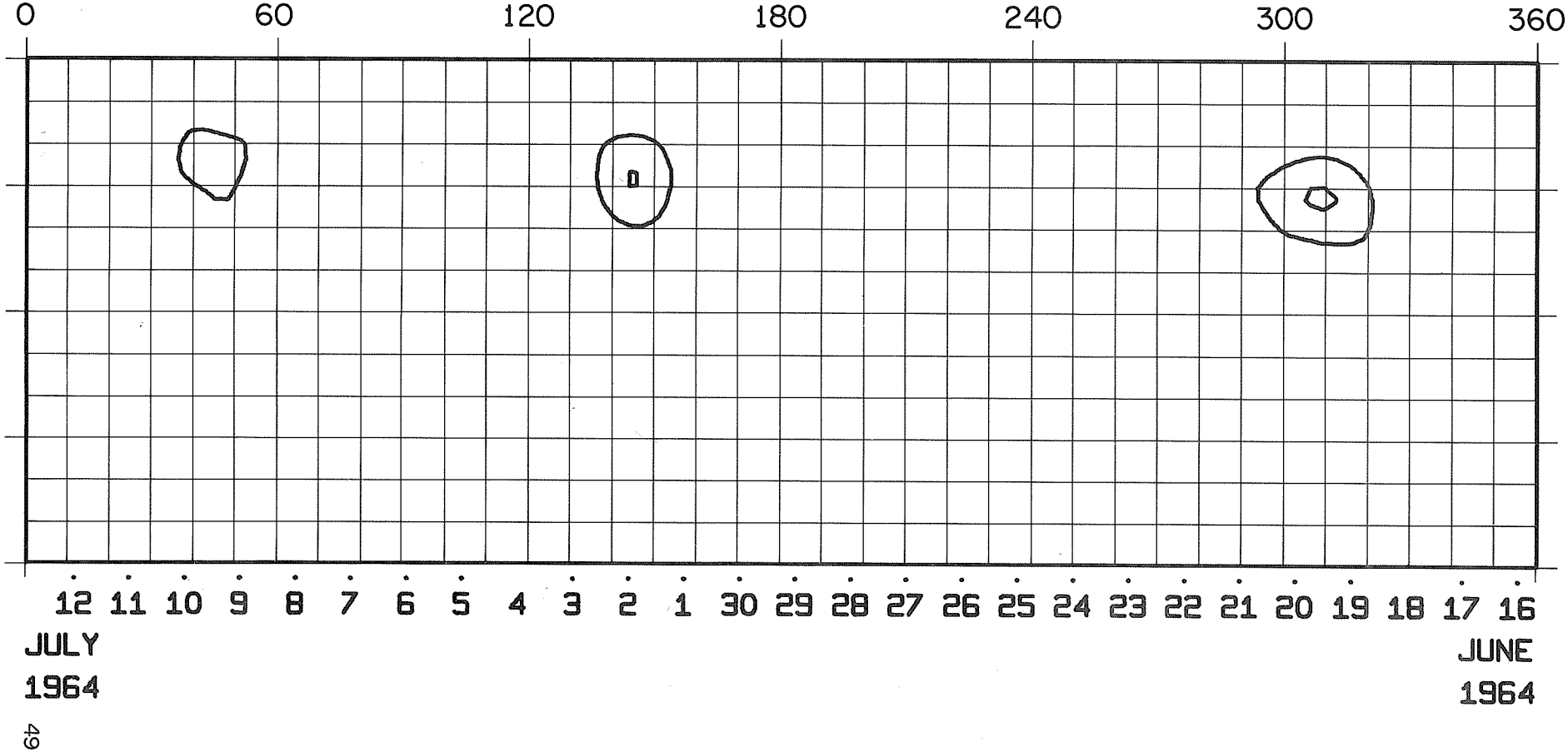

ROTATION NUMBER 1483

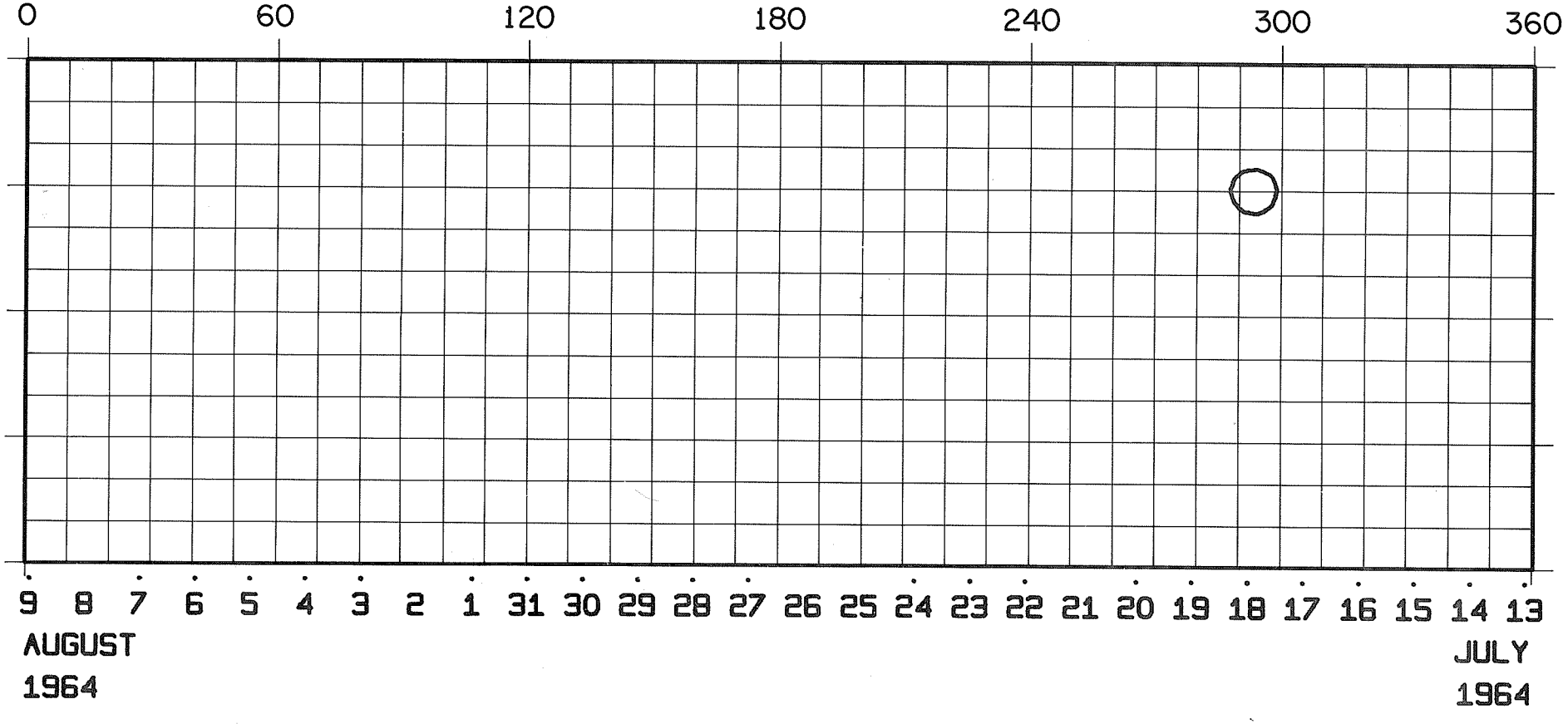

ROTATION NUMBER 1484

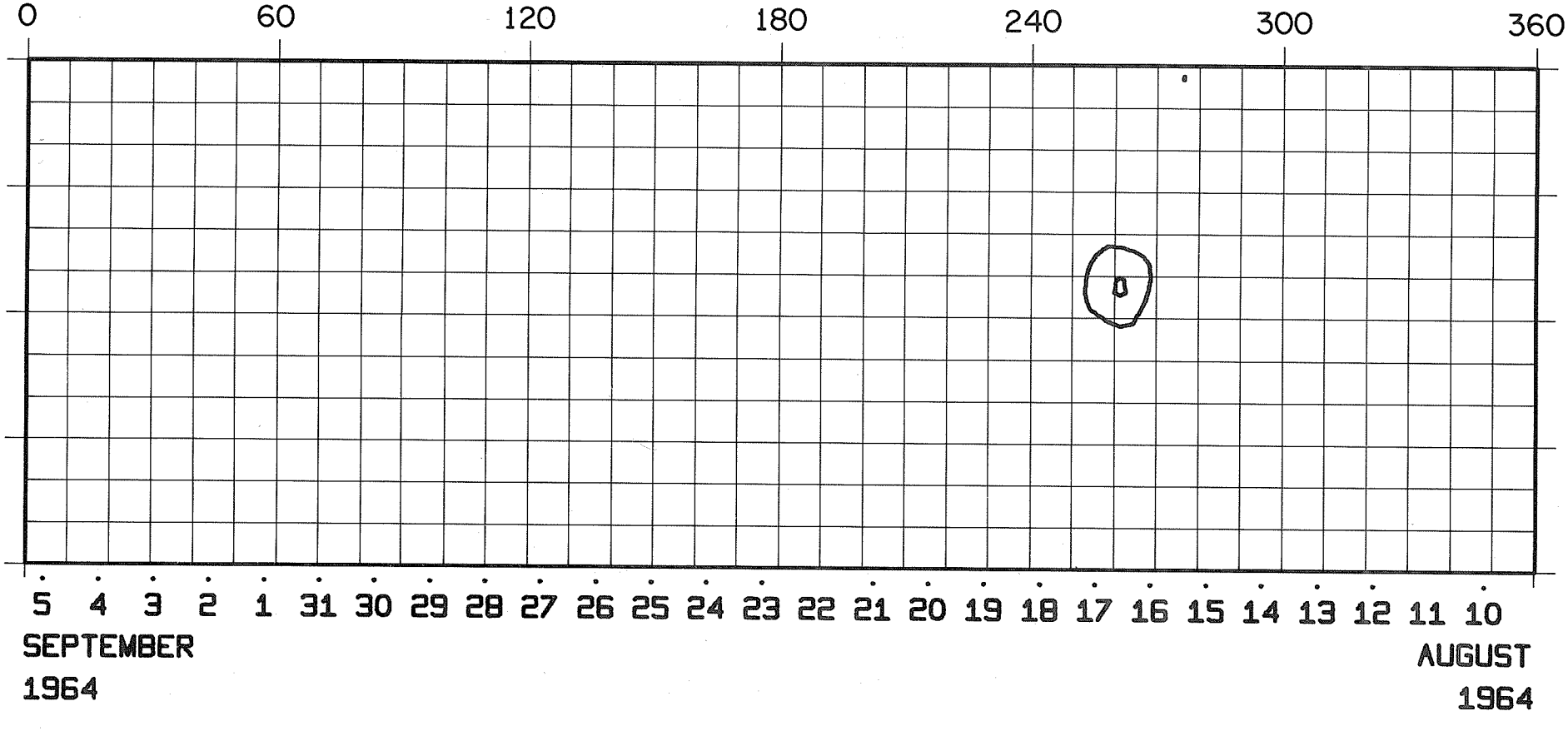

ROTATION NUMBER 1485

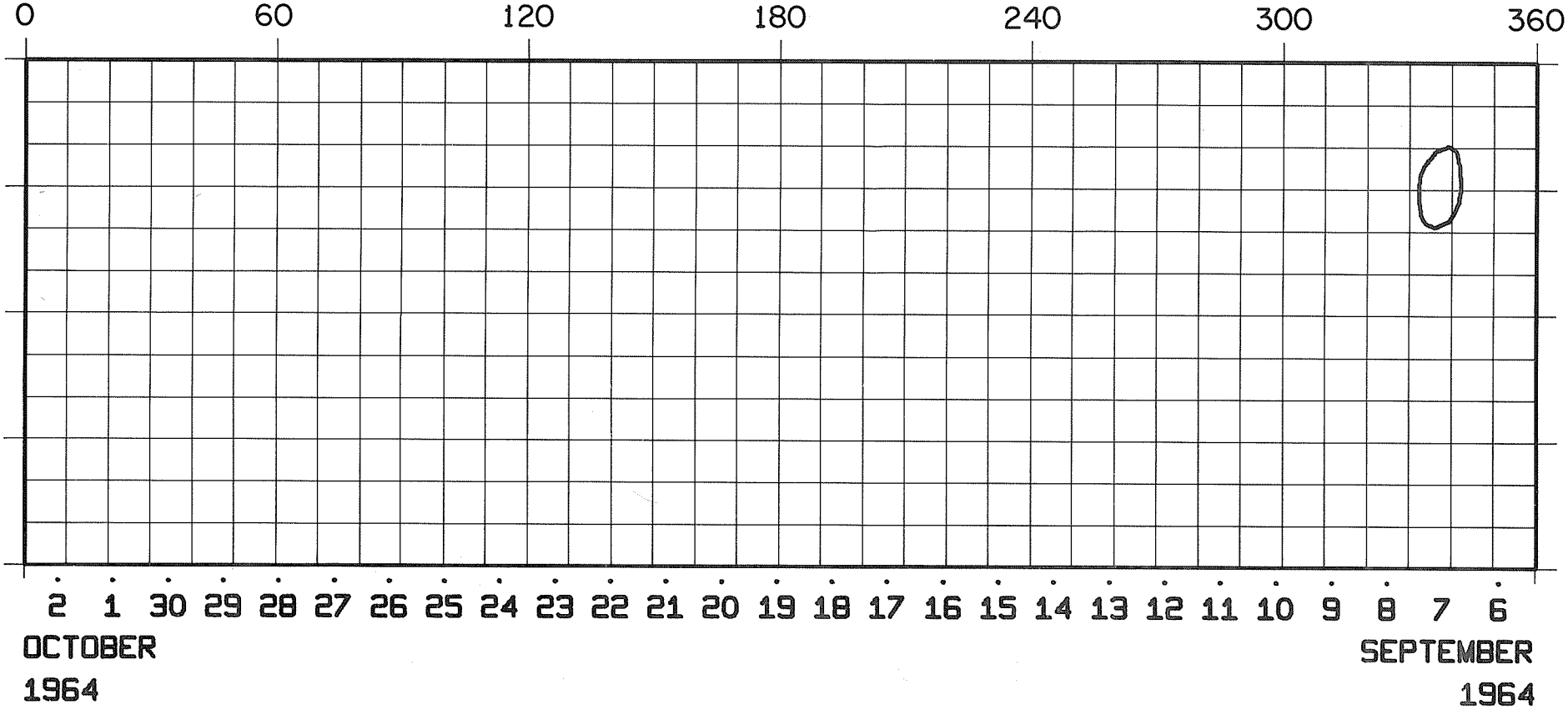

ROTATION NUMBER 1486

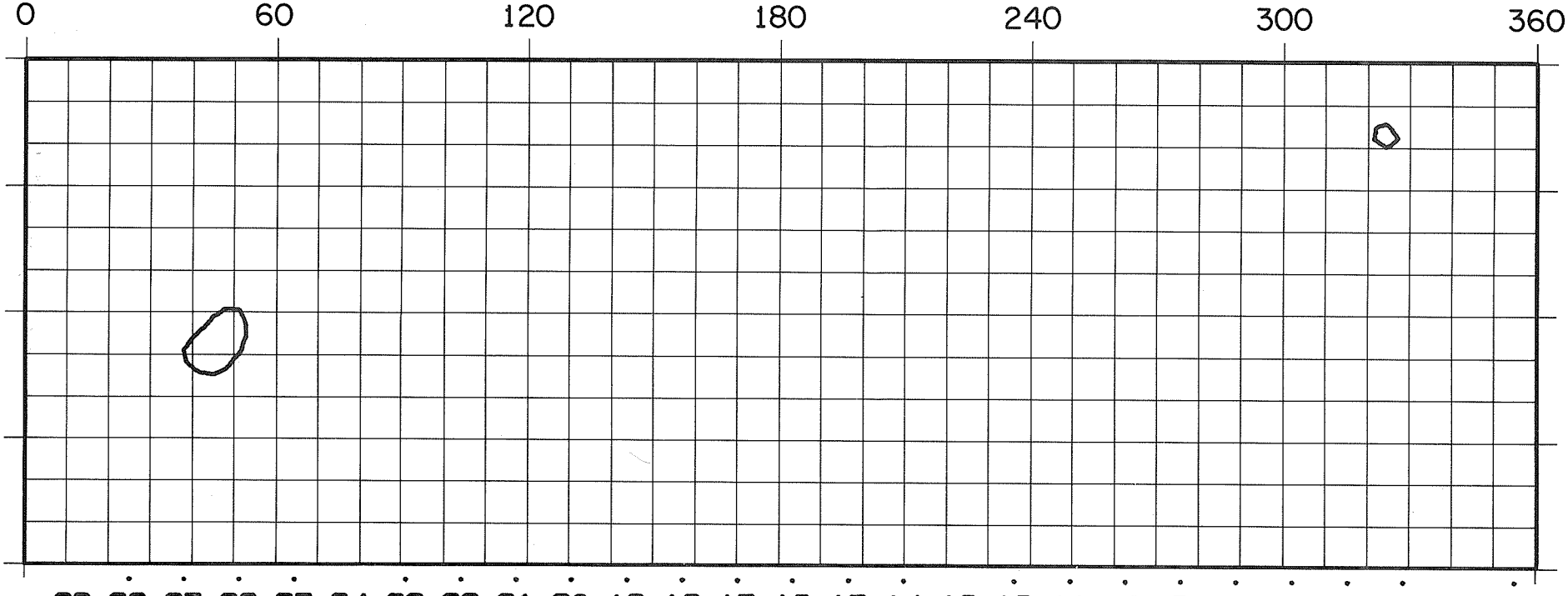

ROTATION NUMBER 1487

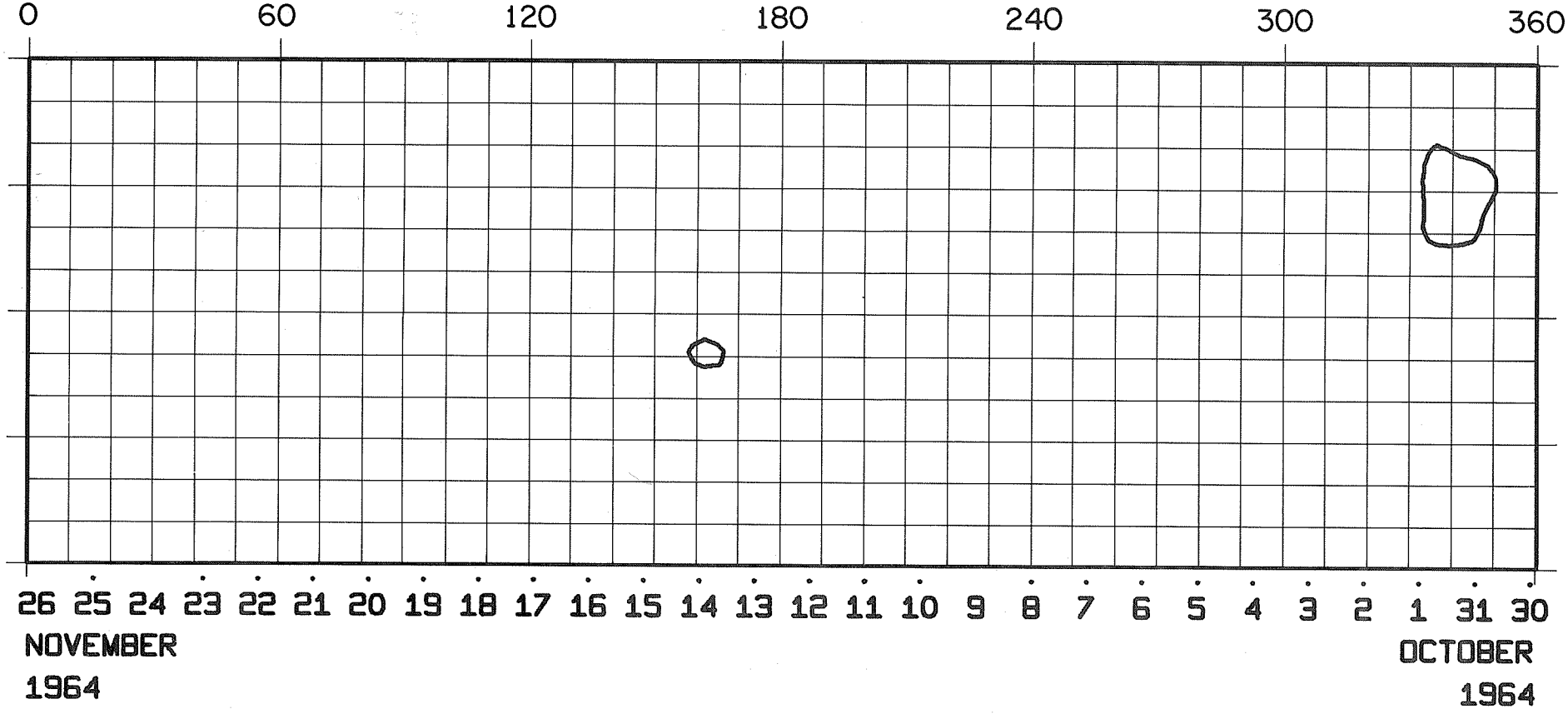

ROTATION NUMBER 1488

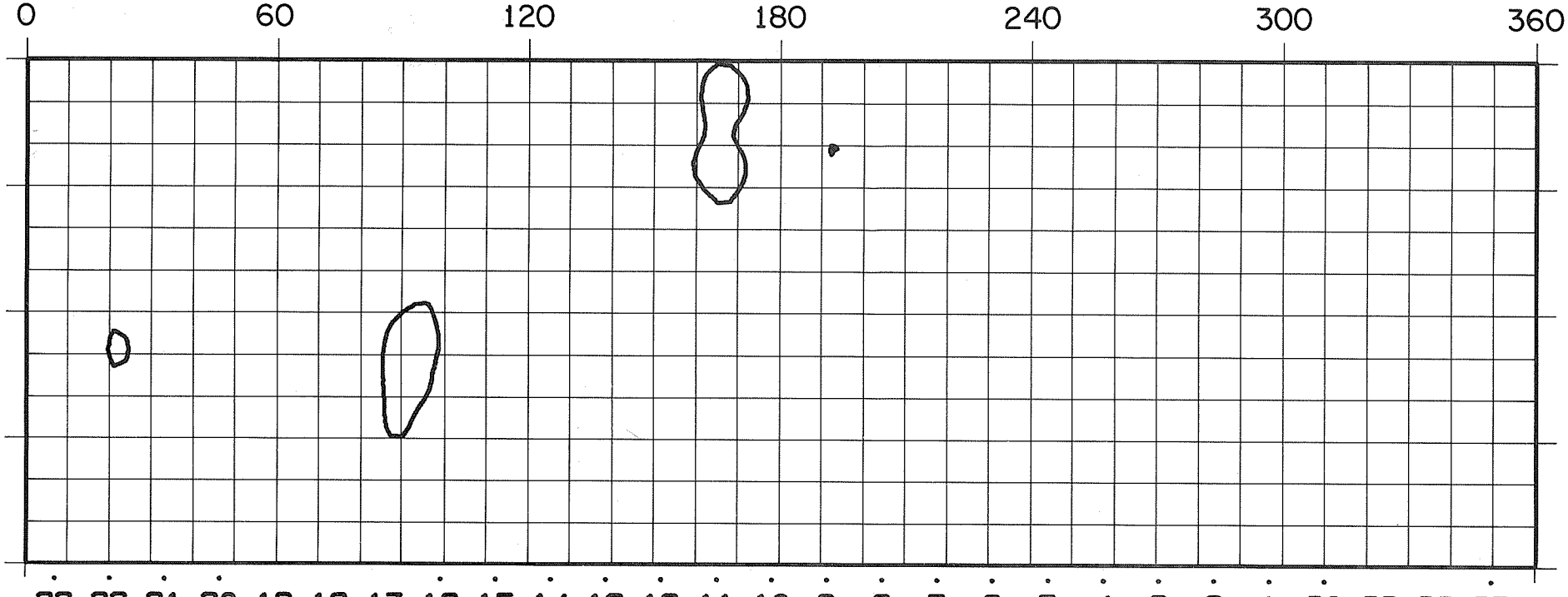

ROTATION NUMBER 1489

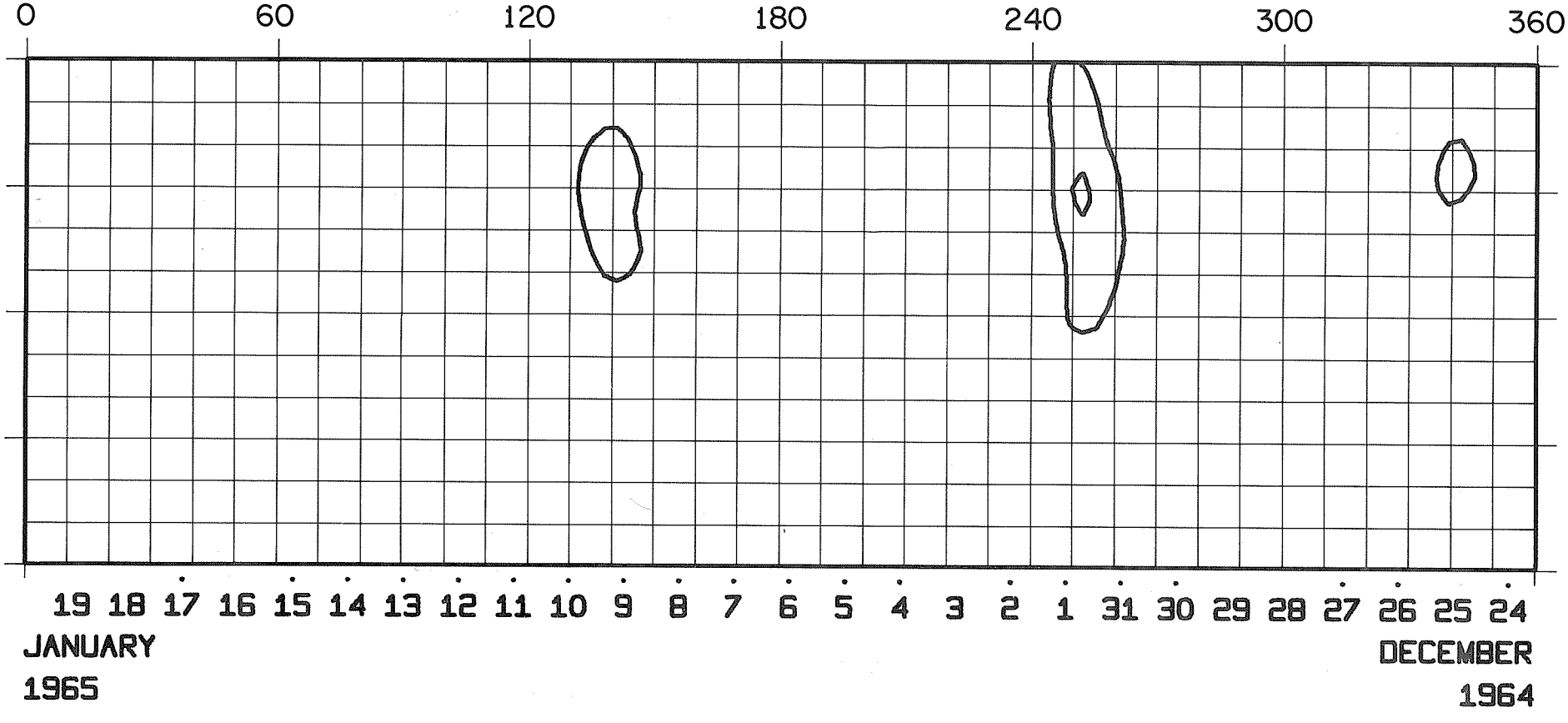

ROTATION NUMBER 1490

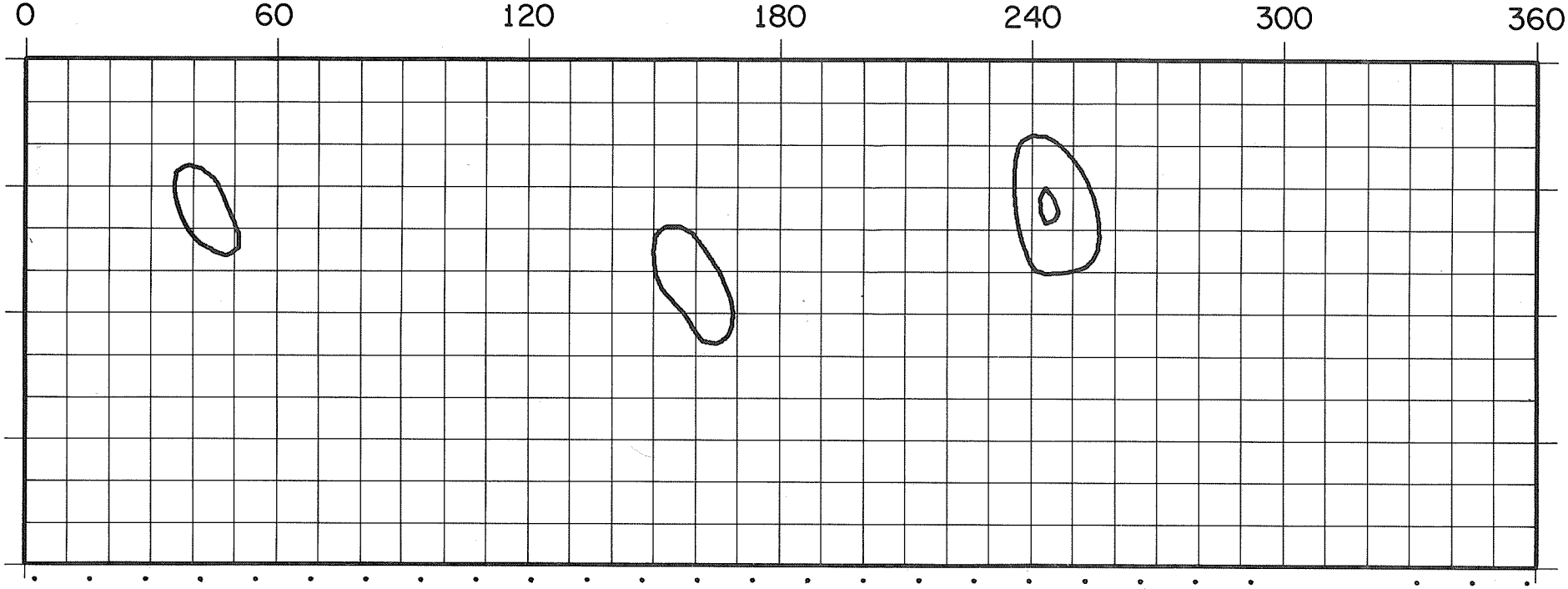

ROTATION NUMBER 1491

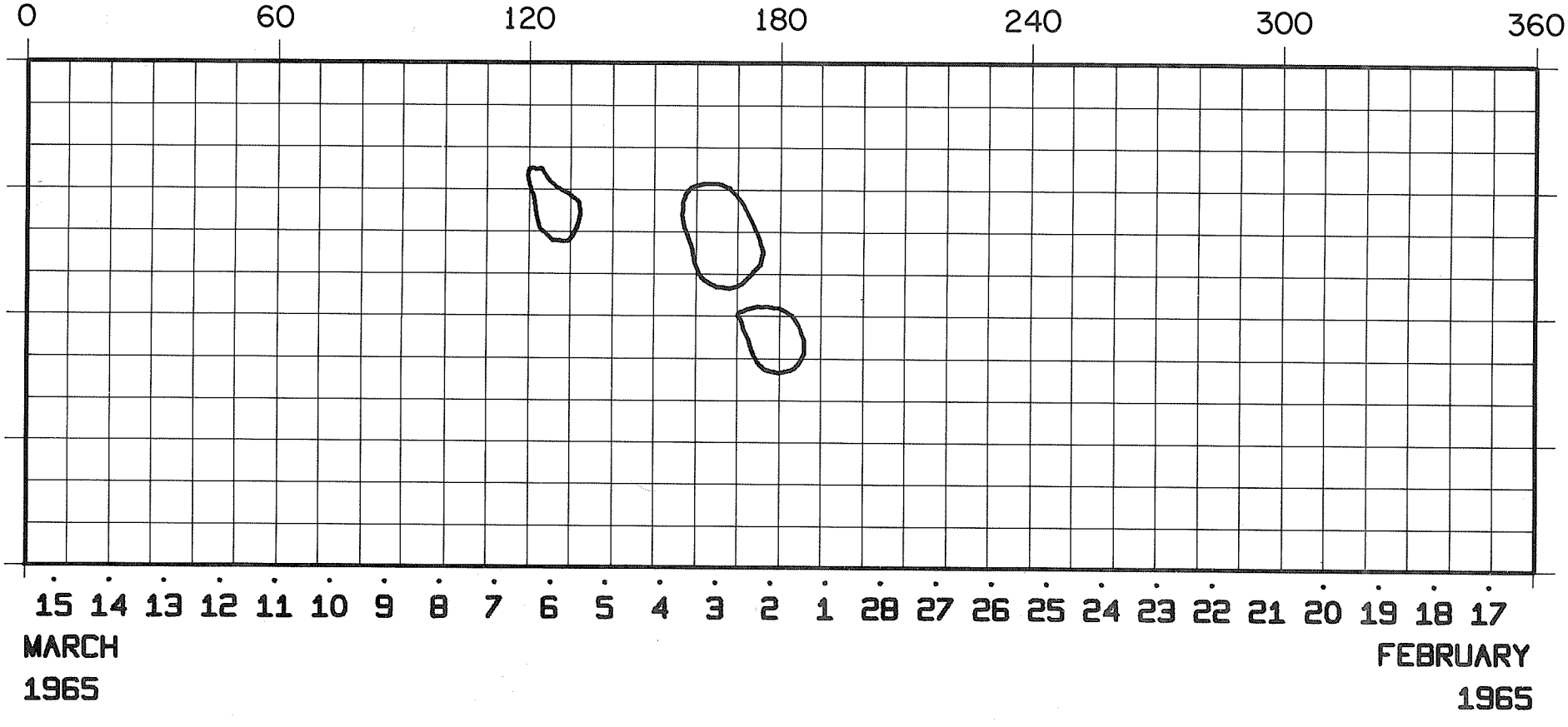

ROTATION NUMBER 1492

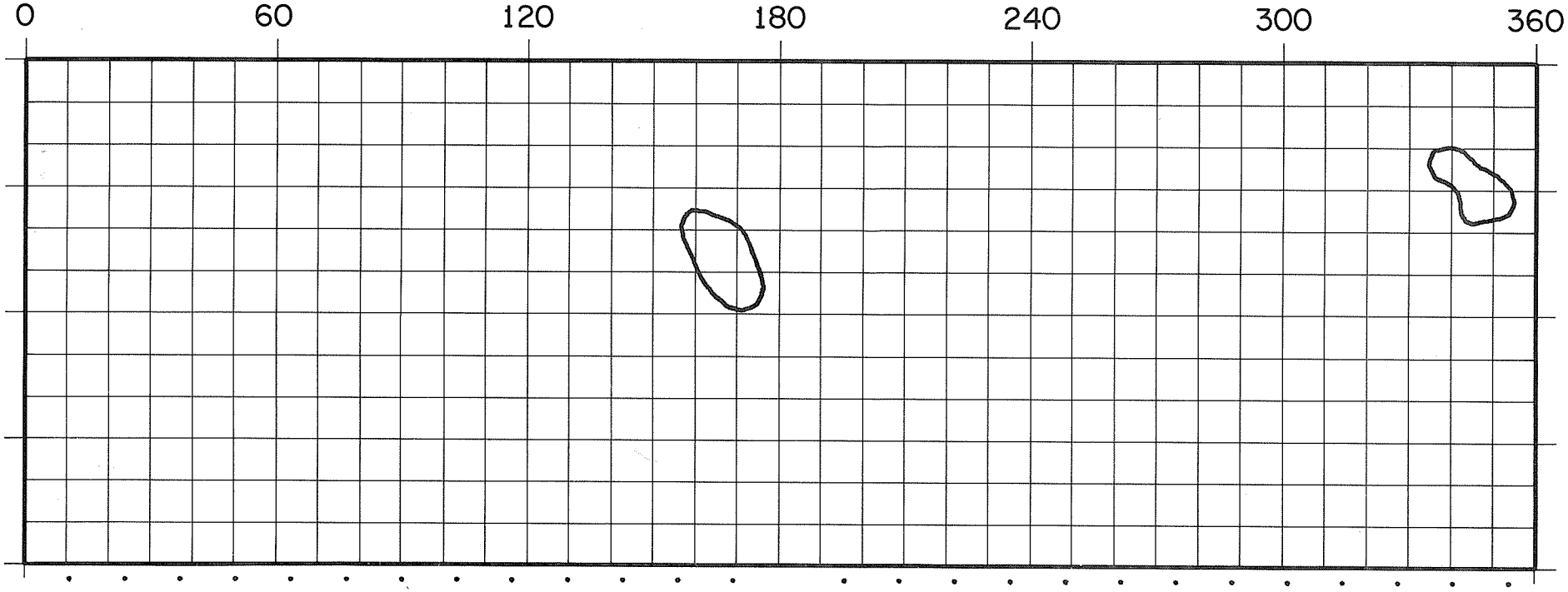

ROTATION NUMBER 1493

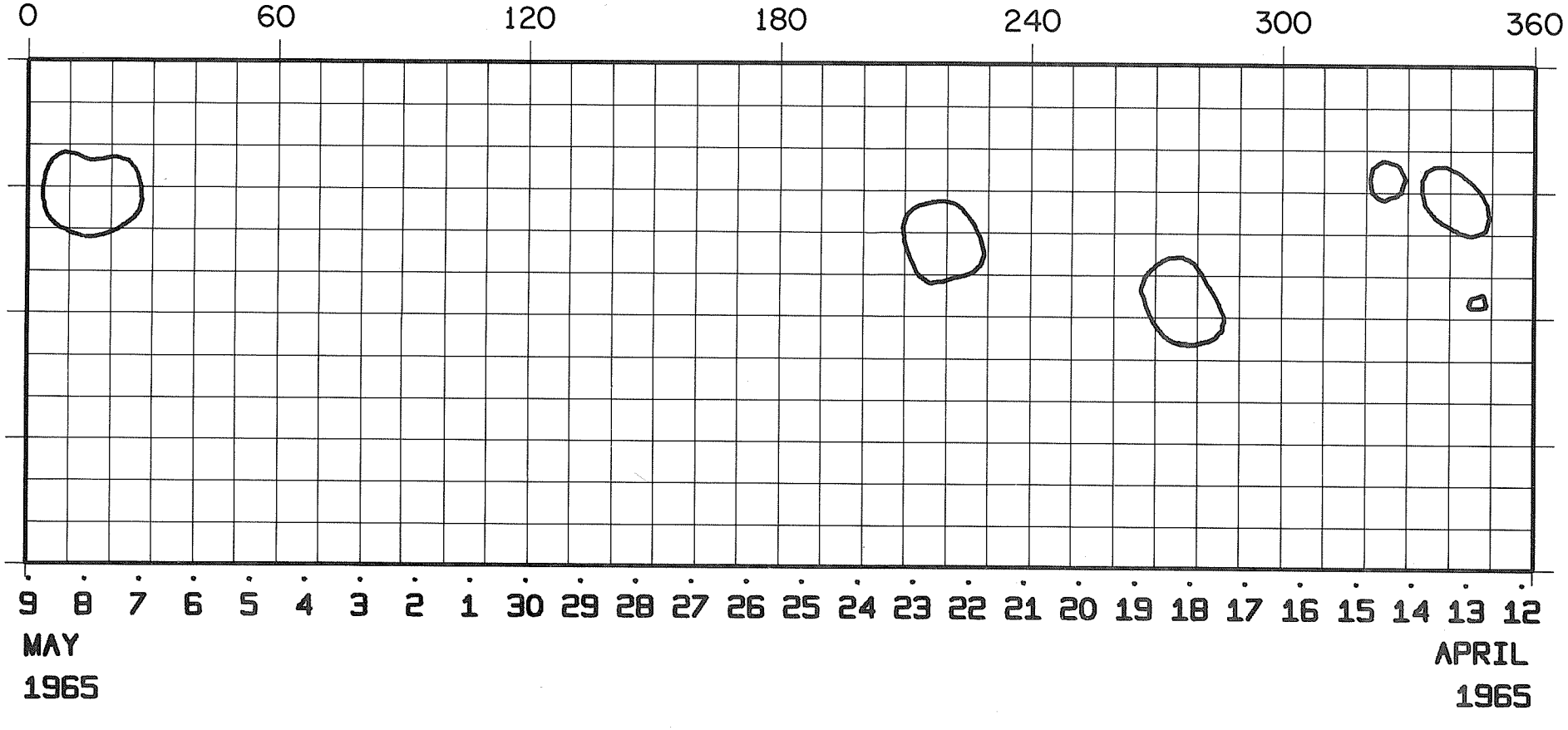

ROTATION NUMBER 1494

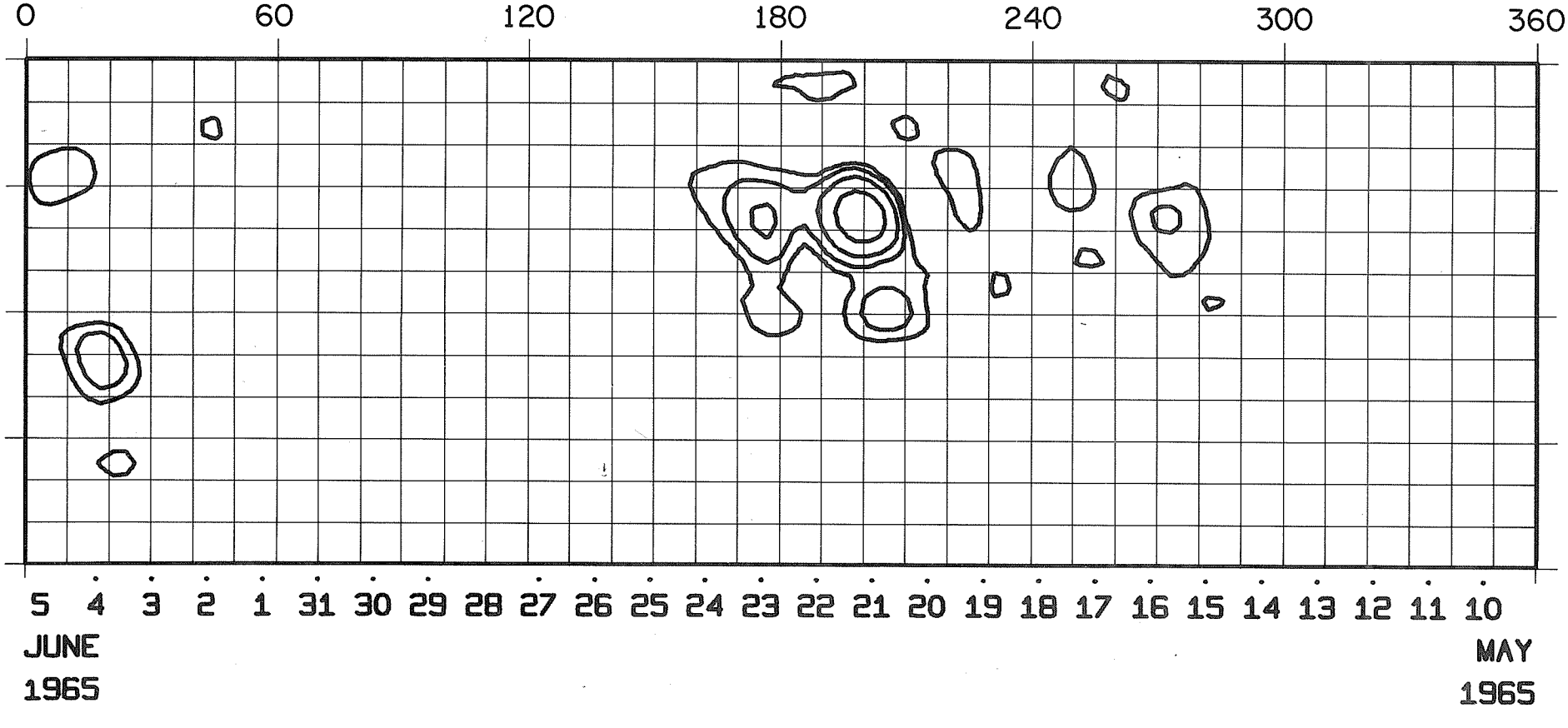

ROTATION NUMBER 1495

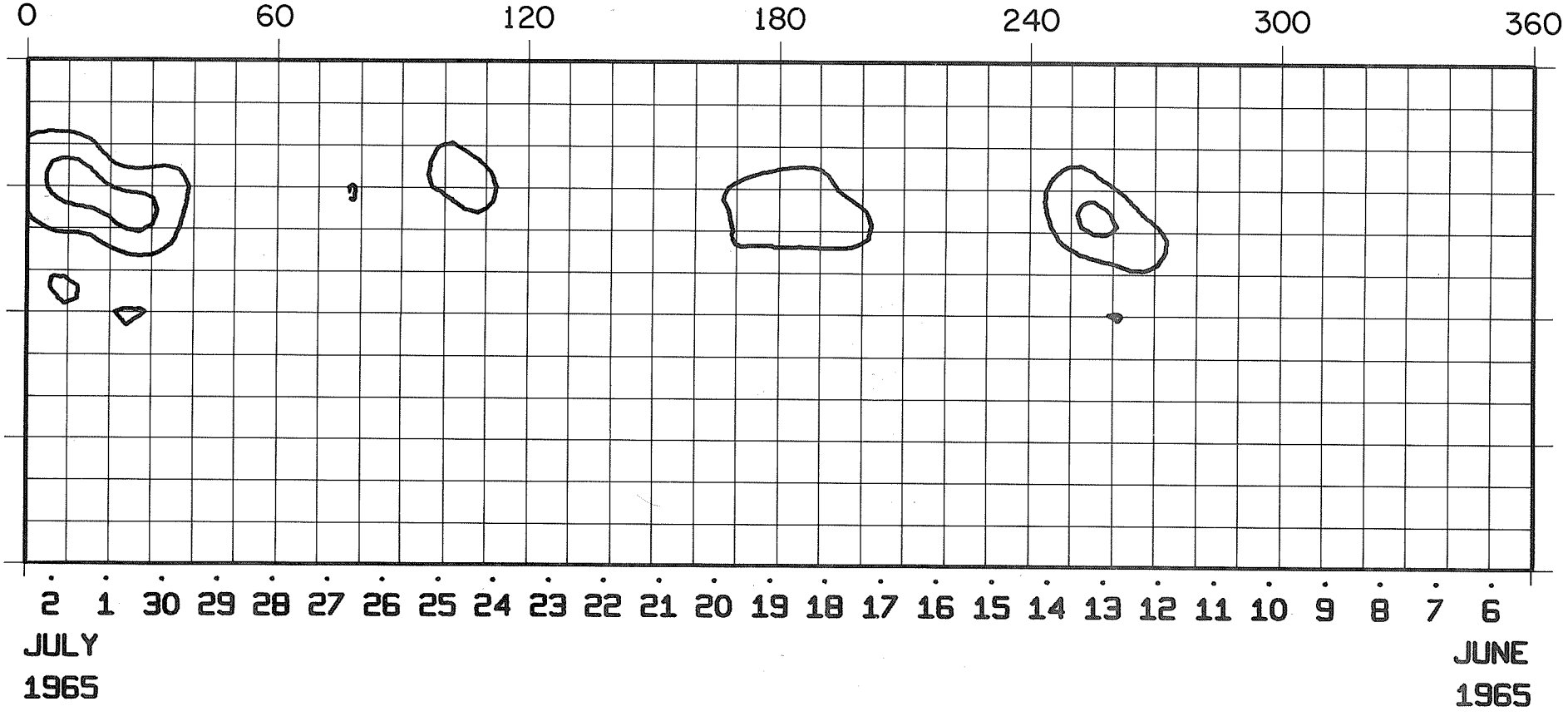

ROTATION NUMBER 1496

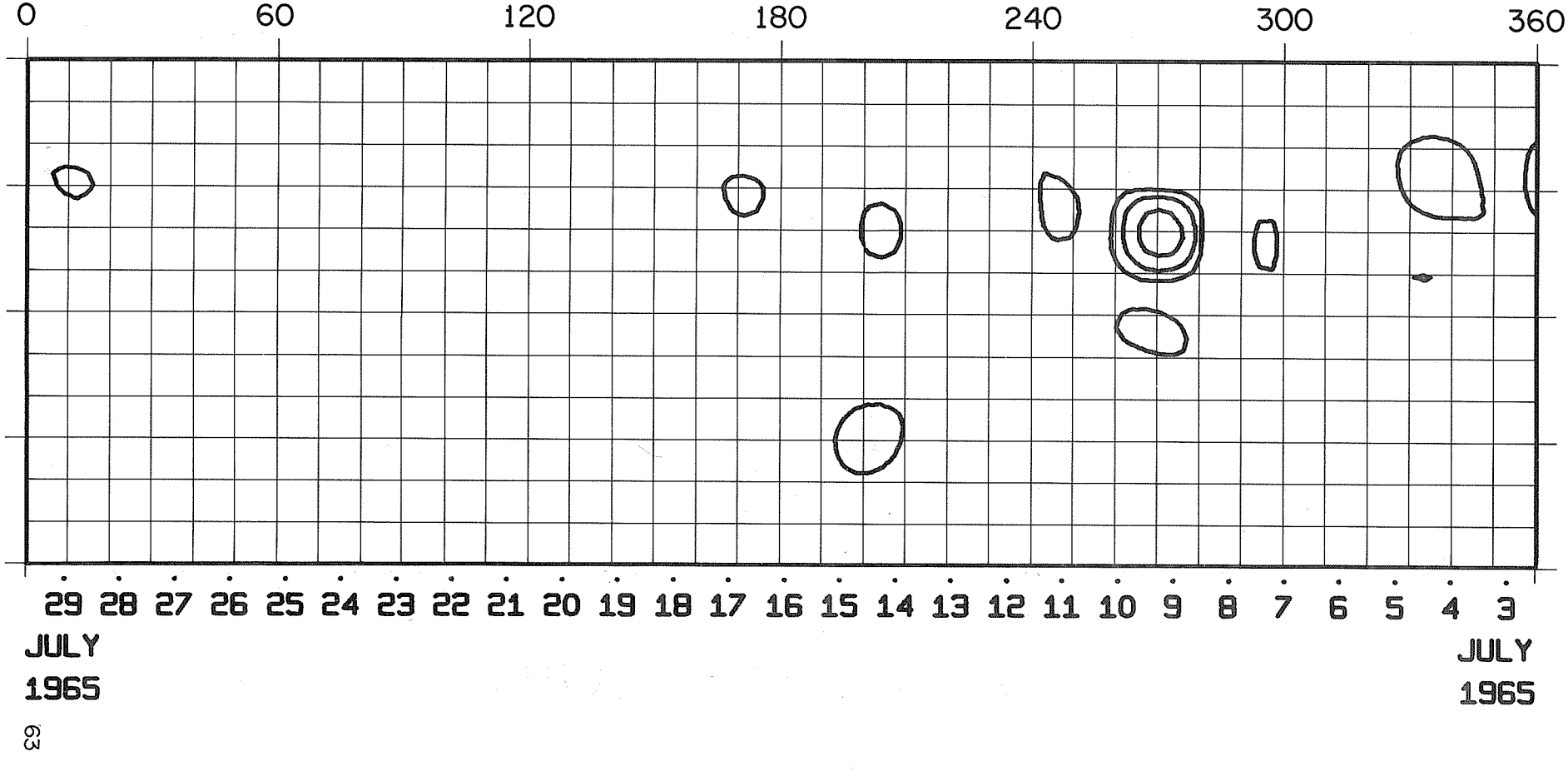

ROTATION NUMBER 1497

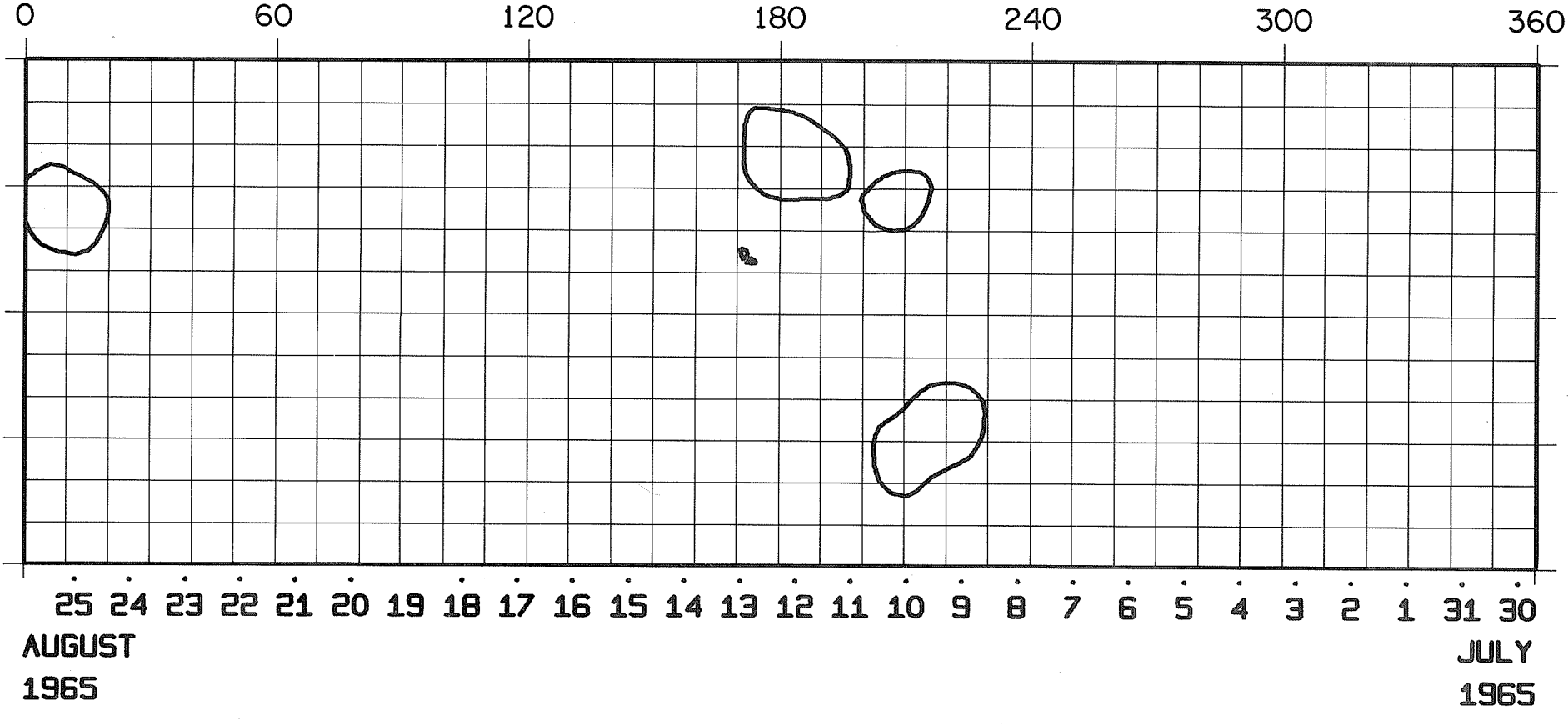

ROTATION NUMBER 1498

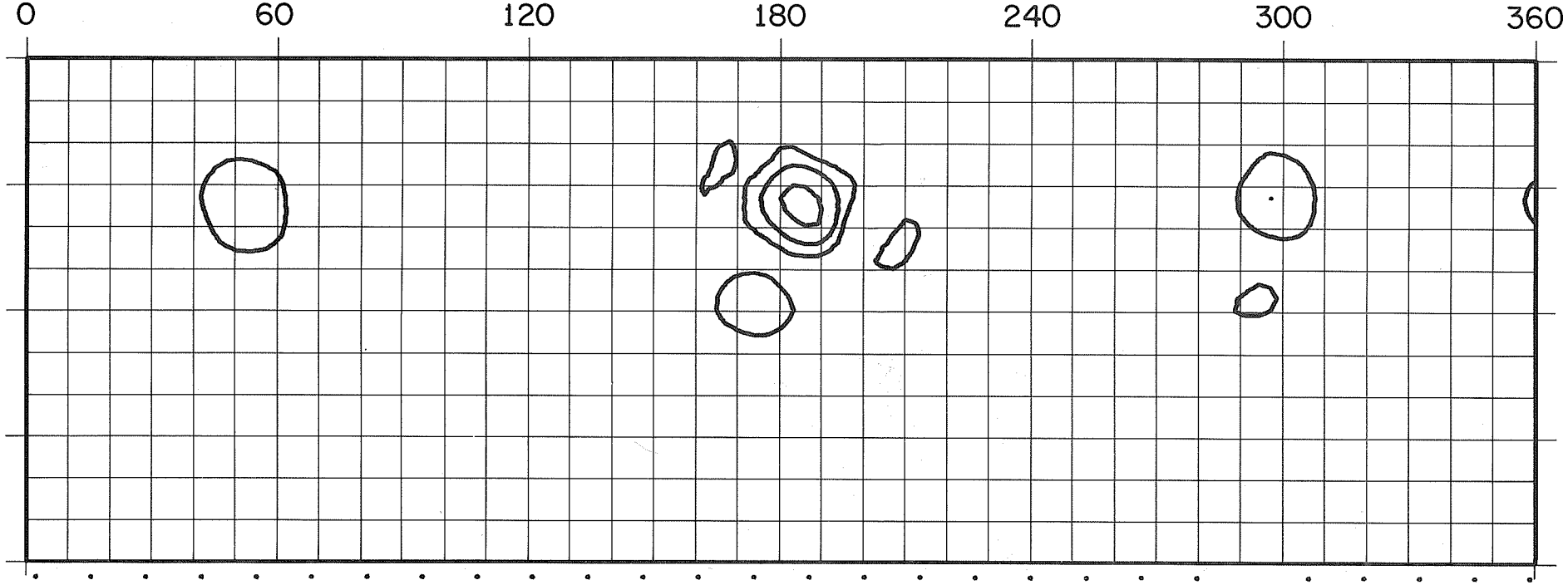

ROTATION NUMBER 1499

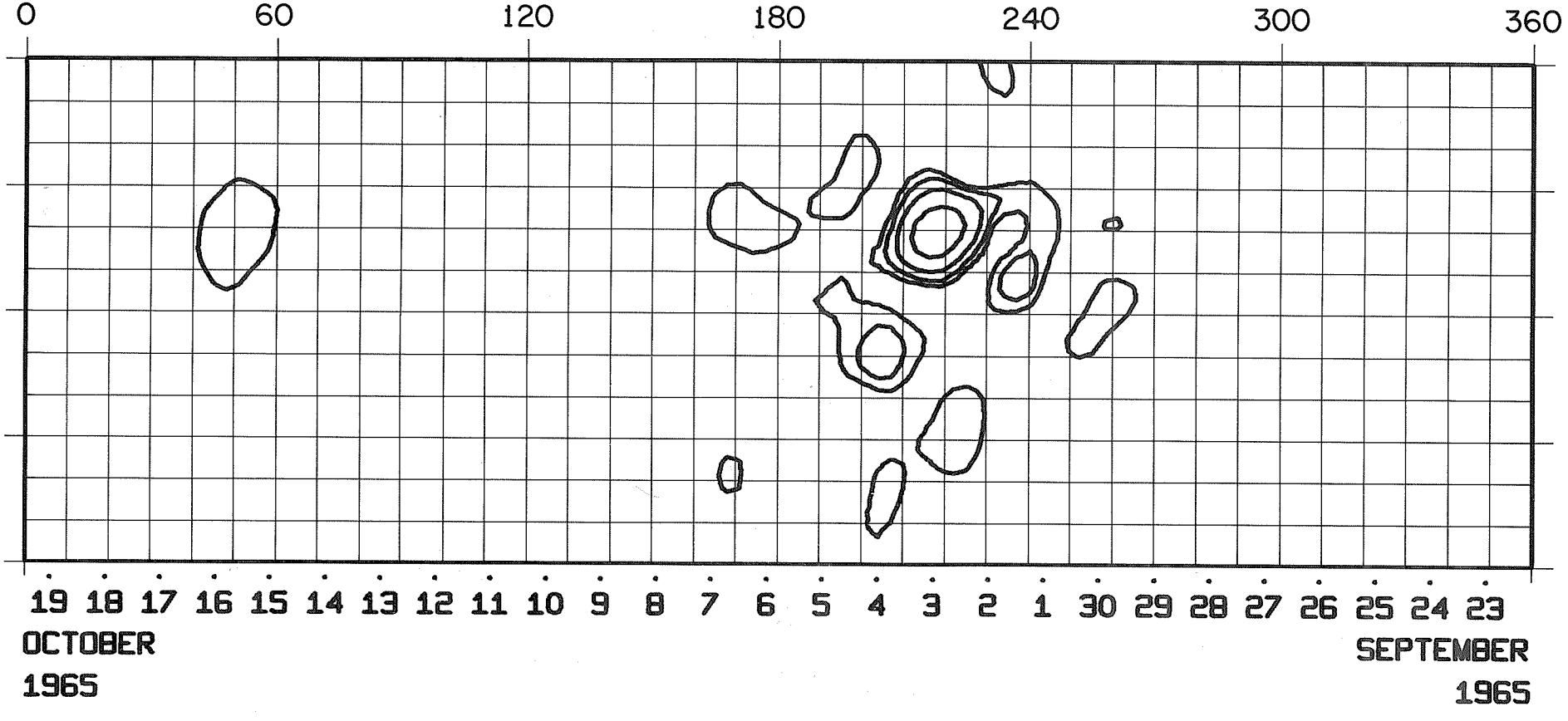

ROTATION NUMBER 1500

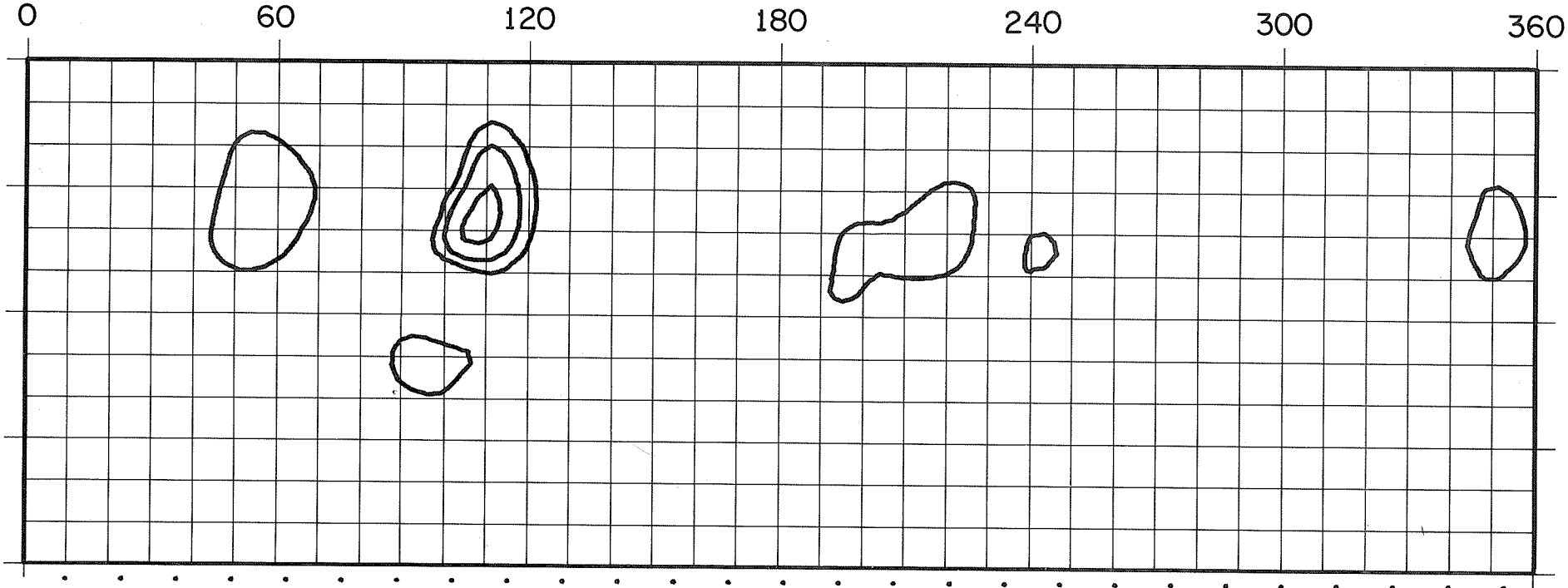

ROTATION NUMBER 1501

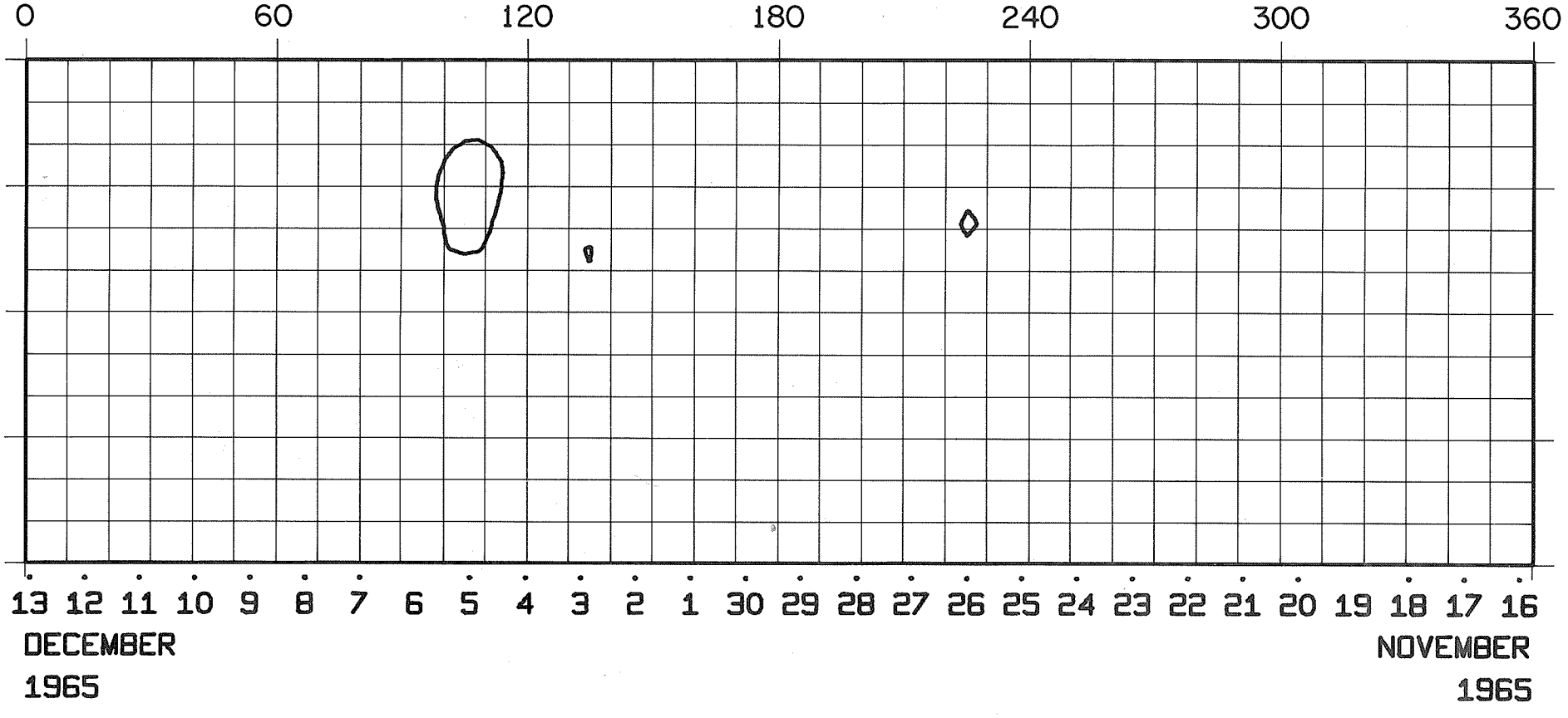

ROTATION NUMBER 1502

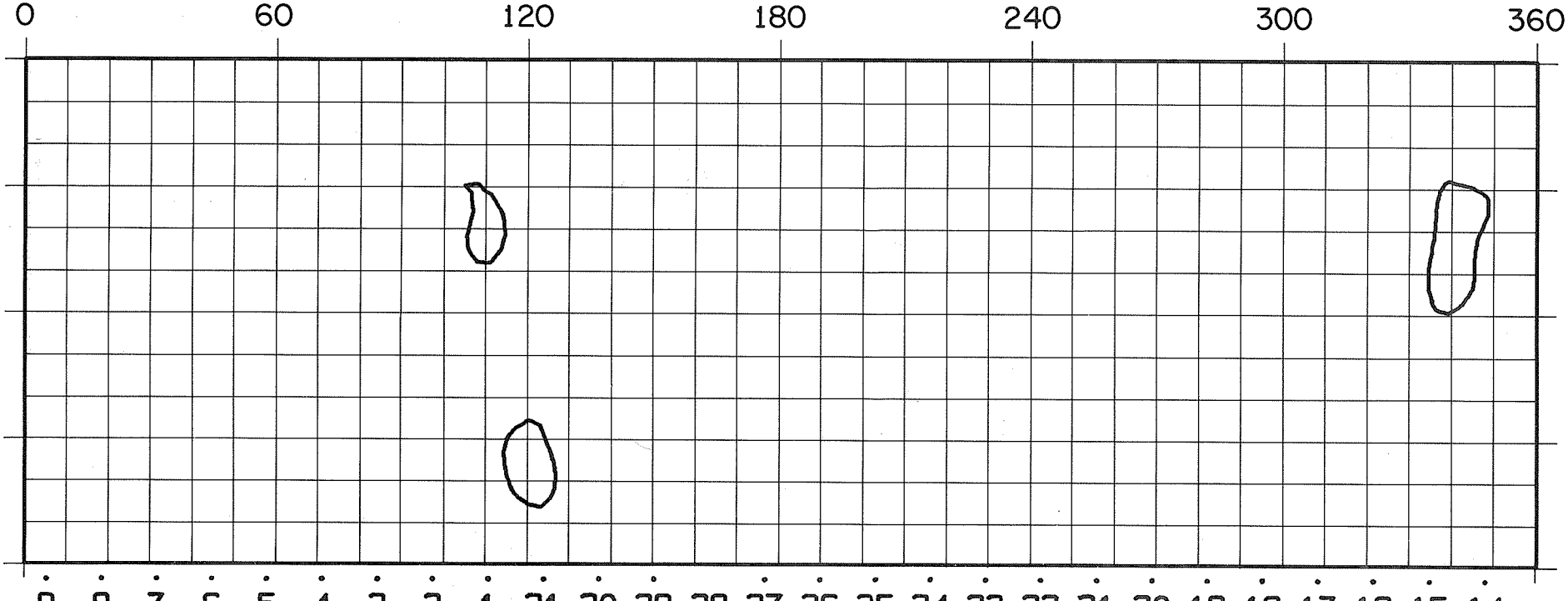

ROTATION NUMBER 1503

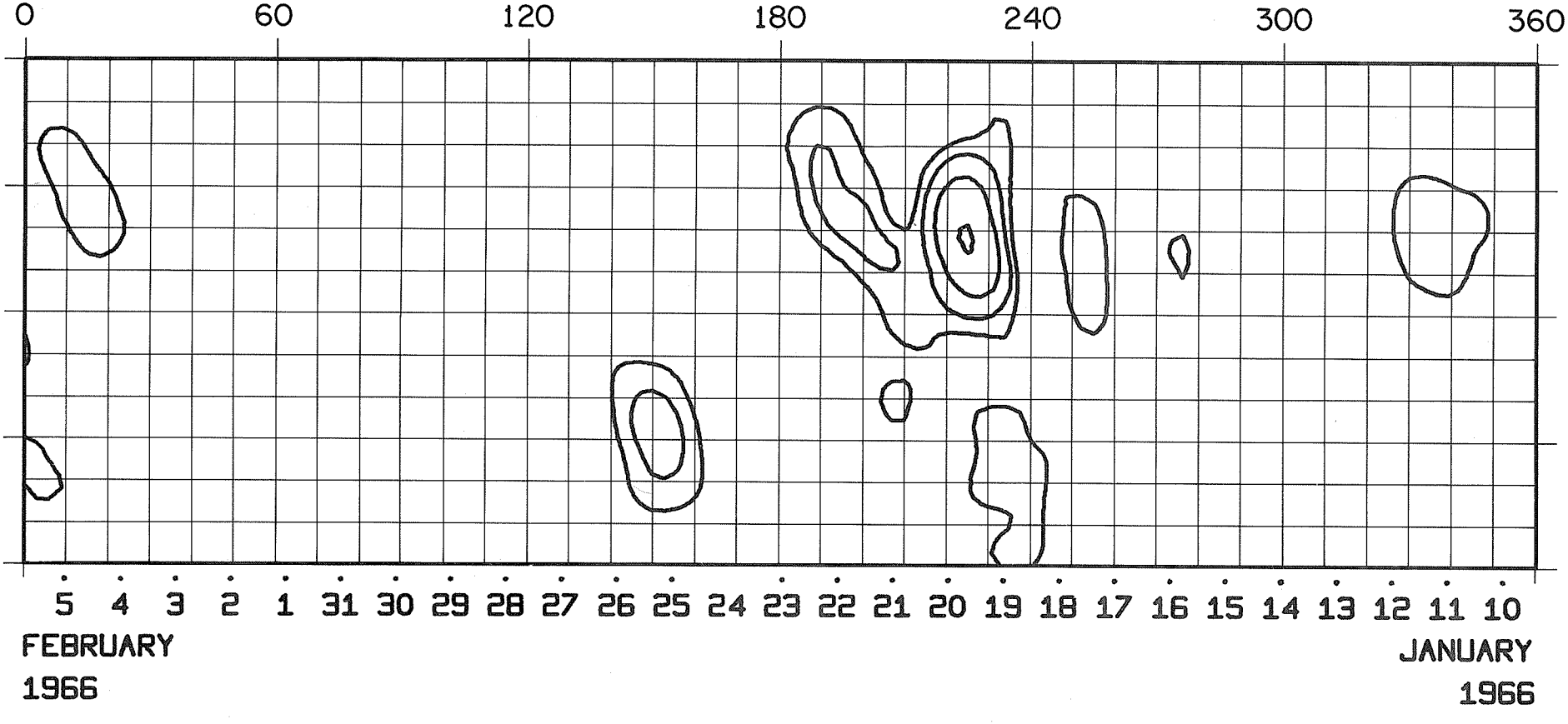

ROTATION NUMBER 1504

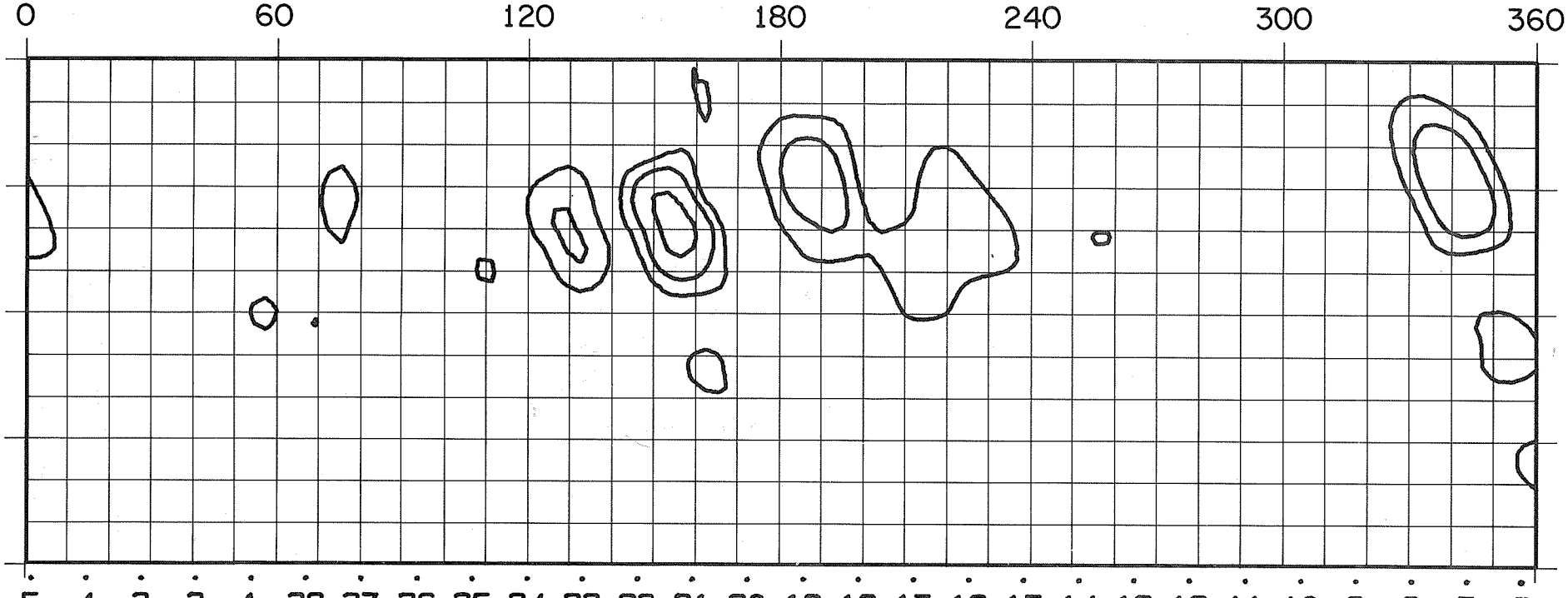

ROTATION NUMBER 1505

ROTATION NUMBER 1506

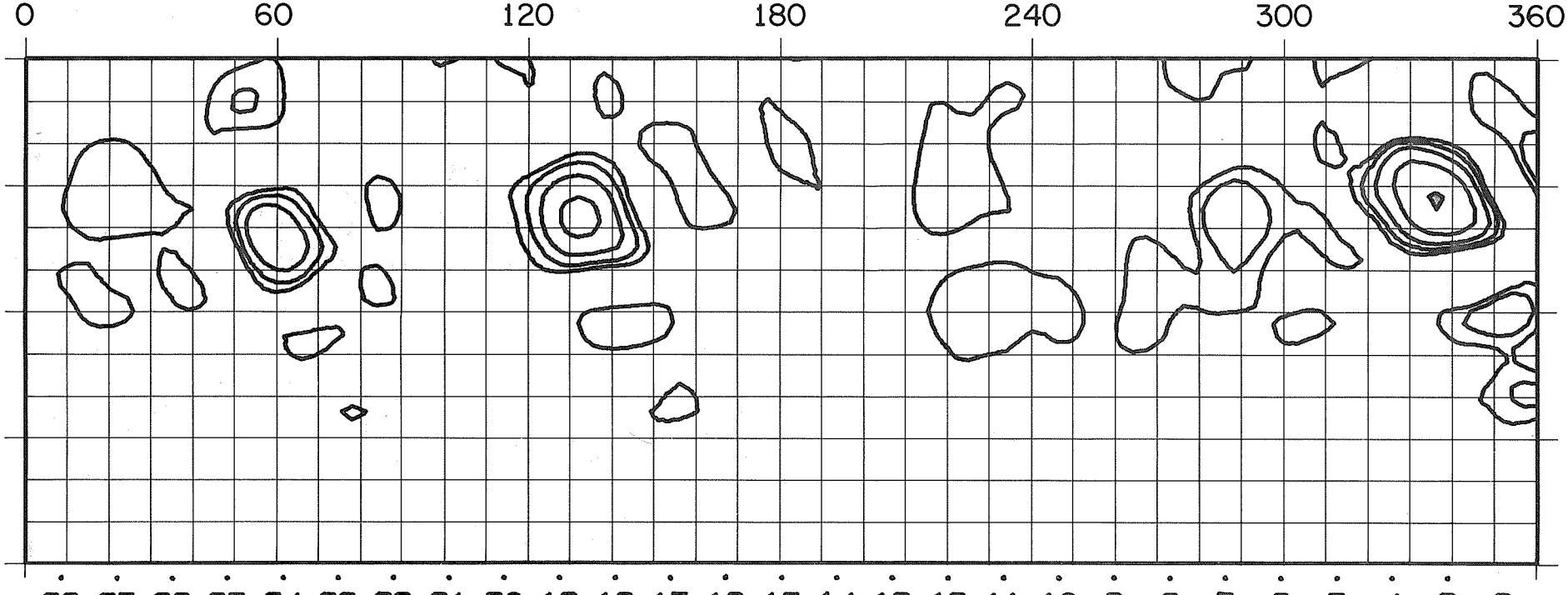

ROTATION NUMBER 1507

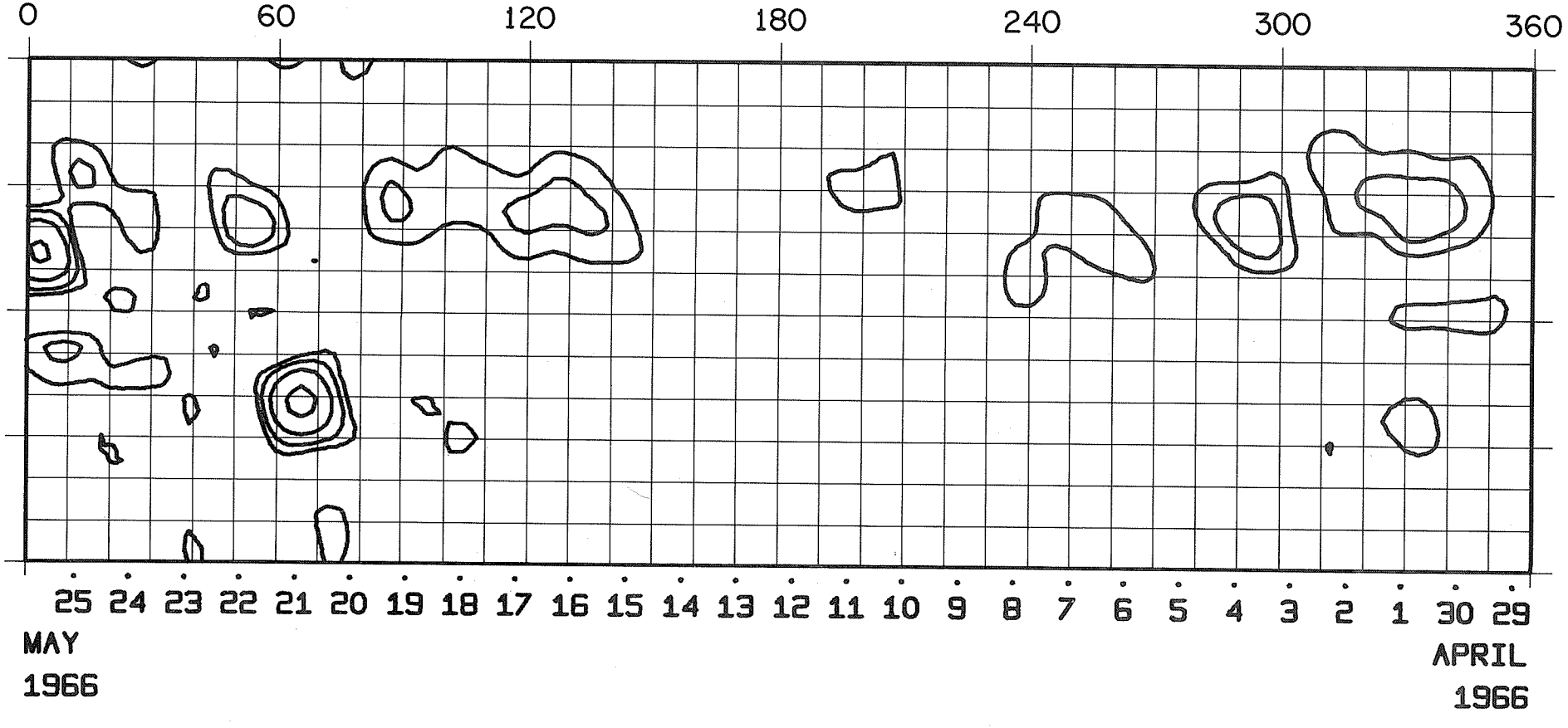

ROTATION NUMBER 1508

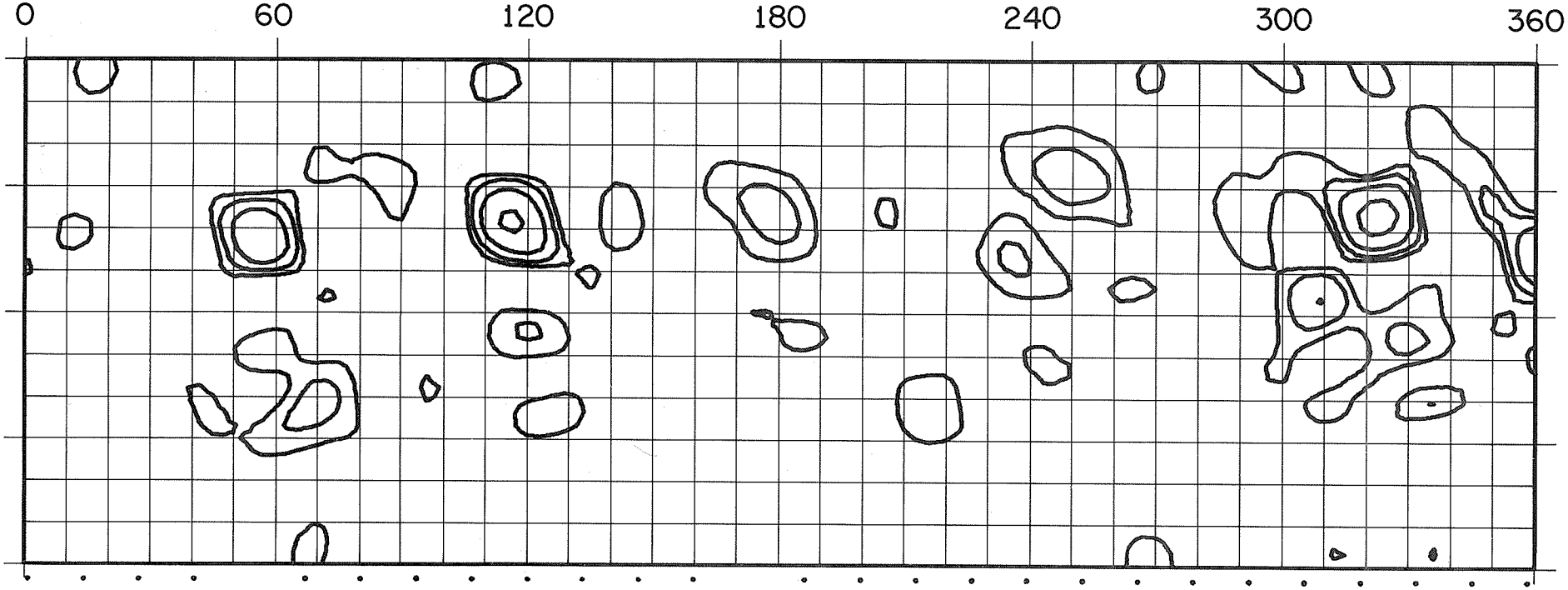

ROTATION NUMBER 1509

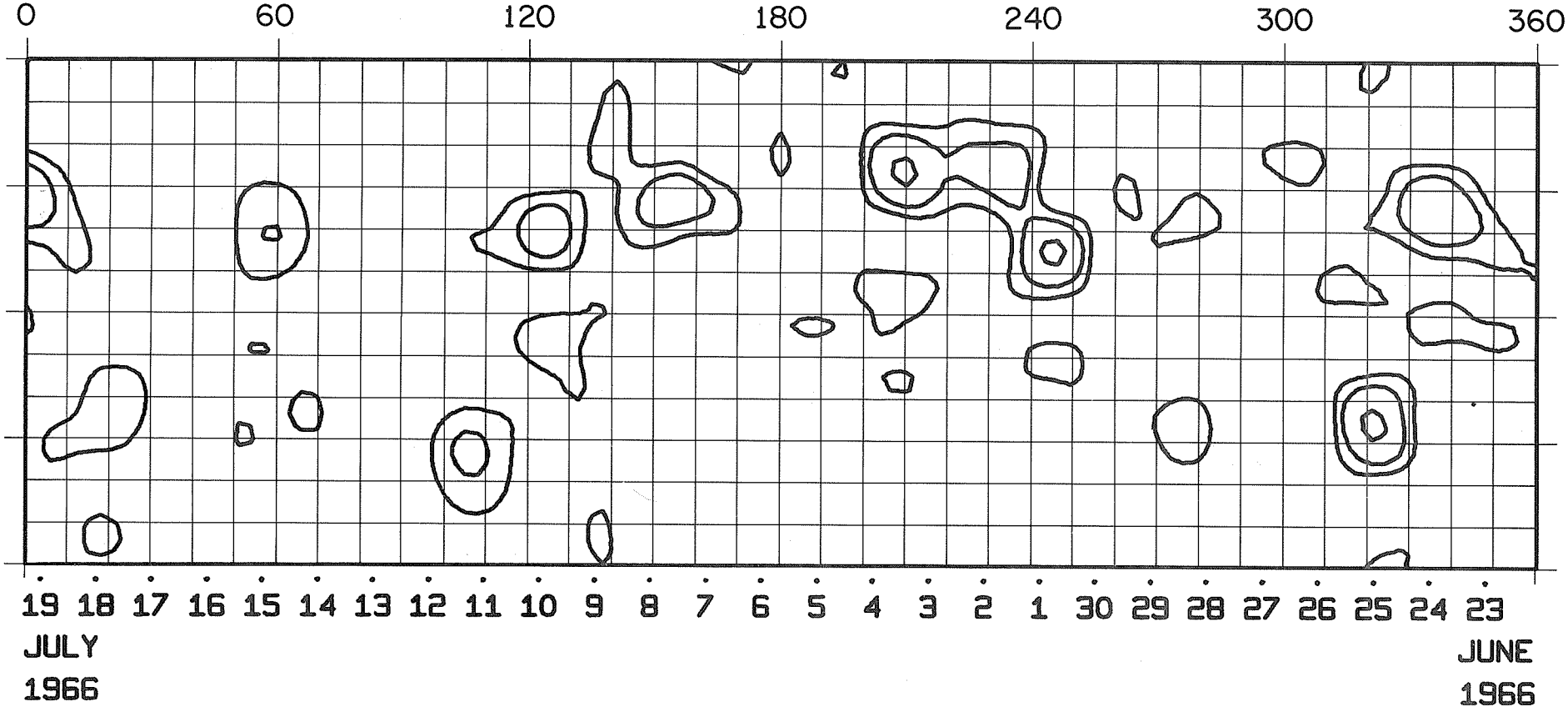

ROTATION NUMBER 1510

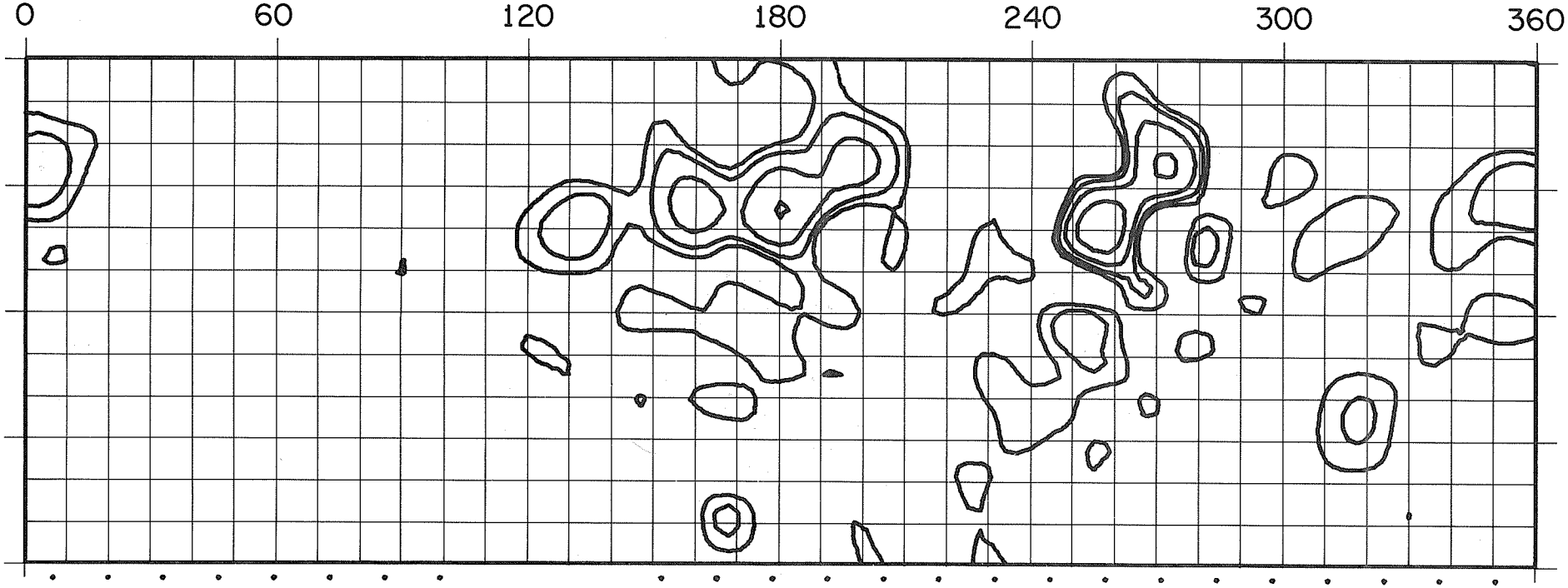

ROTATION NUMBER 1511
0
60
120
180
240
300
360
11 10 9 8 7 6 5 4 3 2 1 31 30 29 28 27 26 25 24 23 22 21 20 19 18 17 16
SEPTEMBER
1966
AUGUST
1966

ROTATION NUMBER 1512

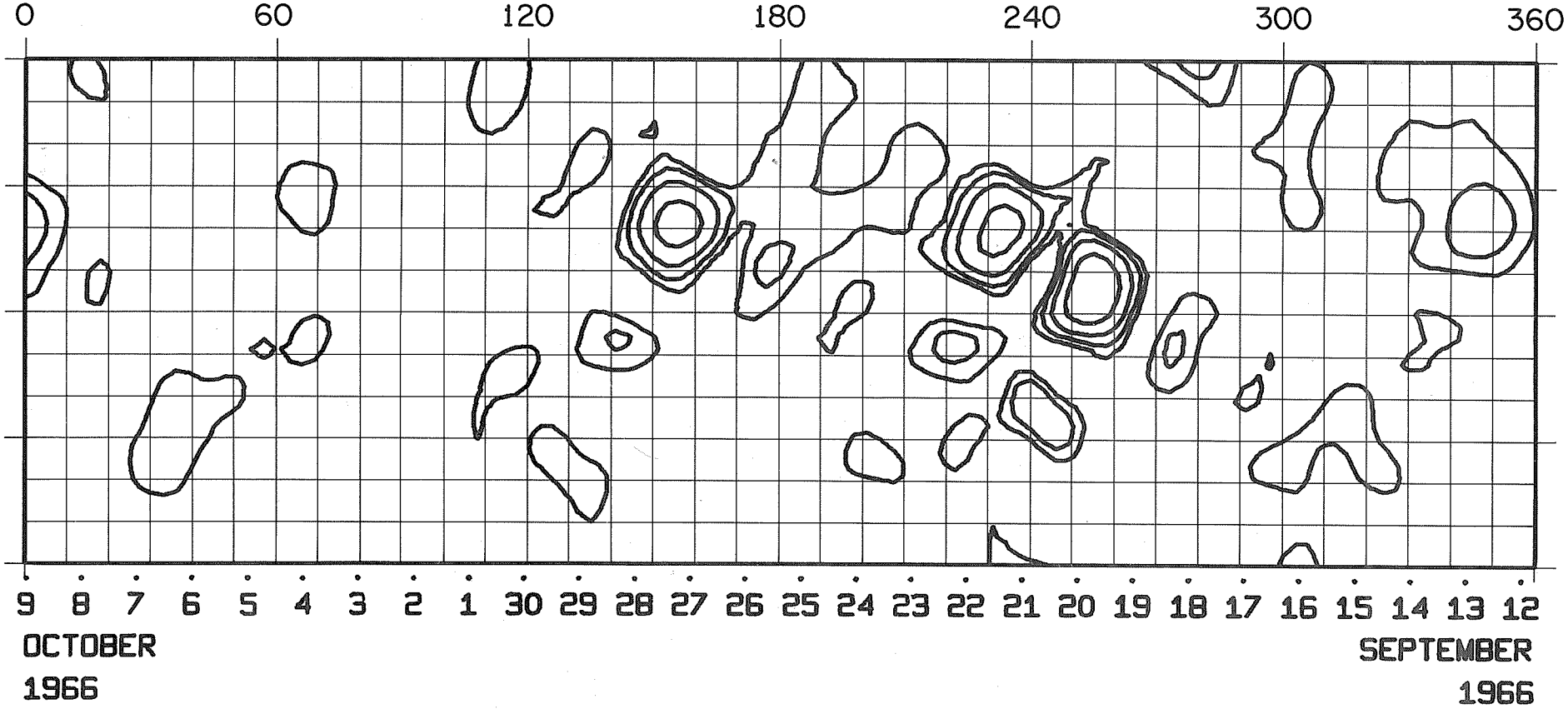

ROTATION NUMBER 1513

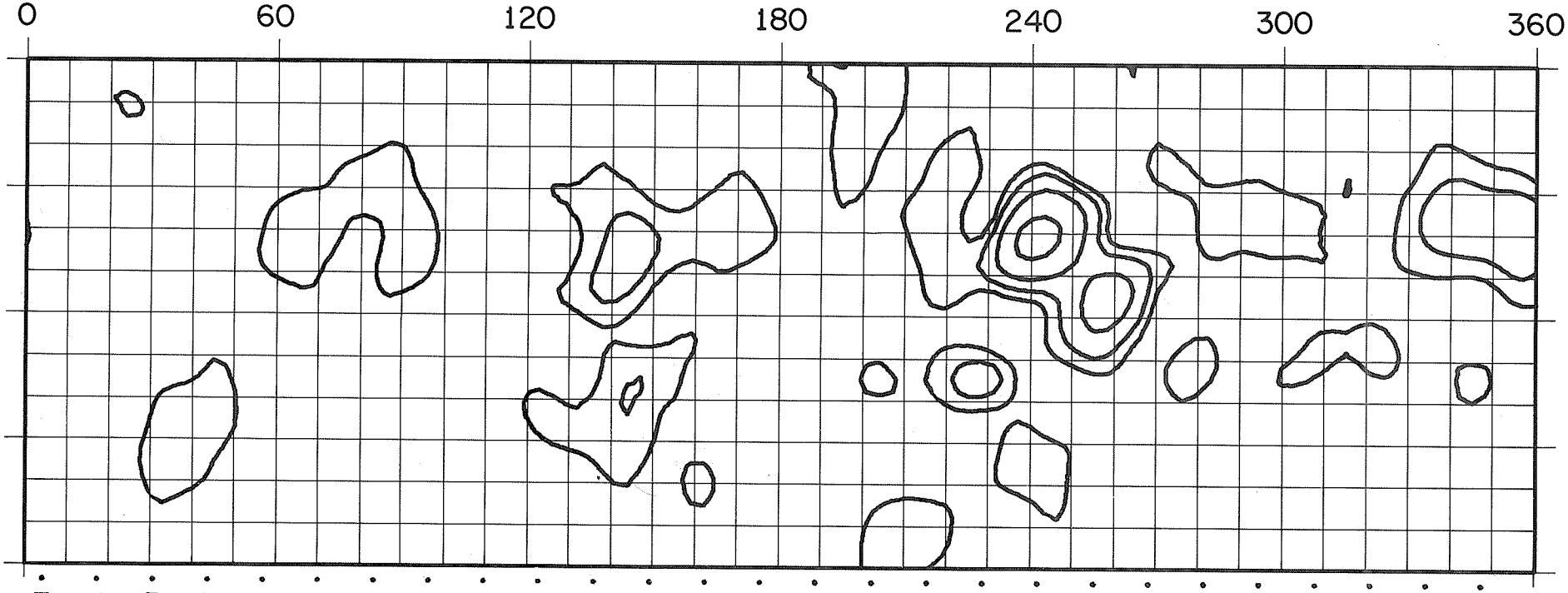

ROTATION NUMBER 1514

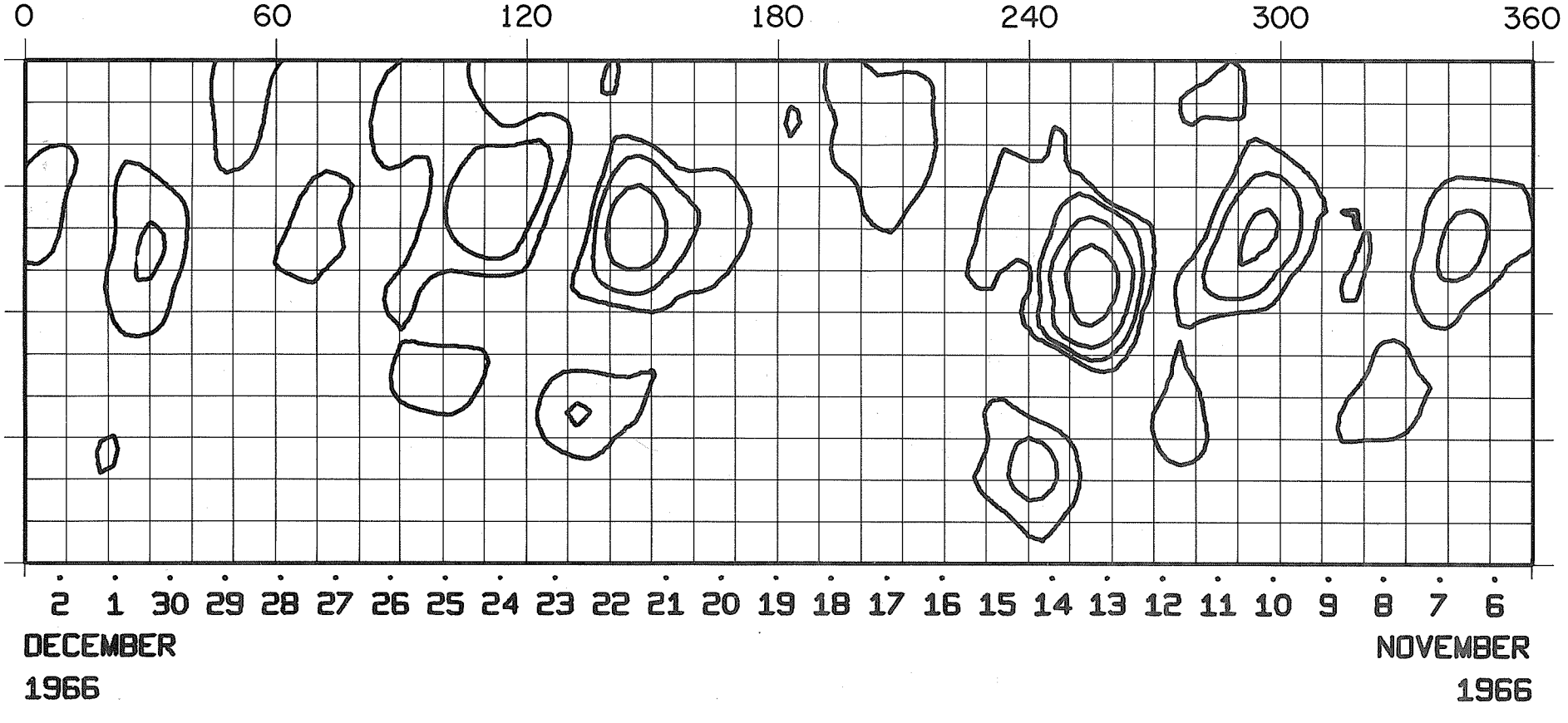

ROTATION NUMBER 1515

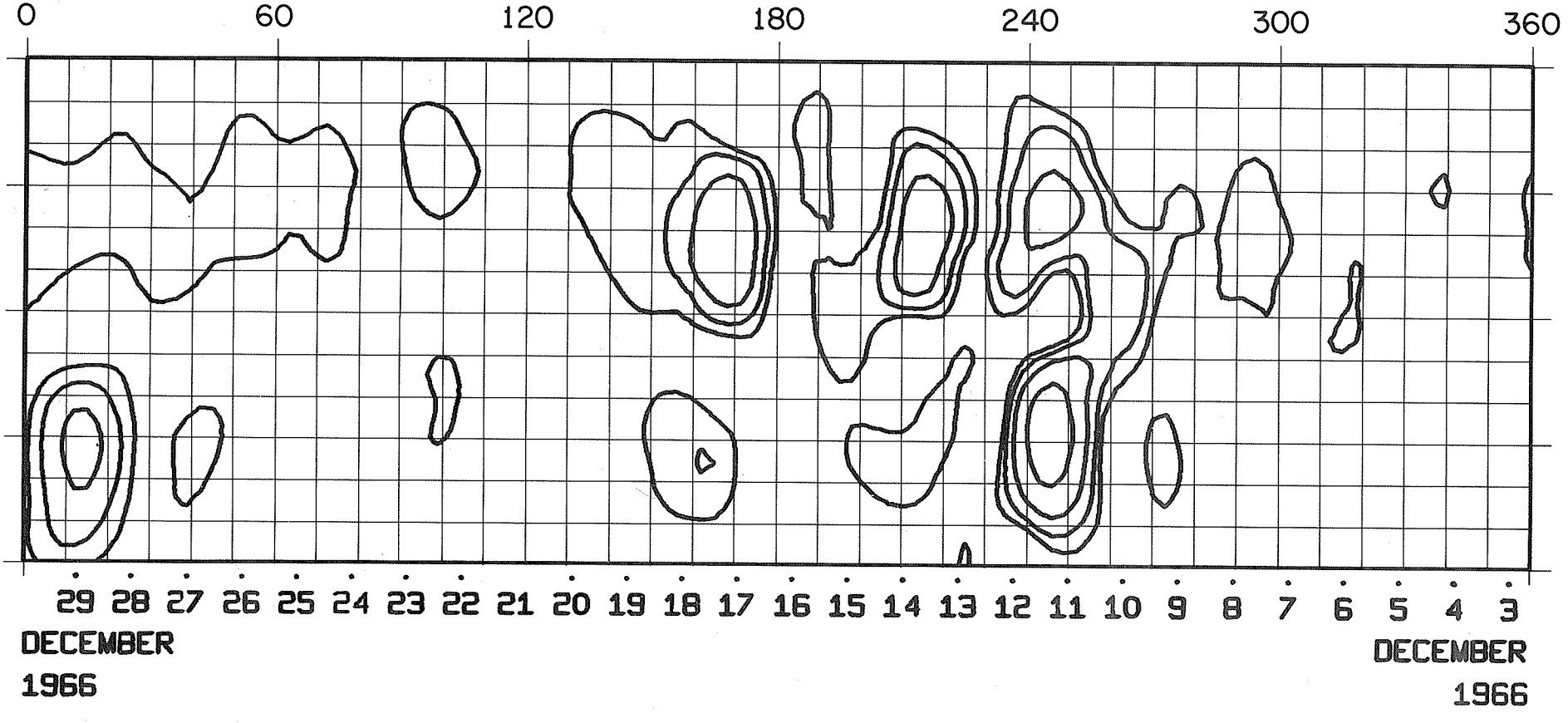

ROTATION NUMBER 1516

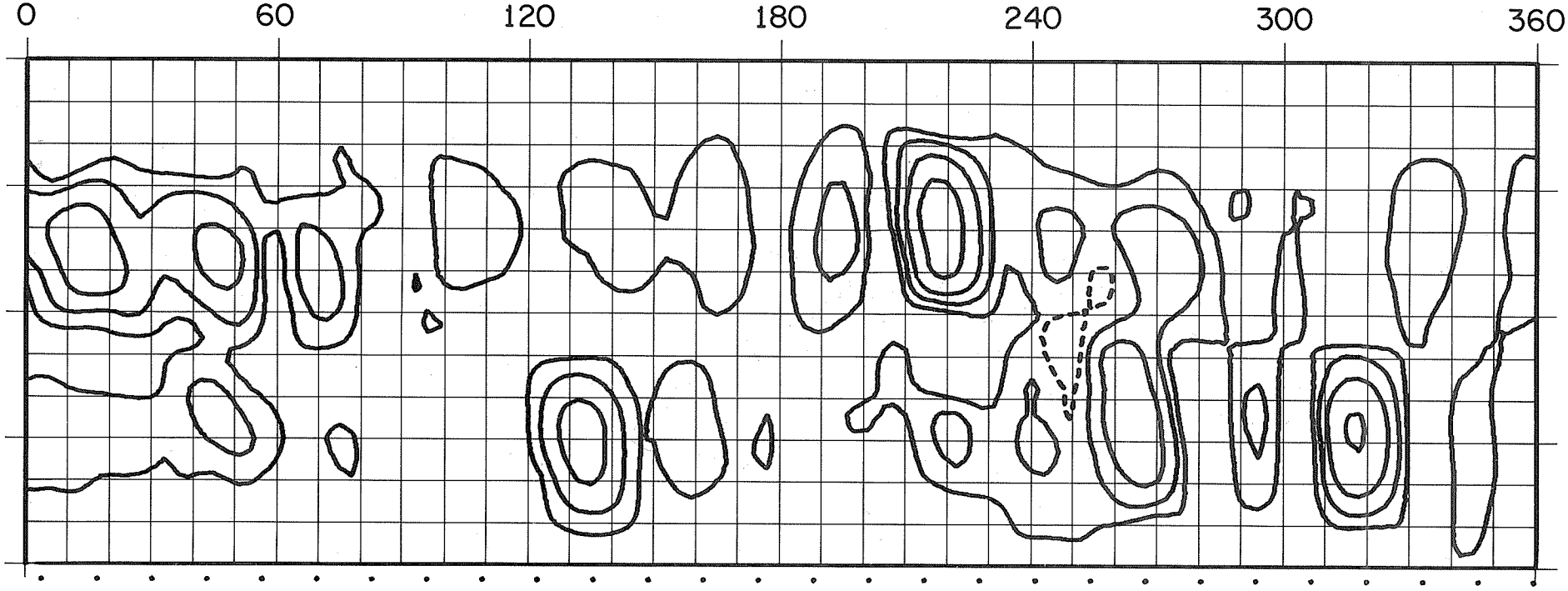

26 25 24 23 22 21 20 19 18 17 16 15 14 13 12 11 10 9 8 7 6 5 4 3 2 1 31 30

JANUARY 1967

DECEMBER 1966

ROTATION NUMBER 1517

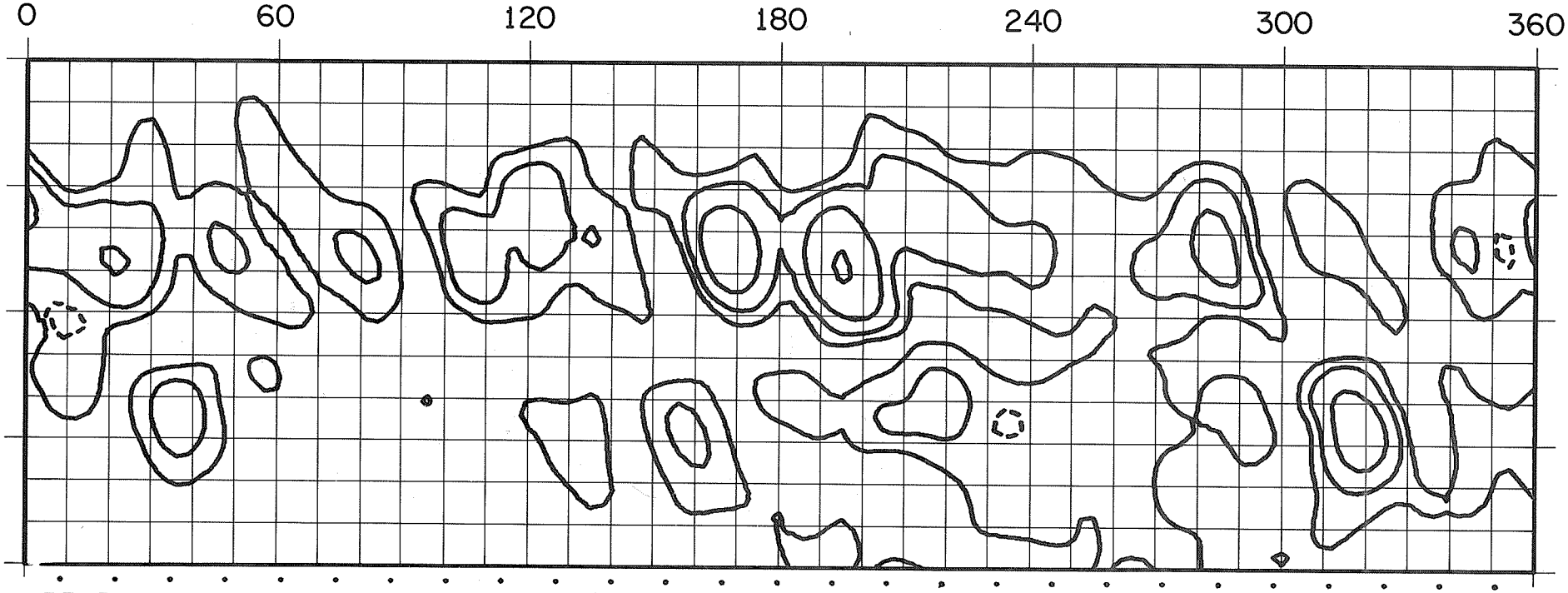

ROTATION NUMBER 1518

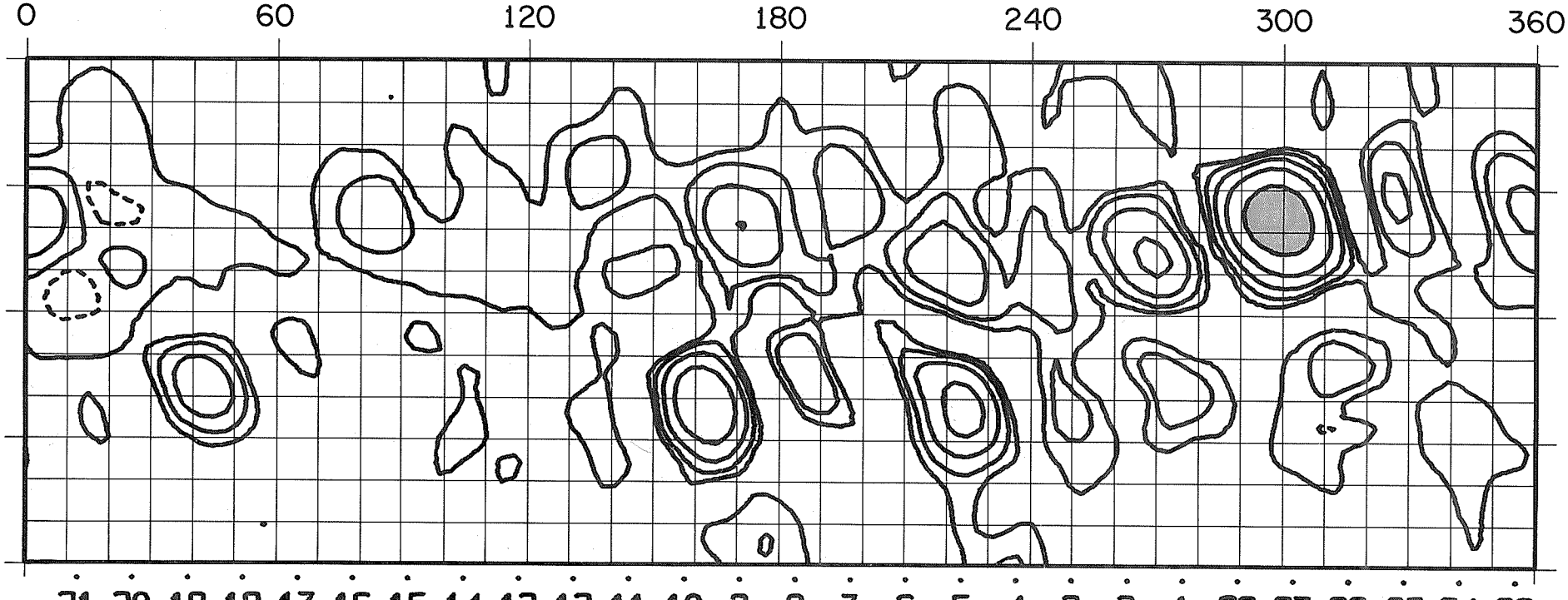

ROTATION NUMBER 1519

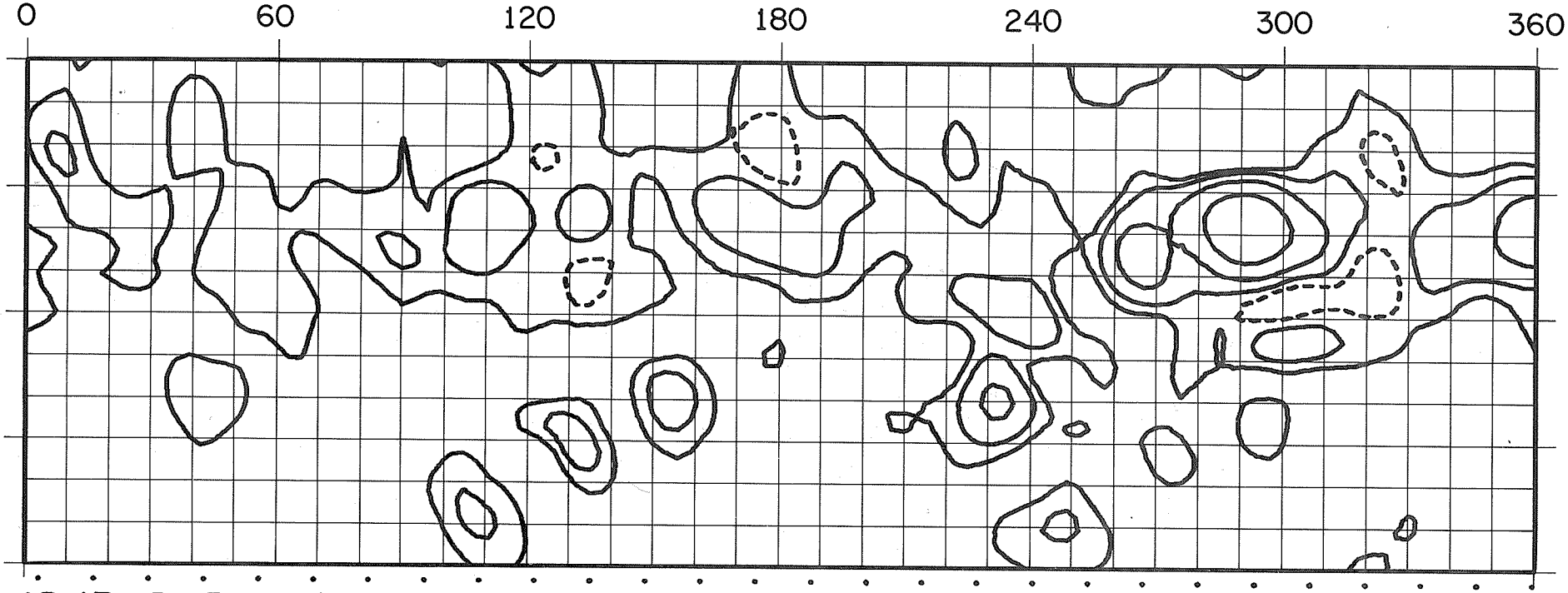

ROTATION NUMBER 1520

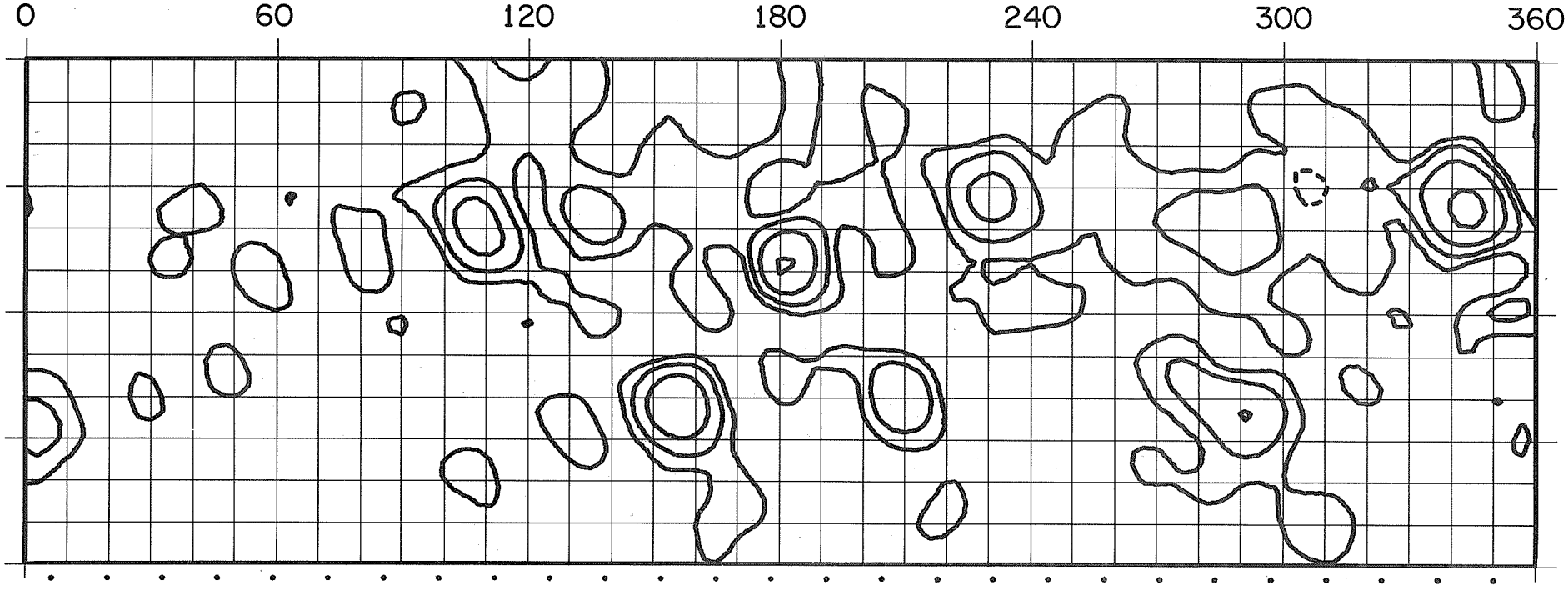

15 14 13 12 11 10 9 8 7 6 5 4 3 2 1 30 29 28 27 26 25 24 23 22 21 20 19

MAY
1967

APRIL
1967

87

ROTATION NUMBER 1521

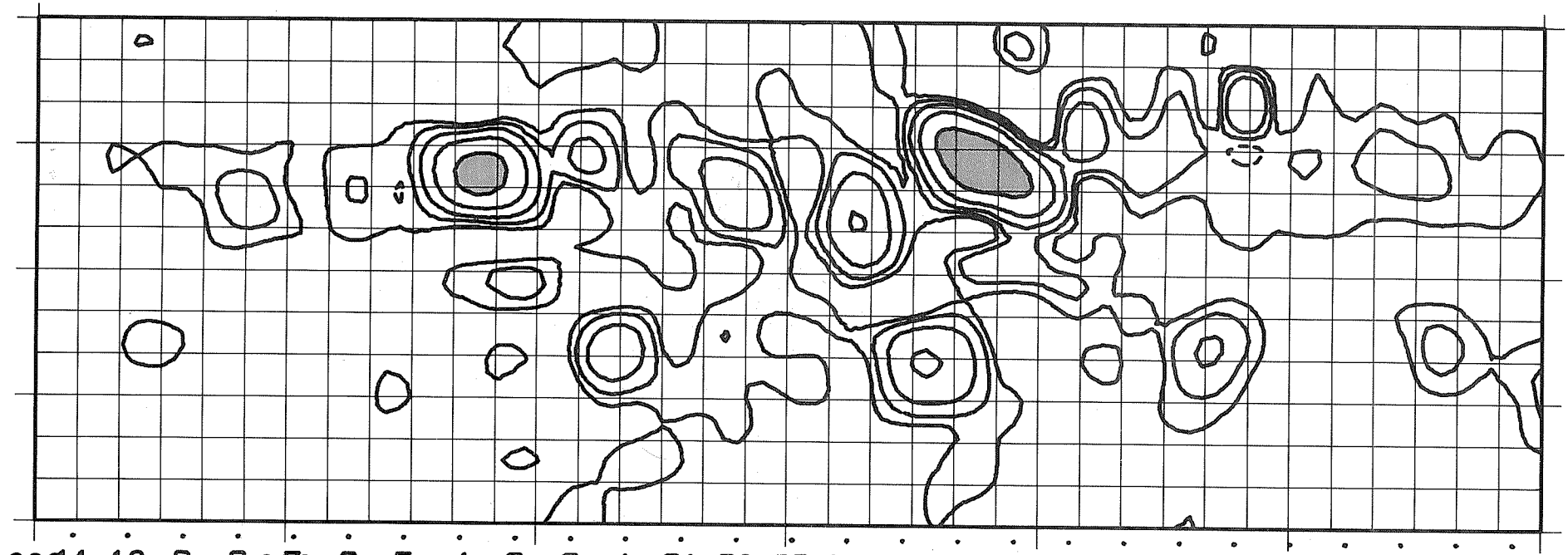

ROTATION NUMBER 1522

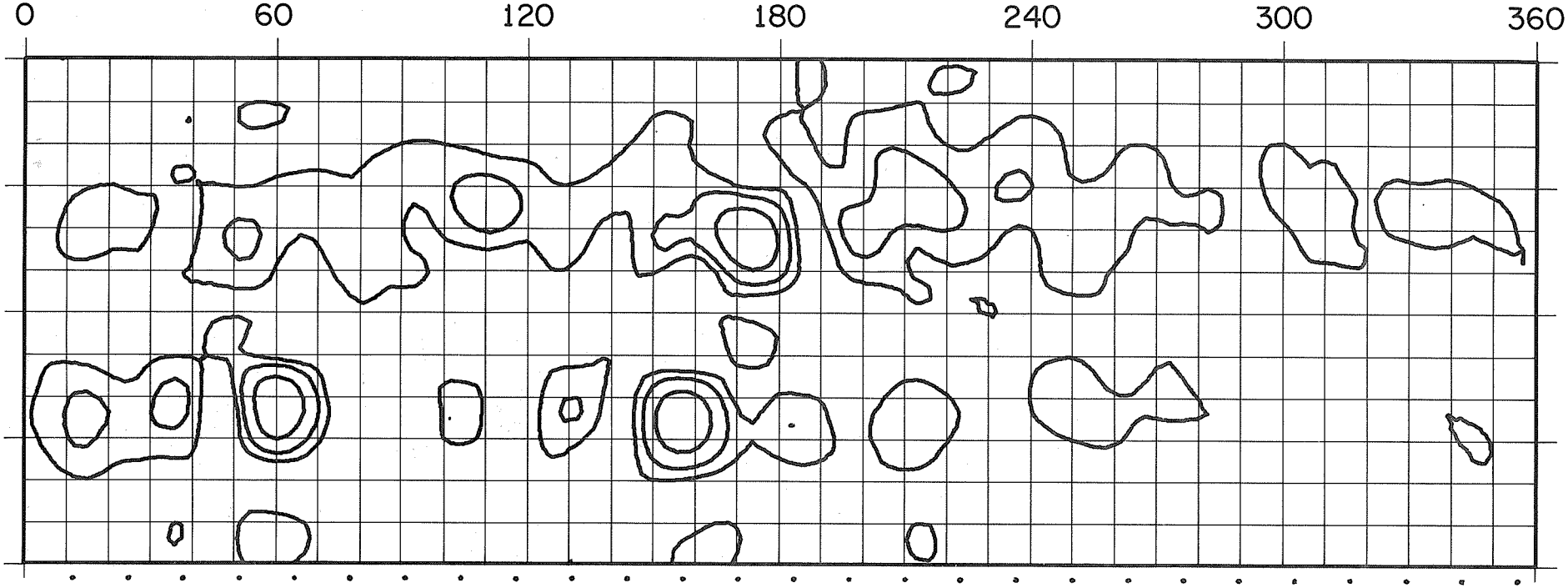

ROTATION NUMBER 1523
0
60
120
180
240
300
360
5 4 3 2 1 31 30 29 28 27 26 25 24 23 22 21 20 19 18 17 16 15 14 13 12 11 10 9
AUGUST
1967
JULY
1967

ROTATION NUMBER 1524

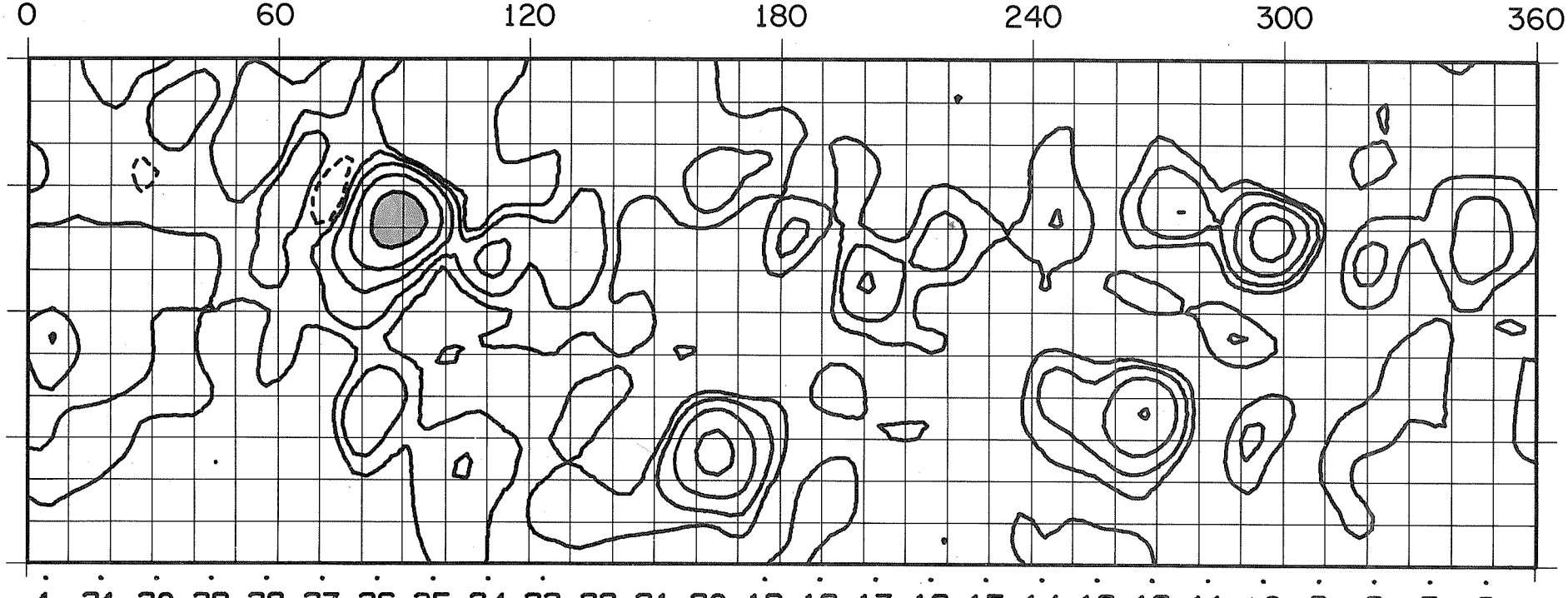

ROTATION NUMBER 1525

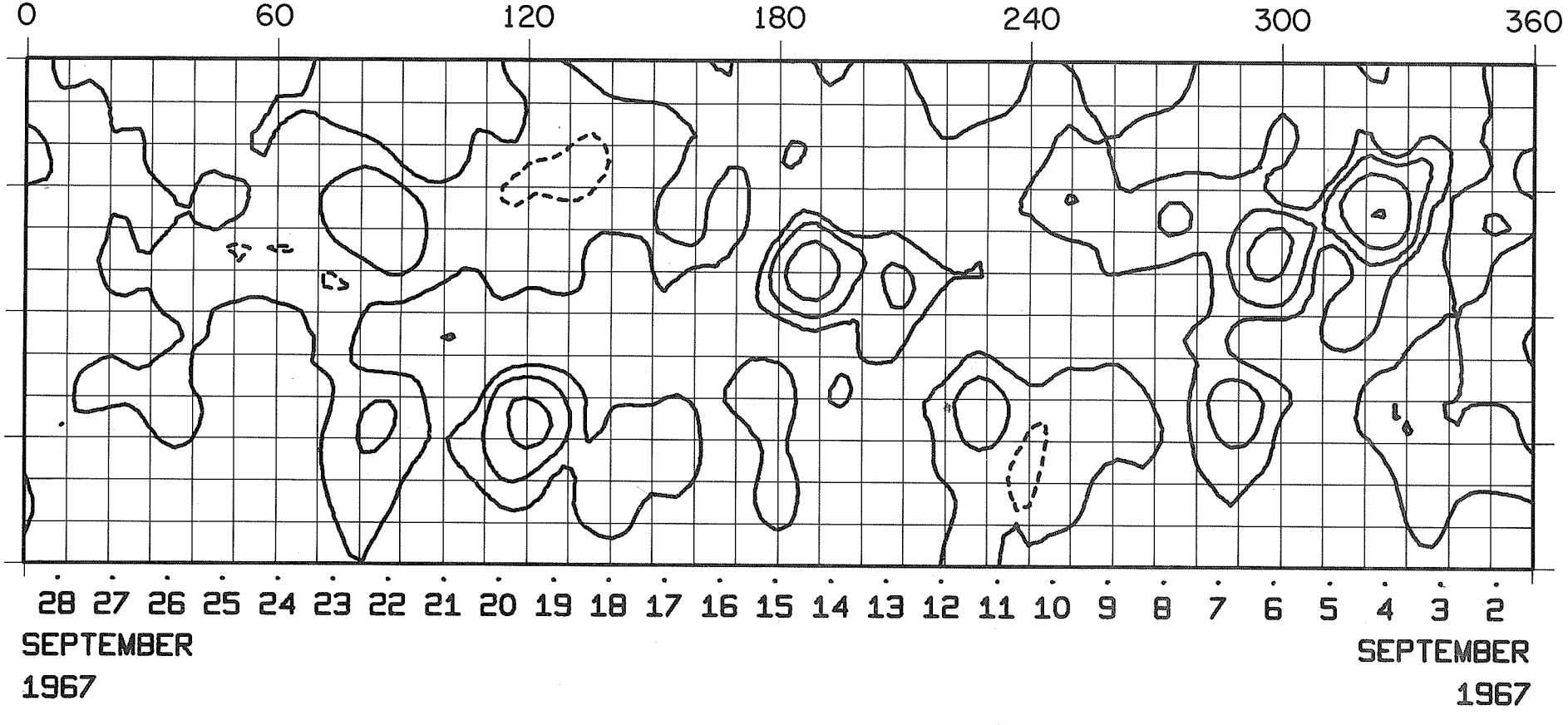

ROTATION NUMBER 1526

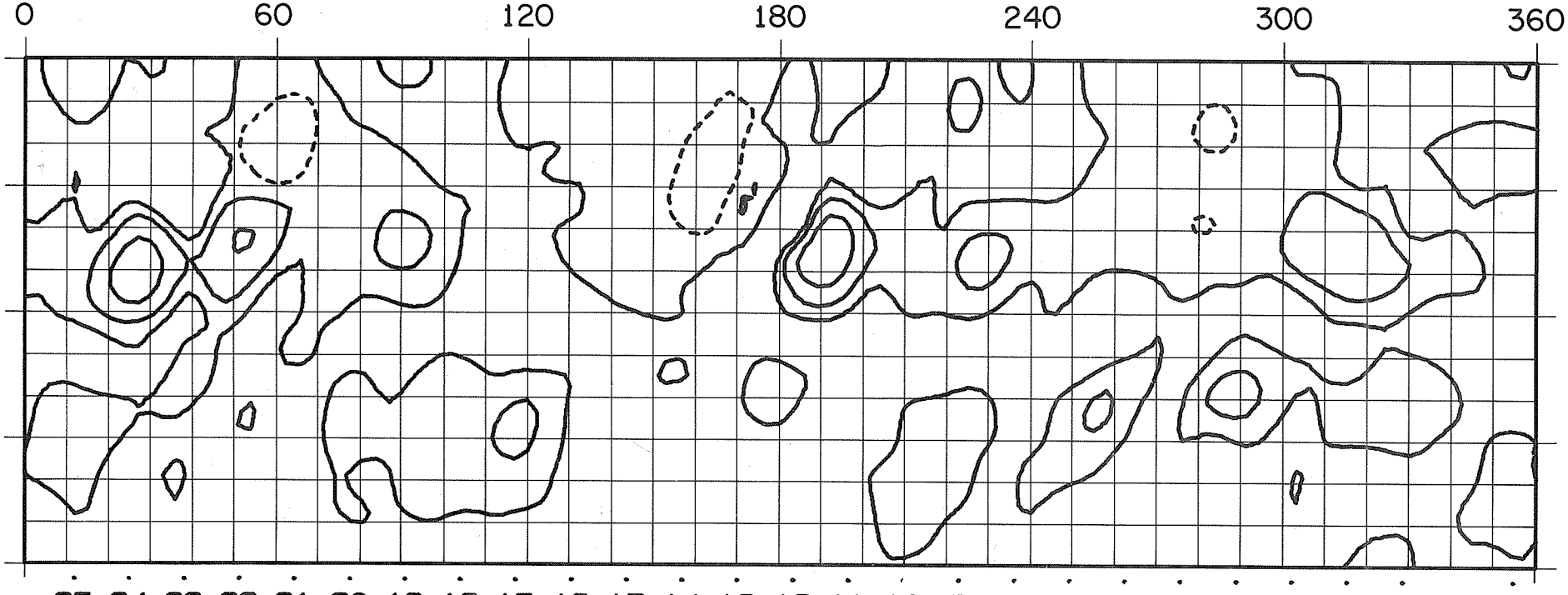

ROTATION NUMBER 1527

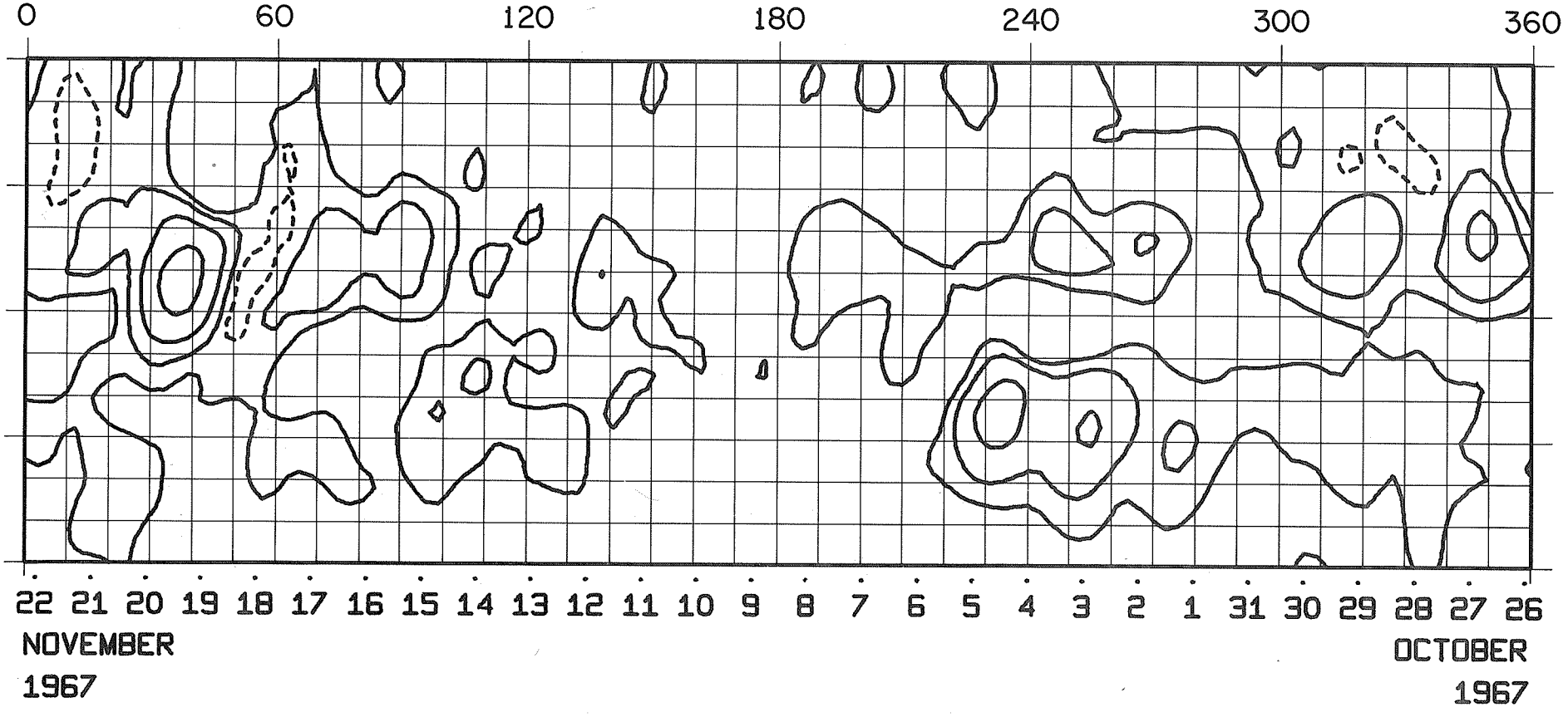

ROTATION NUMBER 1528

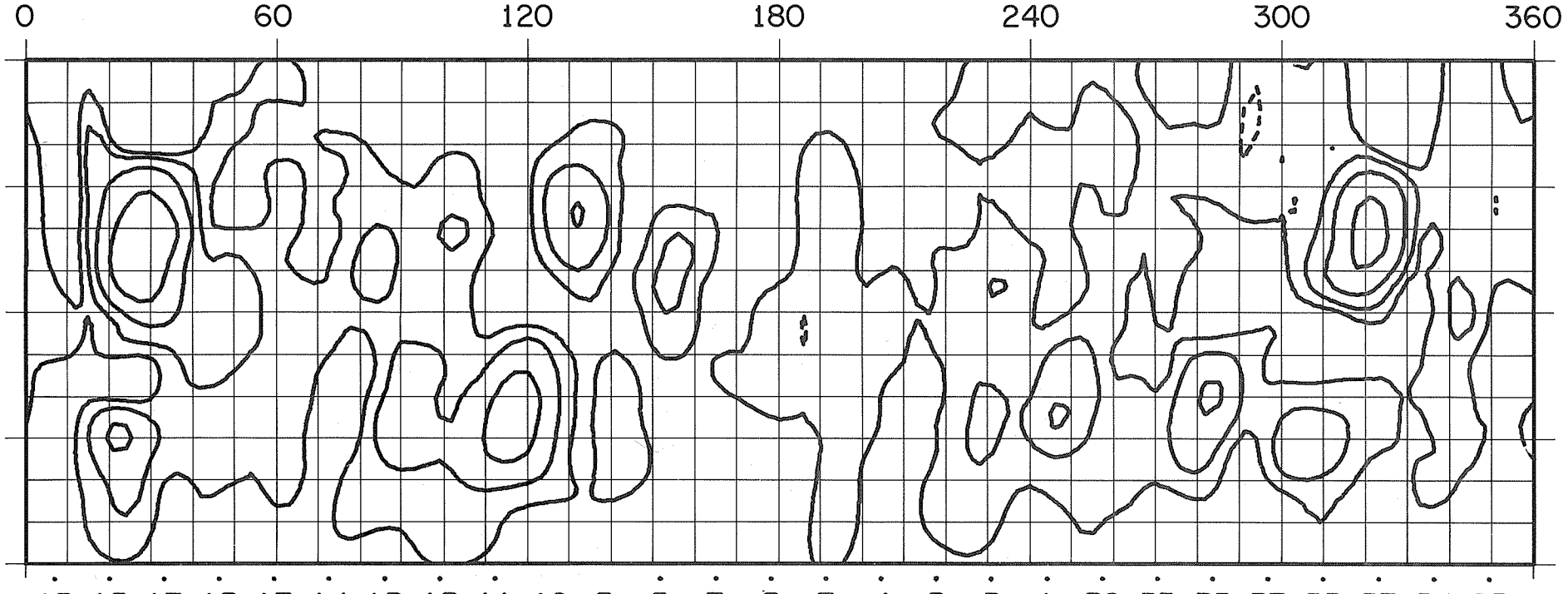

ROTATION NUMBER 1529

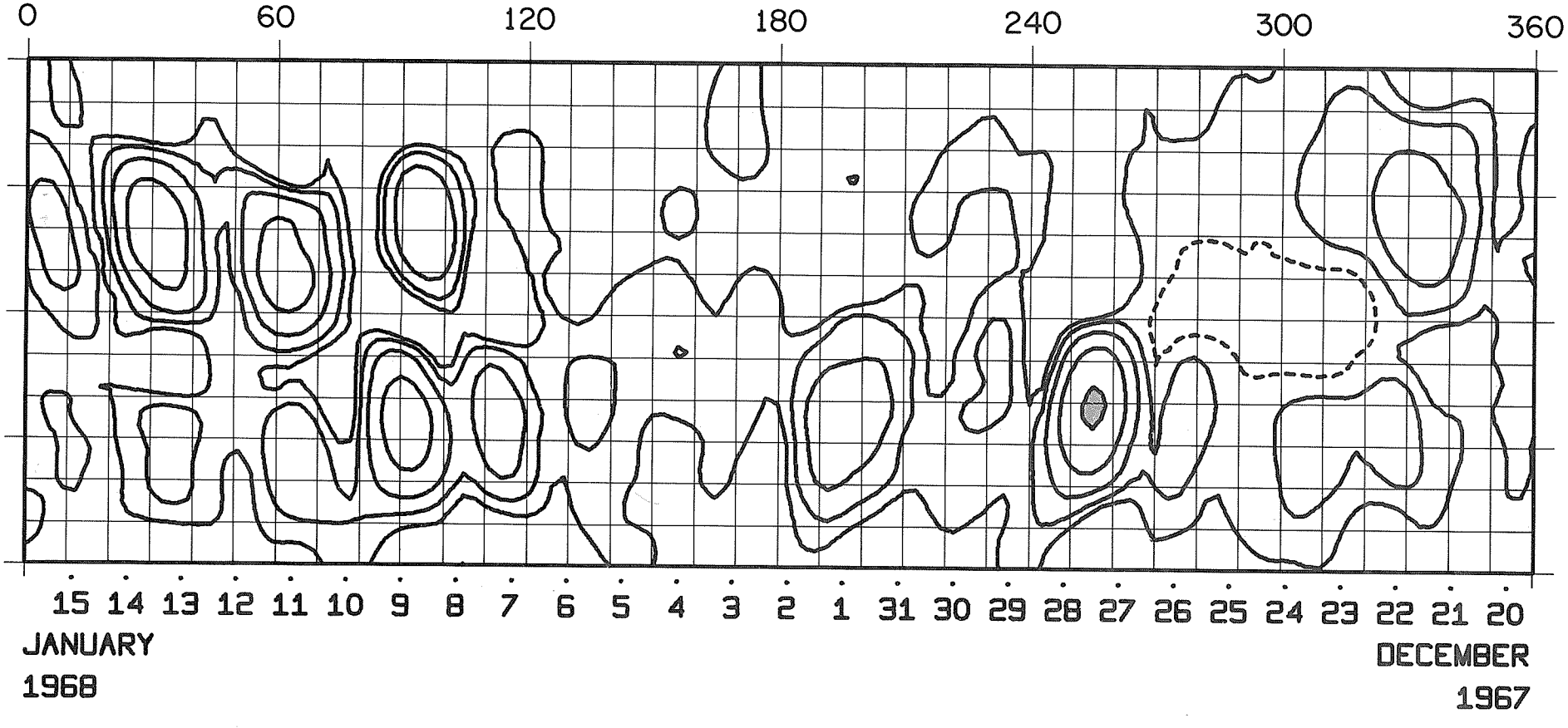

ROTATION NUMBER 1530

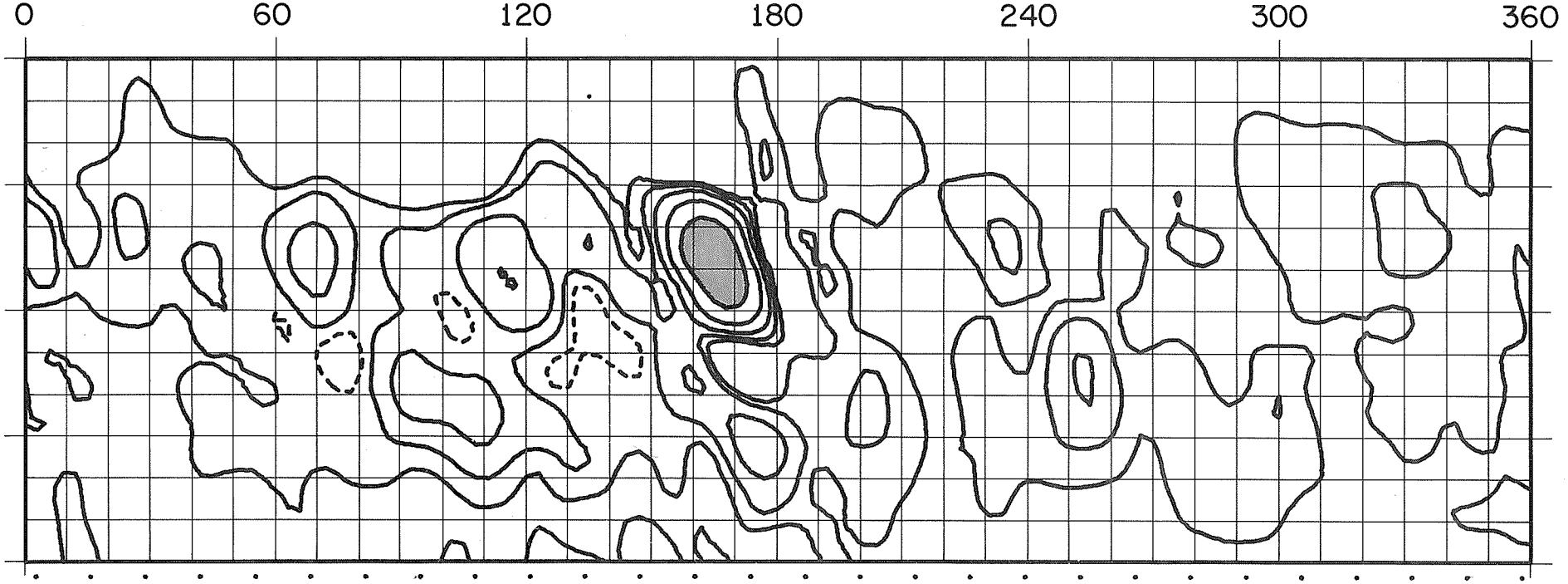

ROTATION NUMBER 1531

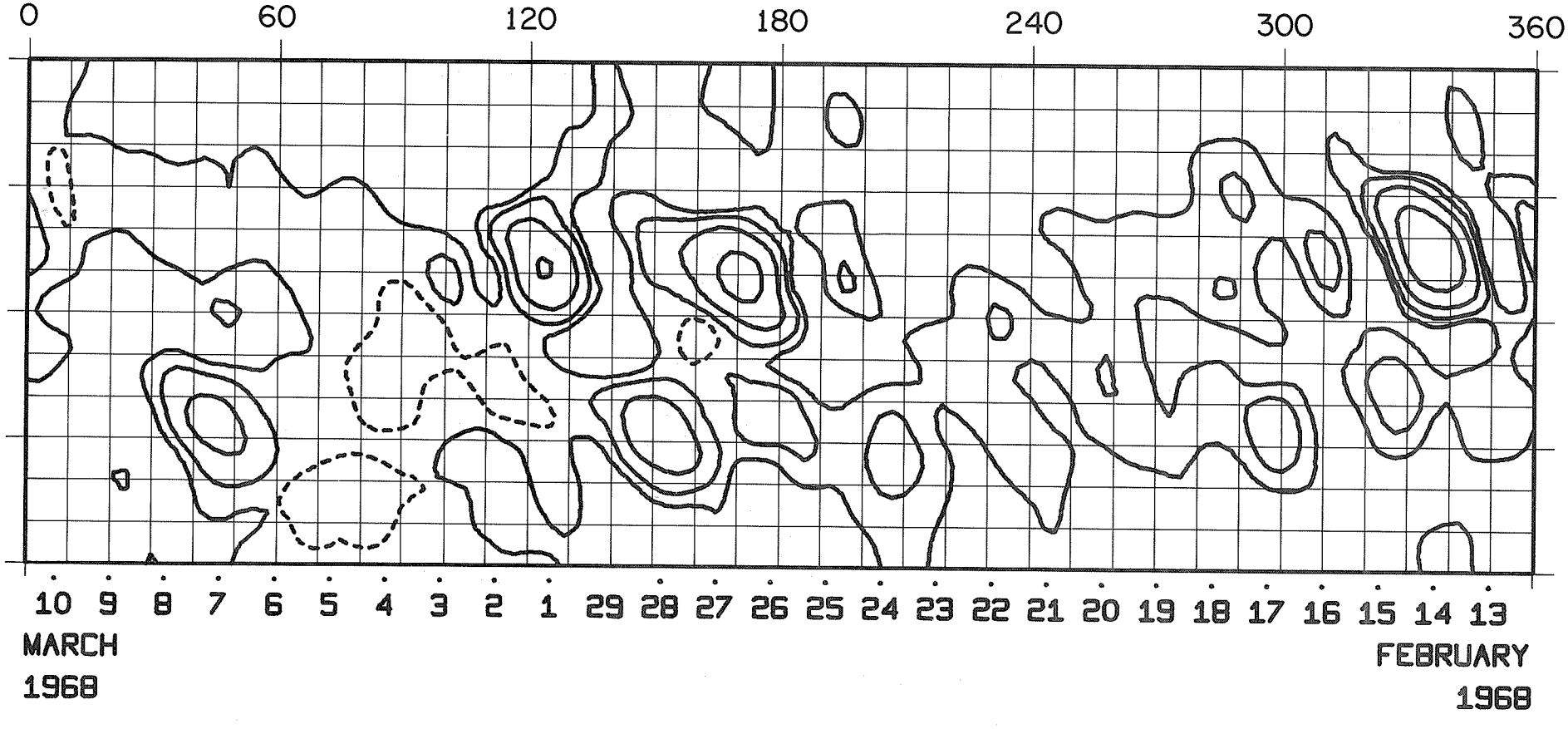

ROTATION NUMBER 1532

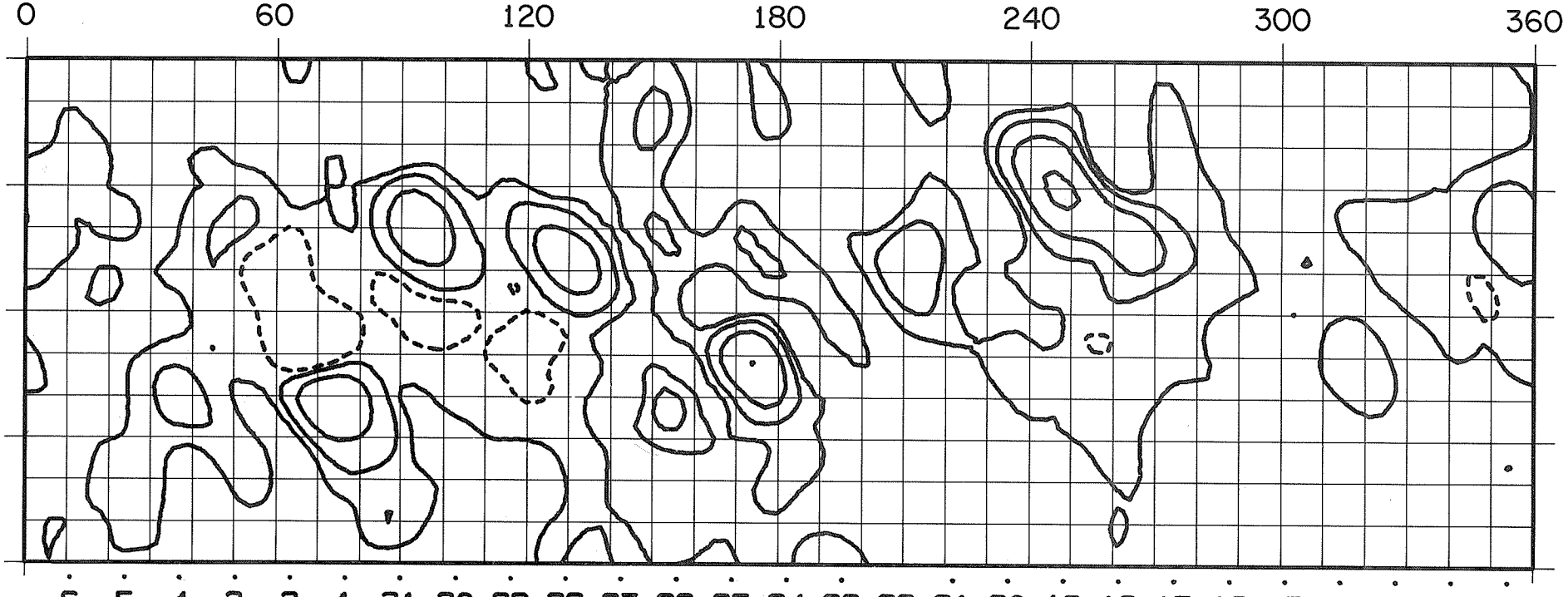

100

ROTATION NUMBER 1533

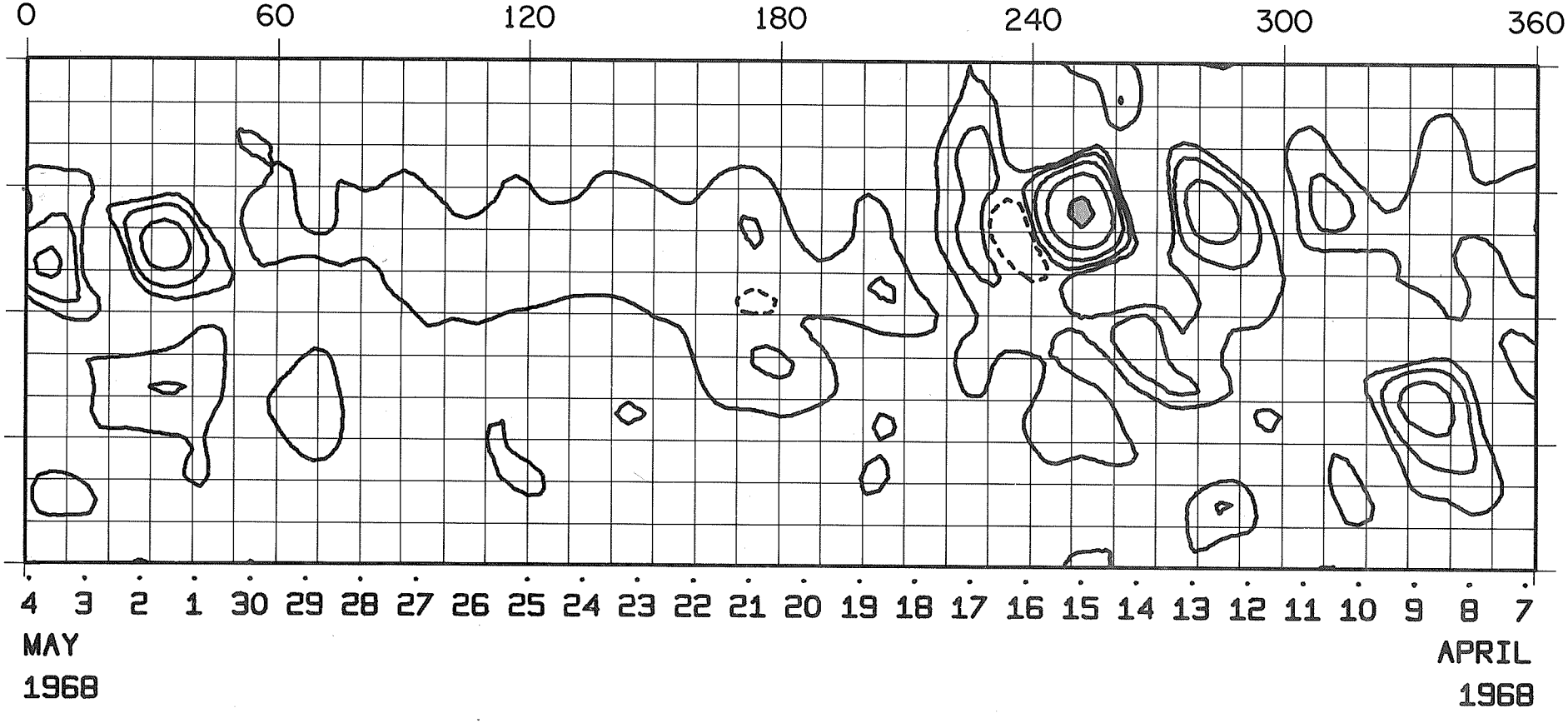

ROTATION NUMBER 1534

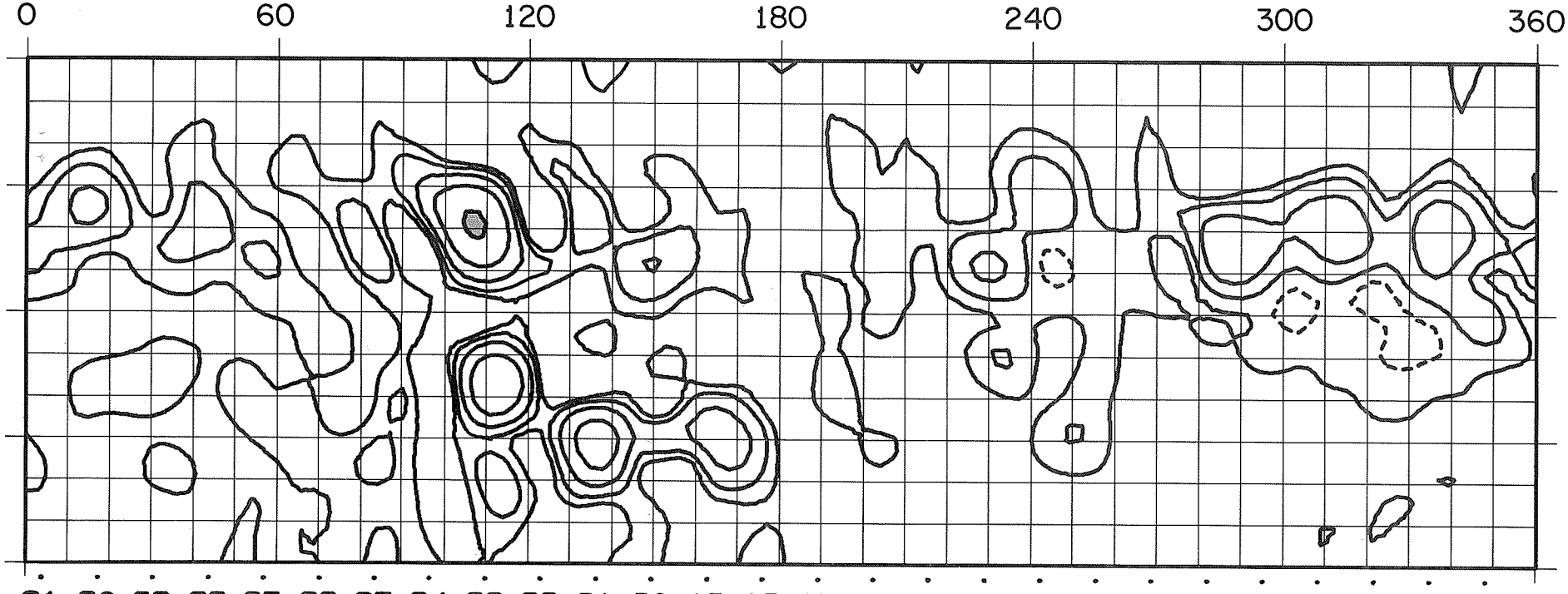

31 30 29 28 27 26 25 24 23 22 21 20 19 18 17 16 15 14 13 12 11 10 9 8 7 6 5

MAY
1968

MAY
1968

ROTATION NUMBER 1535

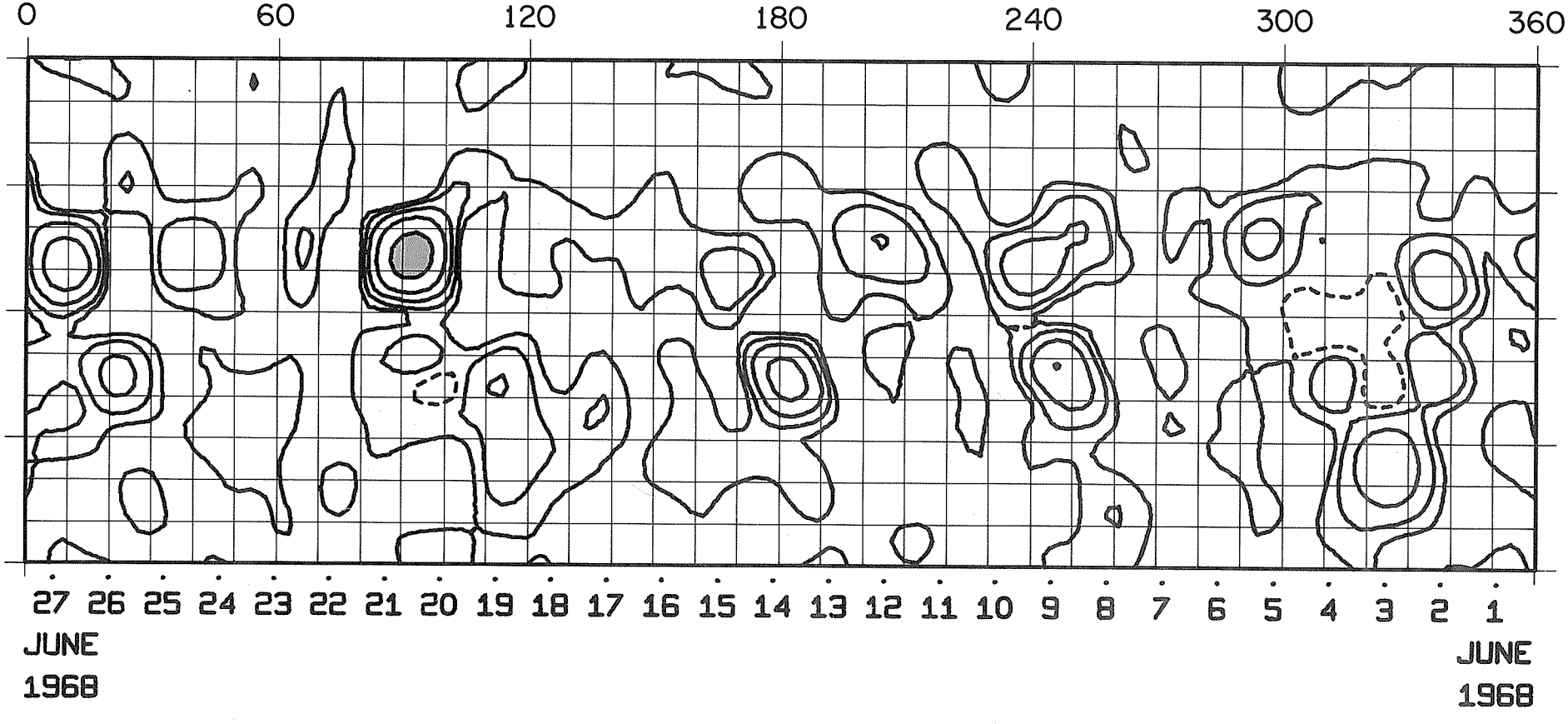

ROTATION NUMBER 1536

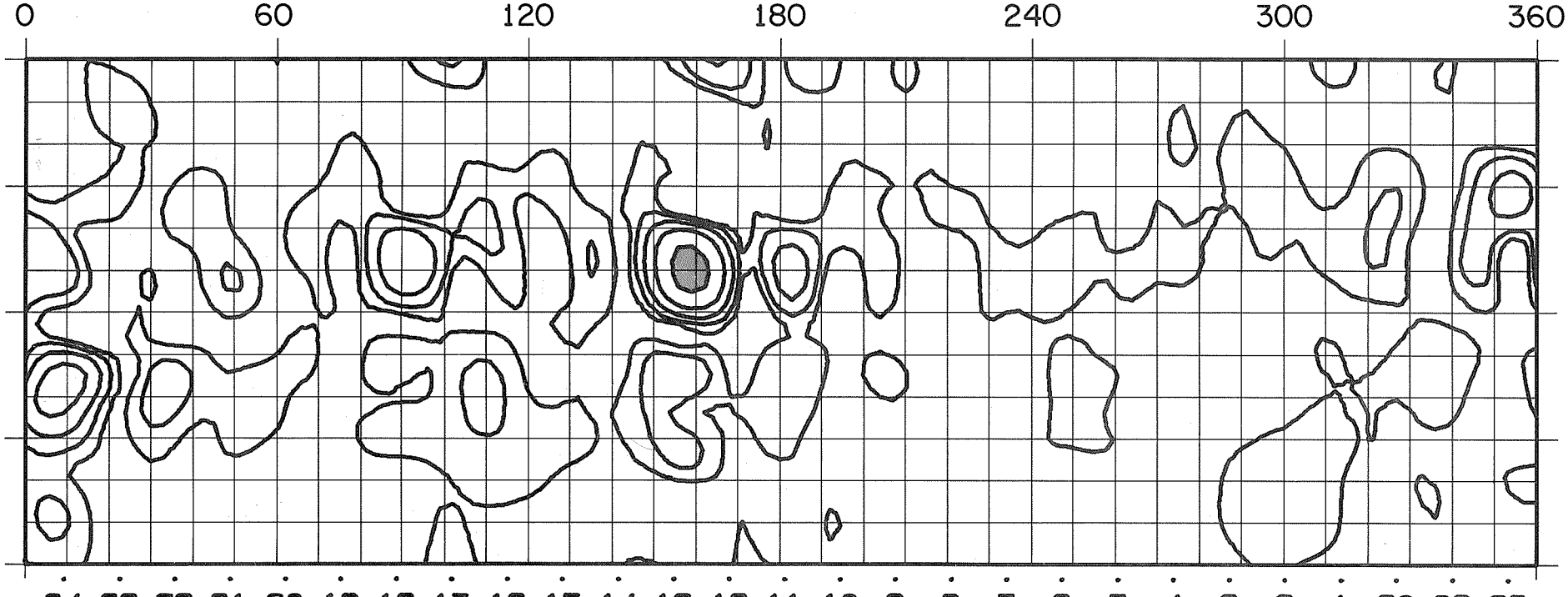

ROTATION NUMBER 1537

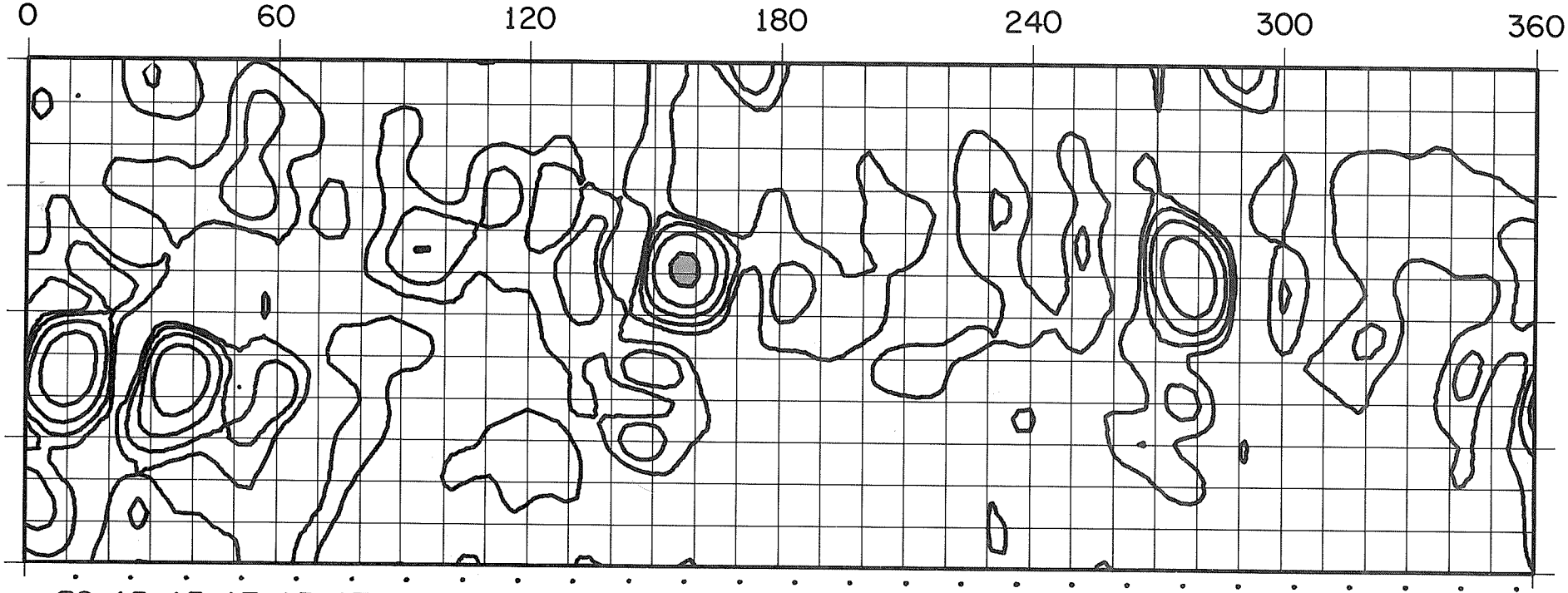

ROTATION NUMBER 1538

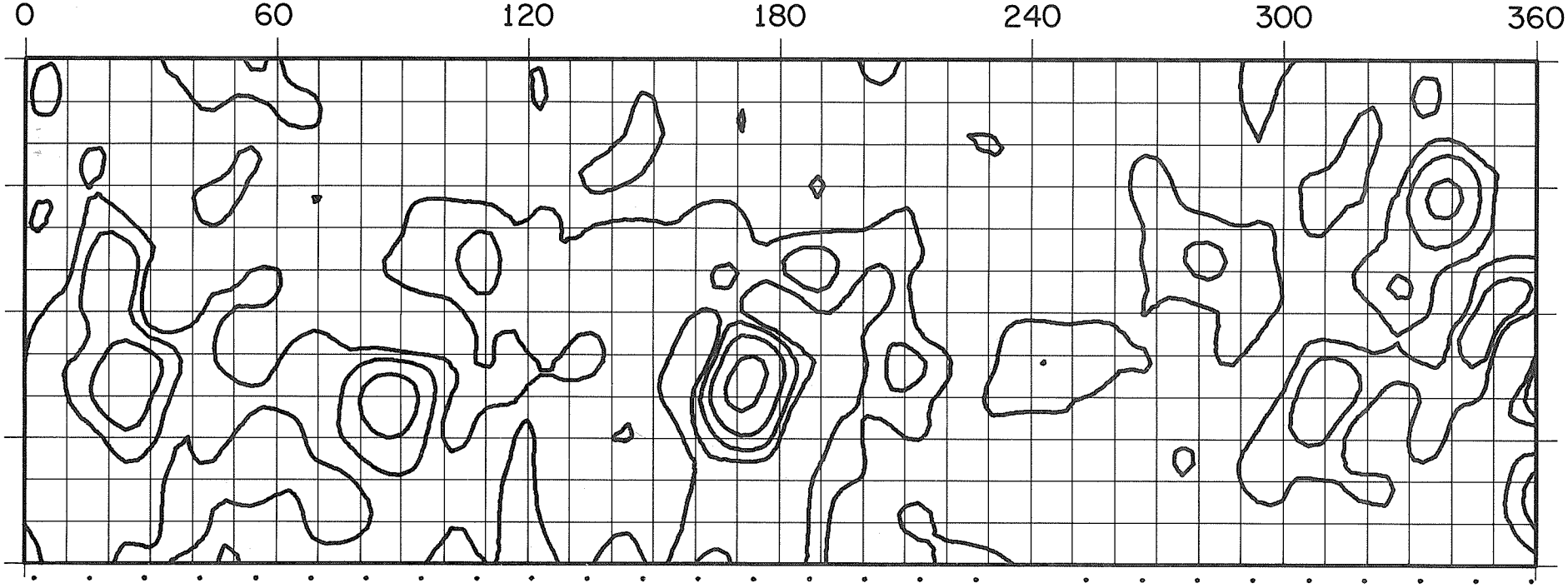

ROTATION NUMBER 1539

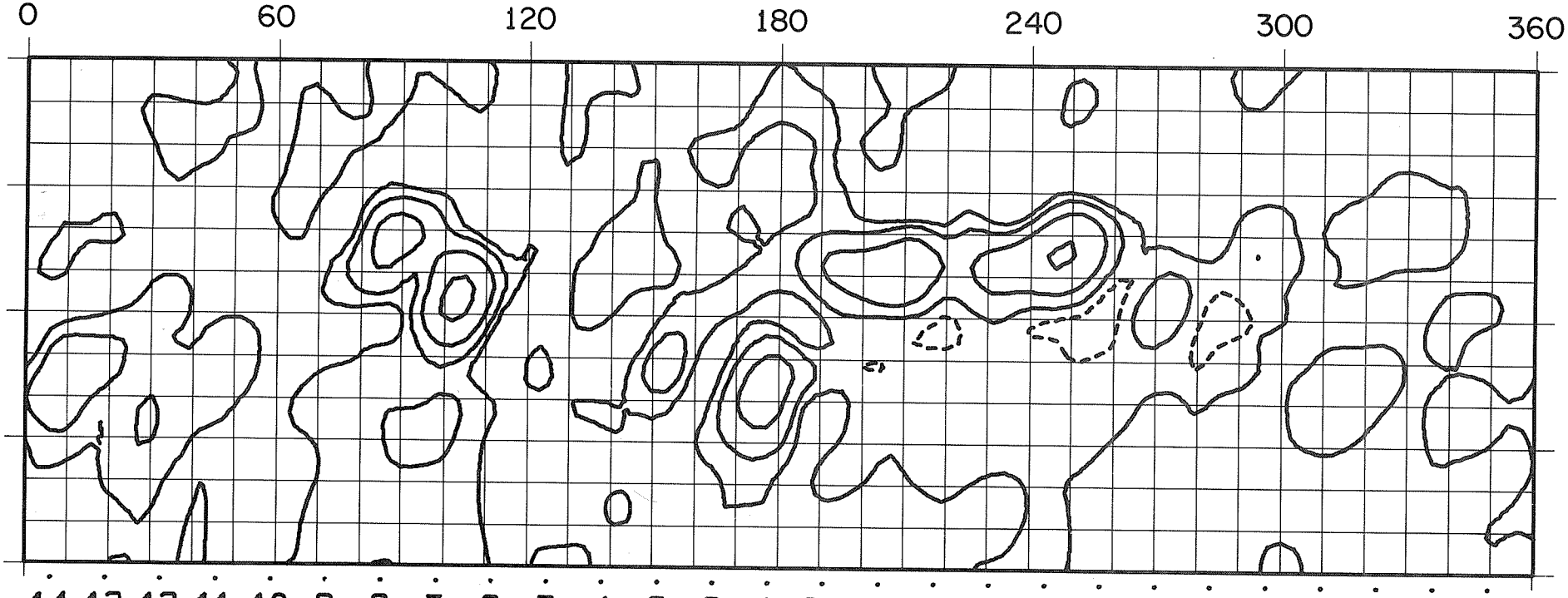

ROTATION NUMBER 1540

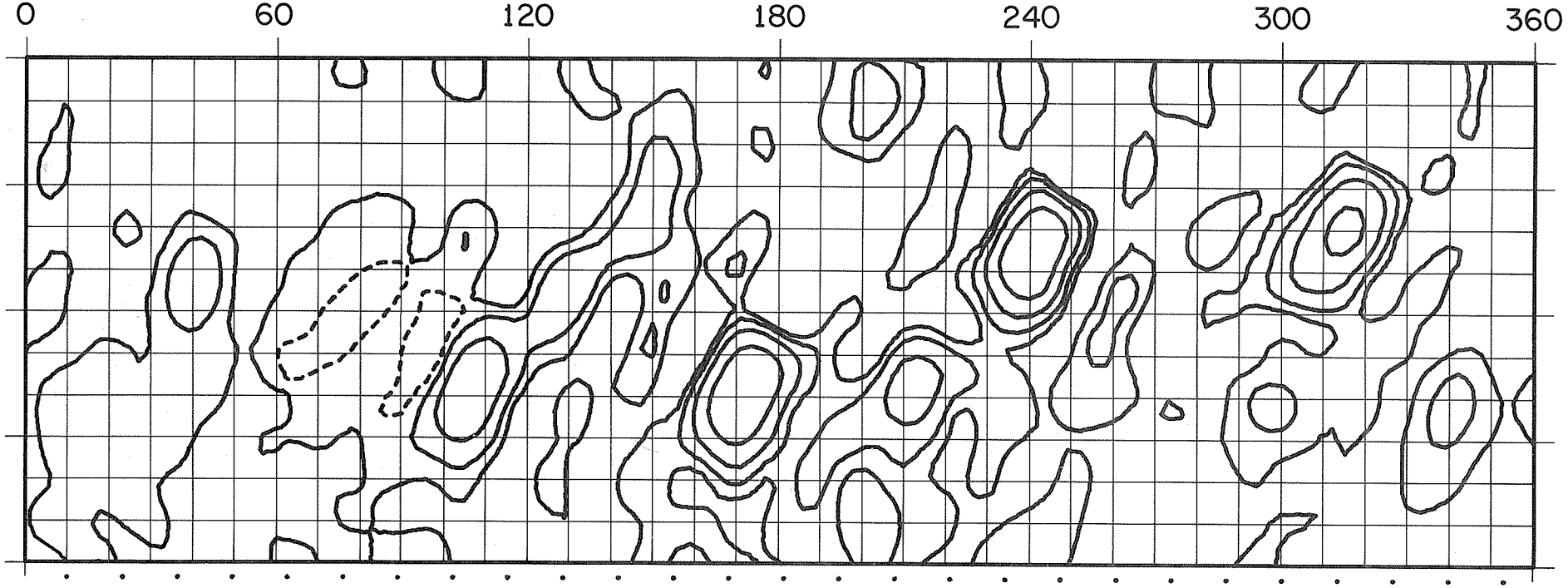

801

ROTATION NUMBER 1541

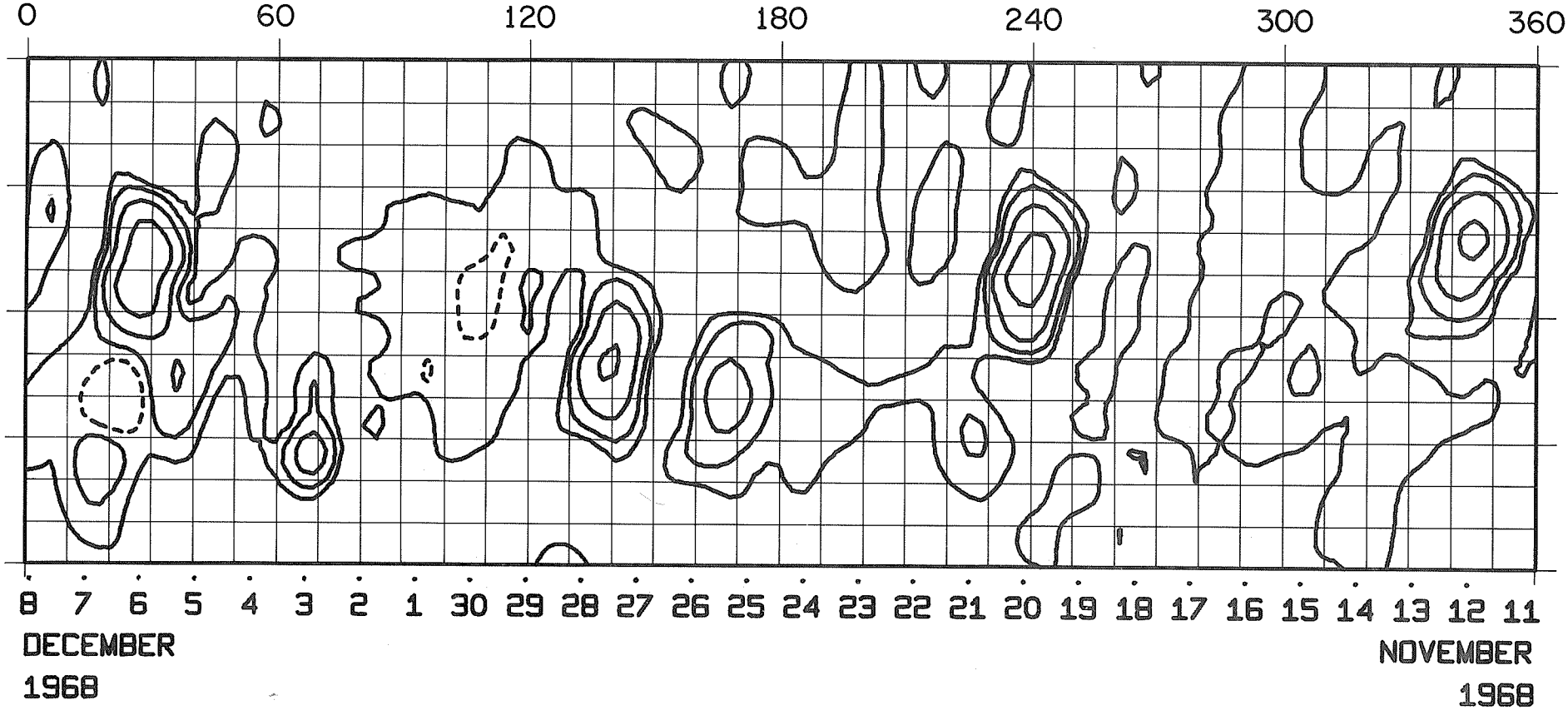

ROTATION NUMBER 1542

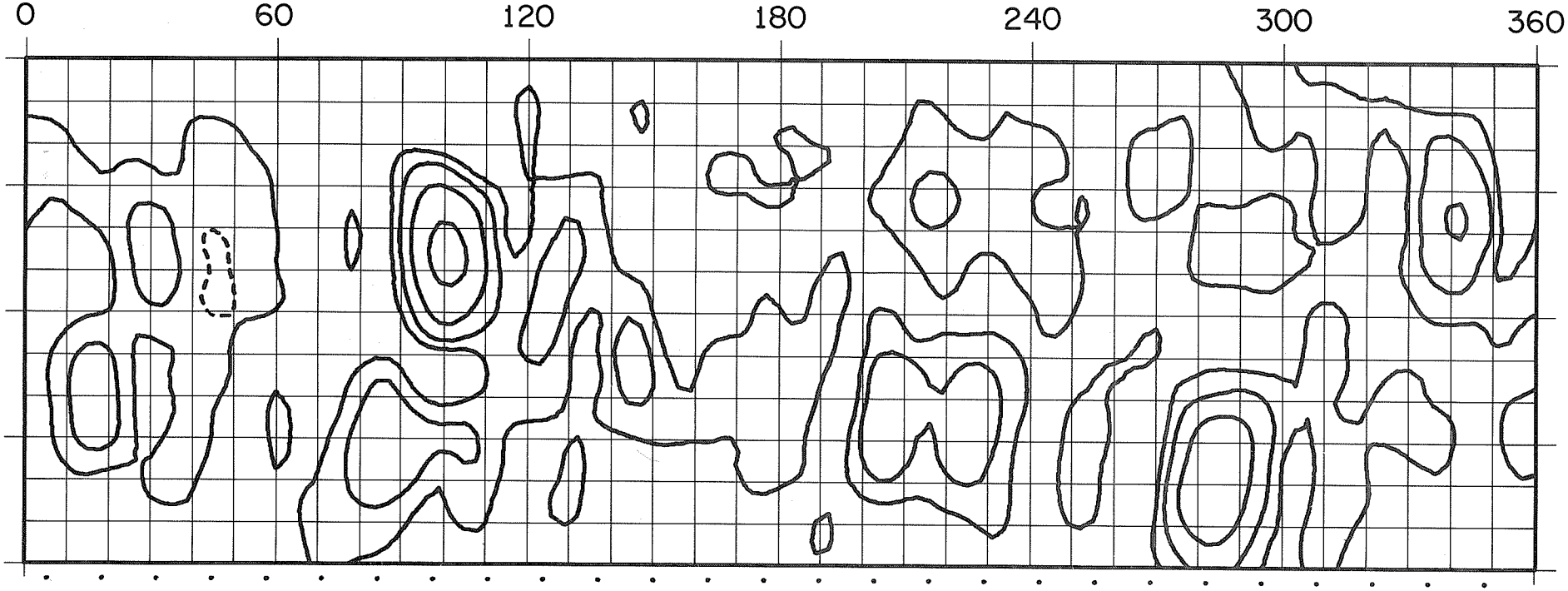

ROTATION NUMBER 1543

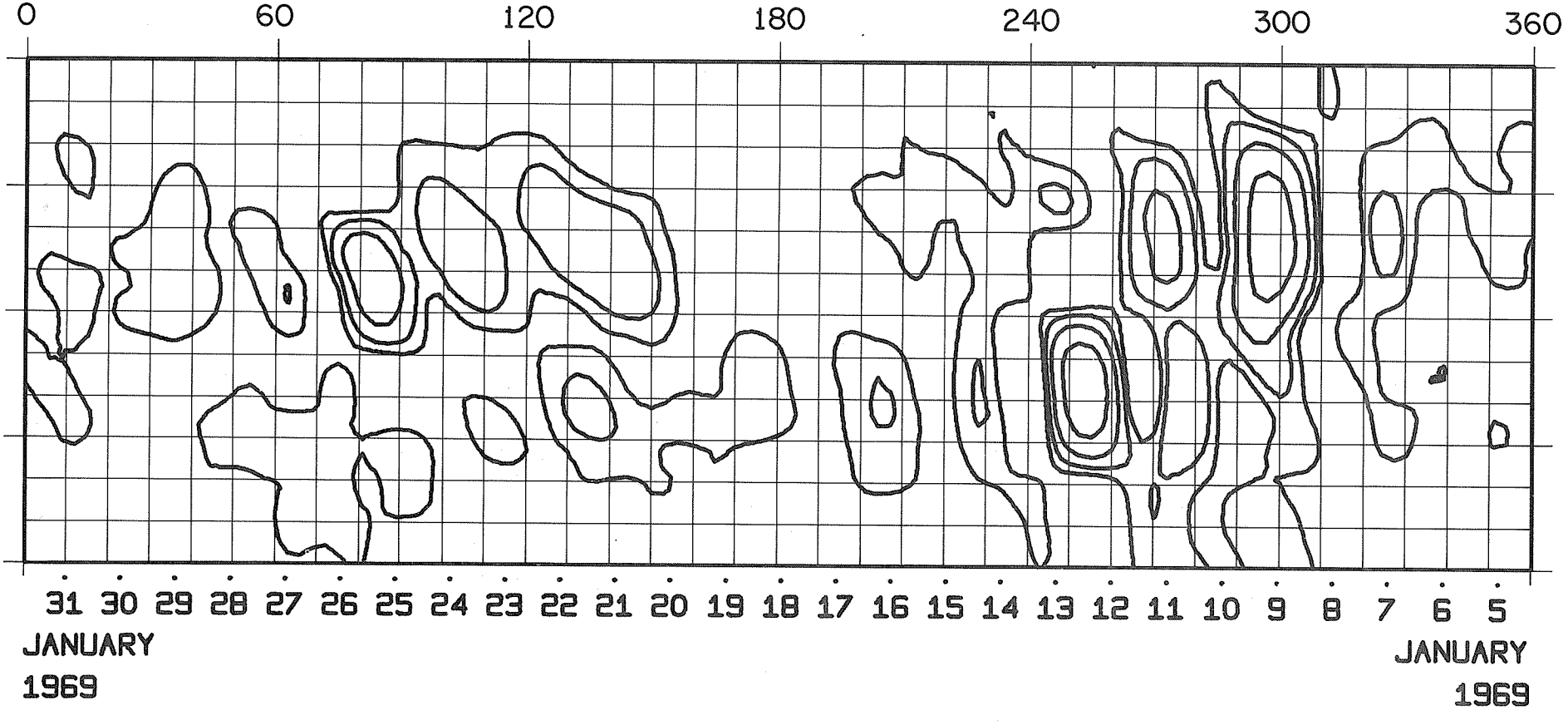

ROTATION NUMBER 1544

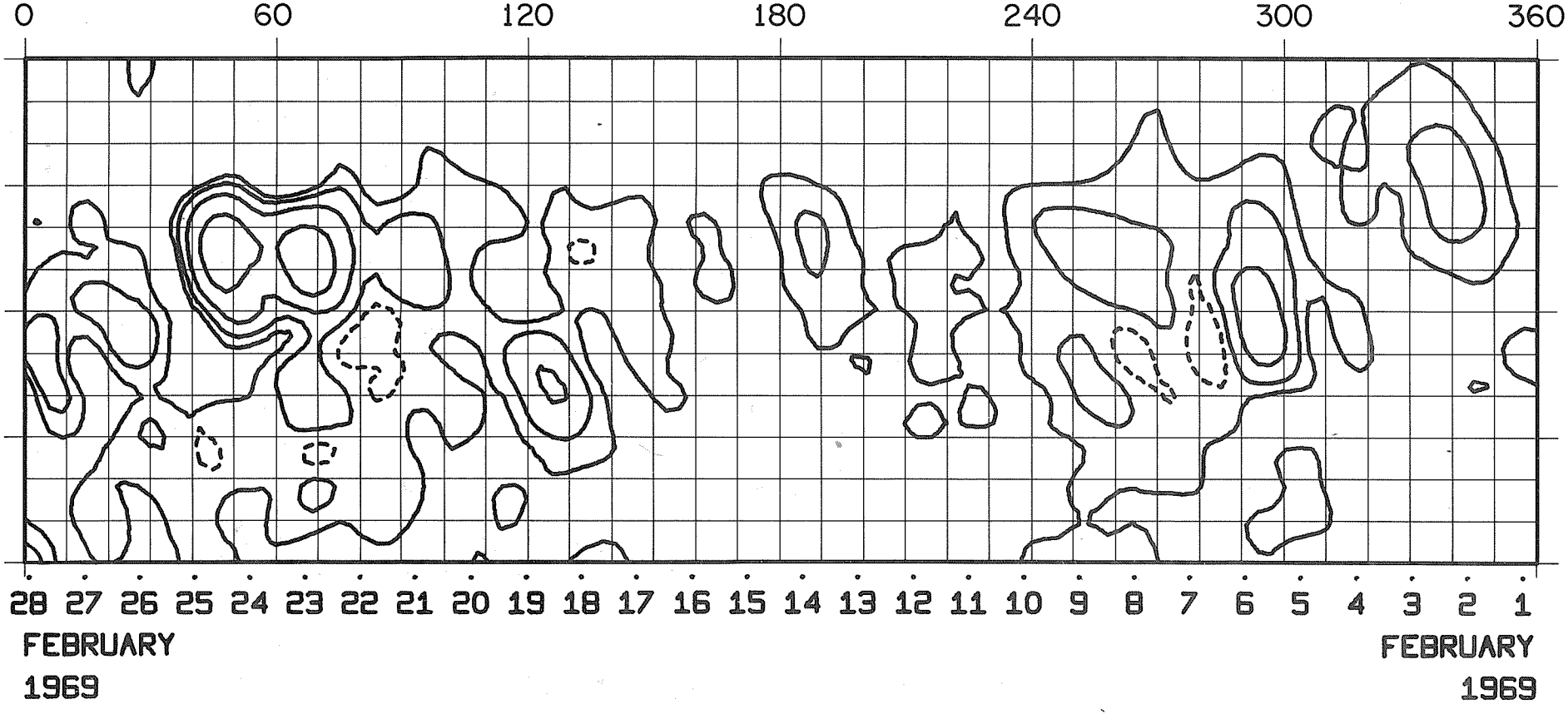

ROTATION NUMBER 1545

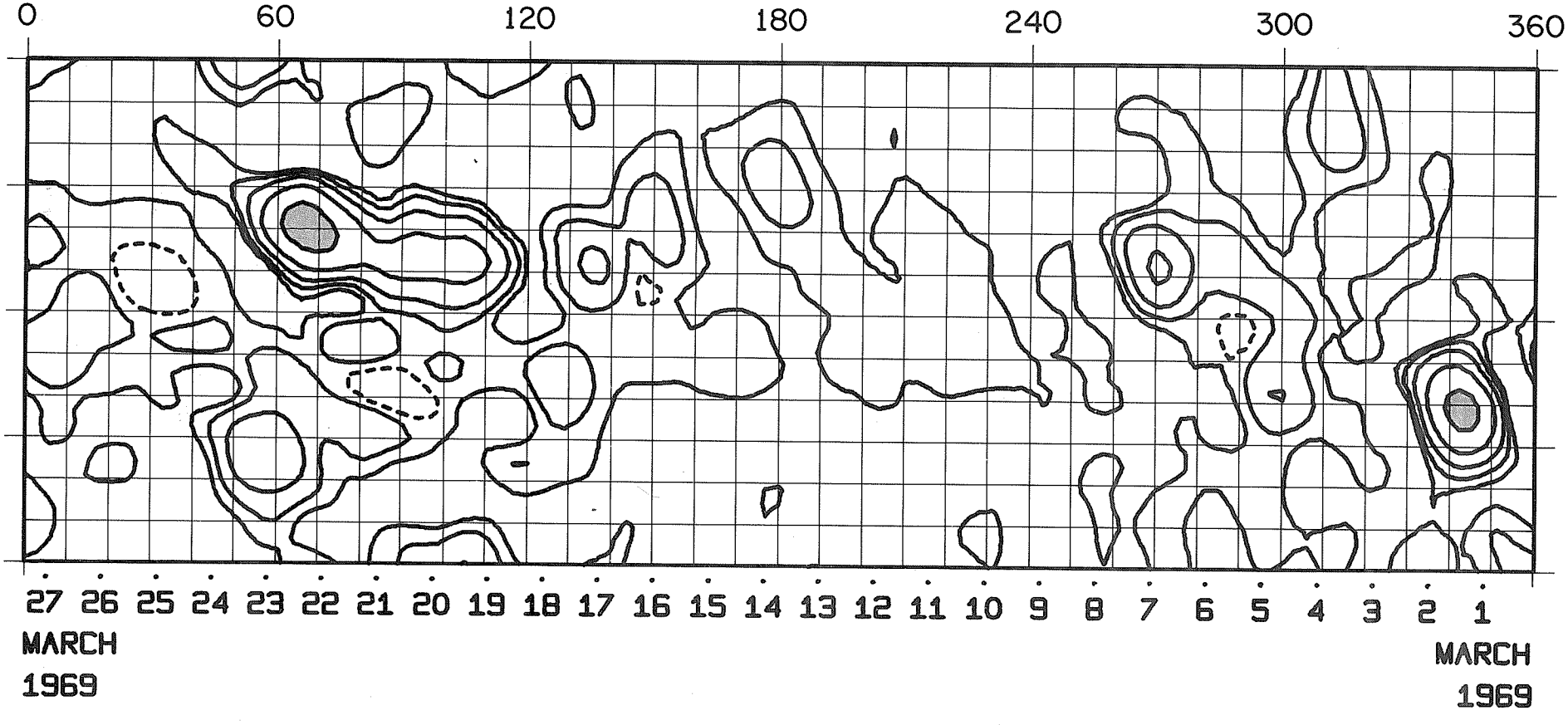

ROTATION NUMBER 1546

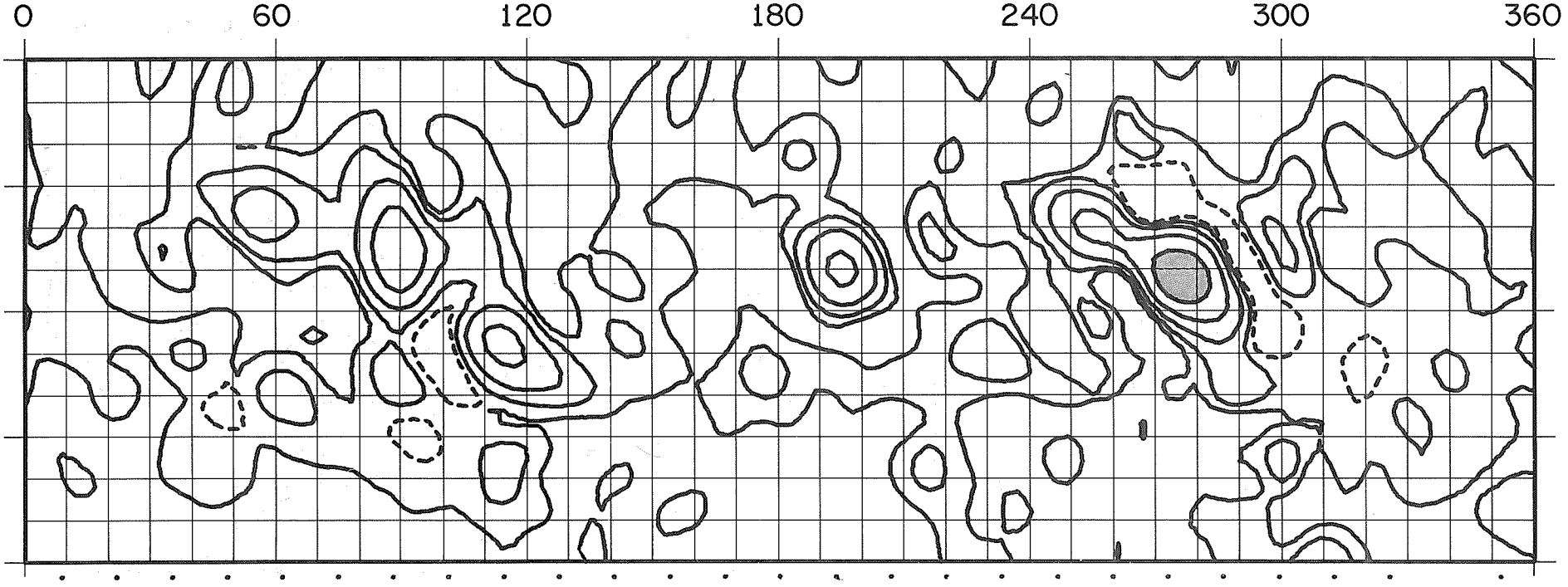

ROTATION NUMBER 1547

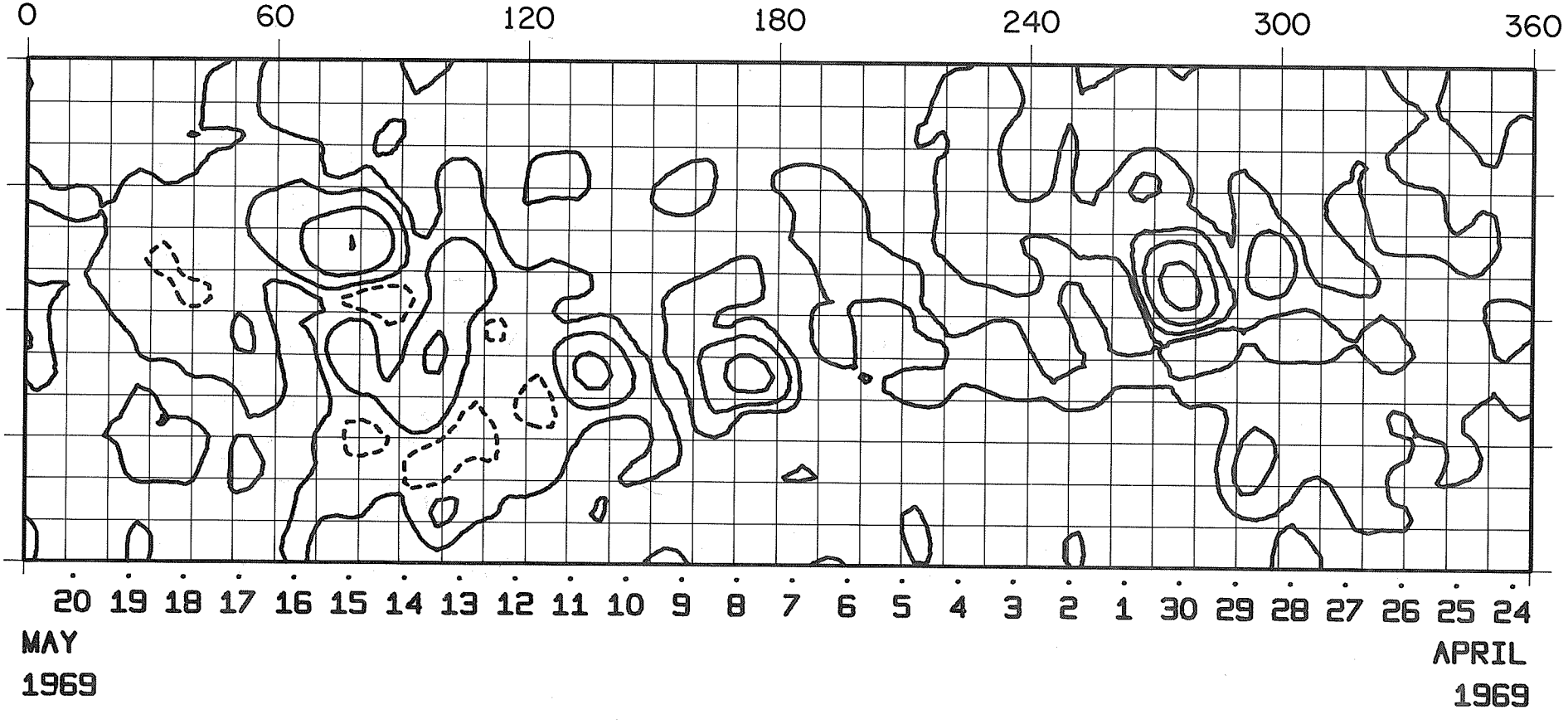

ROTATION NUMBER 1548

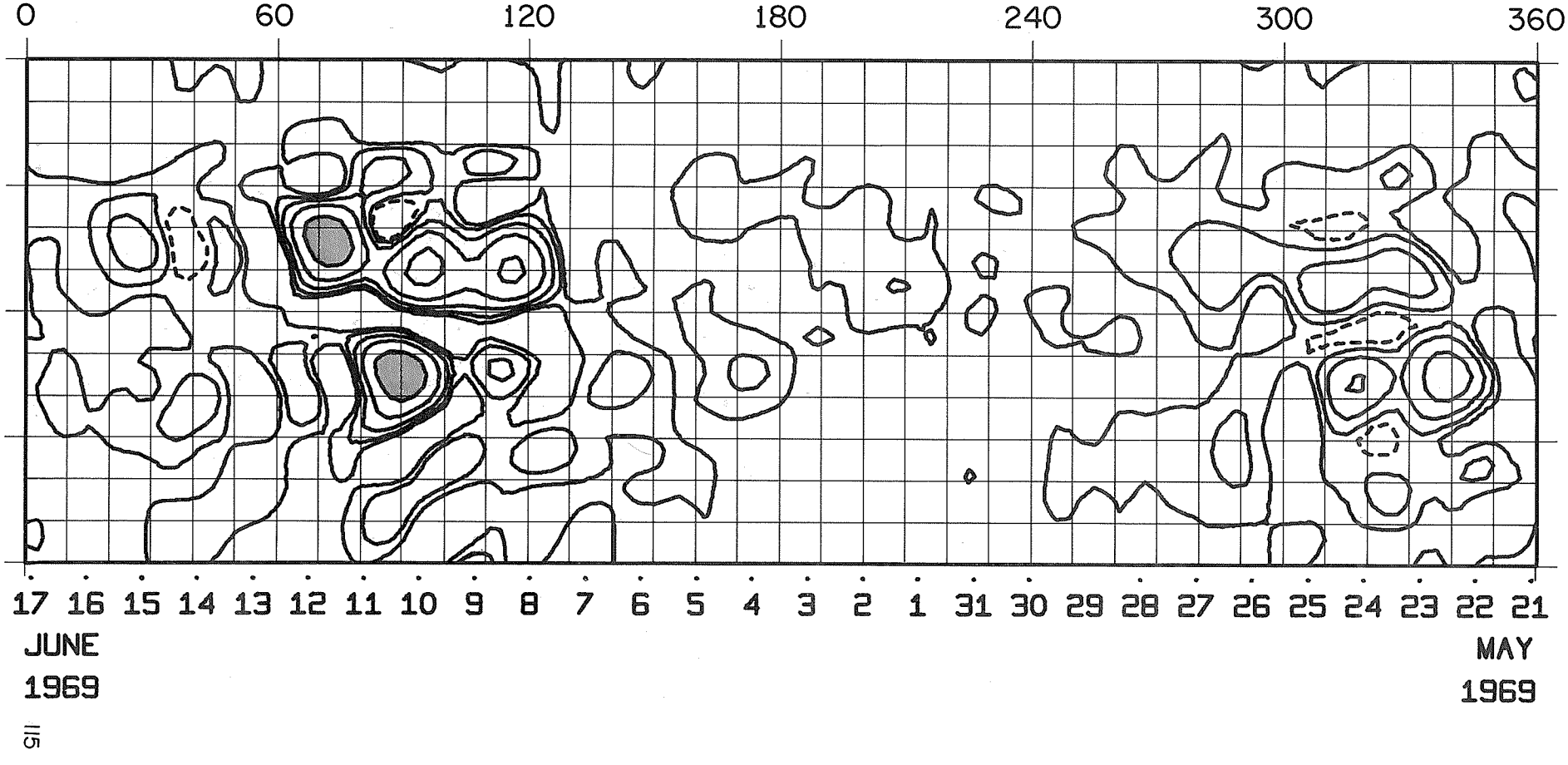

ROTATION NUMBER 1549

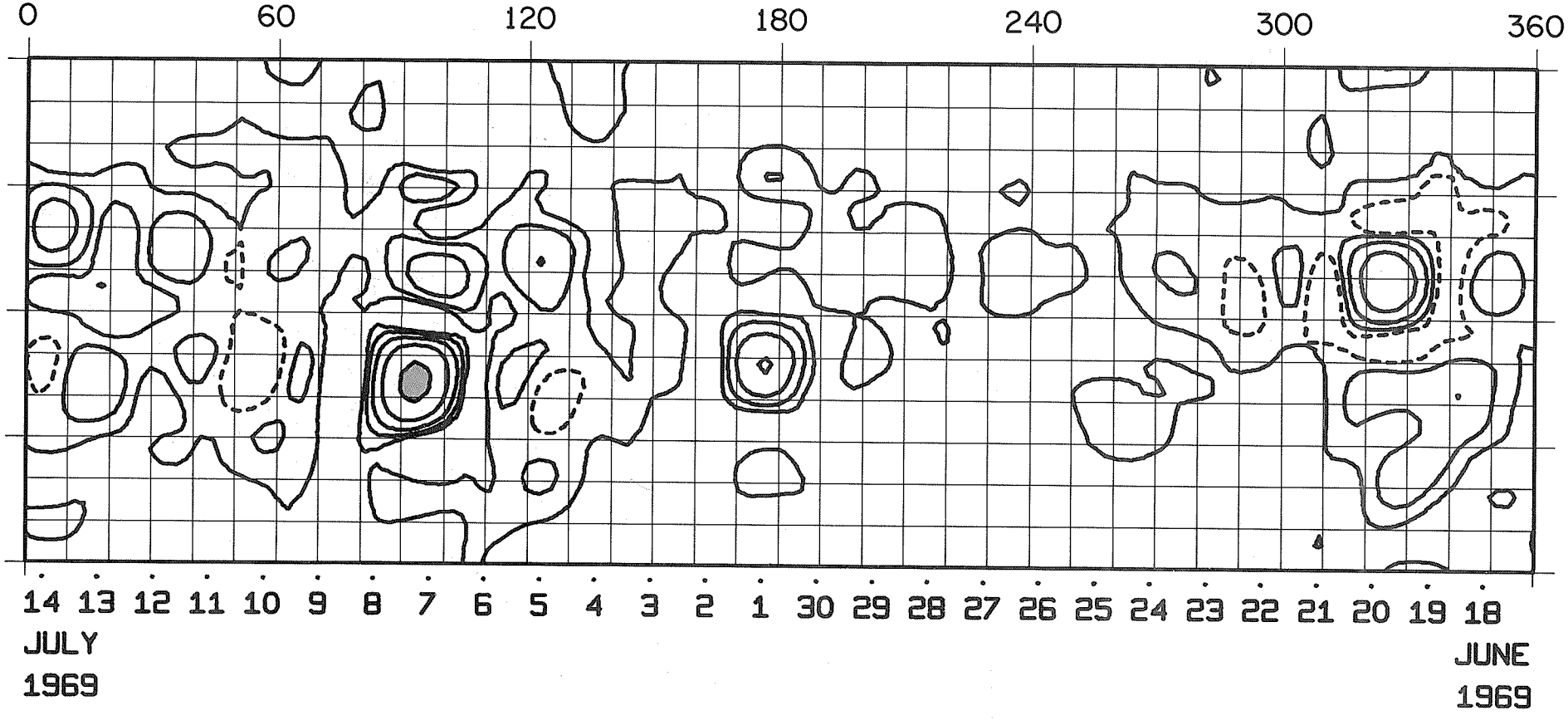

ROTATION NUMBER 1550

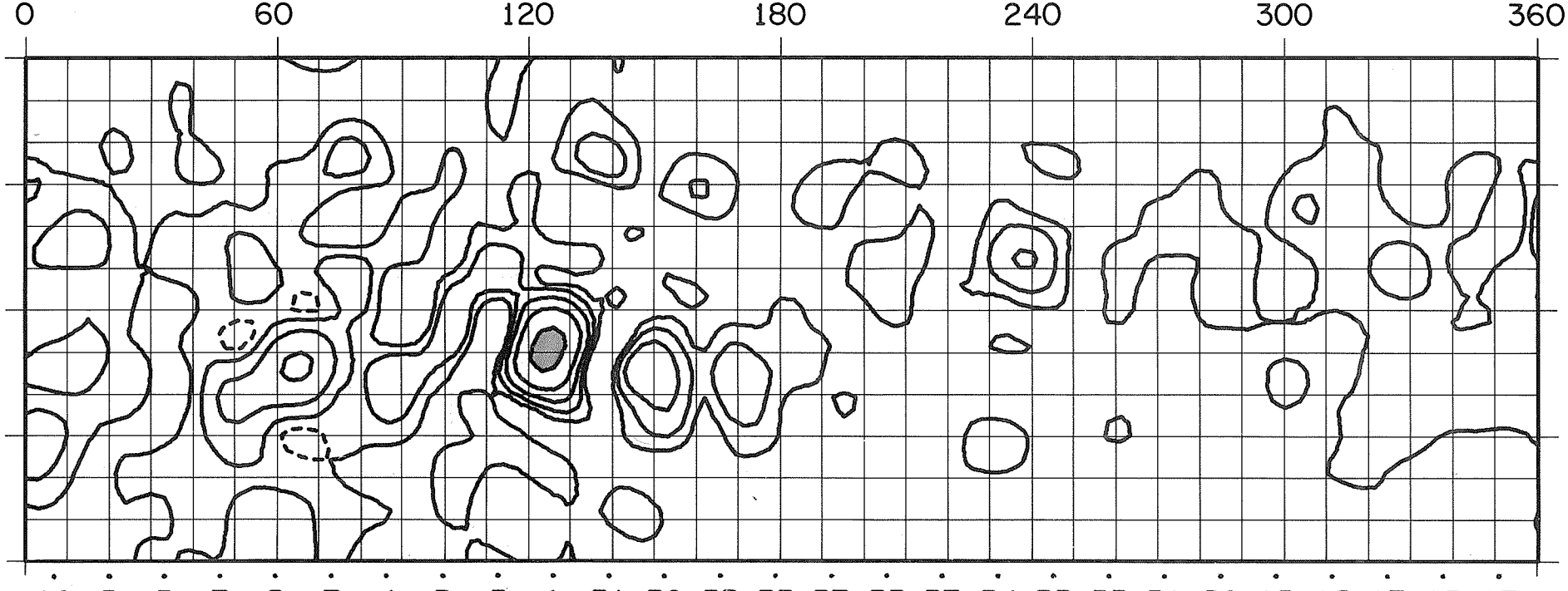

ROTATION NUMBER 1551

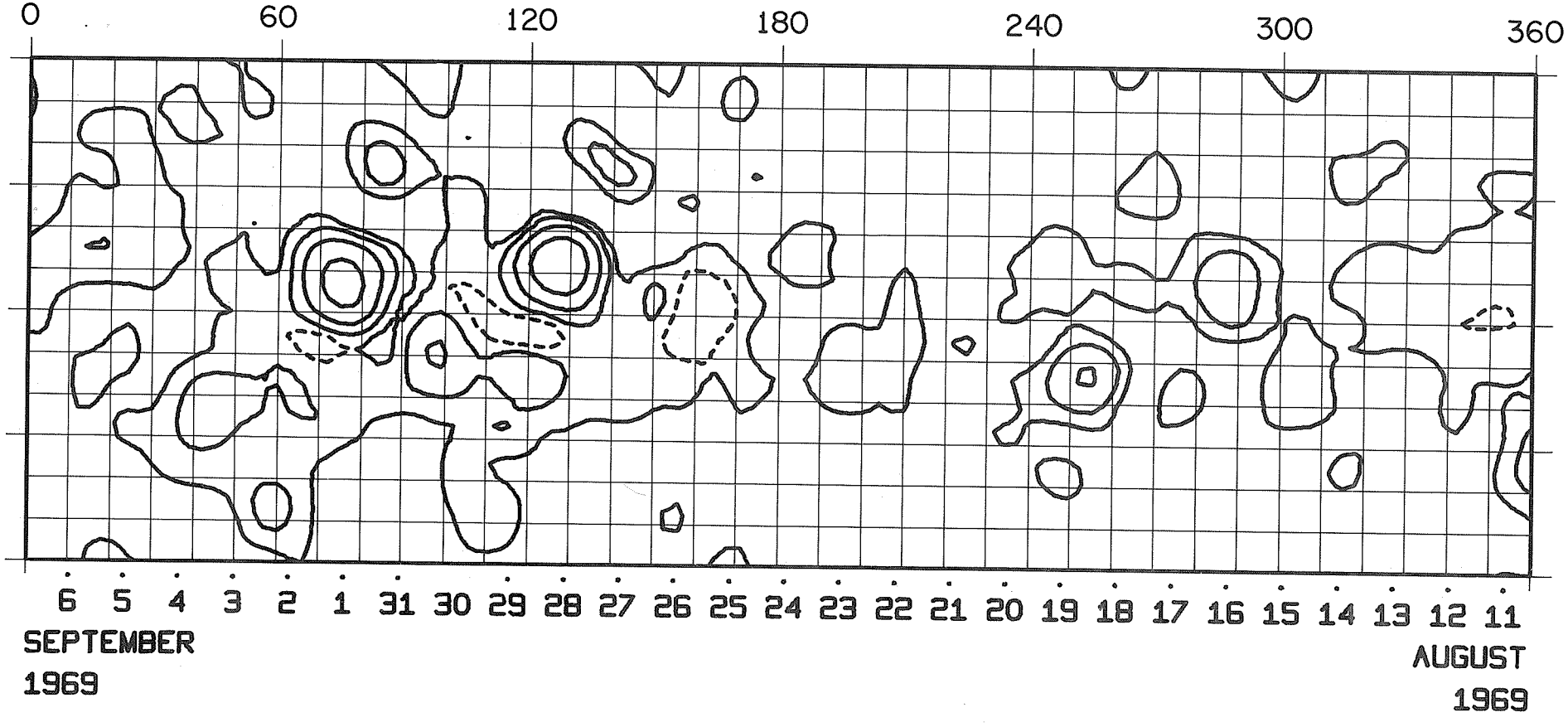

ROTATION NUMBER 1552

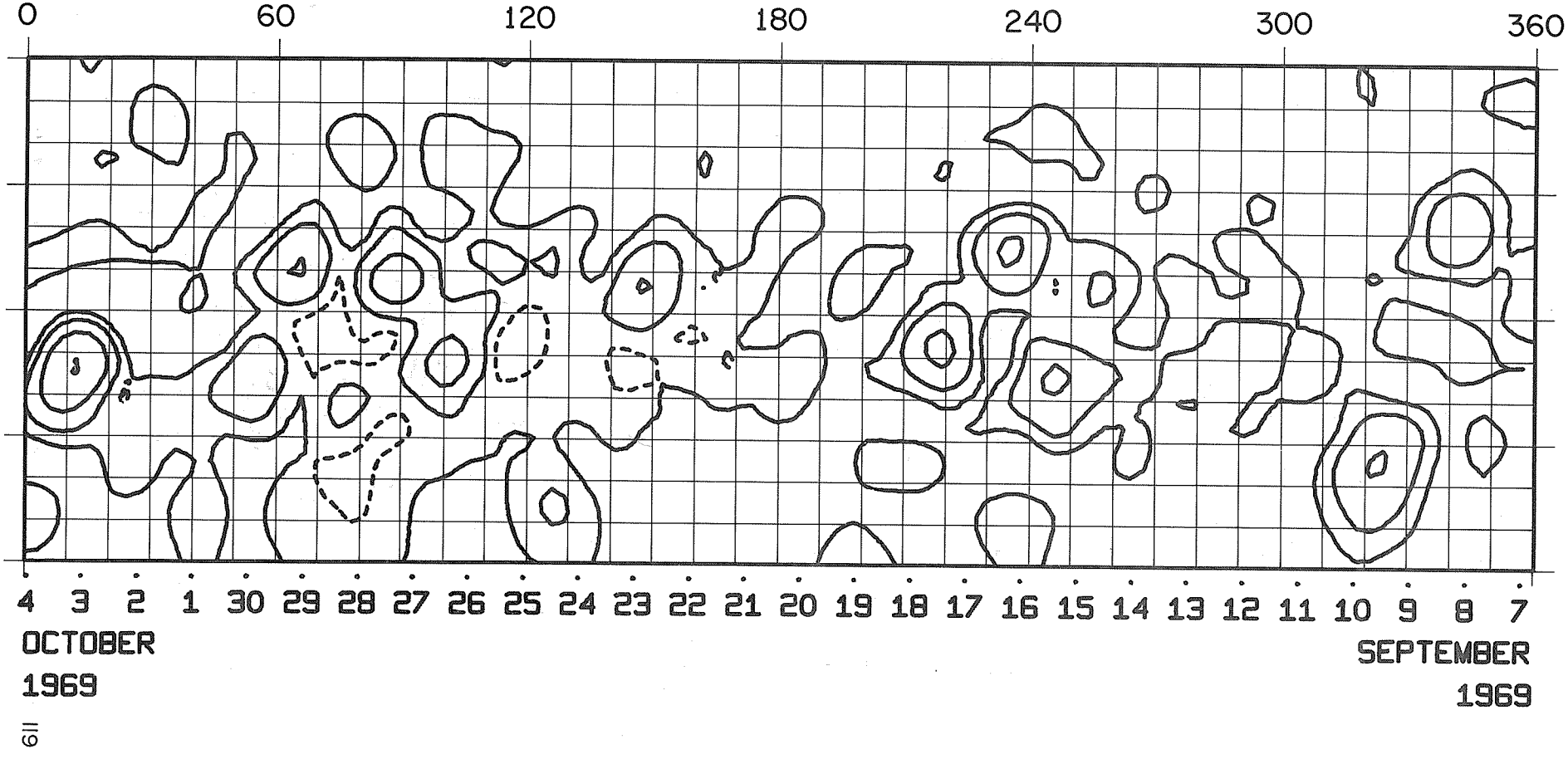

ROTATION NUMBER 1553

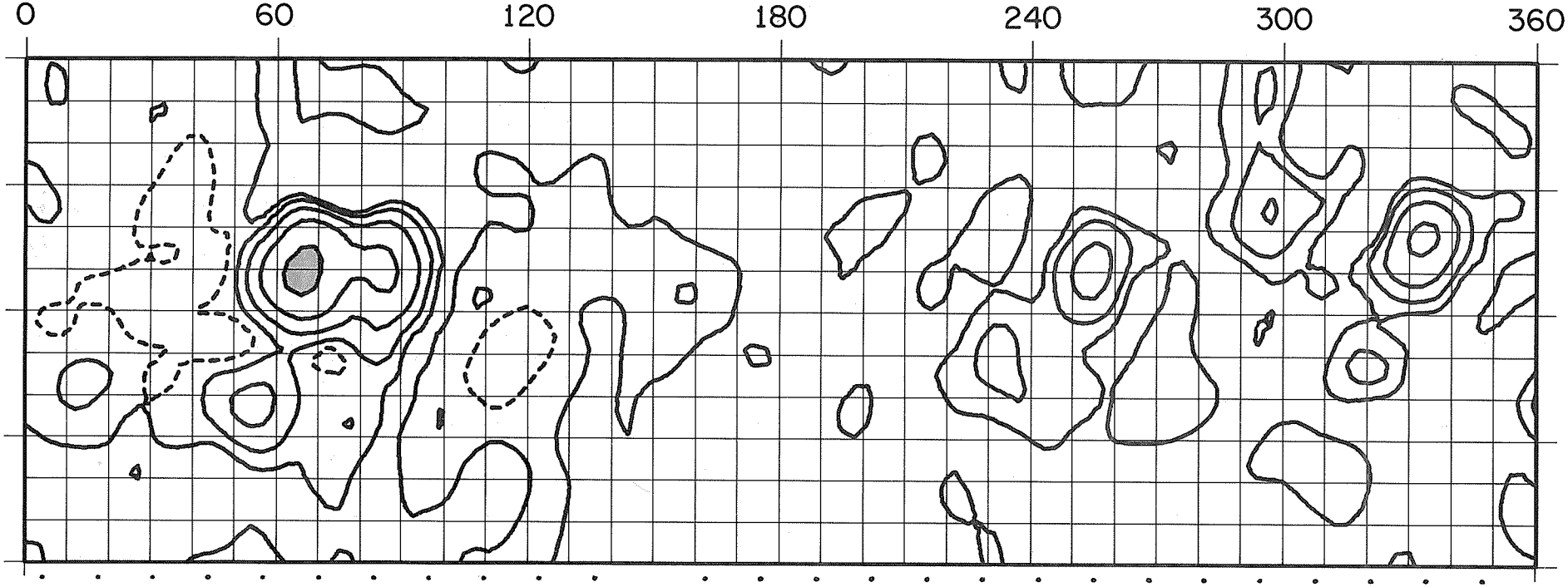

ROTATION NUMBER 1554

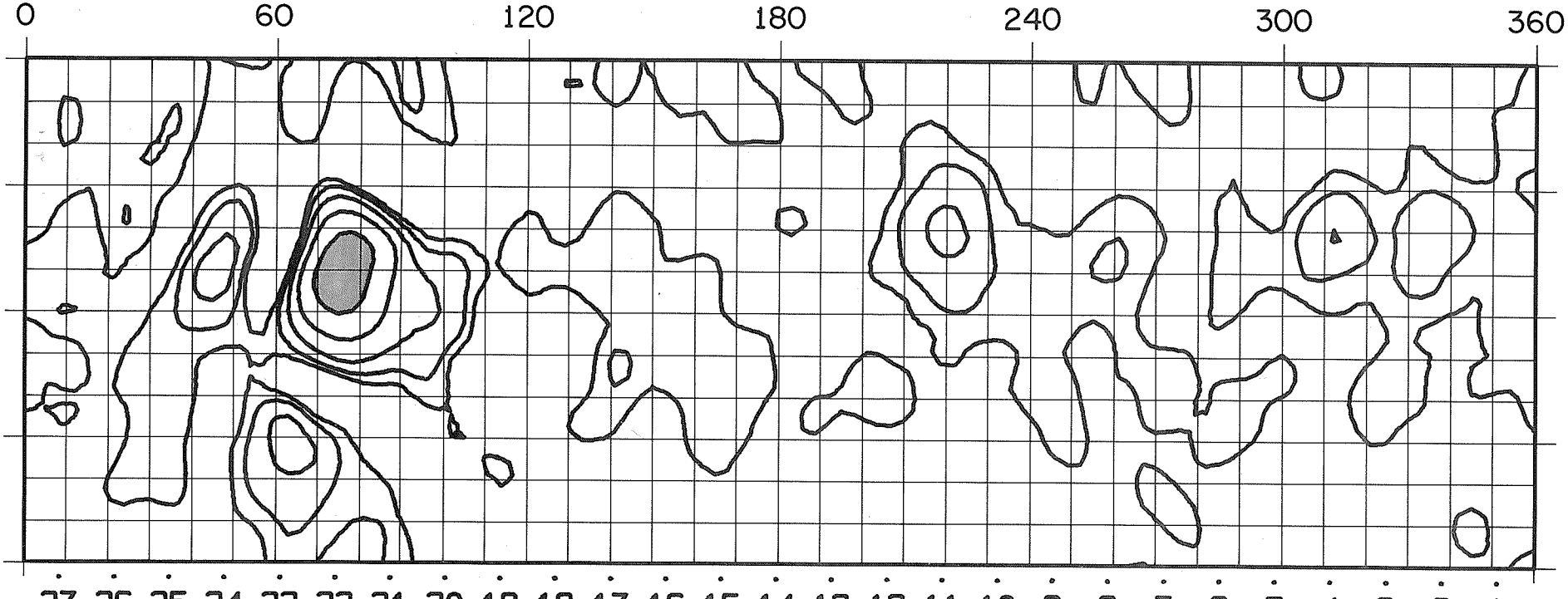

NOVEMBER
1969

NOVEMBER
1969

ROTATION NUMBER 1555

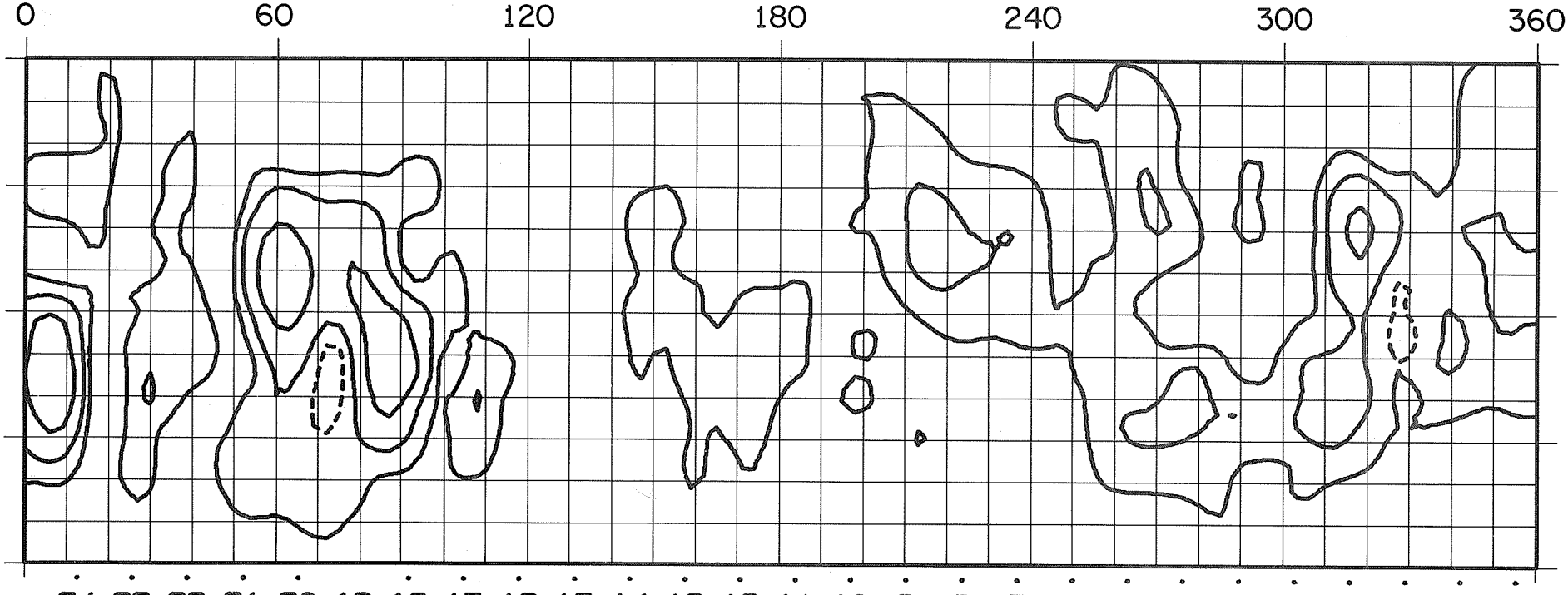

ROTATION NUMBER 1556

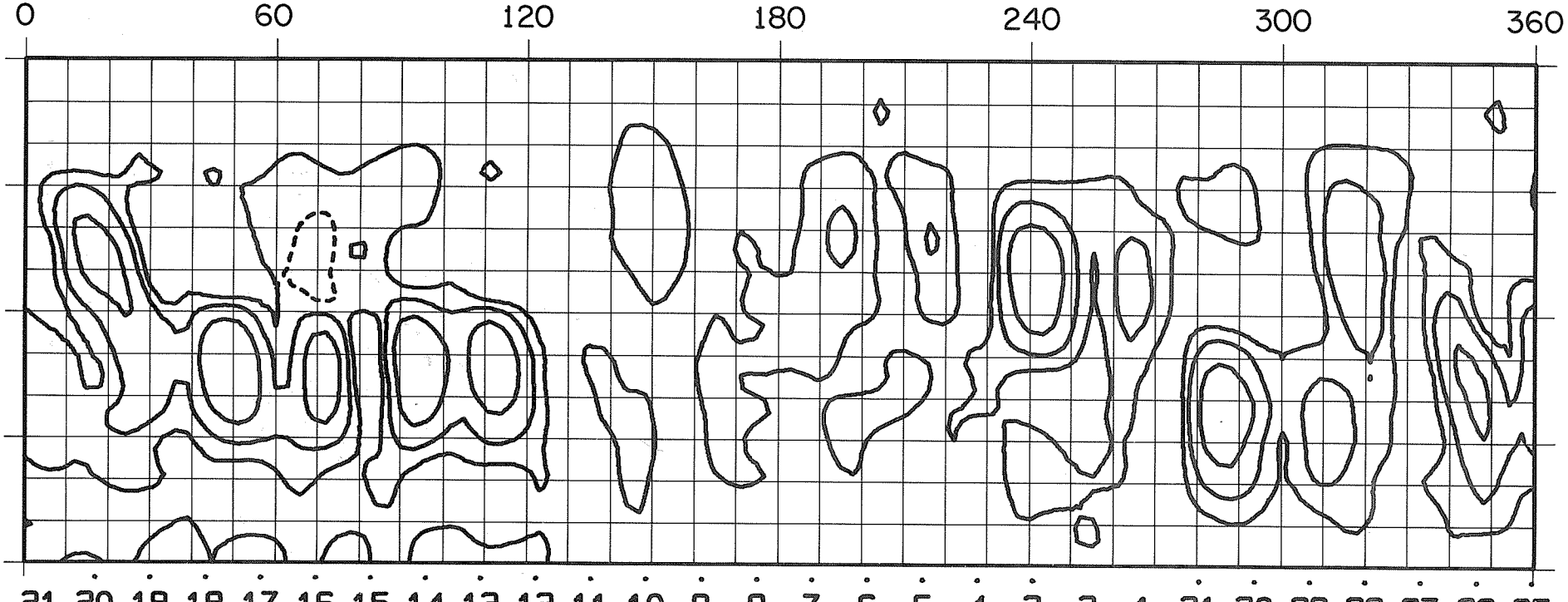

21 20 19 18 17 16 15 14 13 12 11 10 9 8 7 6 5 4 3 2 1 31 30 29 28 27 26 25

JANUARY
1970

DECEMBER
1969

ROTATION NUMBER 1557

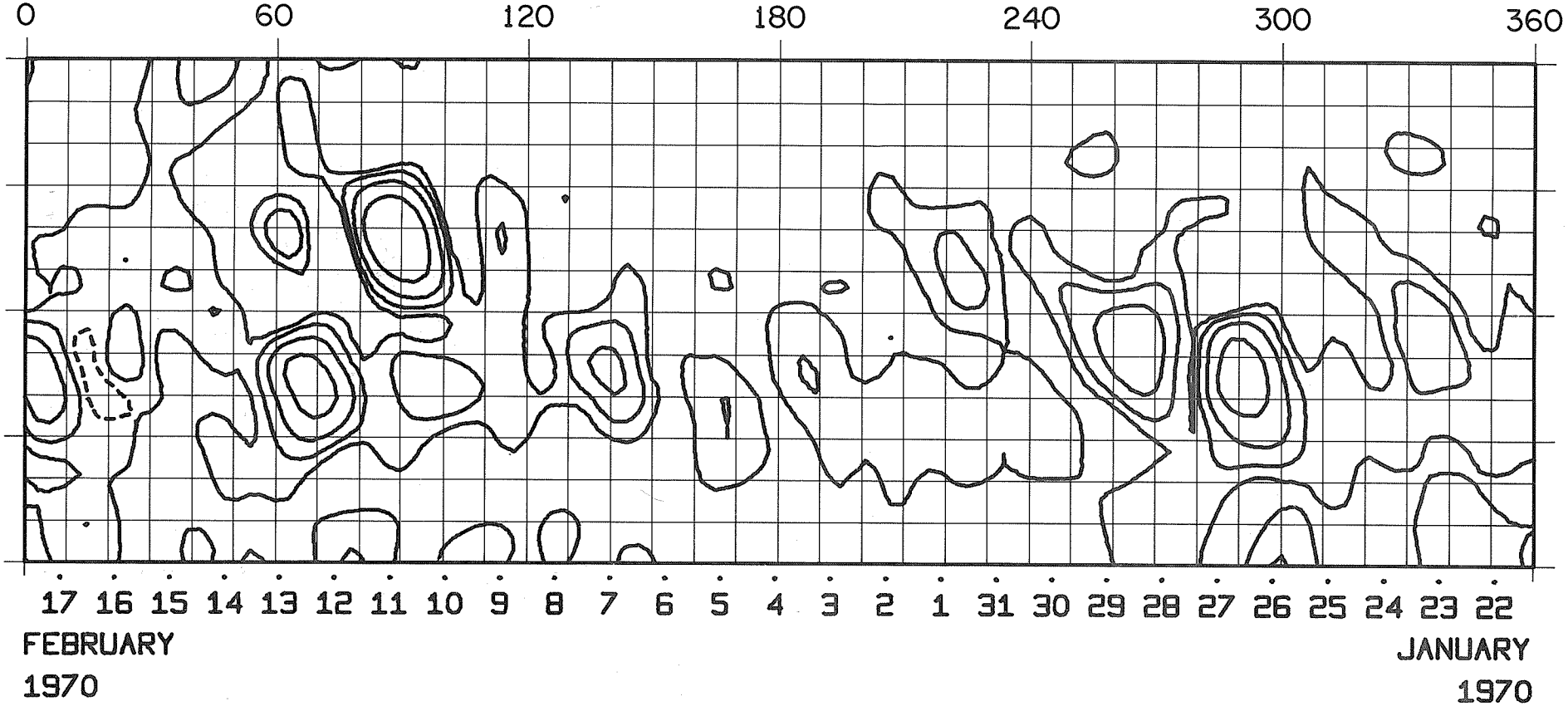

ROTATION NUMBER 1558

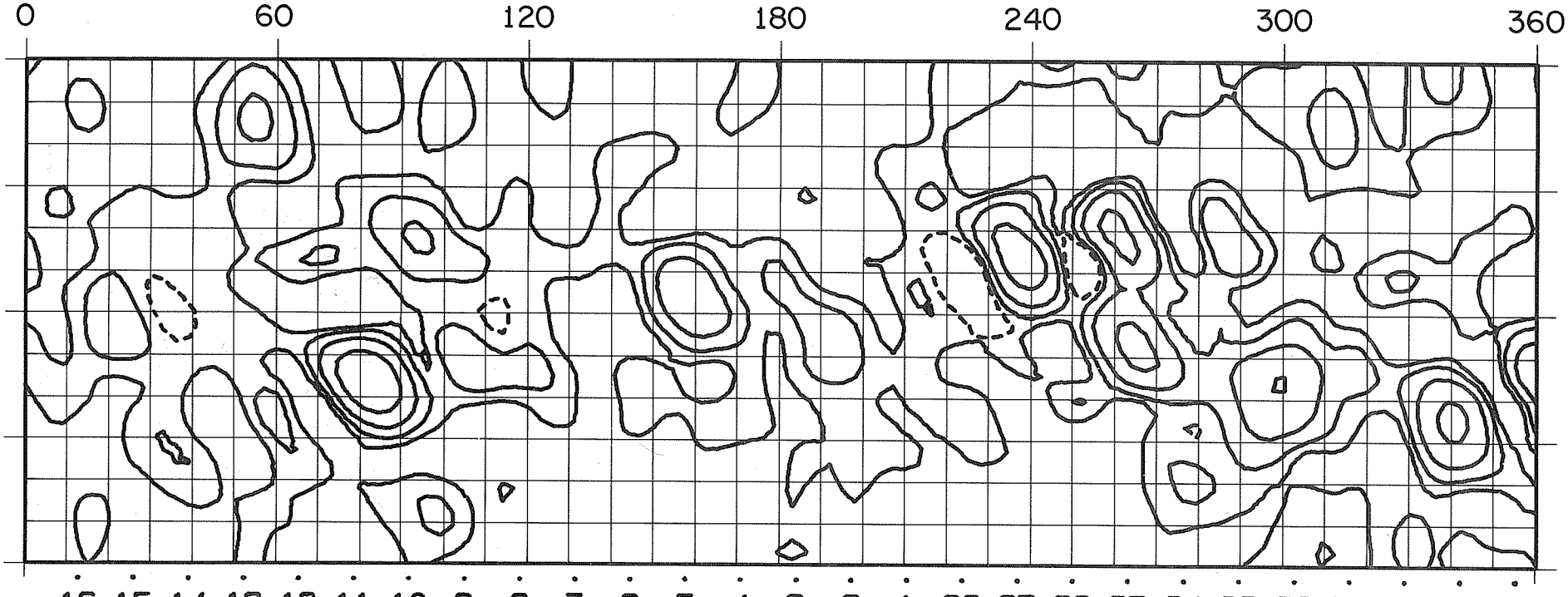

ROTATION NUMBER 1559

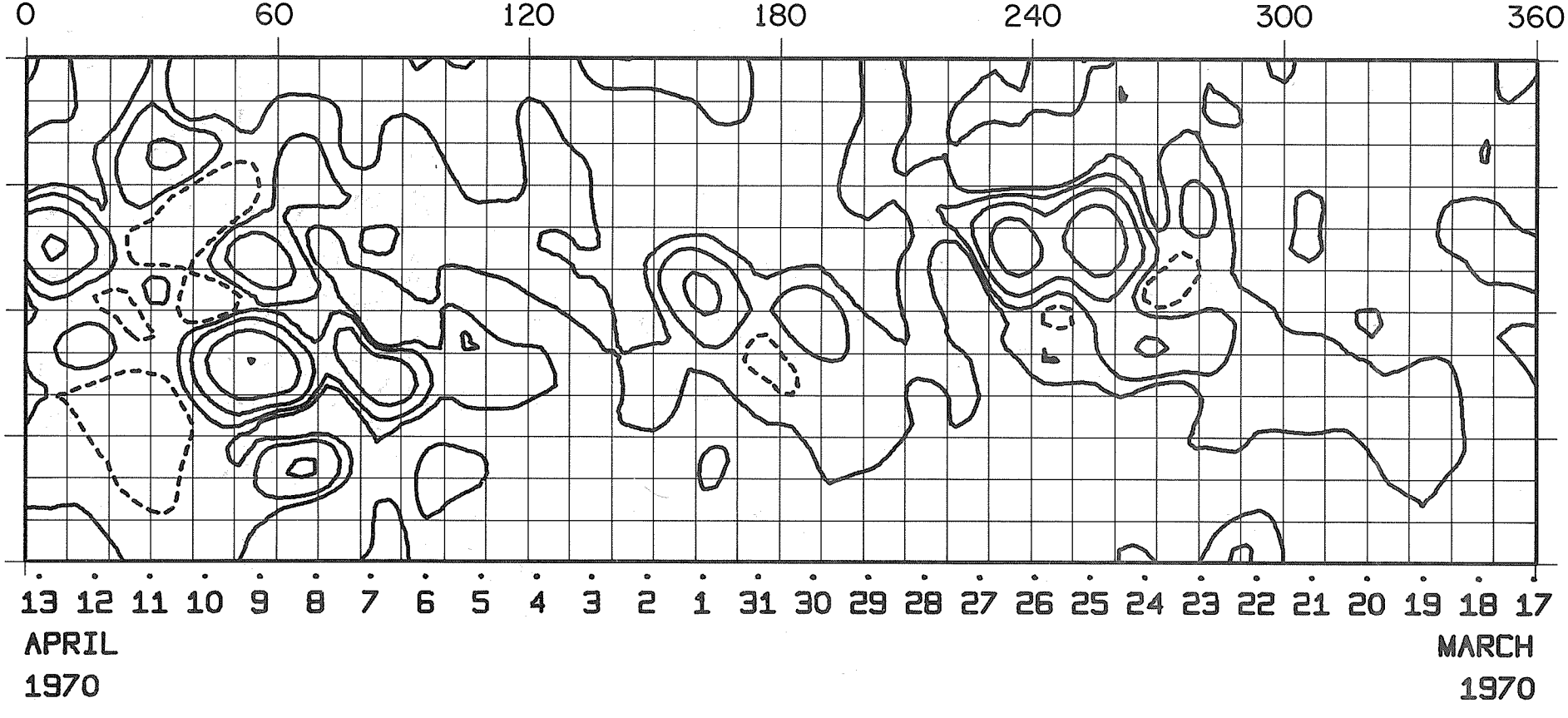

ROTATION NUMBER 1560

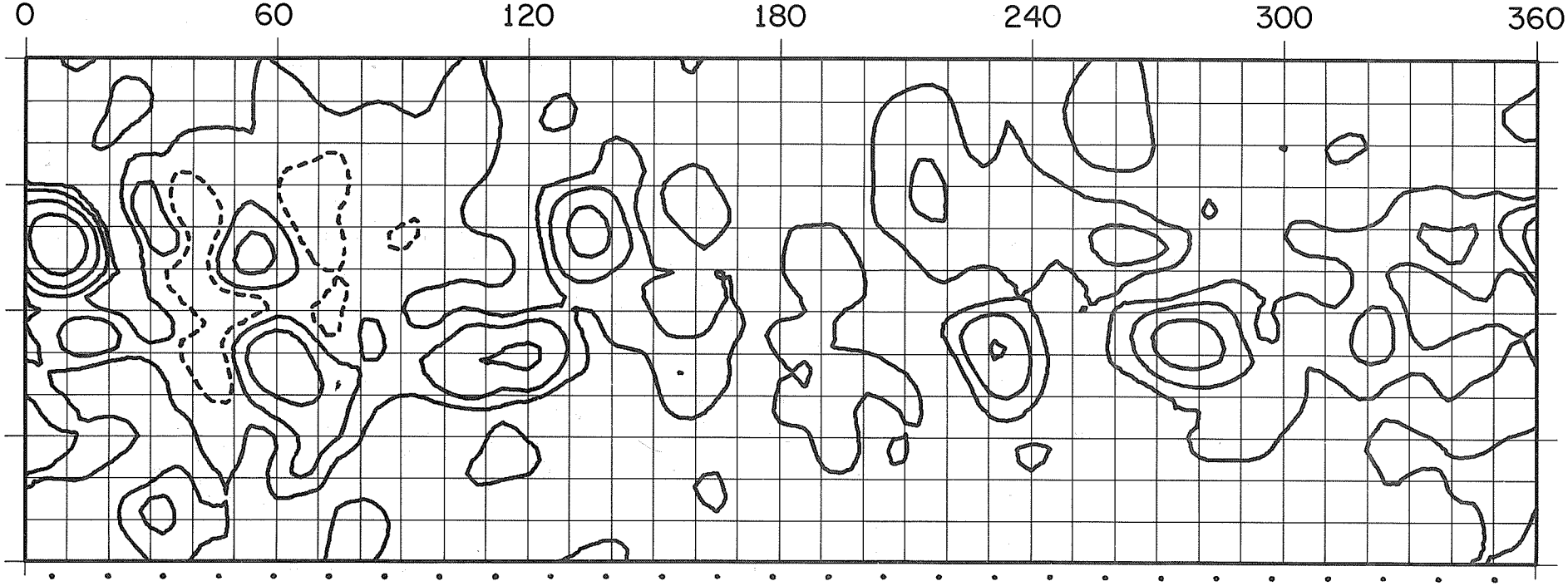

ROTATION NUMBER 1561

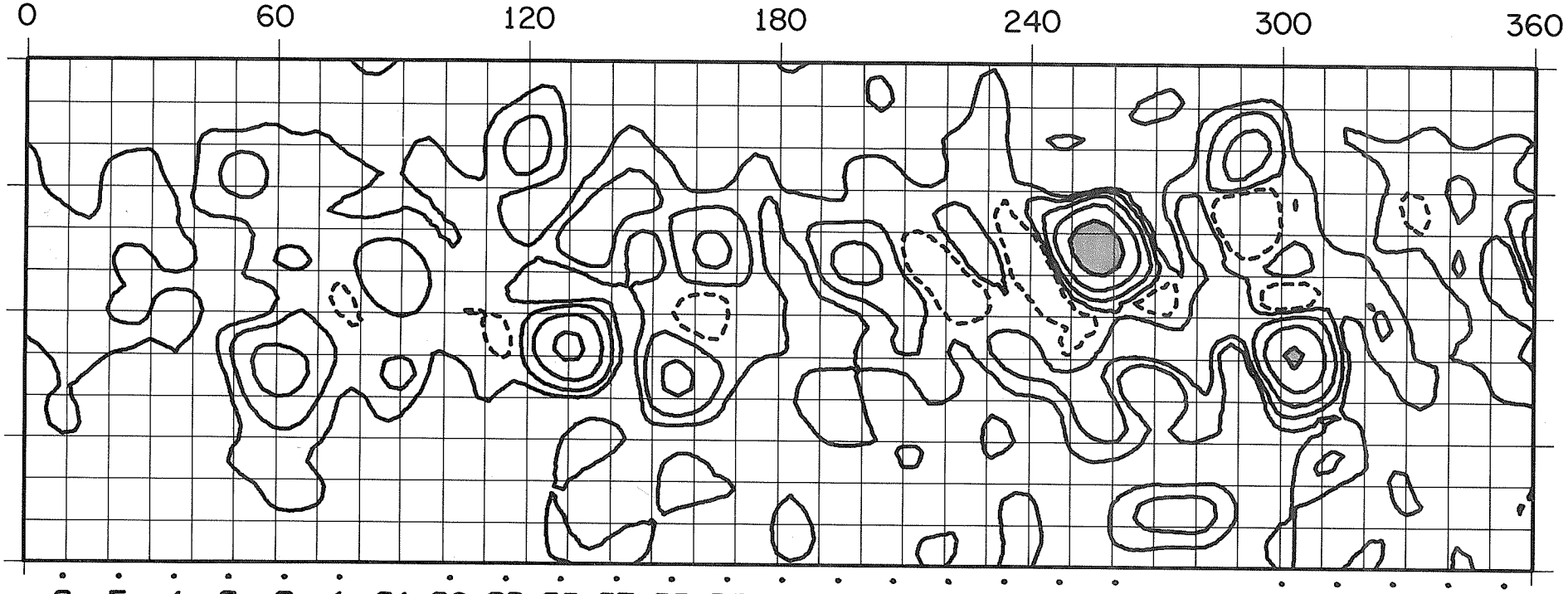

ROTATION NUMBER 1562

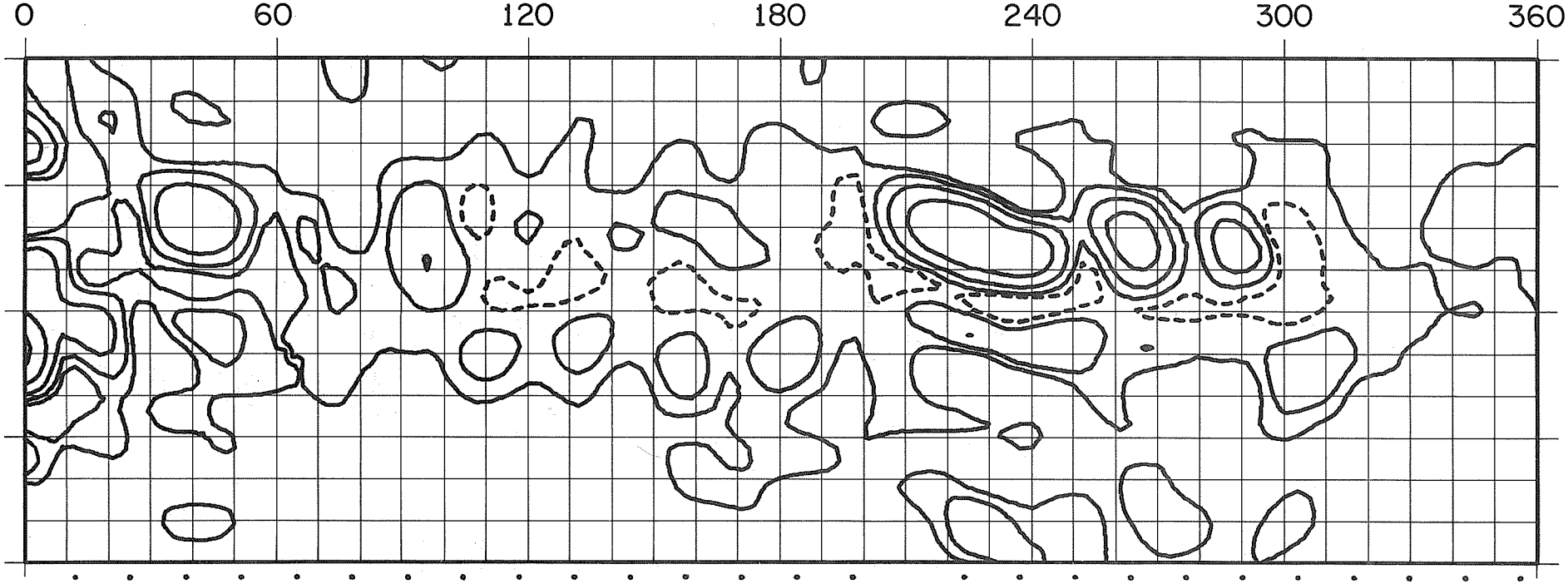

ROTATION NUMBER 1563

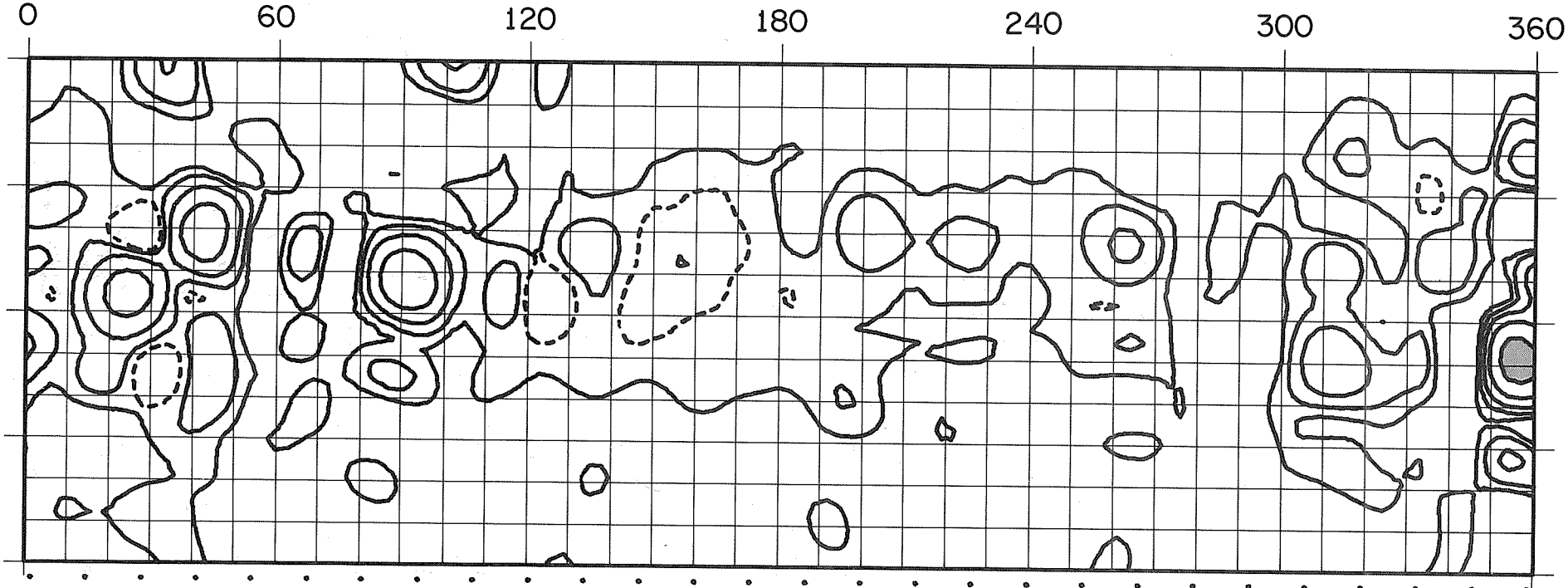

ROTATION NUMBER 1564

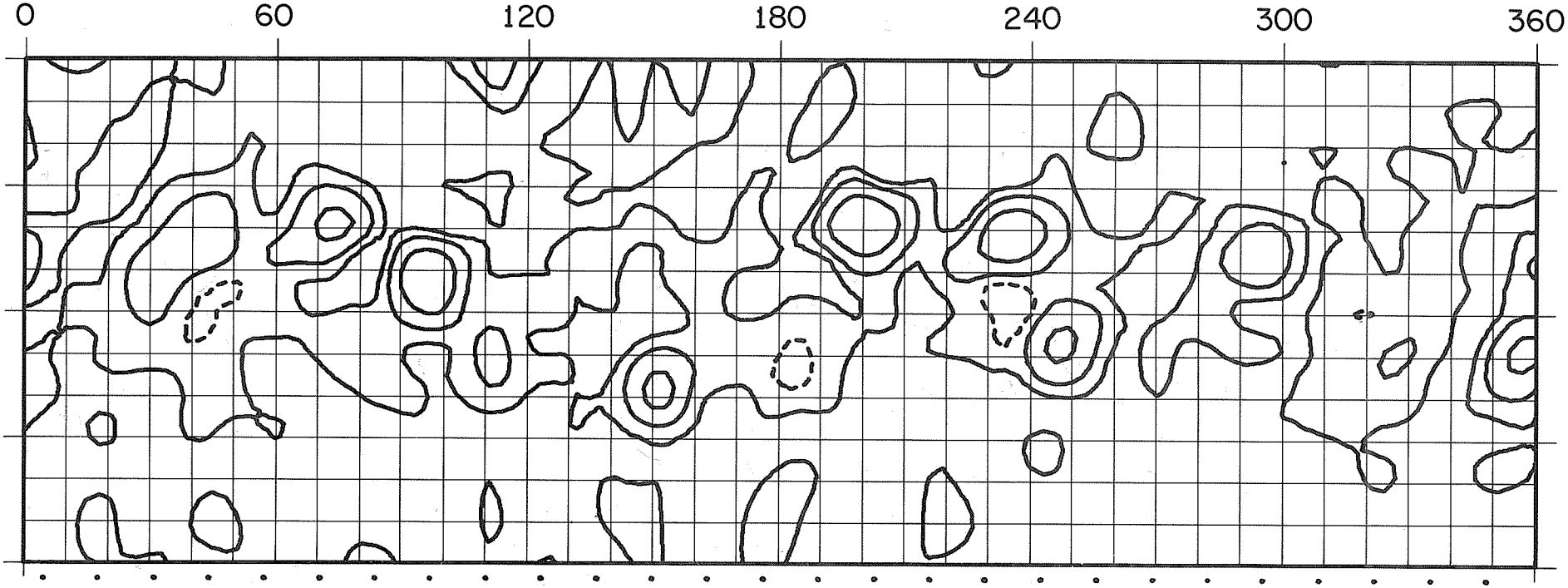

ROTATION NUMBER 1565

ROTATION NUMBER 1566

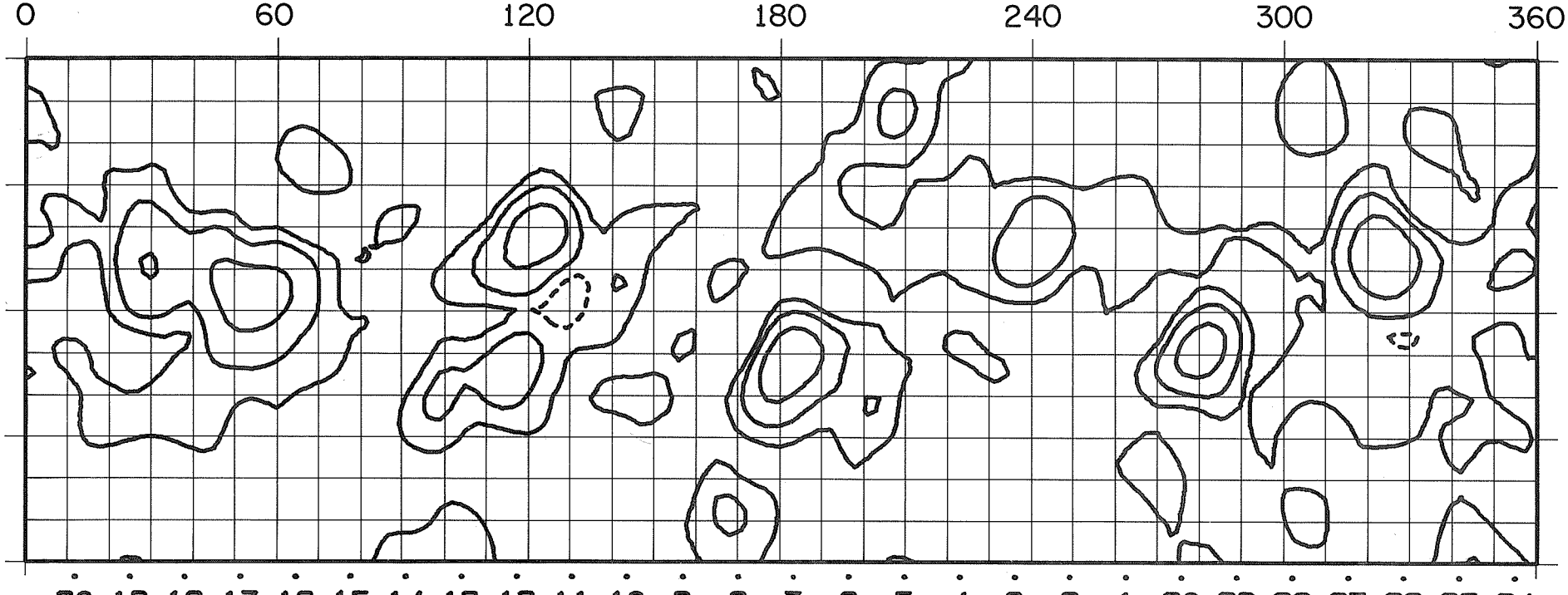

ROTATION NUMBER 1567

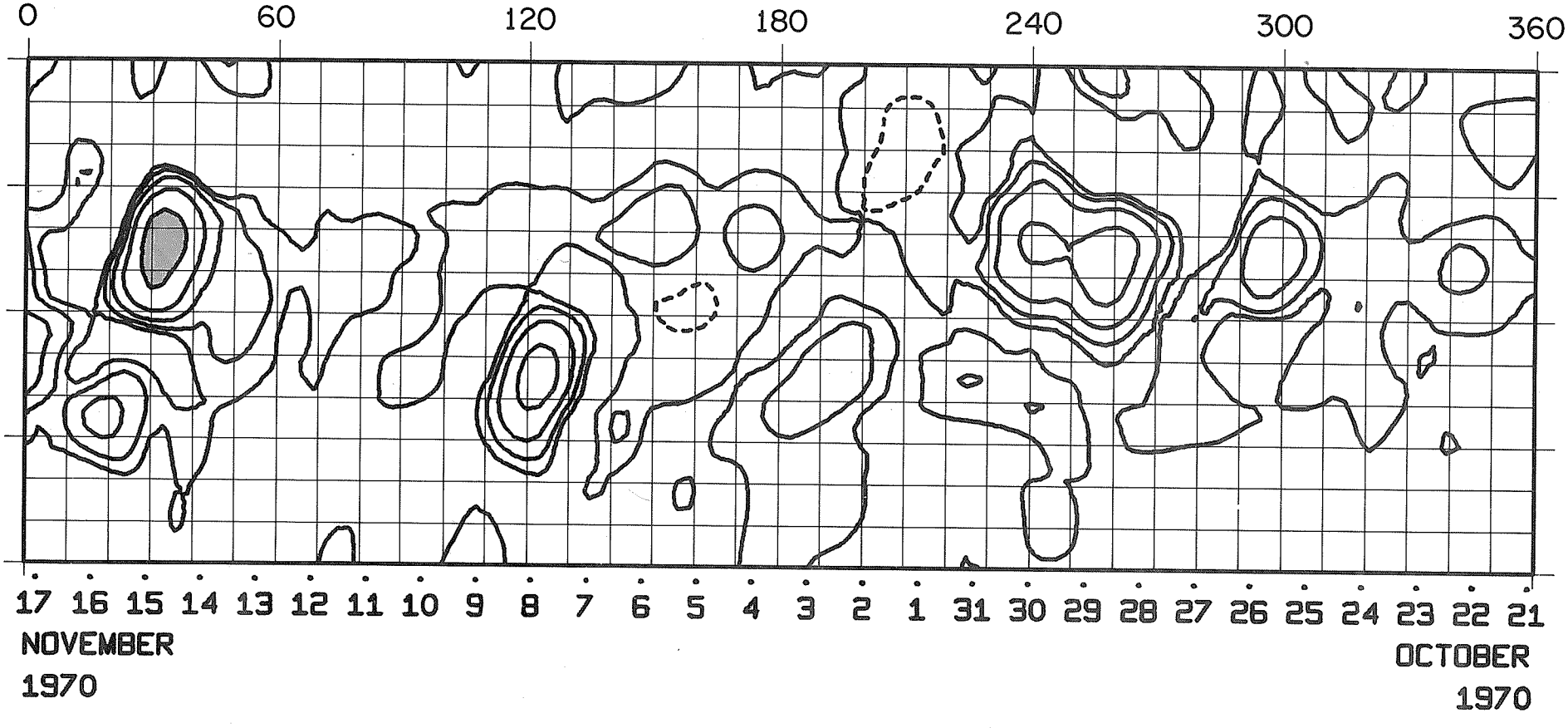

ROTATION NUMBER 1568

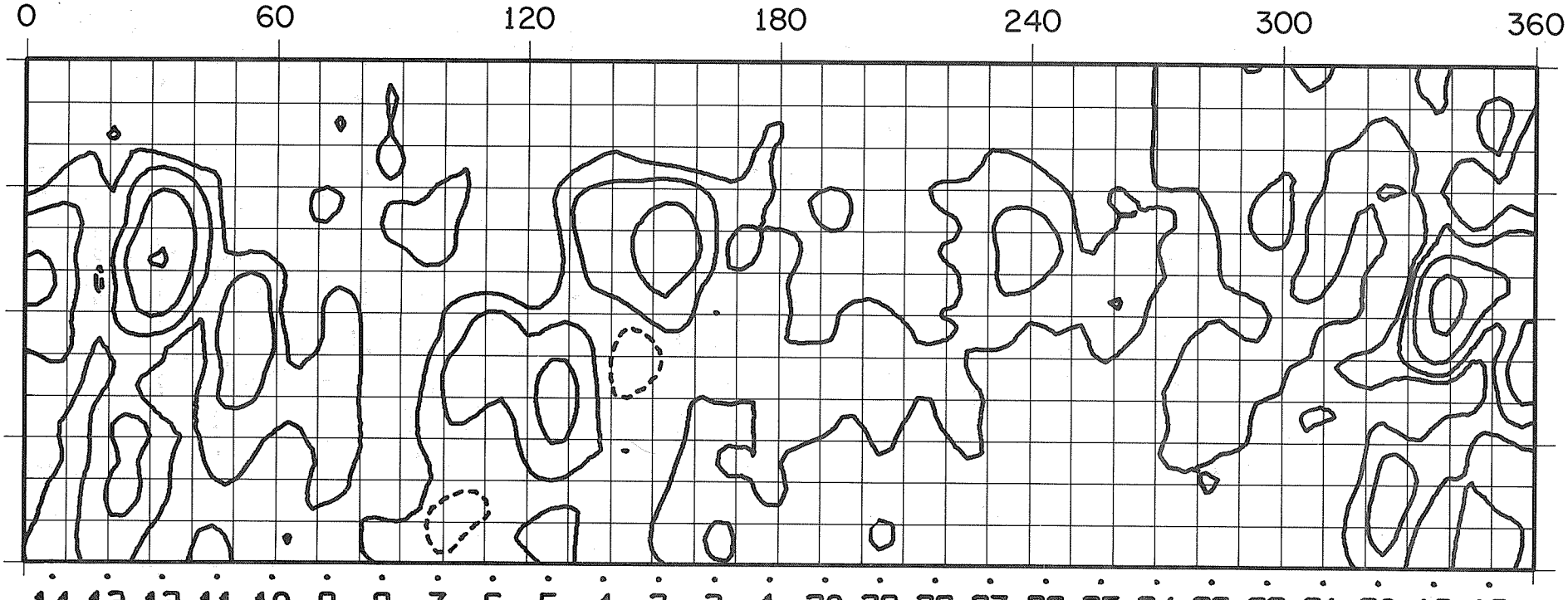

ROTATION NUMBER 1569

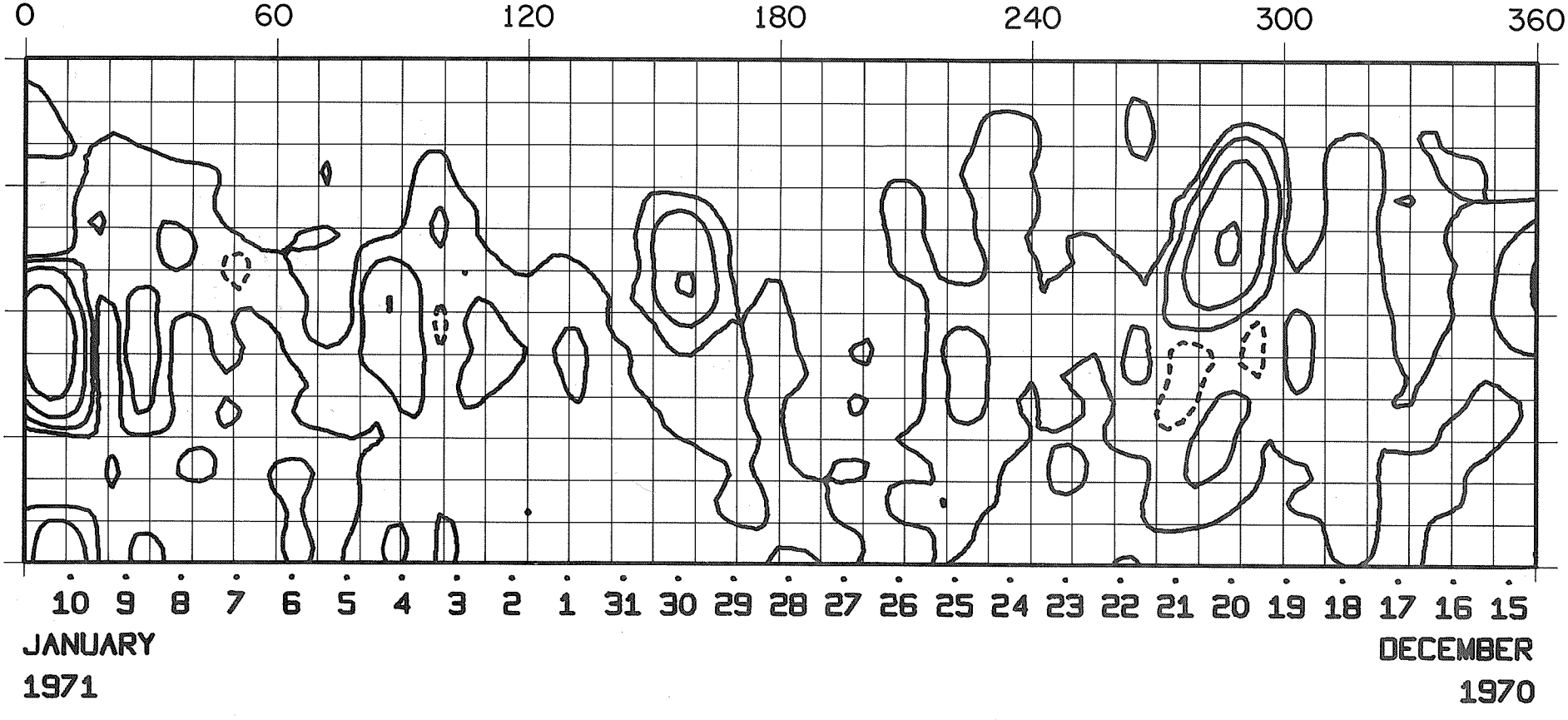

ROTATION NUMBER 1570

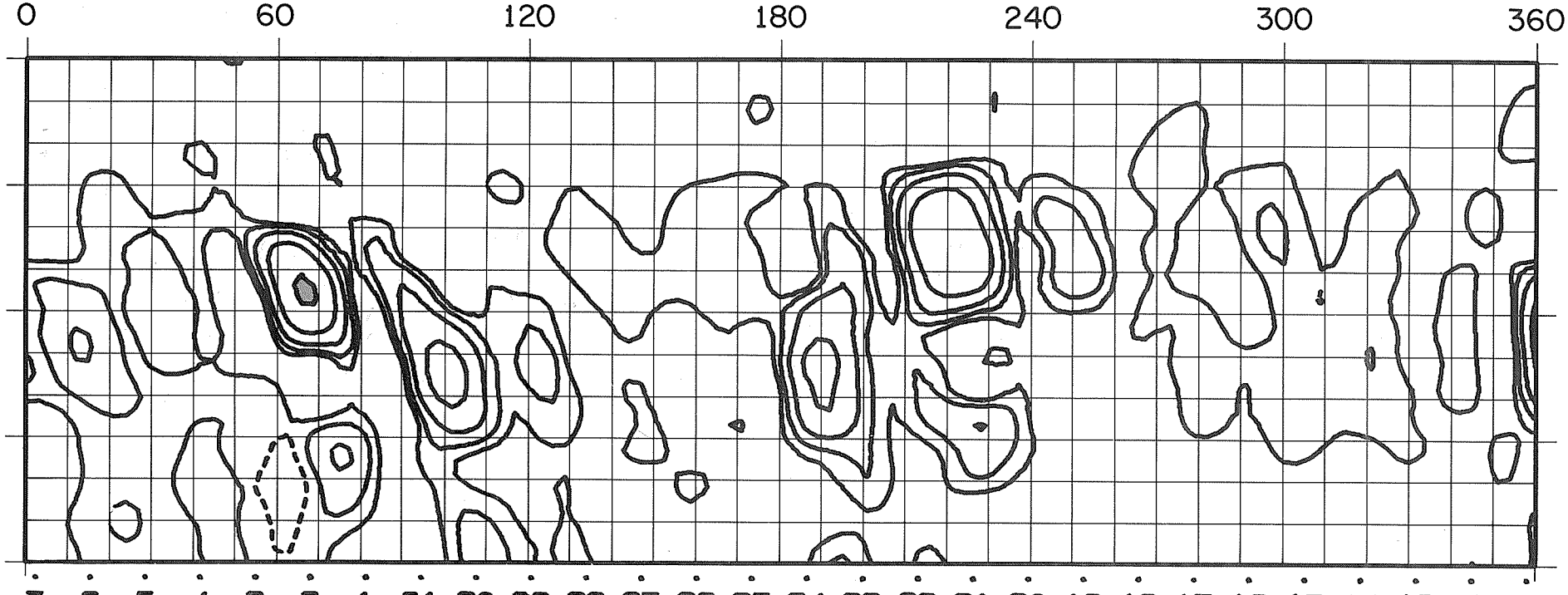

ROTATION NUMBER 1571

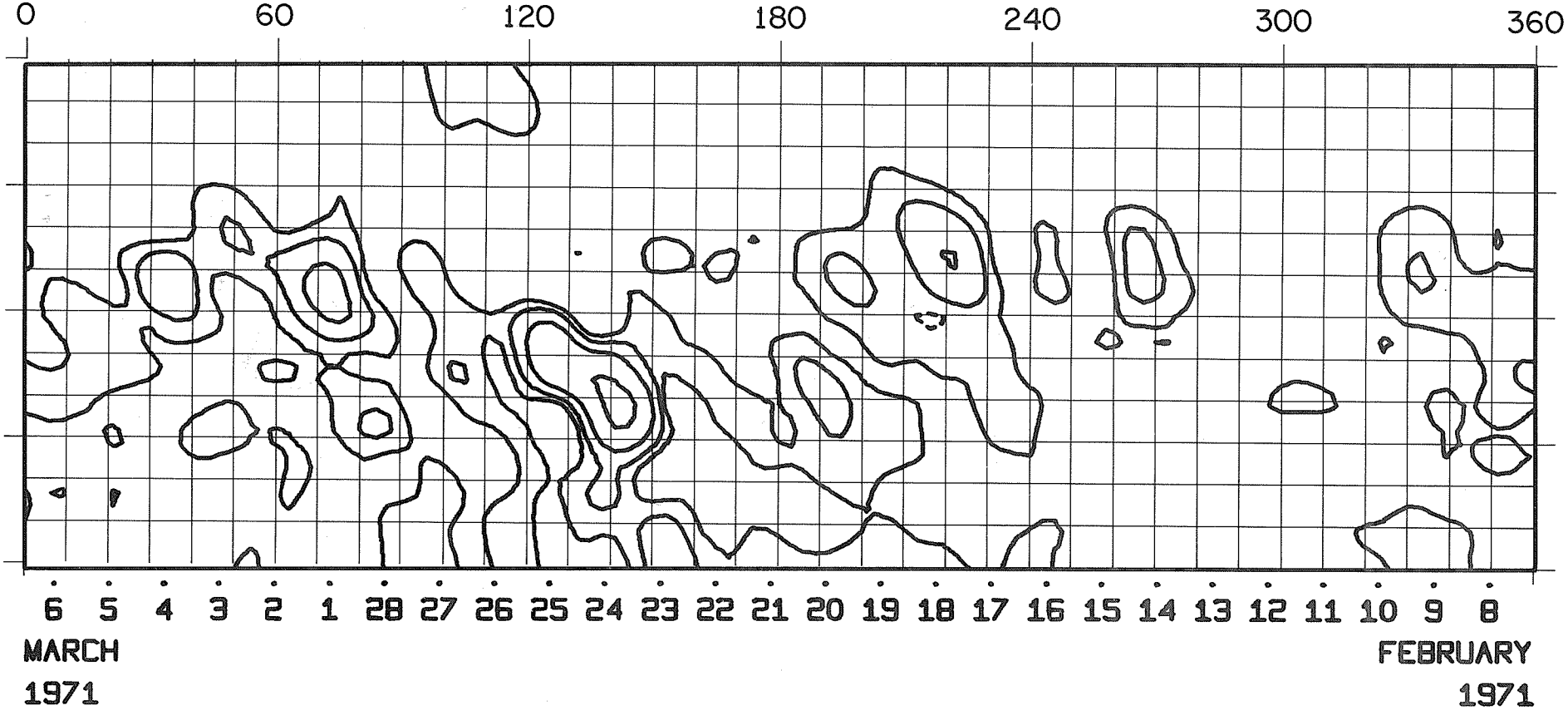

ROTATION NUMBER 1572

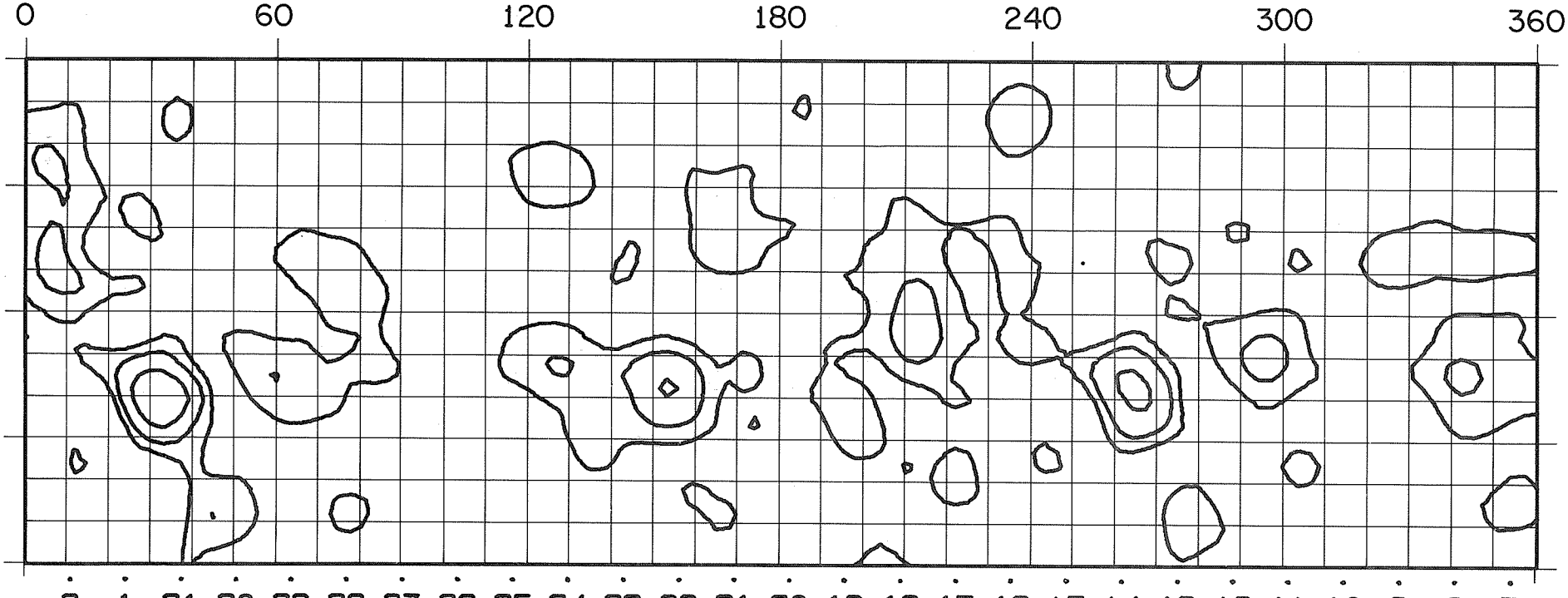

ROTATION NUMBER 1573

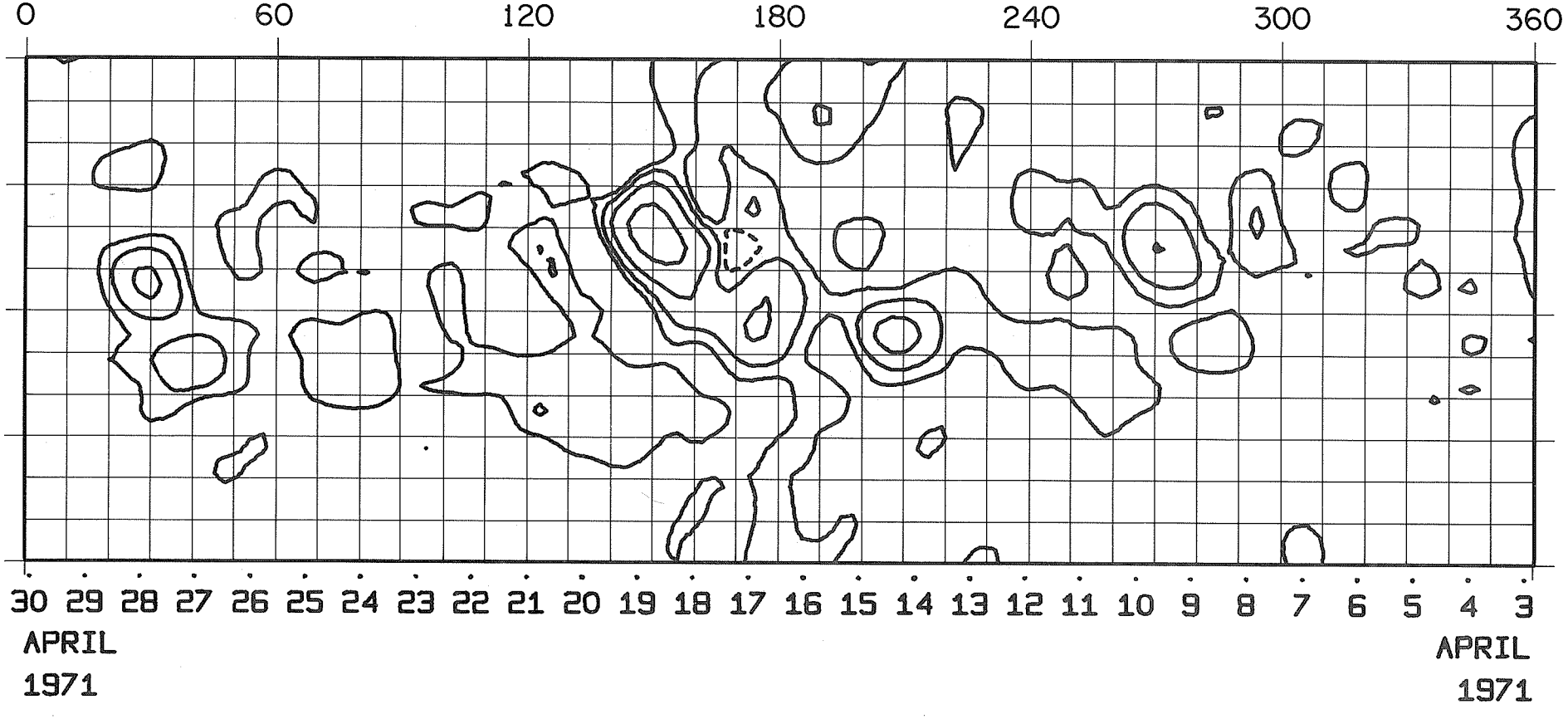

ROTATION NUMBER 1574

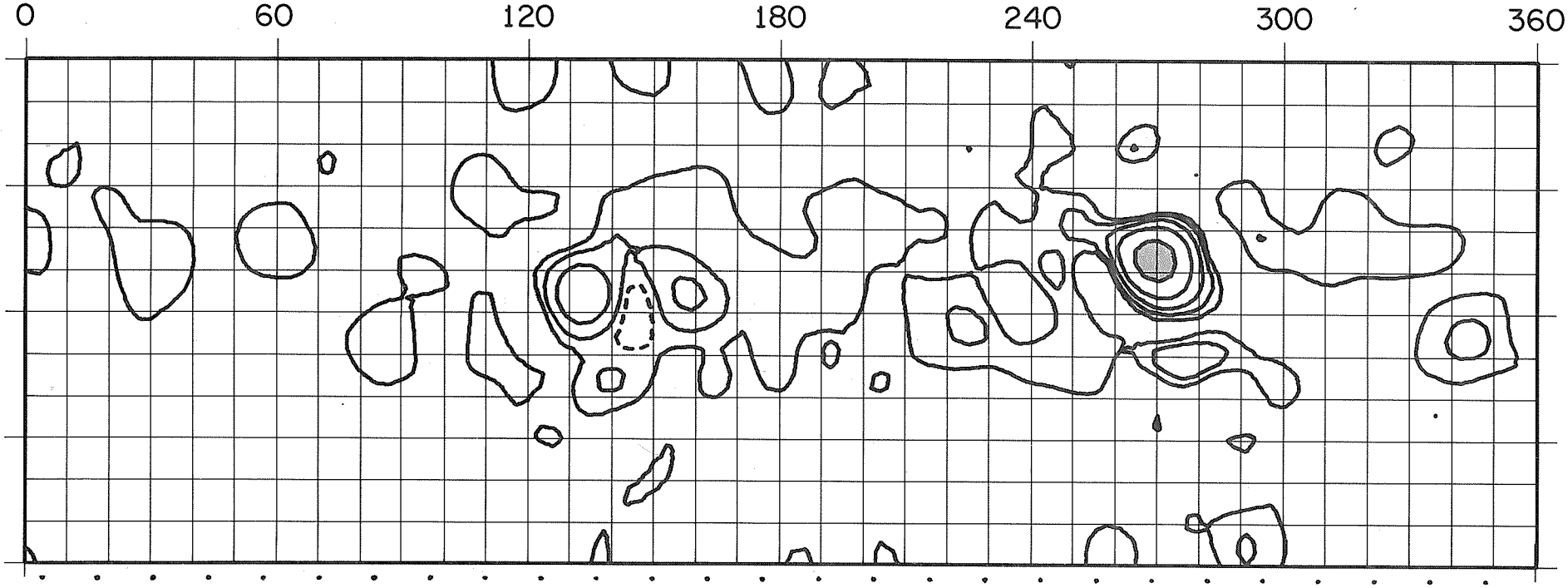

ROTATION NUMBER 1575

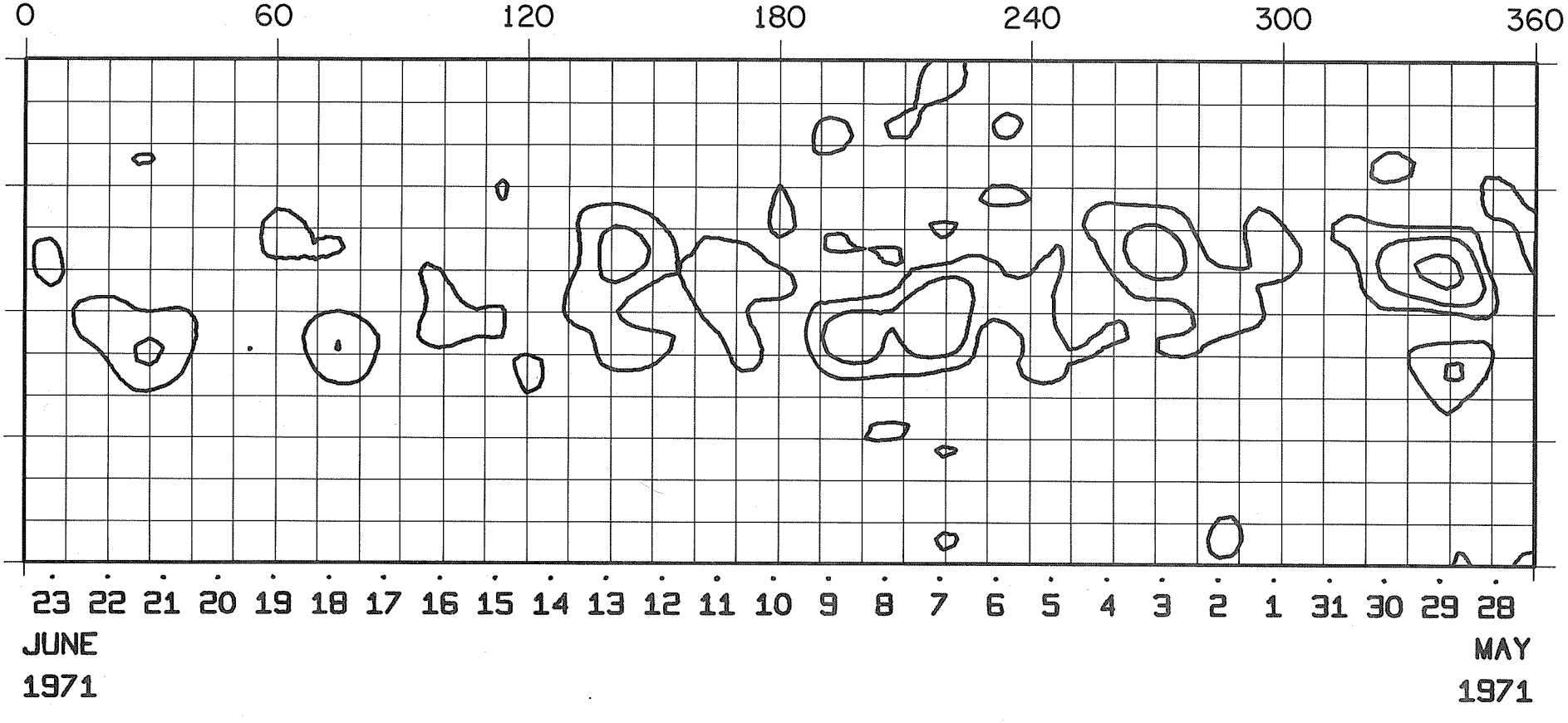

ROTATION NUMBER 1576

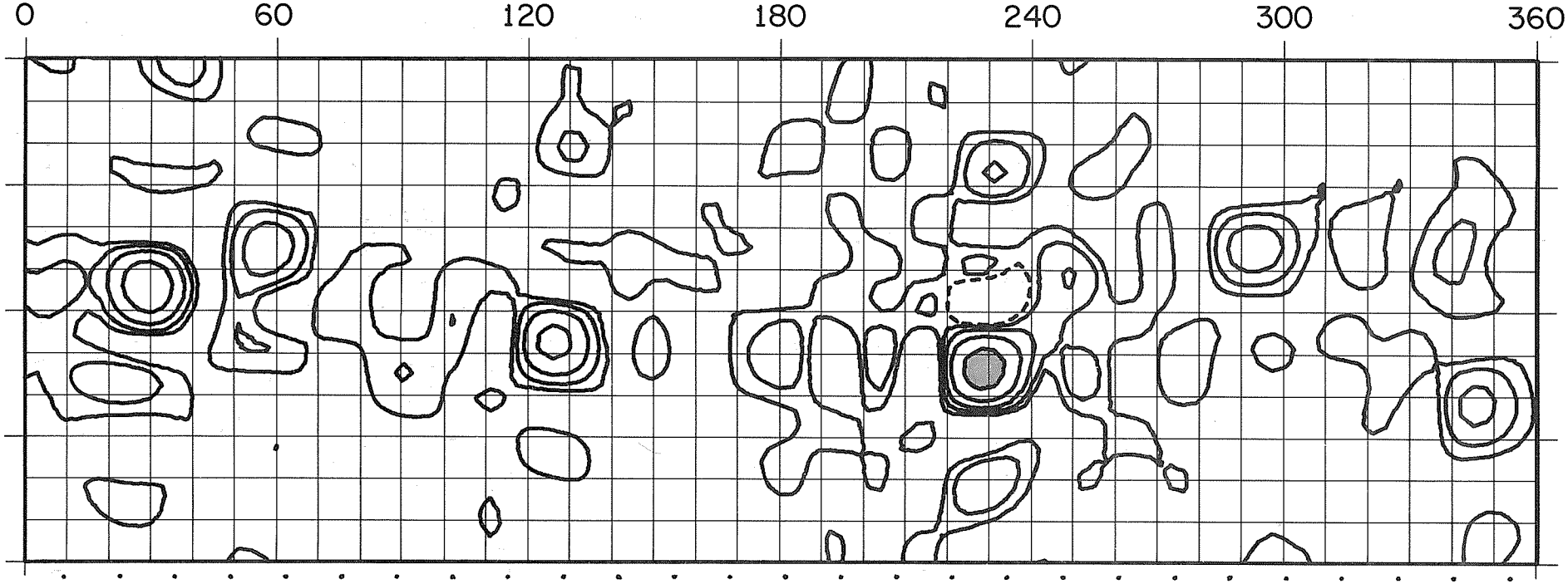

ROTATION NUMBER 1577

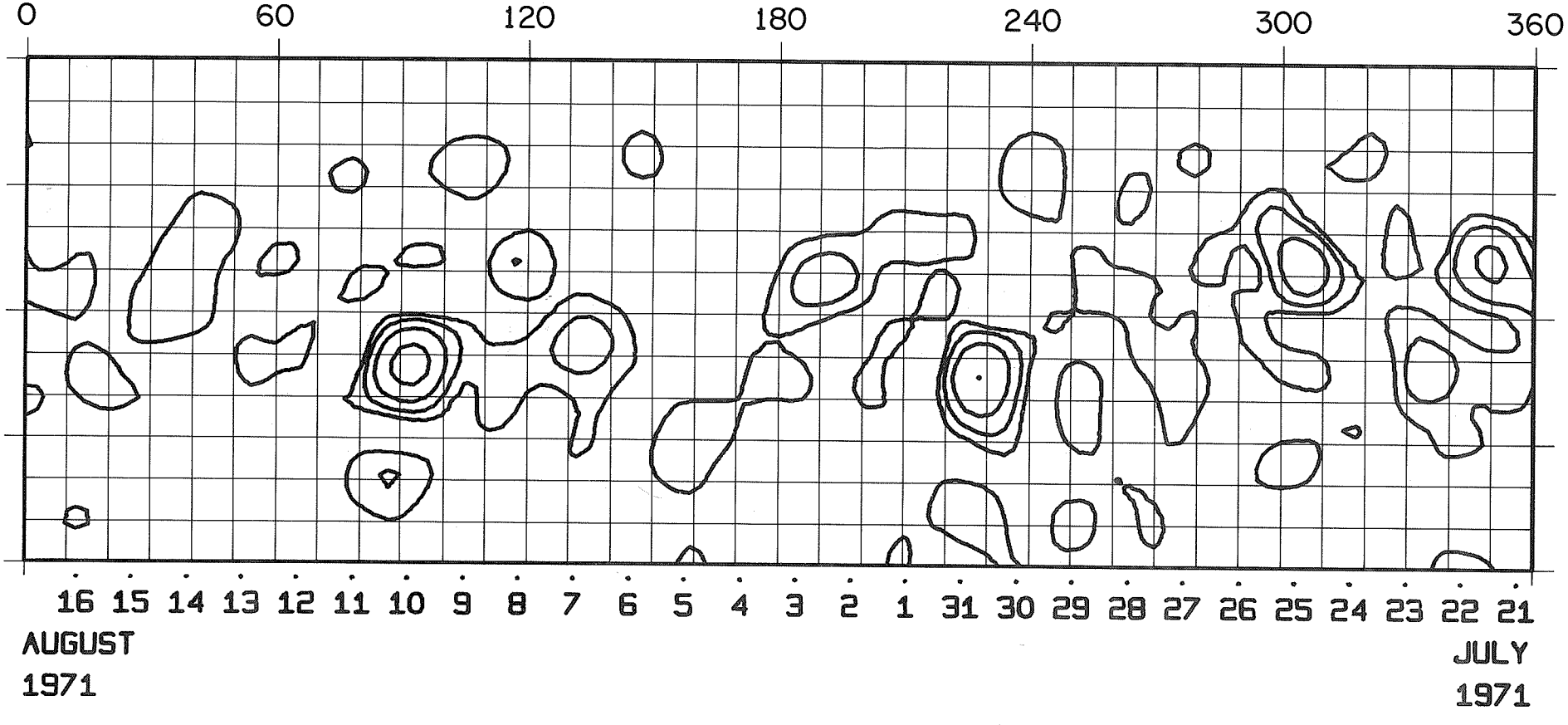

ROTATION NUMBER 1578

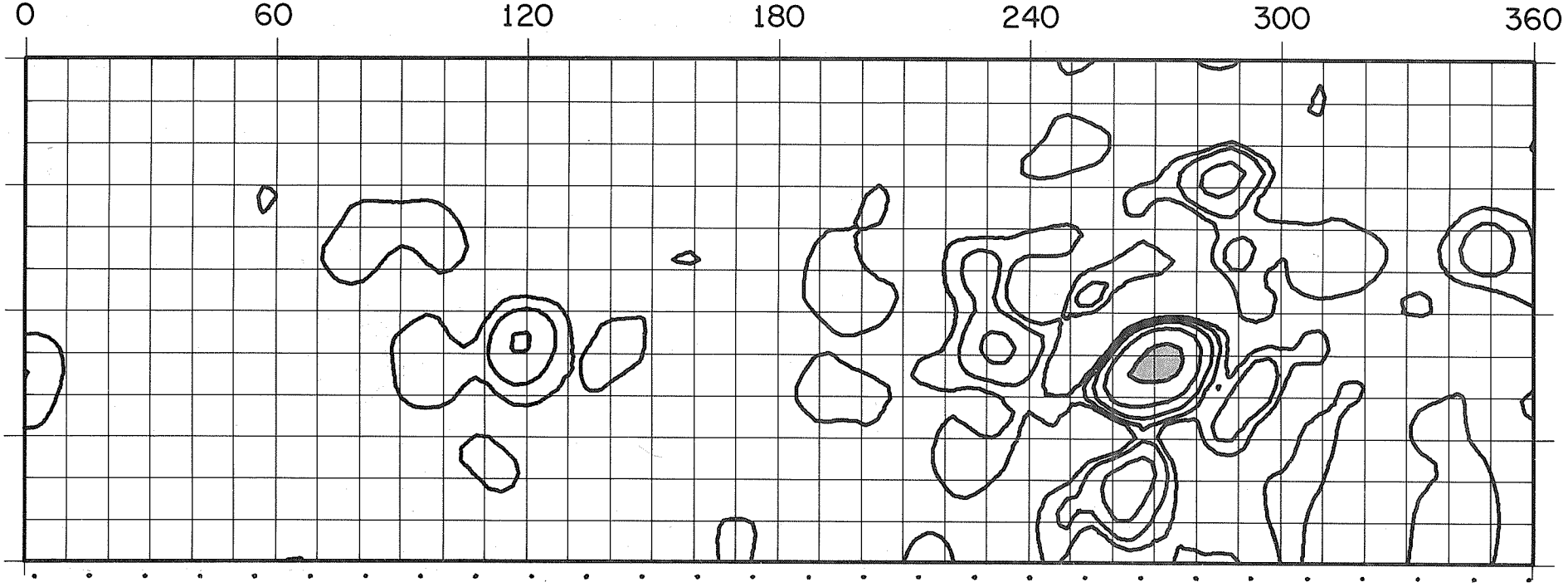

ROTATION NUMBER 1579

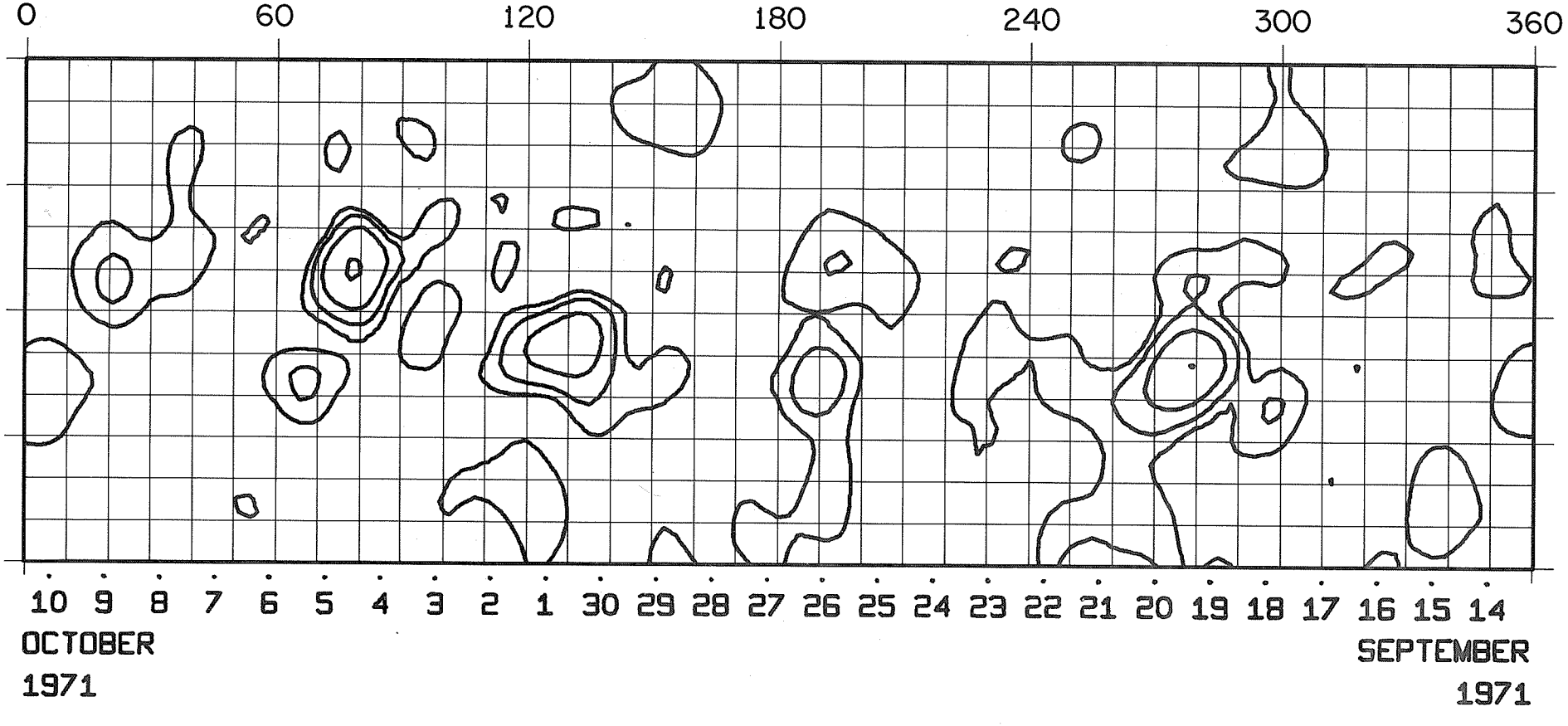

ROTATION NUMBER 1580

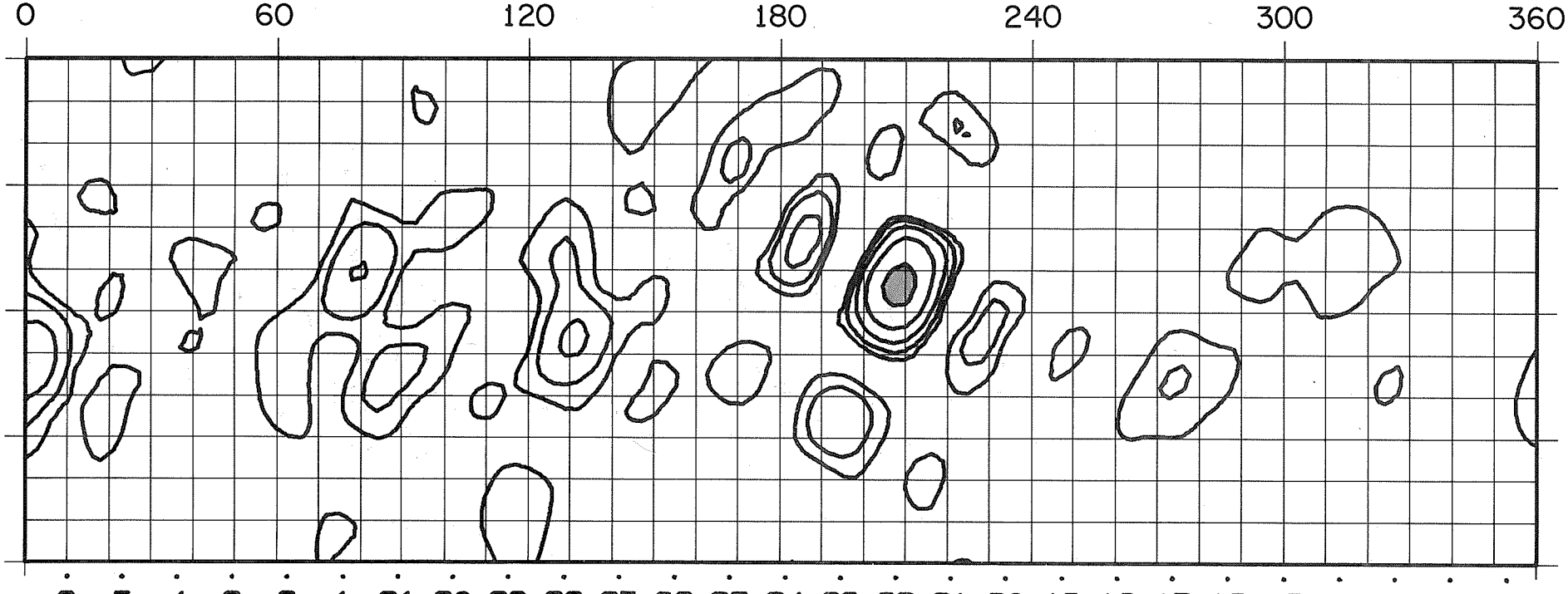

ROTATION NUMBER 1581

ROTATION NUMBER 1582

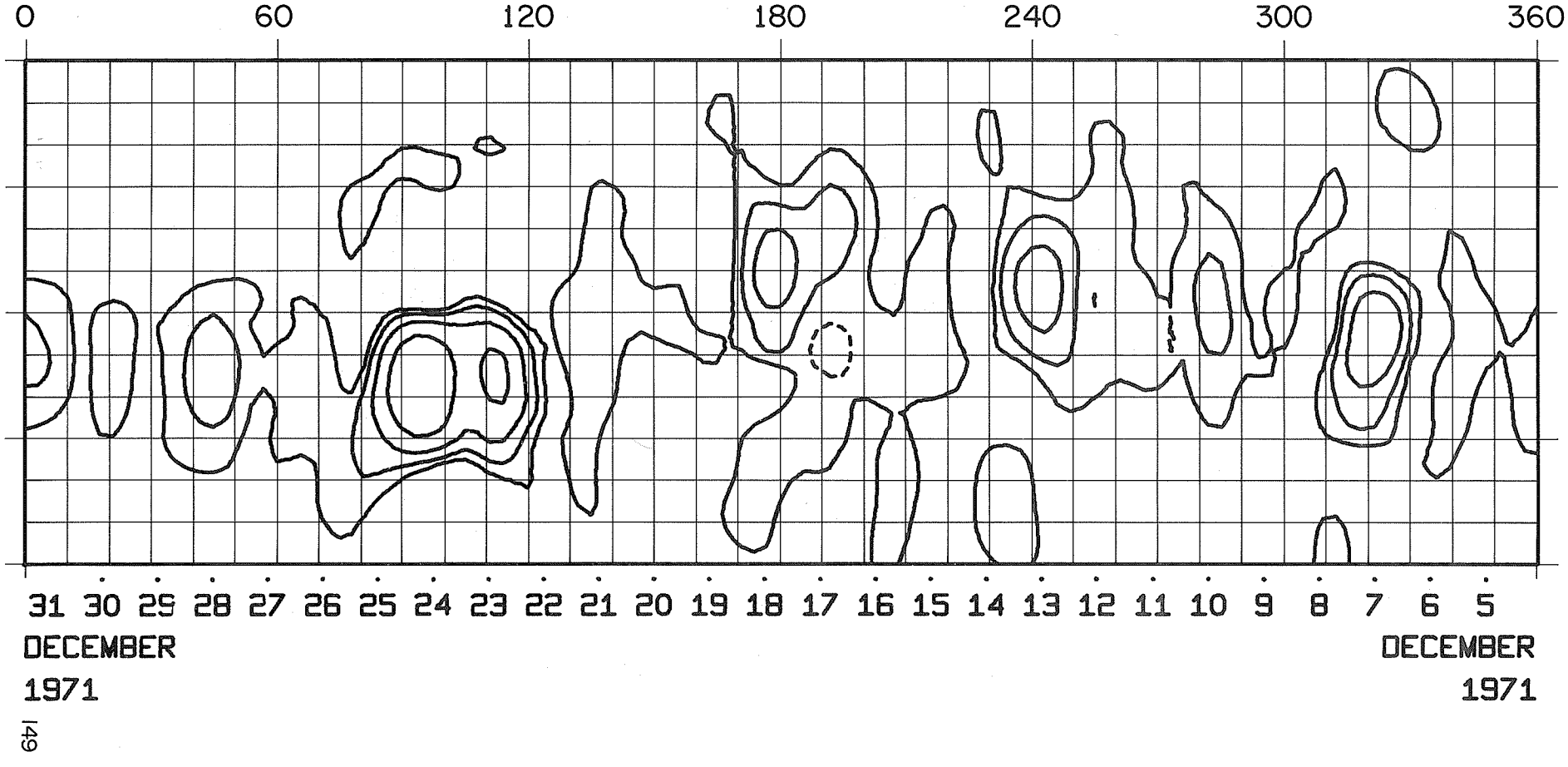

ROTATION NUMBER 1583

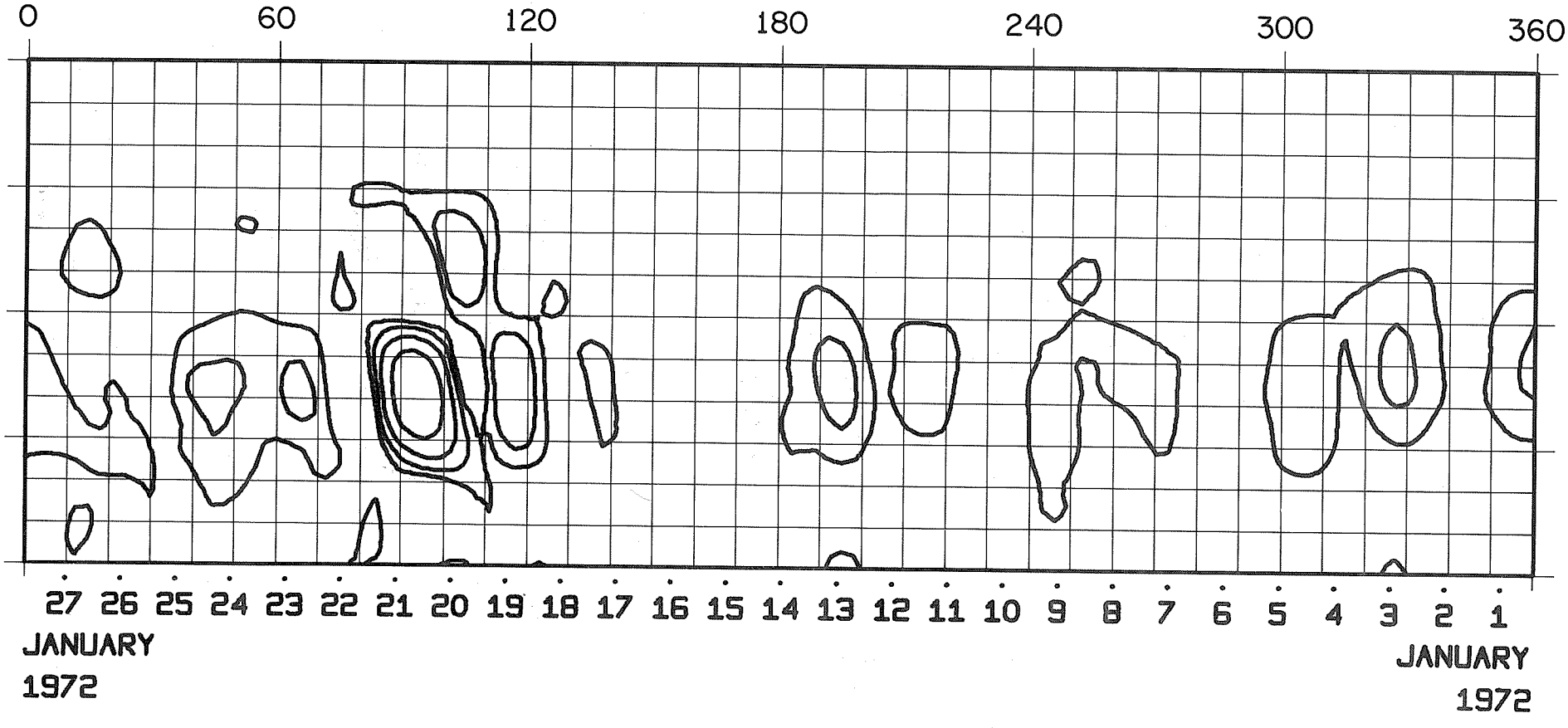

ROTATION NUMBER 1584

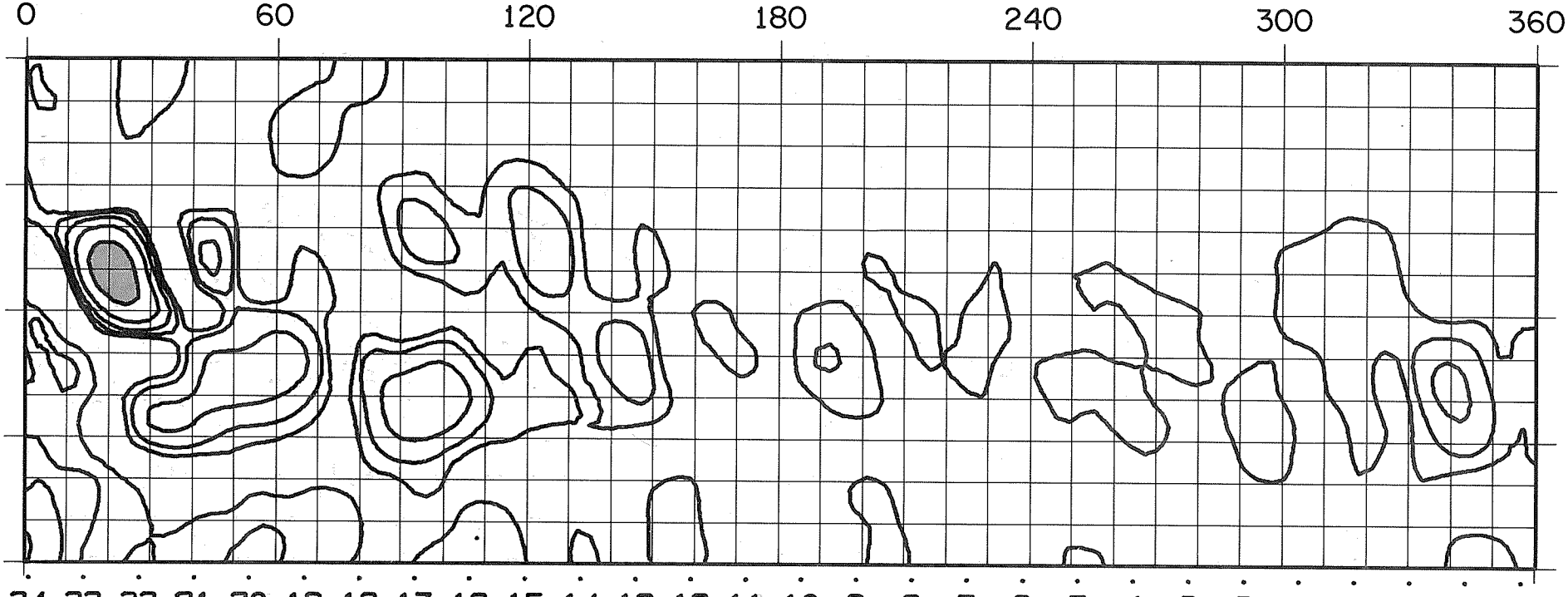

ROTATION NUMBER 1585

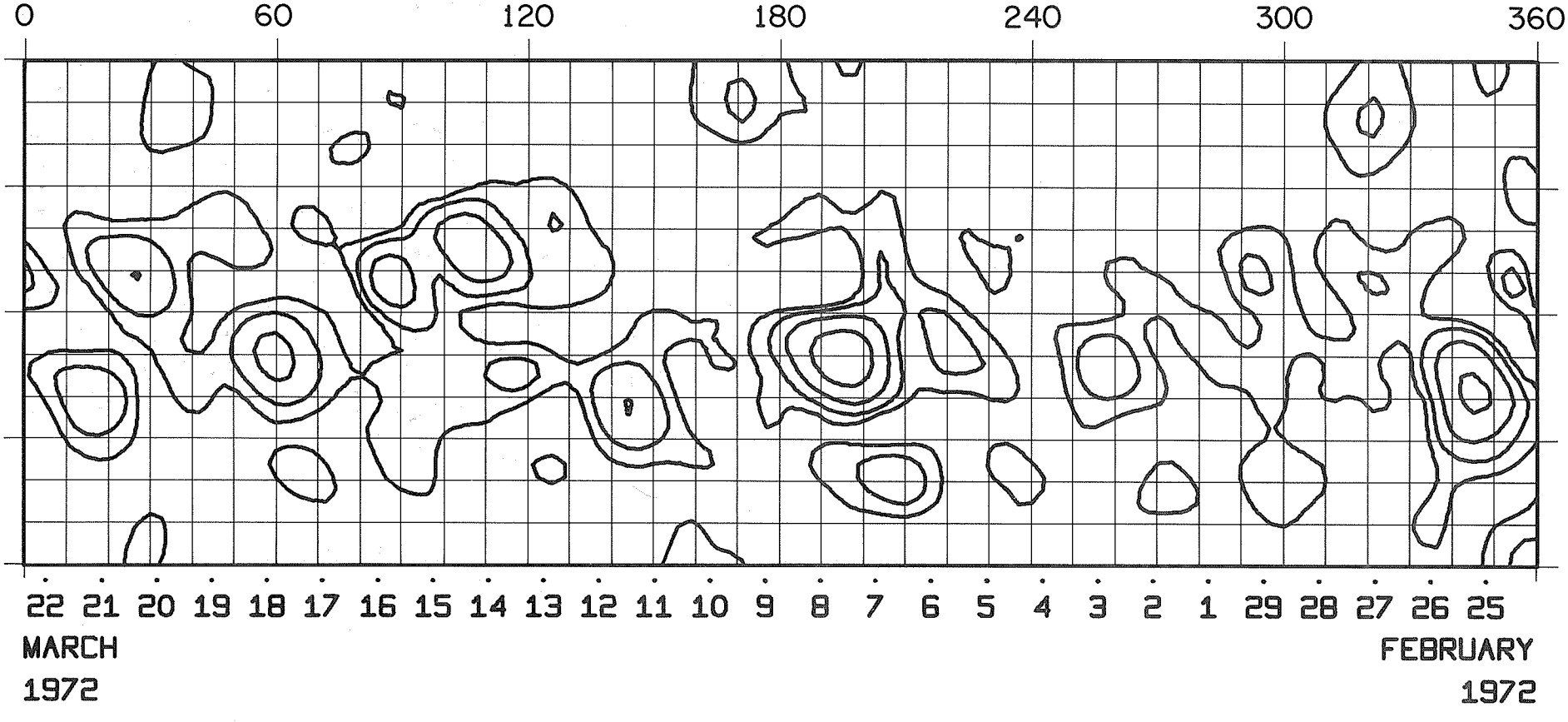

ROTATION NUMBER 1586

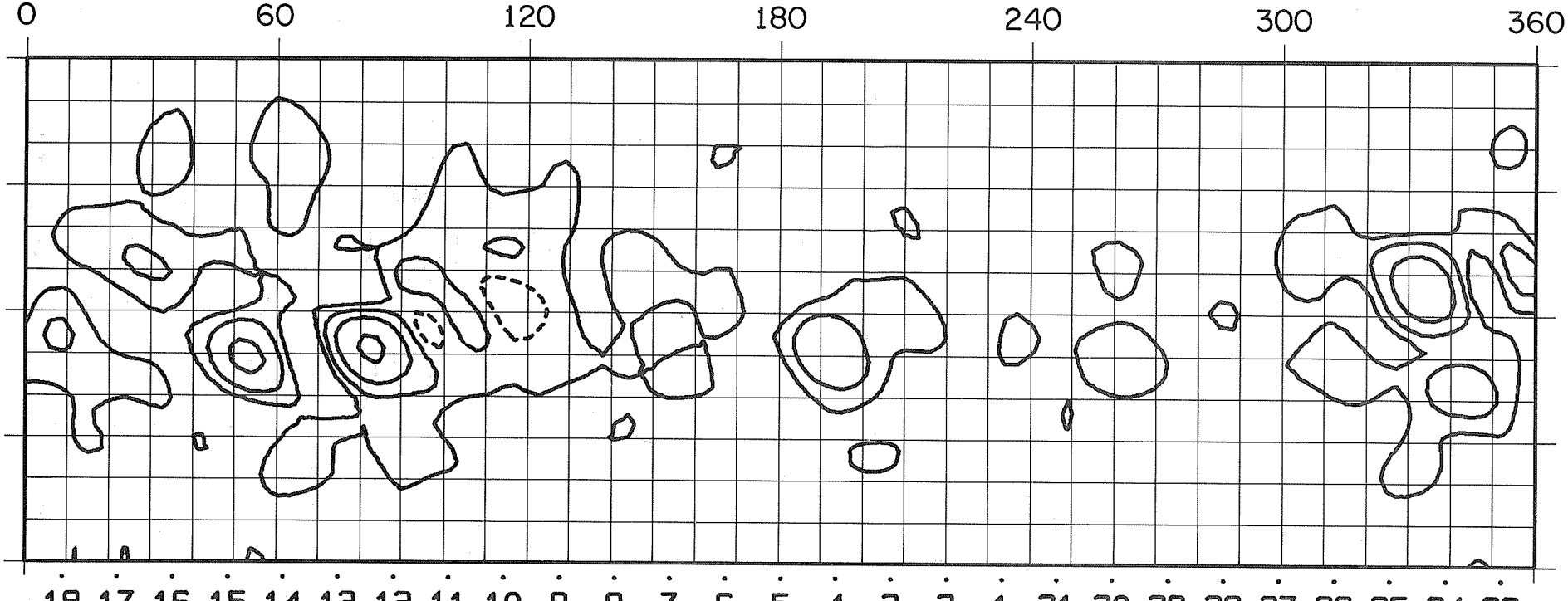

ROTATION NUMBER 1587

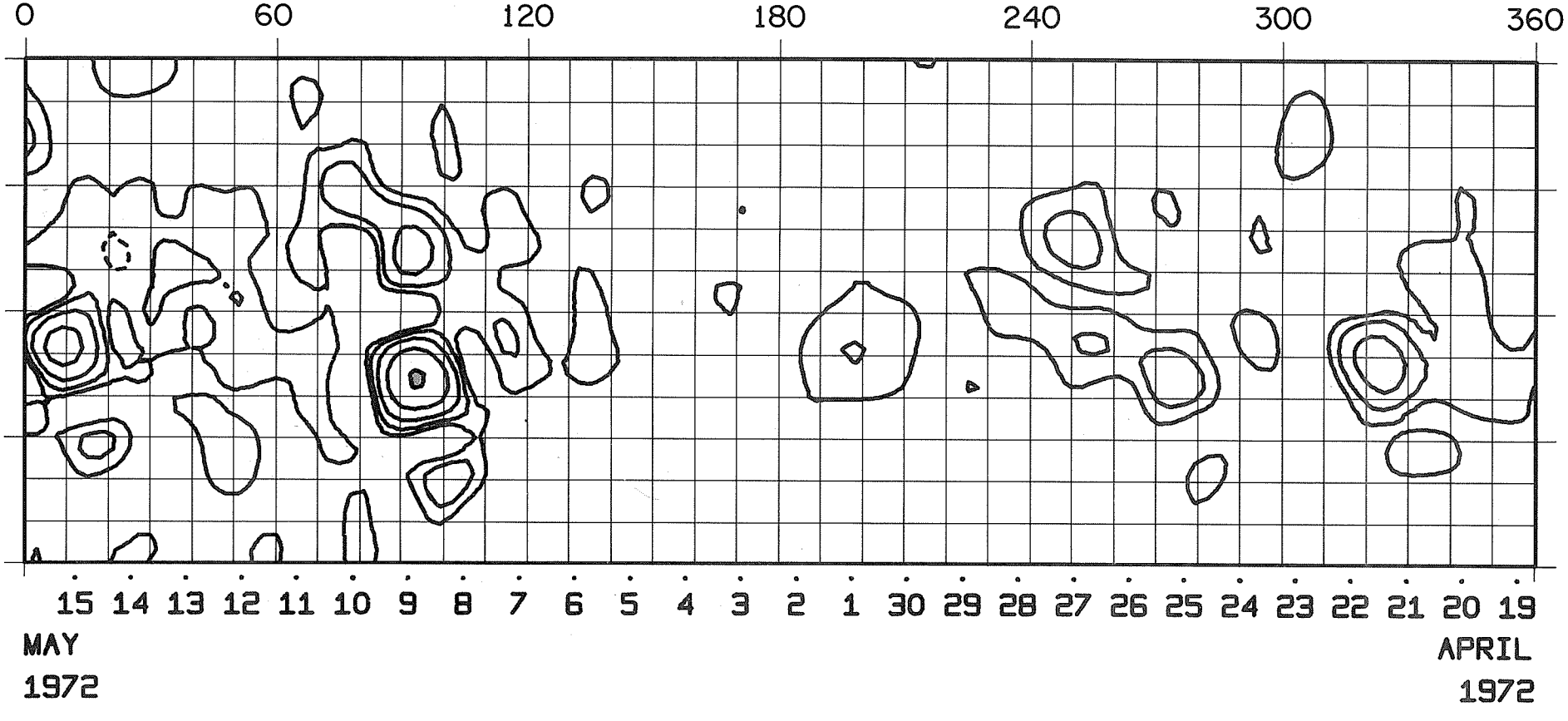

ROTATION NUMBER 1588

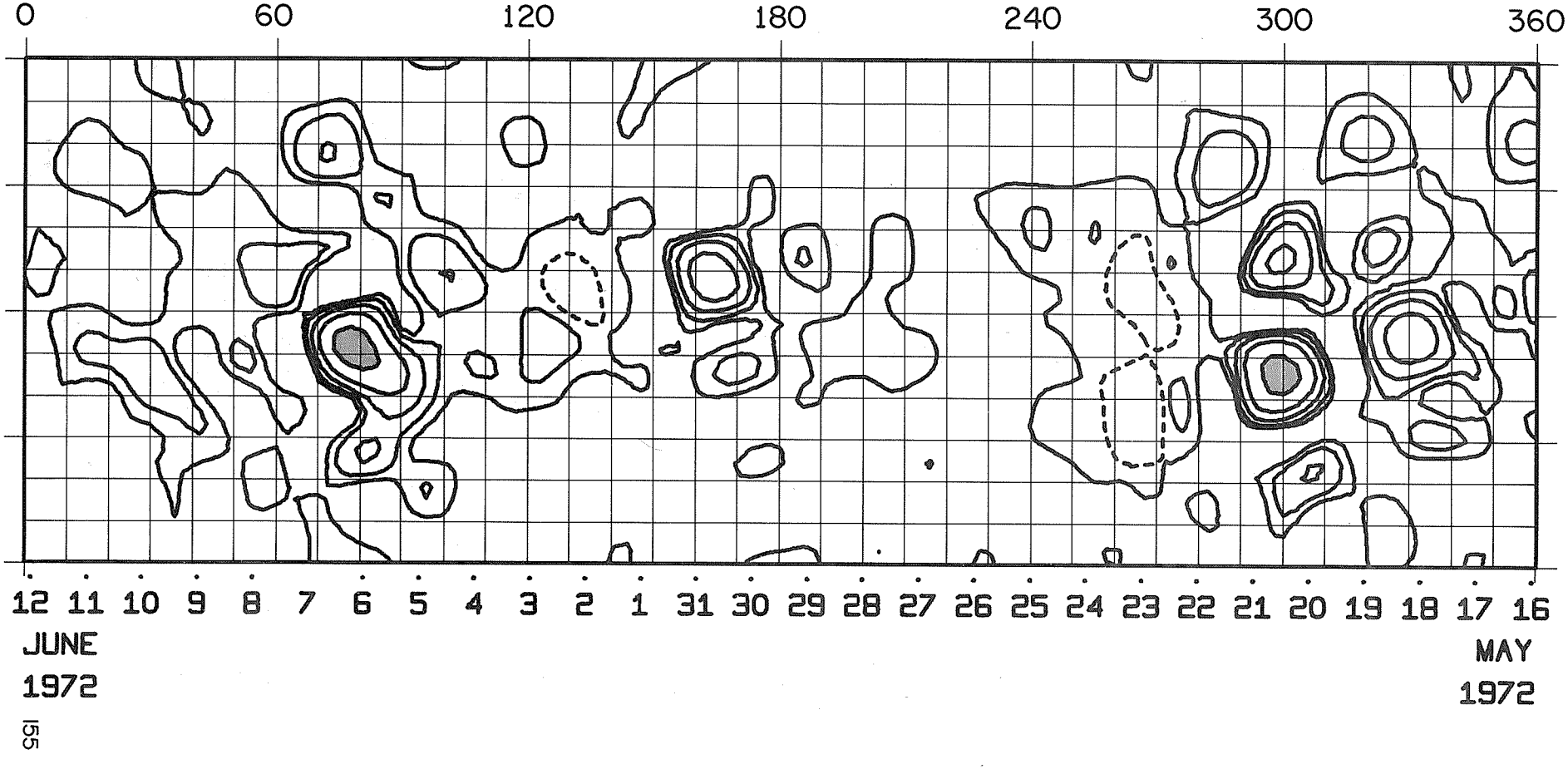

ROTATION NUMBER 1589

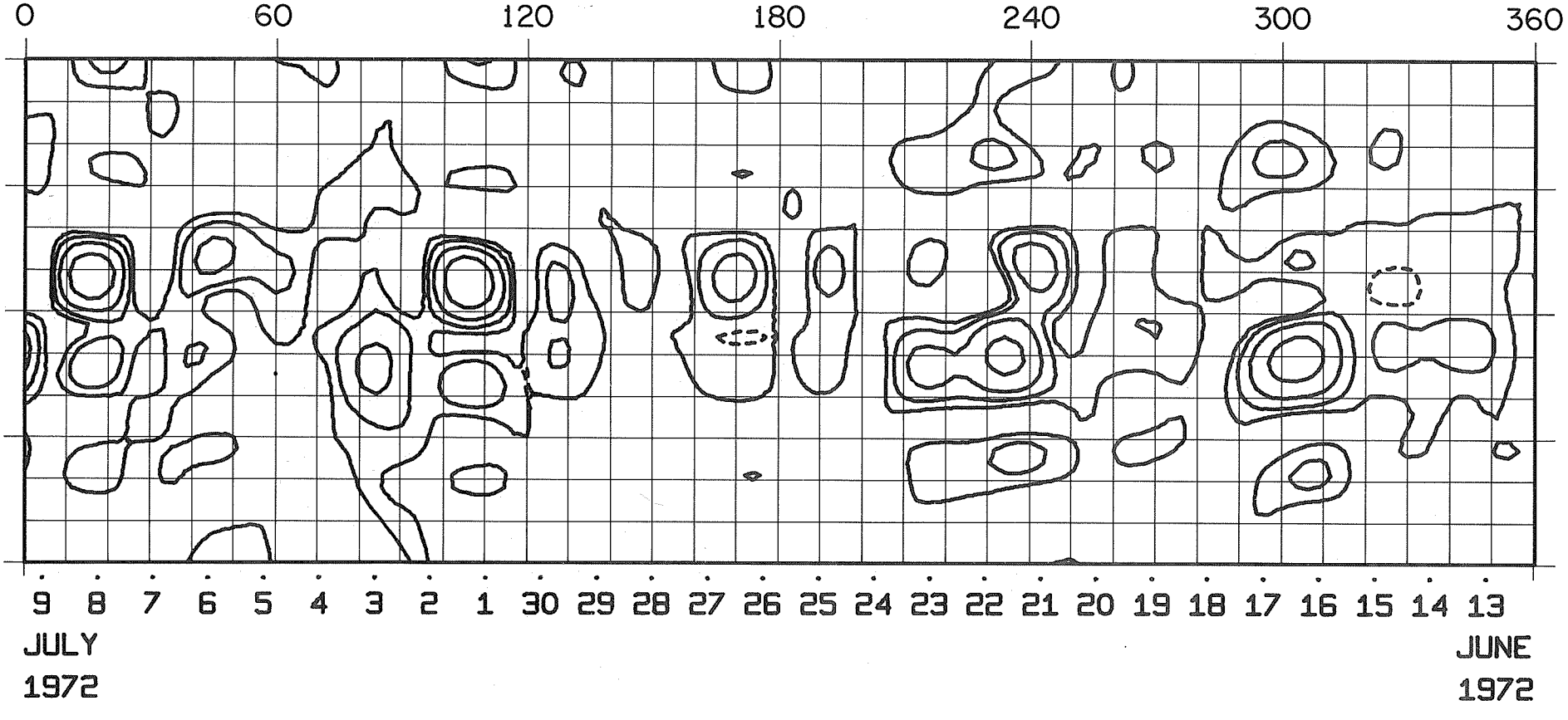

ROTATION NUMBER 1590

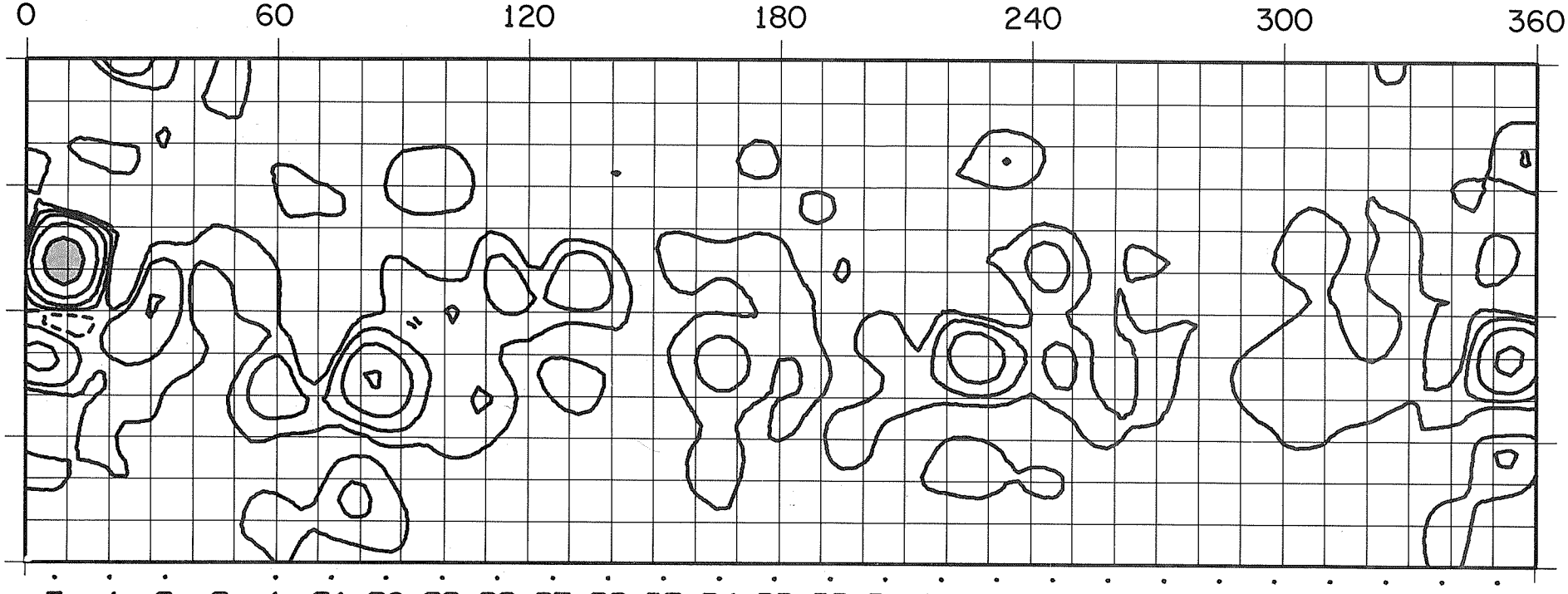

ROTATION NUMBER 1591

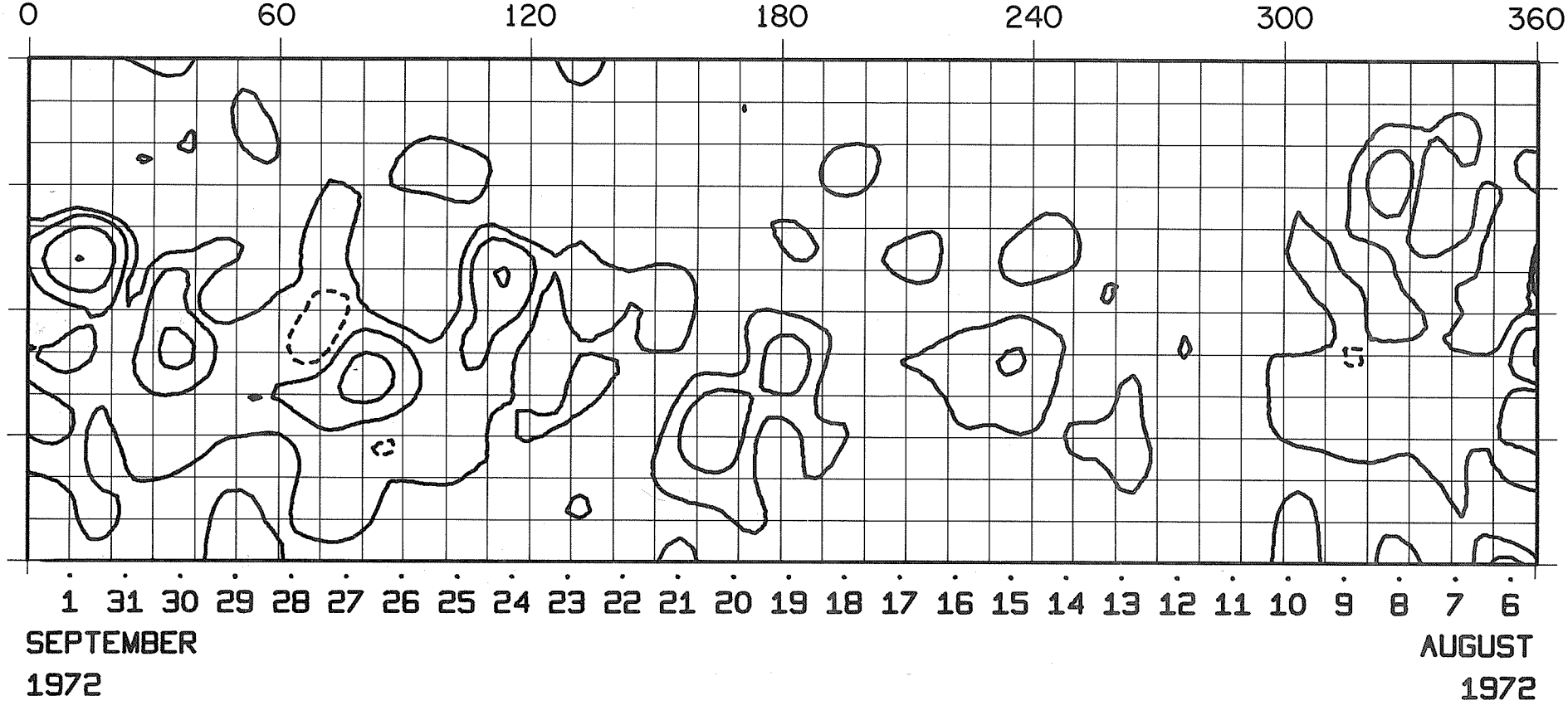

ROTATION NUMBER 1592

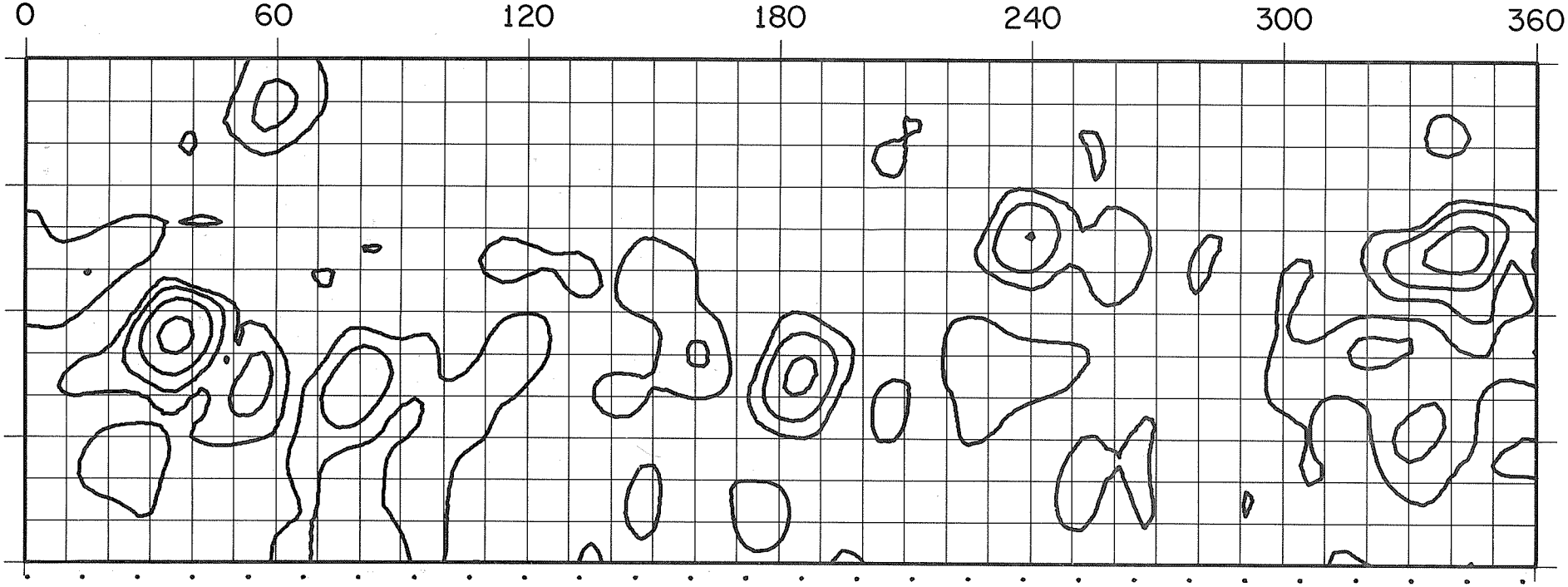

ROTATION NUMBER 1593

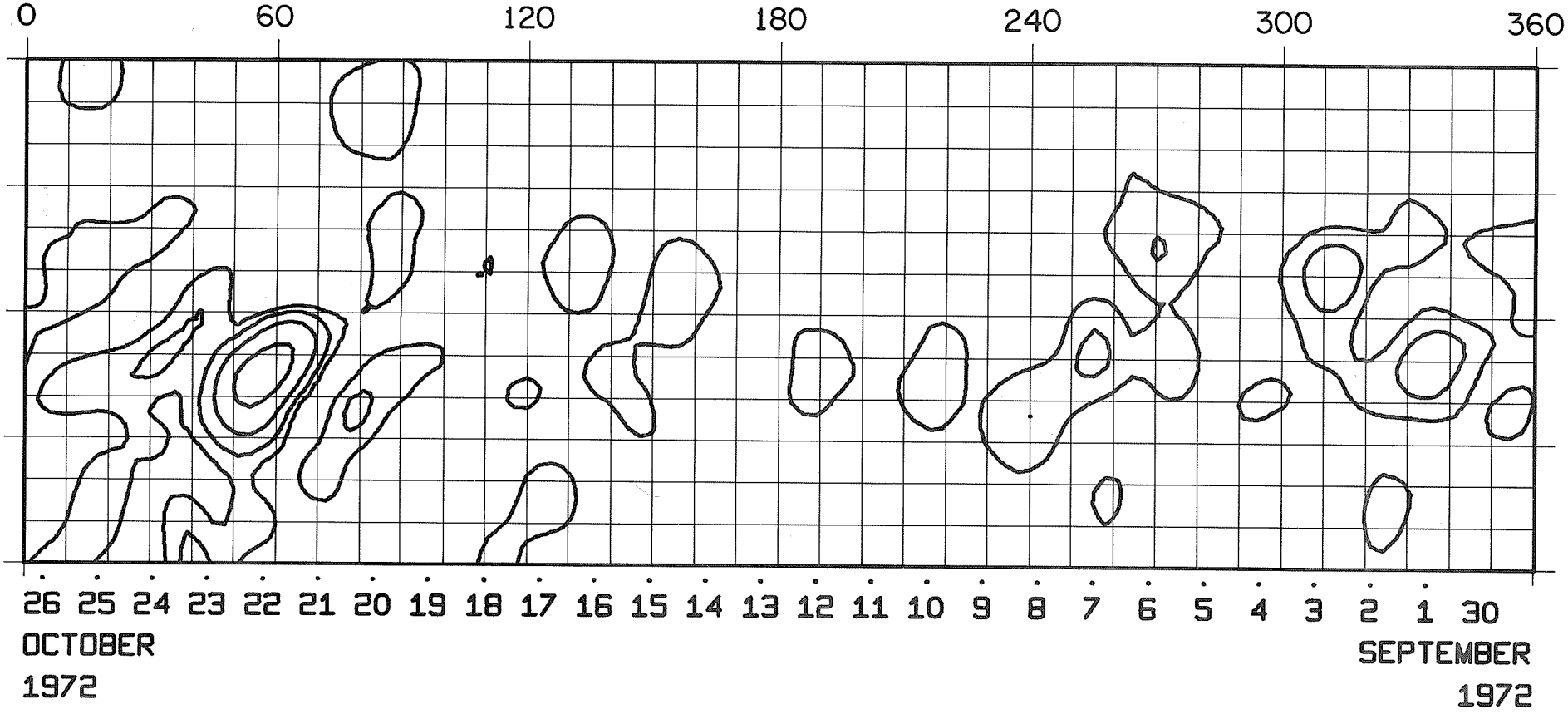

ROTATION NUMBER 1594

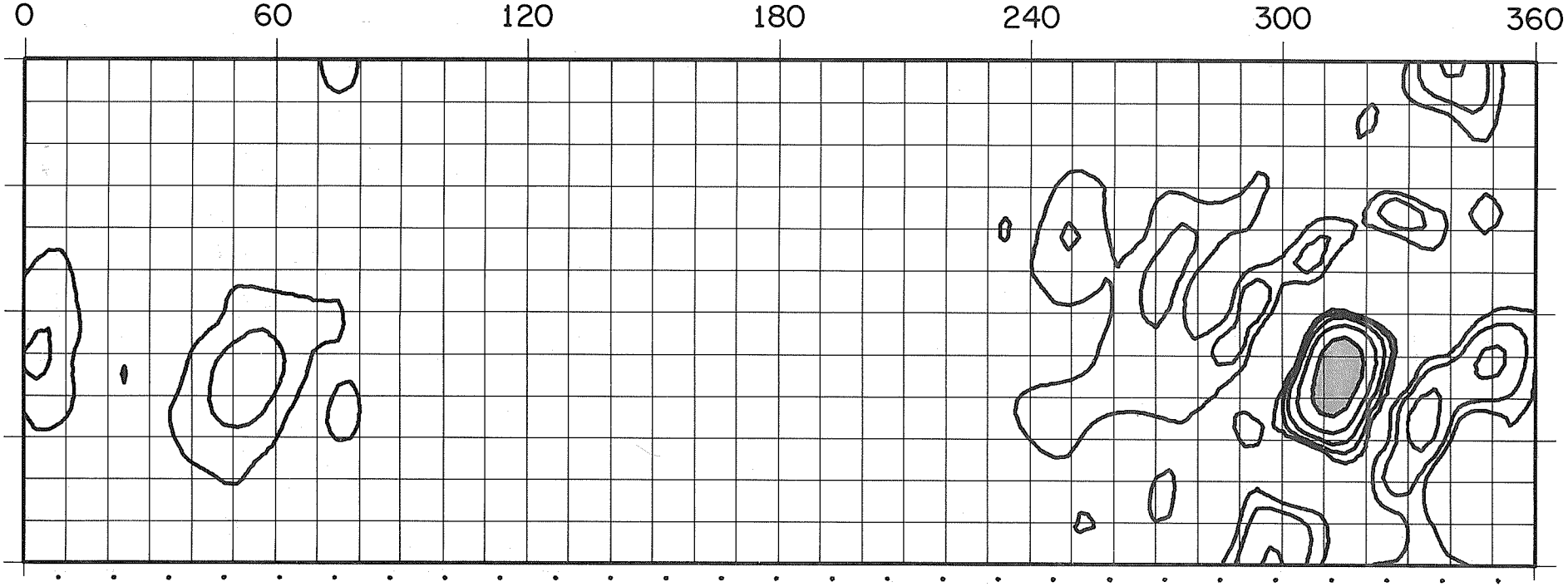

ROTATION NUMBER 1595

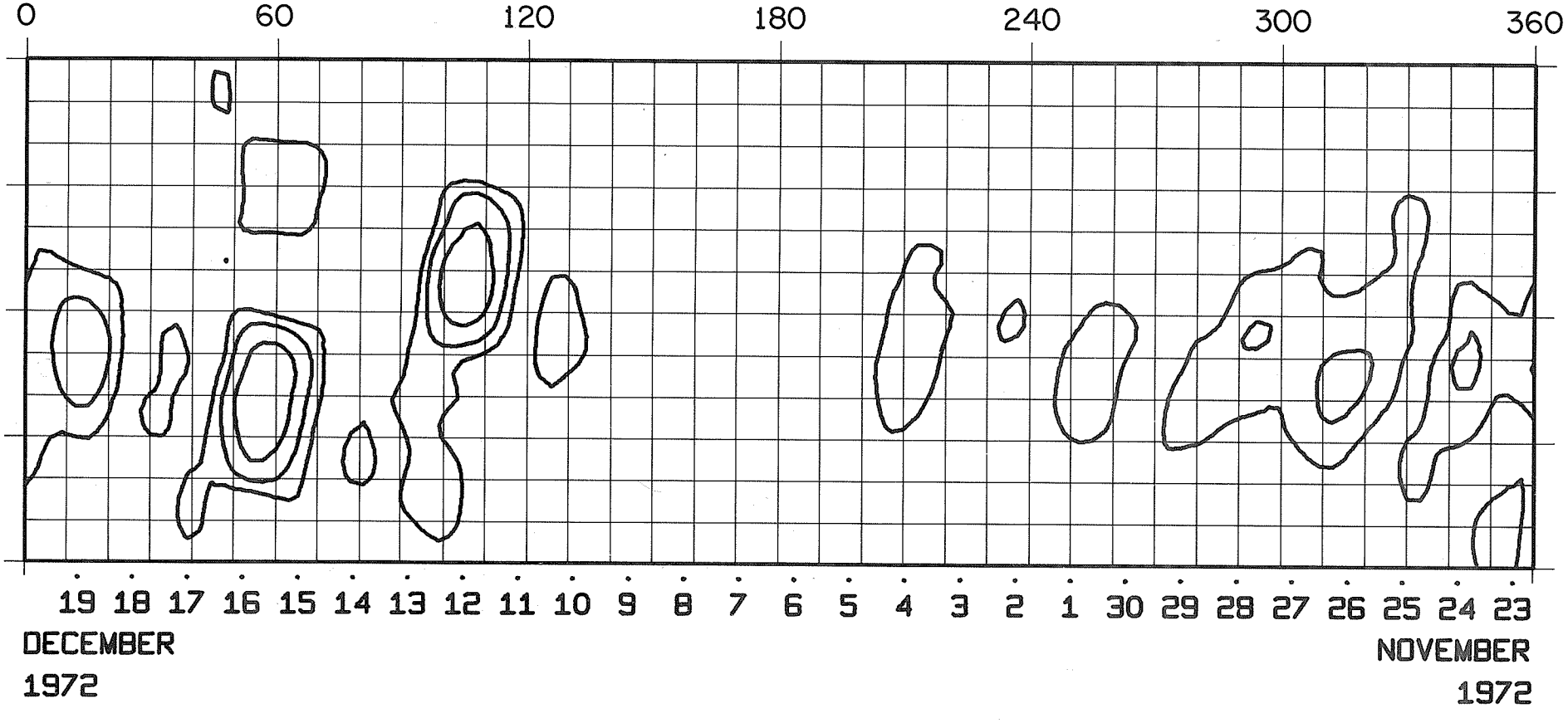

ROTATION NUMBER 1596

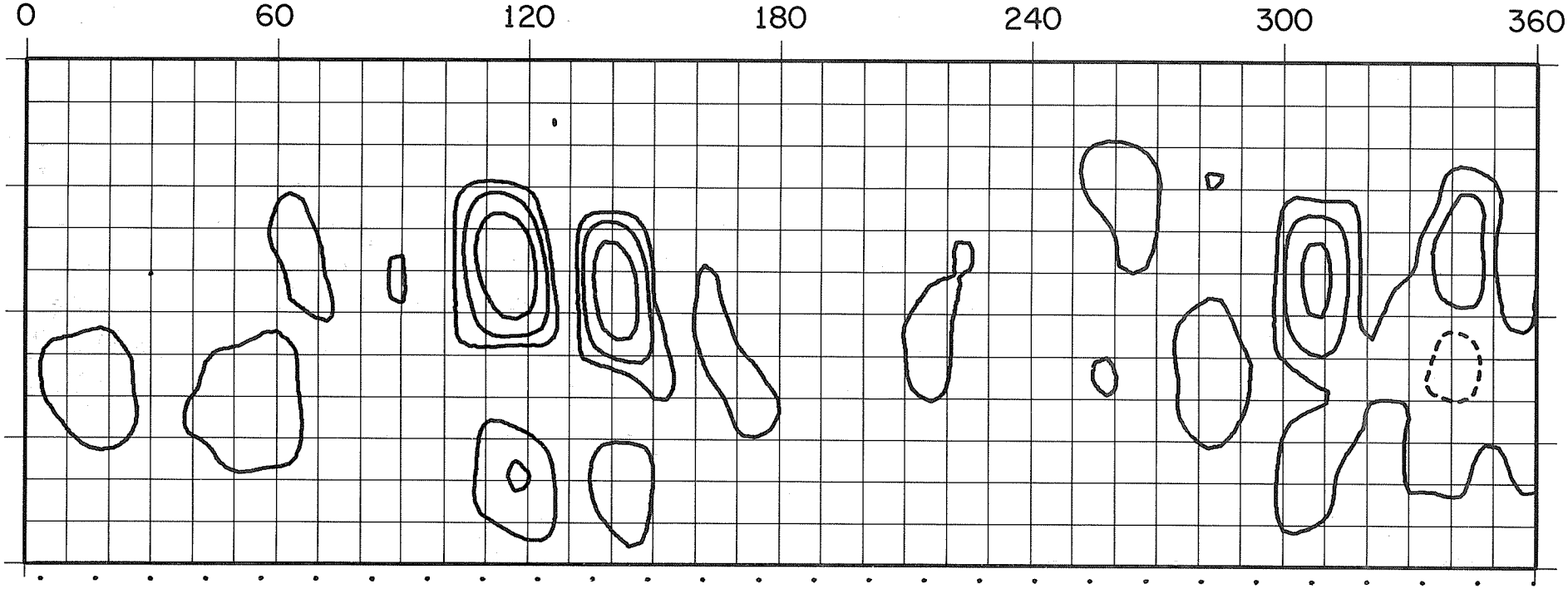

ROTATION NUMBER 1597

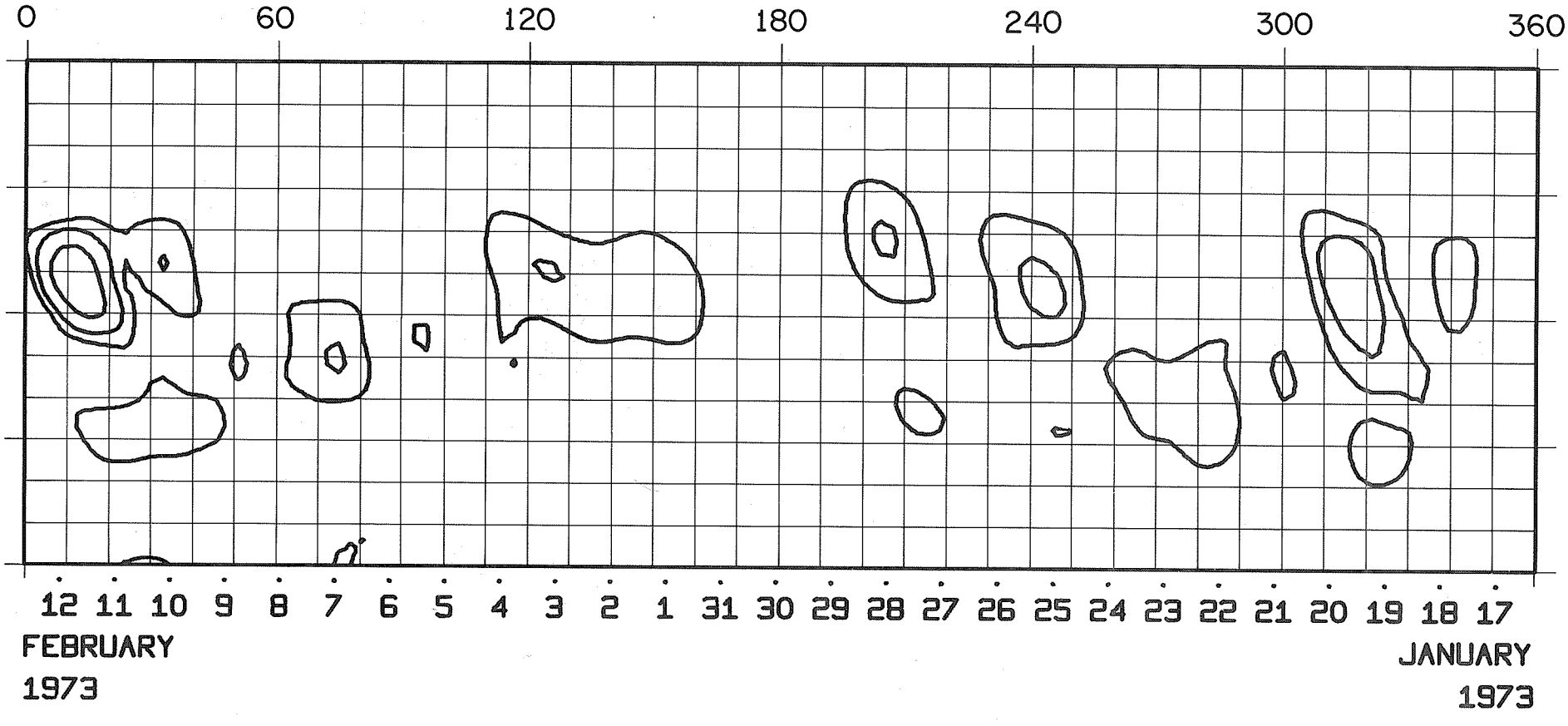

ROTATION NUMBER 1598

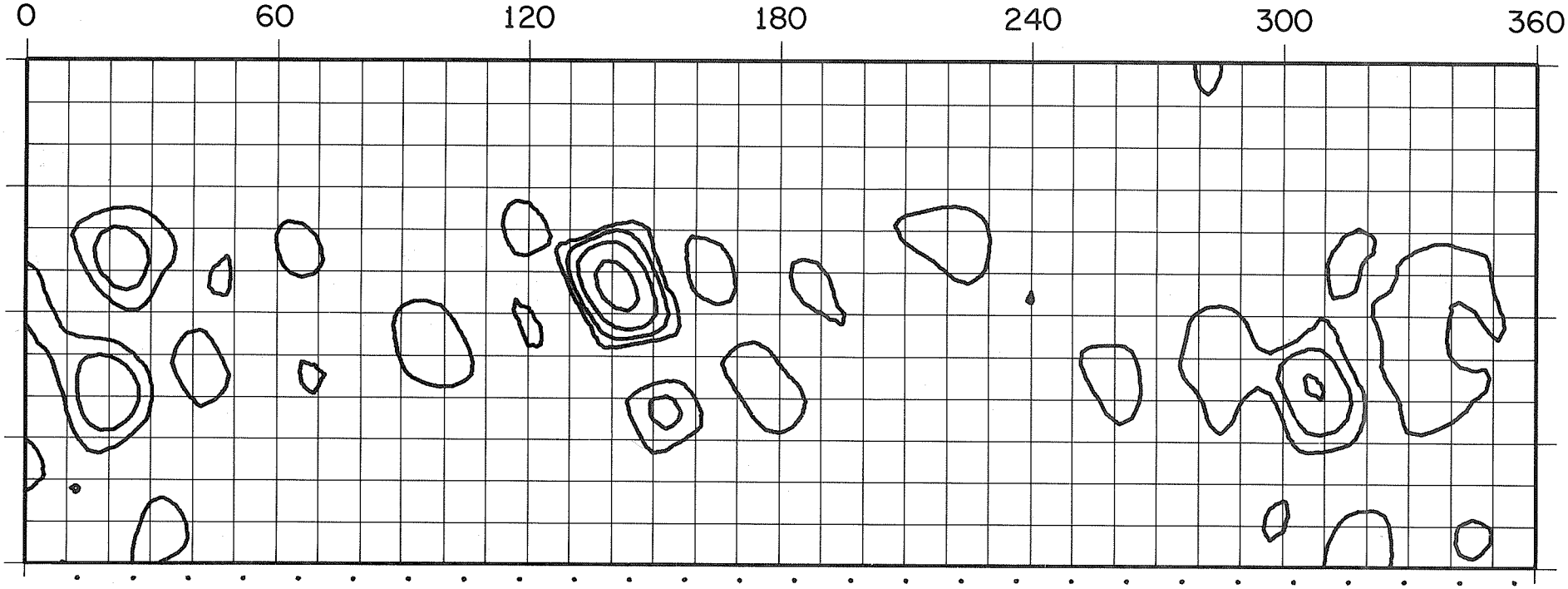

ROTATION NUMBER 1599

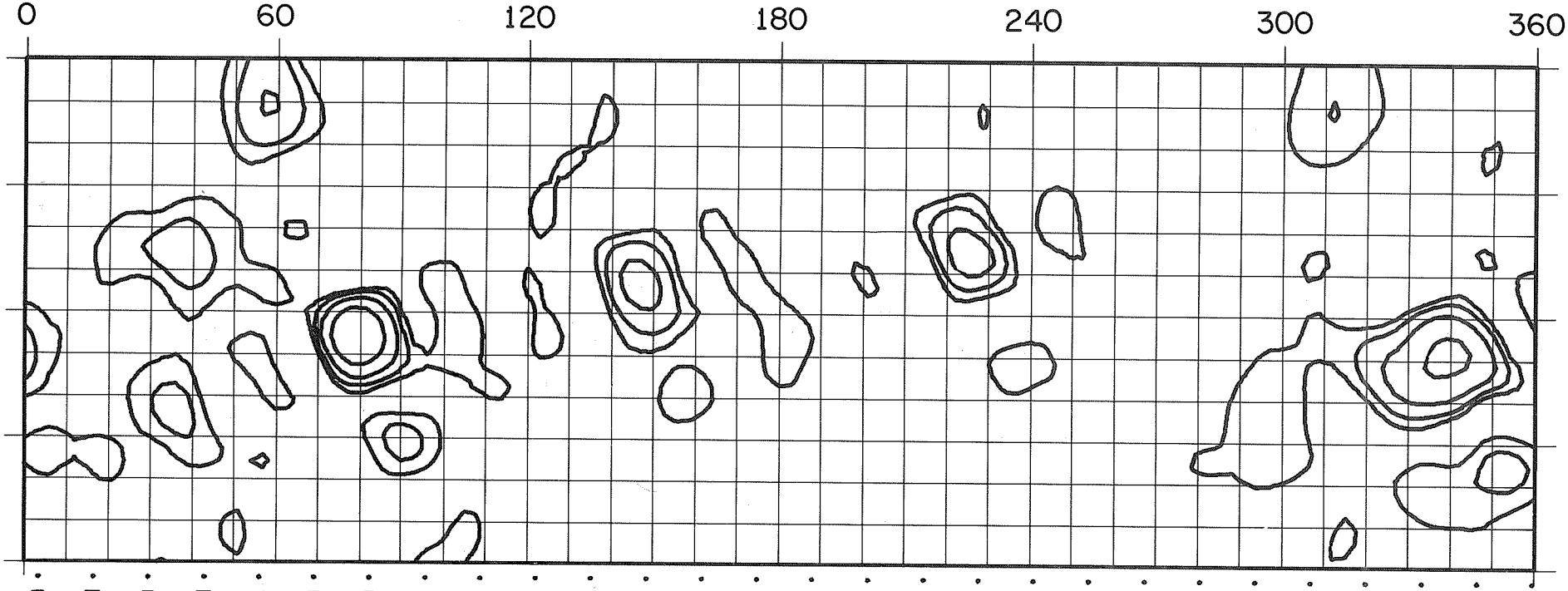

ROTATION NUMBER 1600

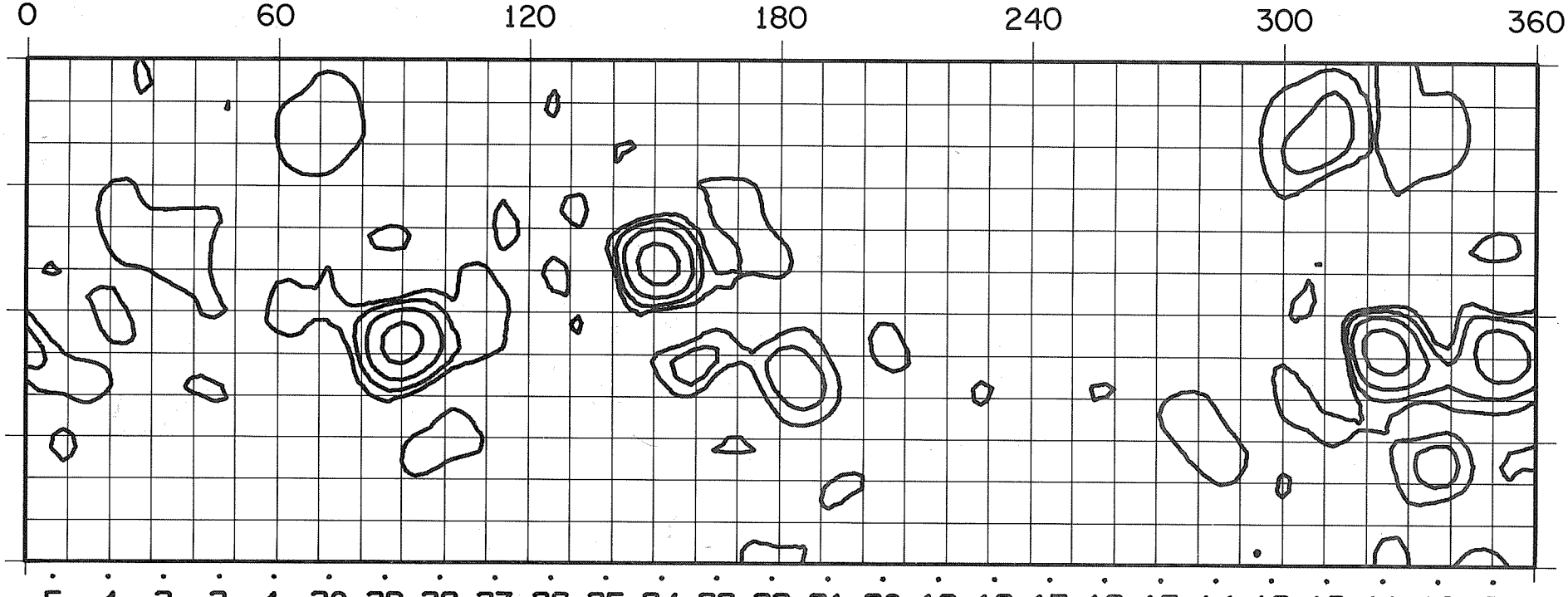

ROTATION NUMBER 1601

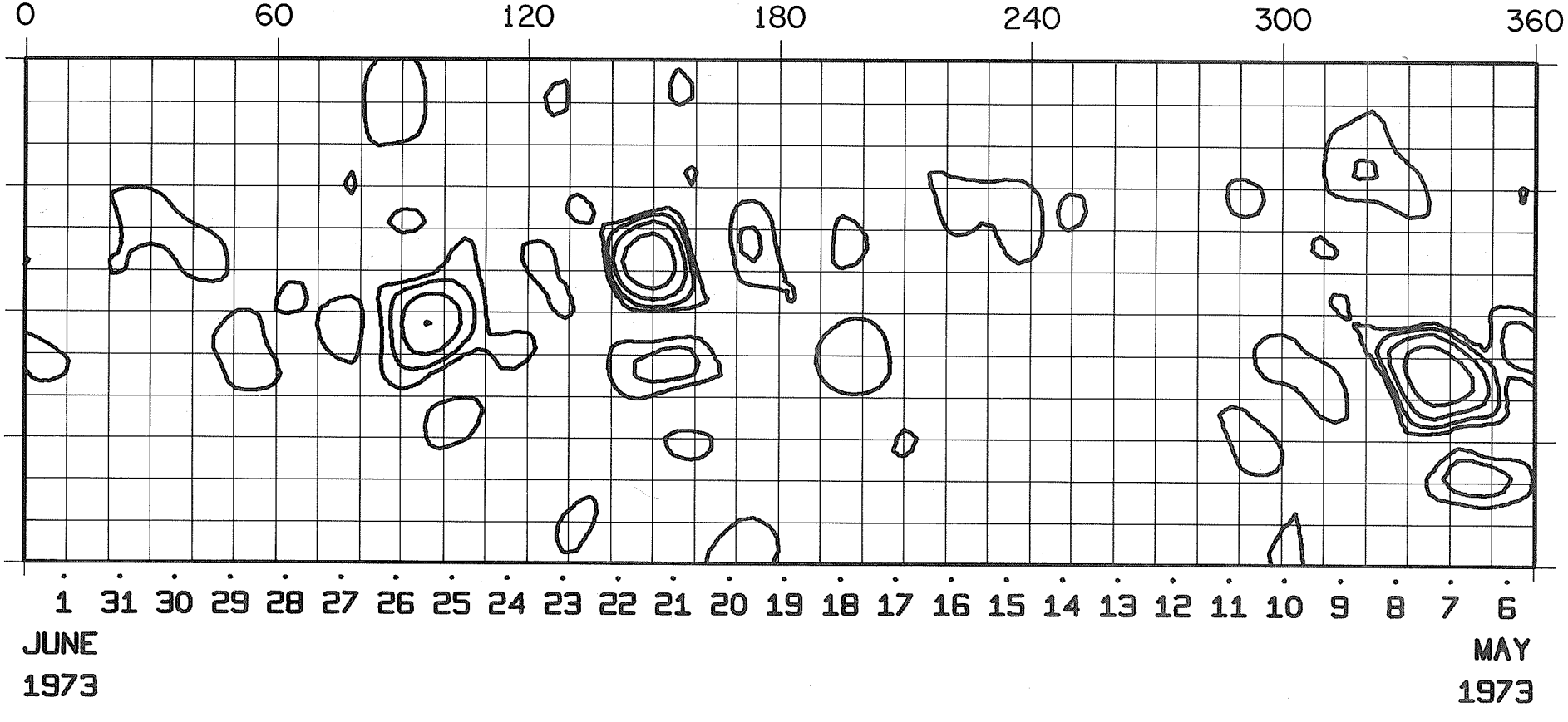

ROTATION NUMBER 1602

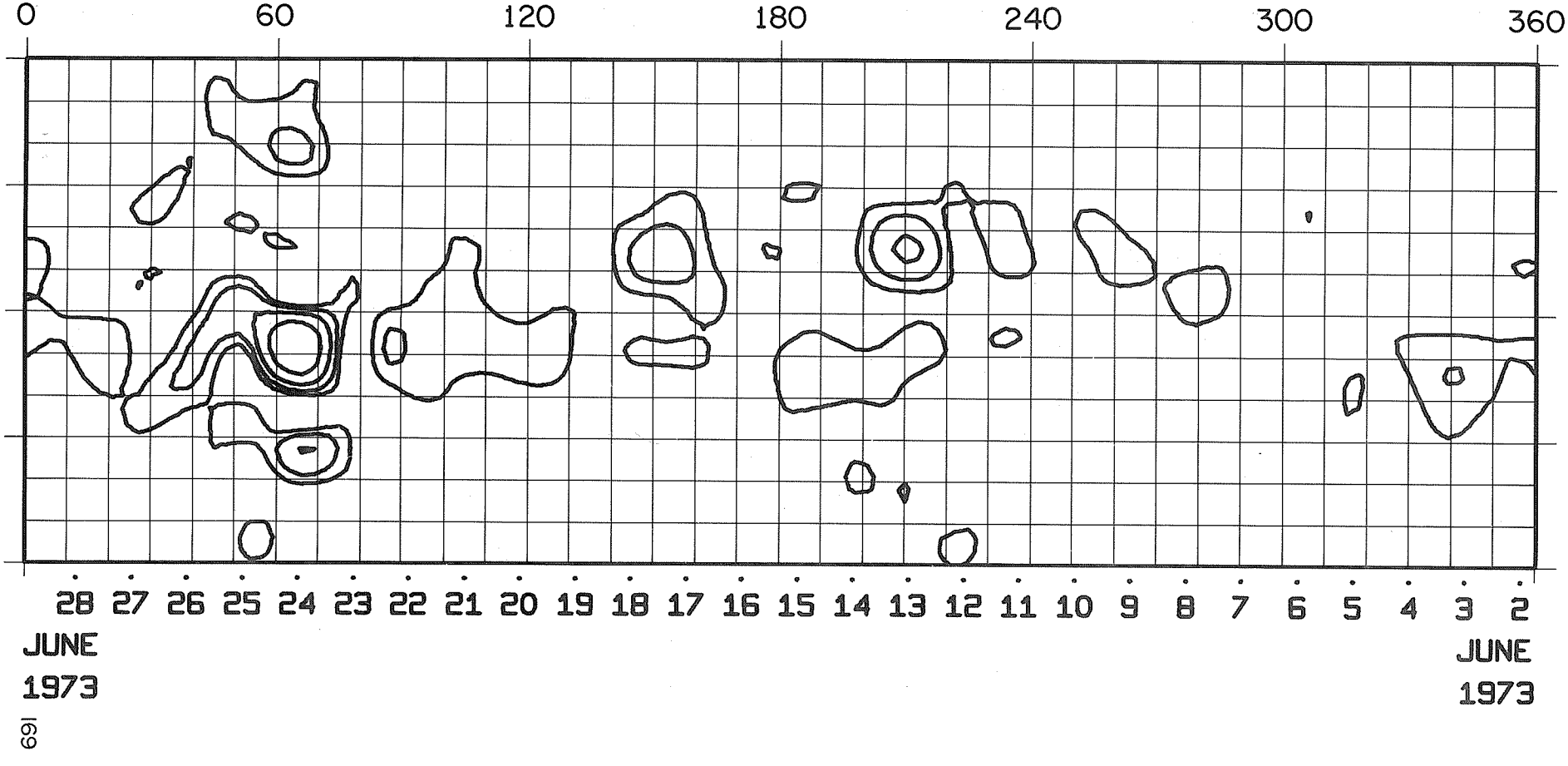

ROTATION NUMBER 1603

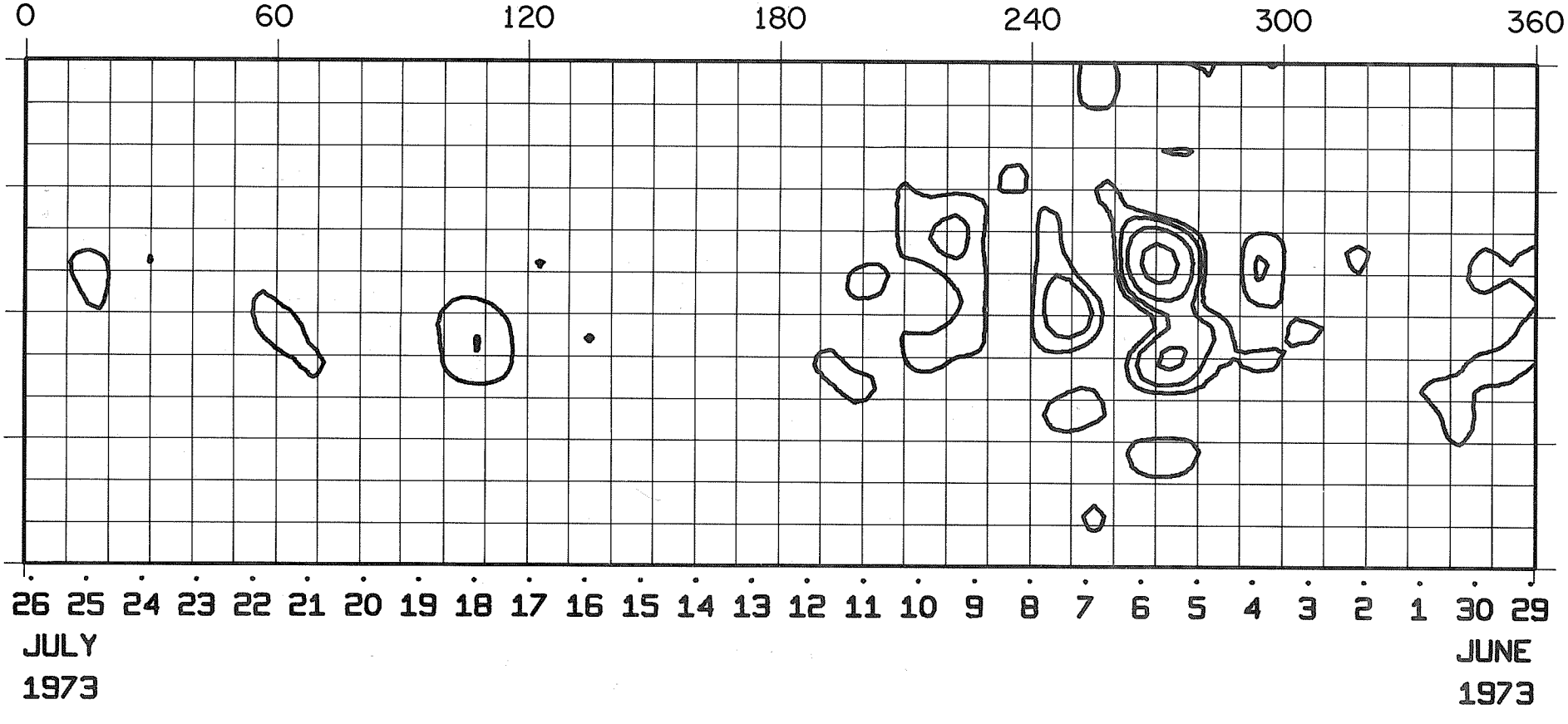

ROTATION NUMBER 1604

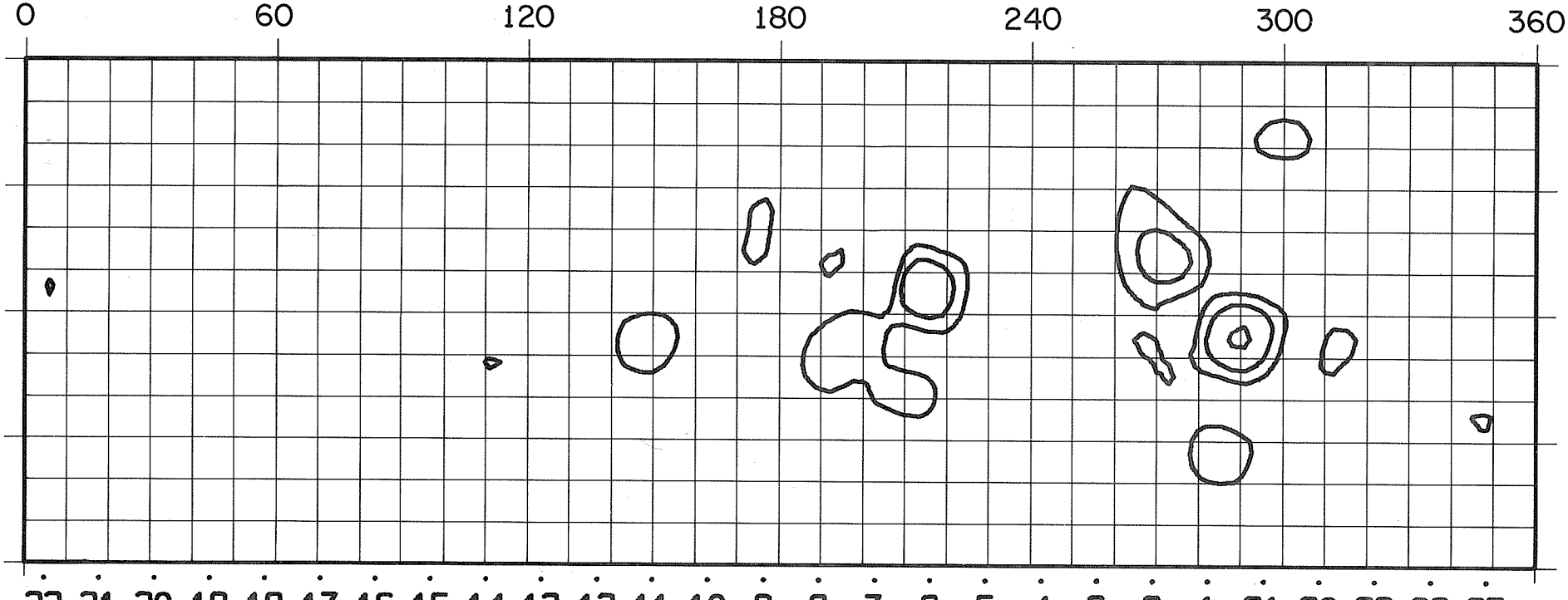

ROTATION NUMBER 1605

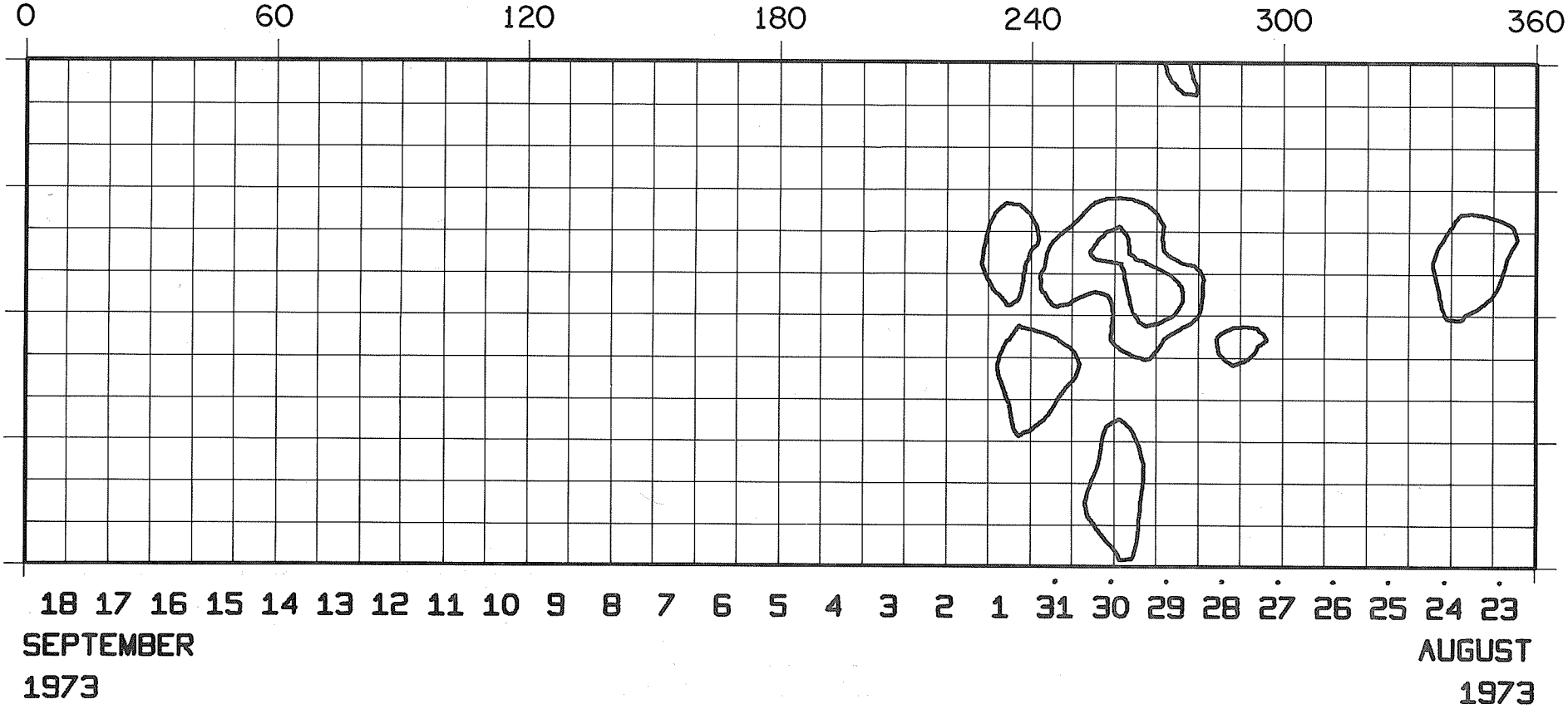

APPENDIX A

The Stanford Microwave Spectroheliograph Antenna, a Microsteradian Pencil Beam Interferometer*

R. N. BRACEWELL†, FELLOW, IRE, AND G. SWARUP†

Summary—A pencil beam interferometer has been constructed at Stanford, Calif., with multiple beams of 3.1 minutes of arc width to half power (0.8 microsteradian). It is composed of two equatorially-mounted, 16-element, Christiansen arrays of 3-m paraboloids, each 375 feet long (1255 wavelengths at a wavelength of 9.1 cm). The half power beamwidth of the fan beam of a single array is 2.3 minutes of arc. To form the pencil beam, the two arrays are switched together as in a Mills cross. Frequency range is from 2700 to 3350 Mc. Phase adjustment and monitoring are handled by a new technique of modulated, weakly reflecting gas-discharges maintained at the focus of the paraboloids. Television-type scanning yields maps of the sun (spectroheliograms) revealing fine details of the microwave source regions in the chromosphere and corona. All the transient bursts and a large fraction of the steady solar emission at 9.1 cm prove to originate in a small number of highly compact centers, whose brightness temperatures may exceed 5×10^{5}°K. The sensitivity of the instrument also allows the thermal emission from the moon (250°K) and a number of galactic and extragalactic sources to be studied with high angular resolution. Illumination of the moon by terrestrial radar can be detected. The pencil beam interferometer furnishes the finest beams currently available from pencil beam antennas of any type. Examination of the fundamentals of extracting high resolution details of a source from its radiation field indicates the fitness of pencil beam interferometers, incorporating steerable multielement arrays, for future development to higher resolving power. Adequate technique of phase preservation over wide spacings is available.

* Received by the PGAP, October 10, 1960. This research was supported by the Office of Sci. Res. of the U.S.A.F., Air Res. and Dev. Command, under contract AF 18(603)-53.

† Radio Astronomy Inst., Radioscience Lab., Stanford University, Stanford, Calif.

I. Introduction

BY 1954 it had become clear that a new type of pencil beam instrument could be built by combining the principles of the Christiansen array and the Mills cross. Practical feasibility of the one had been demonstrated by Christiansen and Warburton [1], [2] on a large, albeit economical, multi-element array, and of the other by Mills and Little [2]–[5] on a scale model designed for the purpose. It was therefore possible to plan an ambitious microsteradian pencil beam project with confidence that the basic principles were sound, an important prerequisite, because in each case objections had been entertained that could only be removed by test. The fruits of the new project would be microwave spectroheliograms, built up television-wise by scanning the sun with the pencil beam. During the tenure of a visiting professorship in the academic year 1954–55, in the Astronomy department of the University of California, Berkeley, the senior author studied the design of an instrument for a wavelength of about 10 cm. Execution of the design was proposed for Sydney (where, however, it was decided to embark on a different but similar project) and for California. The proposal [6] to build the present instrument was submitted to the Office of Scientific Research of the United States Air Force in September, 1955.

The purpose of the instrument was to study the chromospheric microwave emission with a view to ascertaining physical conditions in an optically transparent region which is the seat of important solar disturbance phenomena. Here, in the transition between the corona and the outer chromosphere, occurs the changeover between the steady optical sun and the spectacularly variable meter-wave sun. While the meter-wave radio emission is in itself fascinating, it is a secondary phenomenon associated with ejection of matter from lower levels. An attack on the very little known outer chromosphere therefore offered the possibility of coming to grips with the central problem of solar activity. In fact, as now appears, the maximum of emission from the active centers occurs around the selected wavelength of 9 cm; at shorter wavelengths their lack of opacity renders them less conspicuous, and at longer wavelengths the opacity of the overlying corona obscures them. In the vicinity of 9 cm the active centers have been up to 30 times brighter than the quiet sun.

Section II gives the principle of the instrument and Section III the basic design parameters. Section IV gives physical details of the installation. Section V discusses the vital item of technique on which the whole possibility of adjusting large arrays depends, namely the measurement, maintenance, and control of relative phase over great distances. Section VI gives samples of observations to illustrate the functioning of the instrument; their astronomical significance will be discussed elsewhere. Finally, in Section VII the significance of the instrument for antenna practice is discussed, with attention to possible future development to even greater resolution.

II. Basic Principle

Let an even number N of isotropic point sources be arranged in a straight line, each spaced at a distance d from the next. The field radiation pattern of one pair of identically excited sources at a distance nd apart will be

$$\exp\left[i\frac{2\pi}{\lambda}\,\tfrac{1}{2}\,nd\sin p\right]+\exp\left[-i\frac{2\pi}{\lambda}\,\tfrac{1}{2}\,nd\sin p\right],$$

where λ is the wavelength, and $nd\sin p$ is the path difference between two rays that make an angle p with the plane perpendicular to the line of the array. This expression is equal to $2\cos[(\pi/\lambda)\ nd\sin p]$. If now the whole array is considered to be composed of $\frac{1}{2}N$ symmetrical pairs, all equally excited, the field radiation pattern is proportional to

$$2\sum_{n=1,3,5\cdots}^{N-1}\cos\left[\frac{\pi}{\lambda}\,nd\sin p\right]$$

This is the Fourier series for a periodic function of $\sin p$ consisting of sharp fringes of the form

$$\frac{\sin\left(N\pi\dfrac{d}{\lambda}\sin p\right)}{\pi\dfrac{d}{\lambda}\sin p},$$

repeated with alternation of sign at intervals λ/d. In Fig. 1 this periodic function is plotted for $N=16$ and $d/\lambda=83.68$. The abscissa is 3438 $\sin p$, which is approximately equal to the angle between the ray direction and the median plane, measured in minutes of arc.

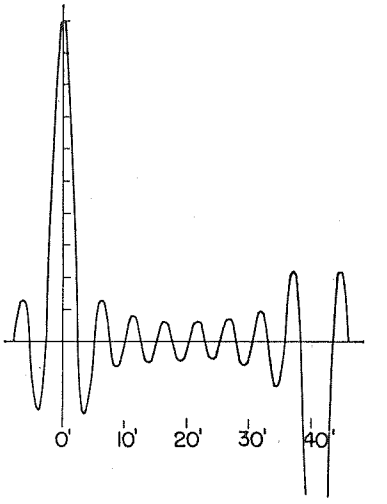

Fig. 1—Field radiation pattern of 16-element array (theoretical).

If now we sum the series by noting that the N exponential terms form a geometrical progression, we obtain the following closed expression for the field radiation pattern:

$$\frac{\sin\left(N\pi\dfrac{d}{\lambda}\sin p\right)}{\sin\left(\pi\dfrac{d}{\lambda}\sin p\right)}.$$

Now if the isotropic point sources are replaced by identical extended elements, the field radiation pattern of the whole is derived from the above by multiplication with the field pattern of a single element. The power pattern is the squared modulus.

It will be seen that when the individual elements are driven so as to track an object moving across the sky, the radiation pattern is the product of a moving envelope and the fixed pattern that is periodic in $\sin p$. Thus the object will be scanned by the sharp fringes of successive order, even though the individual antennas are tracking it.

The potential fringes form small circles on the sky, coaxial with the line of the array, in our case 167 in number (about 160 usable), and may be evoked in any neighborhood where the elements are pointed (Fig. 2).

When one array is crossed with another the principle of the Mills cross enters. Let the voltages received by each array separately from a point source in the direction (θ, ϕ) be respectively $V_1(\theta, \phi)$ and $V_2(\theta, \phi)$. When the two arrays are connected together in phase, the voltage reception pattern of the combination is $V_1(\theta, \phi) + V_2(\theta, \phi)$, and if then a half wavelength of cable is inserted into the second arm before connecting the two, the pattern is $V_1(\theta, \phi) - V_2(\theta, \phi)$. The available power is

$$[V_1(\theta, \phi) \pm V_2(\theta, \phi)][V_1(\theta, \phi) \pm V_2(\theta, \phi)]^*,$$

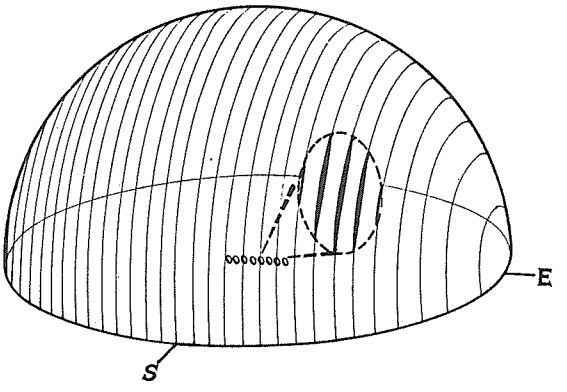

Fig. 2—Potential fringes (small circles) of a multi-element array and effective fringes (those enclosed within the outline representing the pattern of a single element).

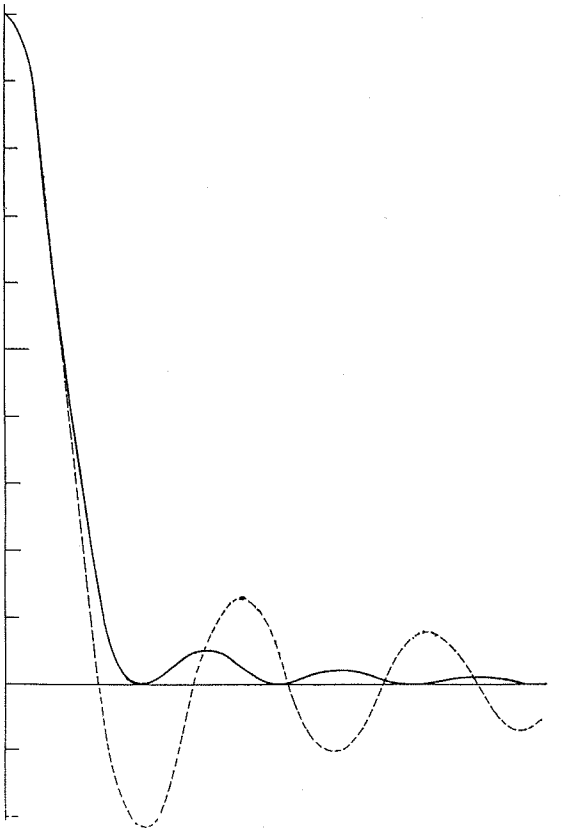

Fig. 3—Skew (heavy curve) and principal (broken curve) sections through the beam of an untapered cross of point sources.

the plus sign referring to the first condition and the minus sign to the second. If now the half wavelength is switched in and out at an audiofrequency (in our case 450 cps), and the receiver pays attention only to the alternating component of the available power, the response of the system as a function of direction will be the alternating part of the previous expression, namely

$$V_1(\theta, \phi)V_2^*(\theta, \phi) + V_2(\theta, \phi)V_1^*(\theta, \phi).$$

Thus the power response of the system to a point source is the scalar product of the voltage responses of the component arrays.

If the arrays produce sharp fringes, the net power response when they are switched together consists of pencil beams at the fringe intersections. The principal sections through the beam, those taken in planes containing one or other of the arrays, have the character of Fig. 1; *i.e.*, the power response may contain the negative lobes characteristic of a field radiation pattern. Sections through the beam in other directions tend towards shapes more usually associated with power patterns, *e.g.*, the 45° section is shown in Fig. 3 (heavy curve) in comparison with the principal section. The magnitude of all the sidelobes is shown in Table I which represents one complete quadrant of one periodic cell of the reception pattern; the ruled lines are null loci. The concentration of the field-type pattern along the principal sections (bold type) is well shown.

Useful alternative explanations that may be given in terms of sensitivity to spatial Fourier components of a source distribution [7], [8] should be referred to for dealing with refinements.[1]

[1] Such as, for example, the question of suitable array tapering, which is still under discussion.

TABLE I

LOBE MAXIMA FOR AN UNTAPERED CROSS OF POINT SOURCES
(PRINCIPAL SECTIONS IN BOLD TYPE)

$\bar{6}$	1	$\bar{1}$	$\frac{1}{2}$	$\overline{\frac{1}{2}}$	$\frac{1}{2}$	$\overline{\frac{1}{2}}$	$\frac{1}{2}$
7	$\bar{1}$	1	$\overline{\frac{1}{2}}$	$\frac{1}{2}$	$\overline{\frac{1}{2}}$	$\frac{1}{2}$	$\overline{\frac{1}{2}}$
$\bar{7}$	2	$\bar{1}$	$\frac{1}{2}$	$\overline{\frac{1}{2}}$	$\frac{1}{2}$	$\overline{\frac{1}{2}}$	$\frac{1}{2}$
8	$\bar{2}$	1	$\bar{1}$	$\frac{1}{2}$	$\overline{\frac{1}{2}}$	$\frac{1}{2}$	$\overline{\frac{1}{2}}$
$\overline{10}$	2	$\bar{1}$	1	$\bar{1}$	$\frac{1}{2}$	$\overline{\frac{1}{2}}$	$\frac{1}{2}$
13	$\bar{3}$	2	$\bar{1}$	1	$\bar{1}$	1	$\bar{1}$
$\overline{22}$	5	$\bar{3}$	2	$\bar{2}$	2	$\bar{1}$	1
100	$\overline{22}$	13	$\overline{10}$	8	$\bar{7}$	7	$\bar{6}$

III. Basic Design Parameters

As a minimum resolving power for revealing detail on the disk of the microwave sun, which has a diameter of about 33 minutes of arc, a beamwidth of 3 or 4 minutes of arc is a reasonable objective. This is about one milliradian. To obtain such a beamwidth an antenna aperture of about 1000 wavelengths is needed, say 100 m at a wavelength of 10 cm. Over the whole of this aperture the excitation has to be maintained constant in amplitude and phase to known tolerances [7], [9], [10] which, in the case of phase, require electrical and mechanical stability to a small fraction of a wavelength. The necessary stability of one part in 10^4 or 10^5 could be achieved only with great effort if the aperture had to be moved bodily to track the sun, especially in two dimensions.

The essence of Christiansen's multi-element interferometer is that the aperture is split into an array, each element of which tracks separately on its own modest mount. However, in doing this, one introduces a periodic variation along the antenna that results in the appearance of multiple beams; if there are N elements in the array, the multiple beams will appear at intervals of about N beamwidths.

The number of elements is consequently set by the requirement that the spacing of the multiple beams shall exceed the diameter of the object to be studied. Under this condition there can never be more than one beam on the object at any time and so the multiple beams can cause no confusion. With a 3 minute beam and a 33 minute sun (36 minutes when the spread due to antenna smoothing is allowed for) one could split the 1000-wavelength array into 12 elements. To allow for deterioration of the beam from various causes a narrower beamwidth was aimed for, however, and 16 elements were adopted.

The size of the individual elements is limited to rather less than the spacing of the elements; in fact unless there is room to spare, the elements will shadow each other when pointing out of the median plane (the plane perpendicular to the line of the array). The elements must be large enough that their combined collecting area is adequate for reception of the part of the source in the beam. While each element receives radiation from the whole source, the adjustment of the array is such that much of this energy is reradiated by other elements, only the contribution from within the 3-minute beam being delivered to the receiver. Standard spun aluminum paraboloids 10 feet in diameter and with 36 inch focal length were selected, and purchased from the Gabriel Company. Feed horns were designed for conservative illumination with low spillover, circular beam, and wideband match; a reflection-compensating window was incorporated in the prototype which was developed by K.-S. Yang. Prodelin Inc. manufactured the feeds complete with gooseneck waveguide supports.

Table II summarizes the design parameters for each of two identical arrays. Table III presents parameters of other existing multi-element arrays of related types, with literature references for further details.

TABLE II

Basic Design Parameters of Each Array

Latitude	37°24′ N
Longitude	122°11′ W
Elevation	20 m
Slope of north-south array	50.5′ (north end low)
Number of elements	16
Element spacing	25 feet (83.68λ)
Over-all length between centers of end elements	375 feet (1255.2λ)
Operating wavelength (frequency)	9.107 cm (3292.1 Mc)
Beamwidth to half power*	2.3′
Peculiar interval	1.28′
Spacing of beams	41′
Diameter of paraboloid	10 feet
Beamwidth of paraboloid	2.3°
Physical area of array	1257 feet² (117 m²)
Feed horn dimensions	3×4 inches
VSWR	<1.4 from 2700 to 3350 Mc <1.1 at 3292 Mc

* Theoretical value. From observations of the most compact solar spots available so far, it has been verified that the beamwidth is less than 2.5′. Under operation as a cross the half-power beamwidth is 3.1′ (theoretical value; observational verification so far, <3.3′).

TABLE III

Parameters of Existing Multi-element Arrays*

Location	Wavelength *cm*	Type of beam	Beam size	Elements		Spacing d/λ	Length $(N-1)d/\lambda$	Mounting	Present sensitivity 10^{-26} Wm^{-2} $(c/s)^{-1}$
				N	Description				
Stanford	9.107	Pencil Fan	3.1′×3.1′ 2.3′×2.3°	16×16 16	3 m dishes	83.68	1255.2	Equatorial	12
Sydney [11]-[13]	21	Pencil Fan	3′×3′ 2′×2.5°	32×32 32	5.8 m dishes	58	1800	Equatorial	2000
Nançay [14]	3.2	Fan	4′×1.7°	16	1.1 m dishes	50	750	Meridian	3000
Nagoya [15]	3.18	Fan	2.25′×1.6°	16	1.2 m dishes	86.05	1290	Equatorial	3000
Nagoya [16]	7.5	Fan	4.5′×4°	8	1.5 m dishes	86.00	602	Equatorial	4000
Ottawa [17]-[18]	10	Fan	1.2′×2°	5	one 46×0.6 m V and four 3 m×2.4 m dishes	450	1800	Meridian	3000
Washington [19]	88	Fan	4.8′×15°	30	Helical antennas	22	640	Meridian	1000
Nançay [20]	177	Fan	3.8′×20°	32	5 m dishes	25	780	Meridian	10
Nançay [21]	177	Fan	7.5′×16°	8	10 m dishes	62	435	Meridian	
Santiago	171	Fan	4′×60°	16	10-element yagis	47	700	Meridian	2000

* Other Christiansen arrays are being brought into operation in Berlin, The Netherlands, and the U.S.S.R. The 90-element array at Pulkovo, USSR, which is of a distinct type, is designed for a fan beam 1′×10′ at the zenith at 3 cm [30].

IV. Physical Description

Each element of the array is mounted on a concrete pier that rises 5 feet above ground level (Fig. 4). The piers extend about 8 feet below ground with a diameter of 30 inches. Bolted to the top of each pier is a machined and scribed cast-iron base-plate which was oriented, leveled, aligned and spaced before grouting. On the base-plate is a cannon-shaped housing containing the polar axle ($32\frac{1}{2}\times 3$ inches) and an oil-filled double worm reduction gear box (360:1). Keyed to the polar axle is a yoke carrying the declination axle ($28\frac{1}{2}\times 3$ inches), two castiron brake bands, and a worm box (20:1). Two cast-iron supporting arms keyed to the ends of the declination axle carry an adapting structure that finally bolts to the back-spinning of the paraboloid at four points on a $43\frac{1}{2}$-inch square. The back spinning is a pan that is riveted to the paraboloid on two circles about 68 and 23 inches in diameter. Counterweight arms bolted to the supporting arms give balance about the declination axis and two other counterweights attached to the polar axle bring the center of gravity down onto the polar axis at a point roughly above the pier.

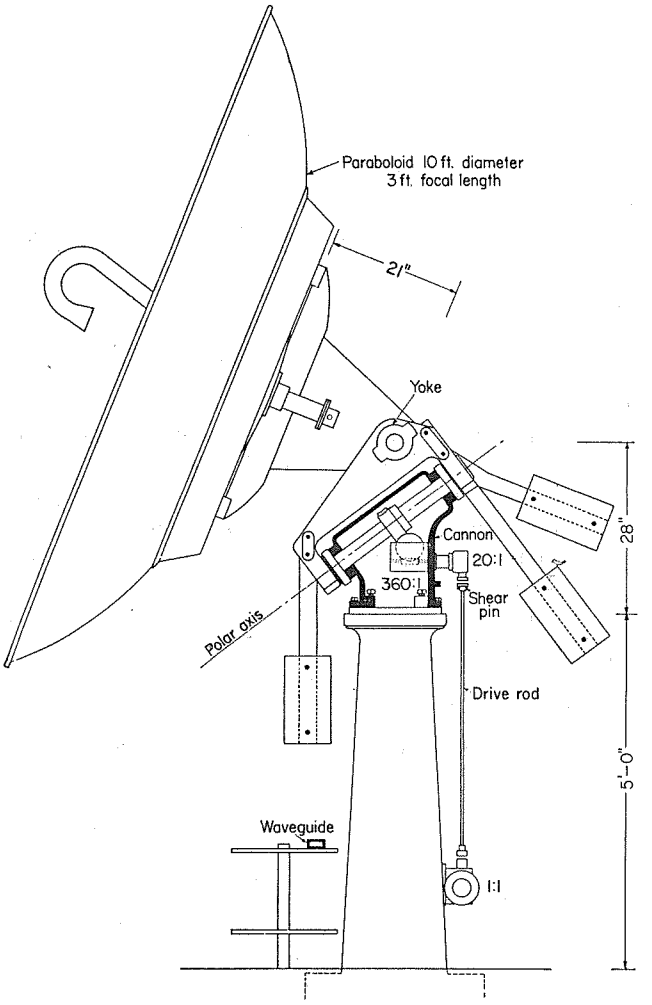

Fig. 4—Equatorial mount for the ten-foot paraboloids.

A mechanical drive system turns all the paraboloids in unison about their polar axes at a tracking rate of $\frac{1}{4}°$ per minute or a slewing rate of 5° per minute. Other rates are available. Two drive shafts, which run the whole length of each array, turn at 5 rpm (tracking) or 100 rpm (slewing) and have flexible couplings and bearings at $12\frac{1}{2}$ foot intervals.

When tracking, all 32 units are turned by a 1500 rpm, 1 hp synchronous motor. The slewing motor is a 1200 rpm, 3 hp induction motor connecting into the drive line through a differential, as shown in Fig. 5. The synchronous drive is accurate enough for tracking the sun, but evidently, whenever the slewing motor is used, absolute position is lost. For this, and other reasons, a further "correcting motor" is connected into the drive line.

If, during the course of the day, it is necessary to bring the antenna onto the sun, one first slews roughly into position and then turns on the tracking motor. A synchronous clock, that is never disconnected from the electrical supply, remembers where the sun should be. A subsidiary shaft S says where the antenna actually is, and a differential D_3 shows the discrepancy with the clock shaft on a counter. A switch on the counter turns on the correcting motor in the correct sense to cancel the discrepancy. The antenna is thus brought automatically onto the sun, after which the tracking

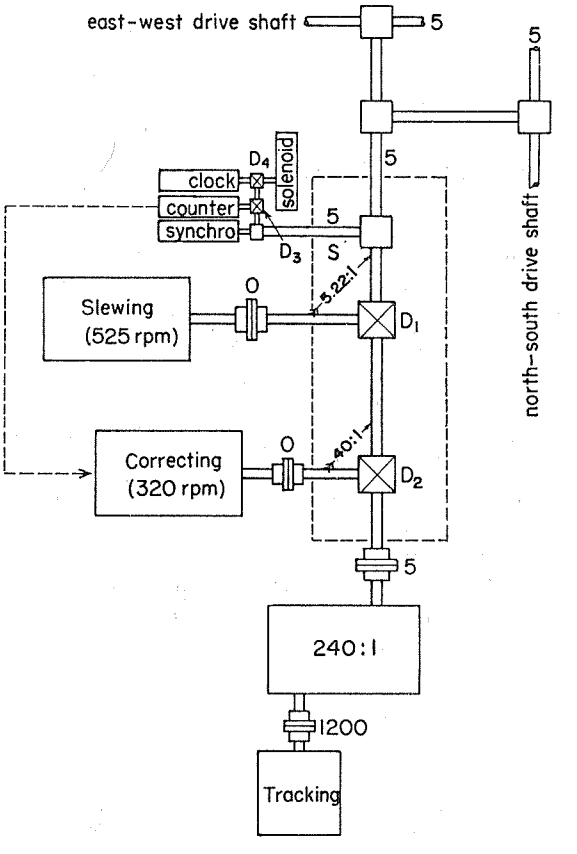

Fig. 5—Mechanical drive system. Numbers on shafts give speeds in rpm during tracking.

motor continues alone; provision is made for automatic slewing back at the end of a run and starting up on the sun the next morning. A synchro-transmitter shown in the figure conveys antenna position to the control console, where a digital indicator shows the "antenna time" (the hour angle at which the antenna is pointed, plus 12 h).

Corrections for equation of time are incorporated manually from the control console by pulsing a rotary solenoid that can insert a lead or lag in the clock shaft through the differential, D_4. The pulses also drive a digital time indicator, and the correct number of pulses has been sent when this indicator shows the sun's meridian transit time at Stanford.

This correction mechanism can also be used for setting on objects with other transit times, and for tracking at nonsolar rates.

The two hour-angle limit switches are located on a dummy polar axle geared to the subsidiary shaft S. They are readily accessible for resetting for special purposes. Two further limit switches, defining the range of safe operation, are actuated directly by the polar axle within the cannon of west no. 1 unit and cannot easily be changed; they are set to ± 4 h 20 m. Shear pins on the drive rods of each unit guard against accidents.

V. Phase Technique

The crucial step determining the success of a large array is the adjustment whereby the excitation of each element is brought into the same phase. Each element must also be excited with the same amplitude, but the measurement of amplitude is not especially difficult for a large array except insofar as the number of necessary measurements is large.[2] There is a basic difficulty in phase equalization over long distances, however, because the same absolute precision in fractions of a wavelength is required regardless of distance. Measuring to an accuracy of 1 mm in 50 m, *i.e.*, one part in 50,000, demands careful attention to mechanical stability, thermal effects, frequency stability, and all measurement procedures.

Swarup and Yang [22] have described the method originally used to bring the arms of the array into phase adjustment. The method which has subsequently proved most satisfactory [23] is to introduce a weakly reflecting, modulated gas discharge at the mouth of the horn of the element under test. When a test signal is sent out from the receiver room a faint, but modulated, reflection is returned from the electron cloud in the discharge. The modulation frequency component in the receiver output can be cancelled by combining the reflection with a strong quadrature reference signal. By sliding a probe in a slotted section of waveguide one finds a null setting that indicates the phase path to the discharge. The method has adequate accuracy and sensitivity for the present purpose, but is also susceptible of refinements suiting it to more extreme applications in the future. Phase path measurements through space by Swarup and Yang [24] show that the figure of giant paraboloids could be continuously monitored without further ado.

Assuming that the phases of both arrays have been adjusted, we would find the potential pencil beams at the intersection of the fringes of the arrays. The fringes of the east-west array lie in the directions where the path difference is an integral number of wavelengths m, *i.e.*, where

$$d \sin p = m\lambda.$$

In this equation, d is the spacing of the elements and p is the co-distance from the west point of the horizon. The number m is the order of interference of the fringes of the east-west array; the zero order fringe lies in the meridian plane. The fringes of the north-south array lie where

$$d \sin q = n\lambda.$$

Here q is the co-distance from the south point of the horizon, and n is the order of interference of the fringes of the north-south array, being zero on the east-west vertical circle (the prime vertical).

In terms of hour angle H and declination δ, coordinates forced on us by the earth's rotation,

$$\sin p = \sin H \cos \delta$$

$$\sin q = -\cos \Lambda \sin \delta + \sin \Lambda \cos \delta \cos H,$$

where Λ is the observing latitude.

To carry out scanning operations, the location of the fringes may be shifted by introducing a linear phase gradient along the north-south arm by means of phase shifters. If the phase gradient is such that the phase path from each element to the receiver exceeds that from its neighbor to the north by Φ meters, then the fringes of the north-south array will be displaced towards the south in accordance with the relation

$$d \sin q = n\lambda + \Phi.$$

Hence the location of the pencil beam of order (m, n) will be given by

$$\frac{m\lambda}{d} = \sin H \cos \delta,$$

$$\frac{n\lambda + \Phi}{d} = -\cos \Lambda \sin \delta + \sin \Lambda \cos \delta \cos H.$$

The following useful version of the formulas gives the coordinates of the pencil beam of order (m, n):

[2] When a signal generator is connected in place of the receiver, reflected waves will return from the elements themselves (due to mismatch) and from transmission system components, such as tee junctions. Some of this energy returns to the generator, but the bulk of it is redistributed among the elements, thus upsetting the amplitude of excitation. If the tee junctions are replaced by hybrid junctions with a matched termination on the fourth port, all returning reflections are absorbed. Excitation errors due to mismatch are then less.

$$\delta = \sin^{-1}\left\{\left[1 - \frac{m^2\lambda^2 + (n\lambda + \Phi)^2}{d^2}\right]^{1/2} \sin \Lambda - \frac{n\lambda}{d}\cos \Lambda\right\}$$

$$H = \sin^{-1}\left(\frac{m\lambda}{d}\sec \delta\right)$$

Values of δ and H for various values of (m, n) have been tabulated on an electronic computer.

To track with a pencil beam on a fixed declination as time elapses, one must vary Φ between scans. As an example, the required change $\Delta\Phi$ over an interval ΔH is given, on differentiation, by

$$\Delta\Phi = -d \sin \Lambda \cos \delta \sin H \, \Delta H.$$

To scan in television fashion, along parallel circles of declination, an additional change in Φ must be inserted between scans, according to the required spacing in declination.

We know by the discrete interval theorem (Bracewell and Roberts [25], Bracewell [26]) that the brightness distribution across the sun is completely determined by parallel scans spaced a distance $\lambda/Nd \cos q$ apart. Thus one can make N independent scans per unit of n, and provision must therefore be made for N path length increments Φ up to one full wavelength.

Of the various ways of inserting phase gradient we have chosen to place separate phase shifters at each element. They must then insert phase at rates proportional to $\pm 1, \pm 3, \pm 5, \cdots \pm 15$, in order to produce equal increments between one element and its neighbor.

The phase shifter is simply a piece of dielectric about 1 m long that can be rotated into and out of the strong electric field along the center line of the waveguide. The difference in phase delay between the extreme positions is exactly one wavelength. The dielectric is turned by a pulsed rotary solenoid through a gear that inserts the required factor mentioned above. A cam gives a linear relationship between the number of pulses to the solenoid and the amount of phase. Eighty pulses insert one half cycle into Number 1 unit, which changes Φ by one wavelength. At noon, five minus pulses (*i.e.*, 75) would be needed between successive scans, but as the sun begins to cross the fringes, the number of pulses alters, following a simple program. For example, for a map beginning at 11 hours 09 minutes 37 seconds at the equinox, the program is 9, 9, 8, 8, 7, 6, 5, 5, 5, 4, 2, 3, 2, 1, 1, 0, 79, 79, 77, · · · , 2.79 minutes elapsing between each batch of pulses. The program can be punched on a card, inserted in a matrix switch on the control console, and followed automatically by a timer, or the program can be sent out manually. It is also practical to take maps with the unequal scanning intervals that result when the phase shifters are not used.

VI. Operational Behavior

Records taken with a single arm of the cross show that the design parameters have been essentially realized. Very sharp multiple beams have been observed, up to about the 80th order, located at equal intervals of sin p and in the calculated positions within about one minute of arc. A record taken tracking Cassiopeia A shows that the effective area remains substantially constant out to large hour angles, but that the beamwidth increases progressively. The precise value of the beamwidth has not yet been measured for want of a source of sufficiently small angular diameter. However, from the fact that ten or more maxima and minima have on occasion been observed within a half degree of the sun's diameter, it is clear that the beamwidth is approximately as planned. Occasionally, compact sources appear on the sun that permit an upper limit to be set to the beamwidth; from such cases we have concluded that the half power beamwidth of the east-west array is less than 2.5 minutes of arc. The expected value is 2.3 minutes.

Fan-beam scans of the sun are shown in Fig. 6. The repetitive character of the record is apparent and it will be seen that the repetition interval just exceeds the width of the sun. A transient event accompanying a solar flare may be seen taking place in one of the active centers.

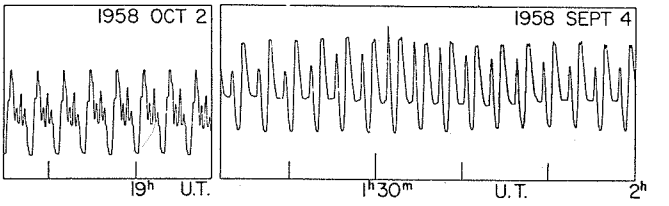

Fig. 6—Fan beam scans of the sun; (a) showing much fine structure, (b) showing a burst in one active center.

The effective area of the east-west array is now about 15 m²; *i.e.*, it is equivalent to a single paraboloid of about 6 m diameter. With the sun receiver, whose noise temperature is about 1500°K, this means that four or five of the brightest discrete sources, and the moon, have proved observable. Since at present the transmission system has an efficiency of only 25 per cent, there is a considerable margin in hand for high resolution studies of nonsolar sources, which can be exploited with superior receivers.

When the instrument is operated as a cross and used to map the solar emission, again it is apparent that the design has been realized. The procedure of phase adjustment is more critical for the cross than for the single arm, (Swarup and Yang [23]); and in fact the quality of the maps is a rather sensitive indicator of maladjustment. Fig. 7 shows a sample map, together with one of

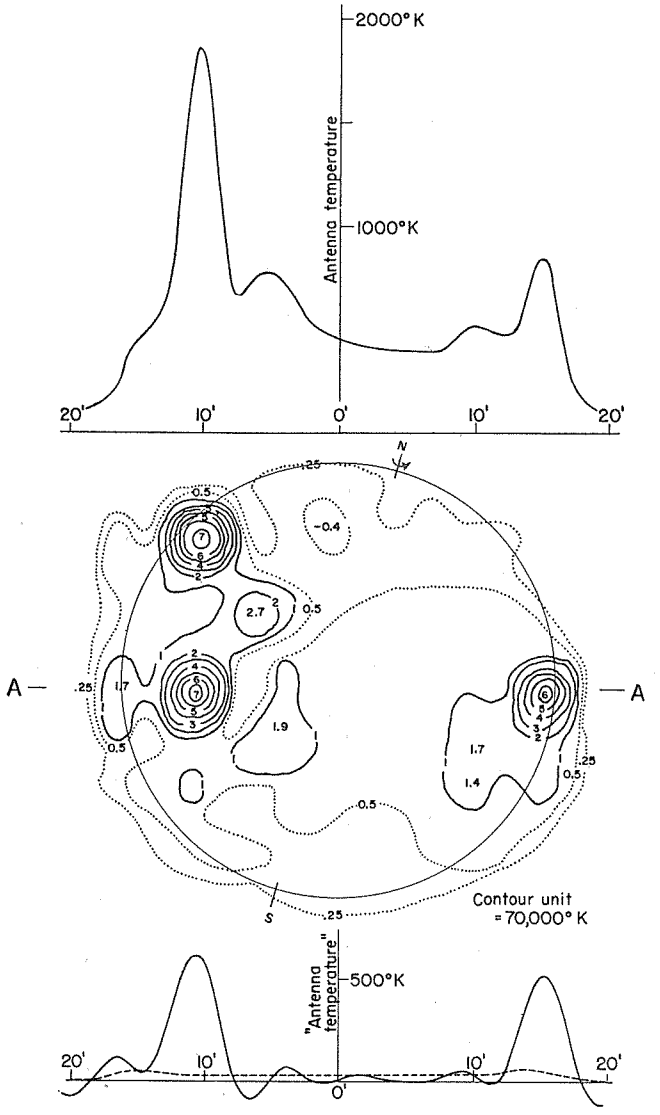

Fig. 7—A map of the 9-cm solar emission prepared from pencil beam scans such as that along A–A (below), together with a fan beam scan (above). May 30, 1960, 19–20h u.t.

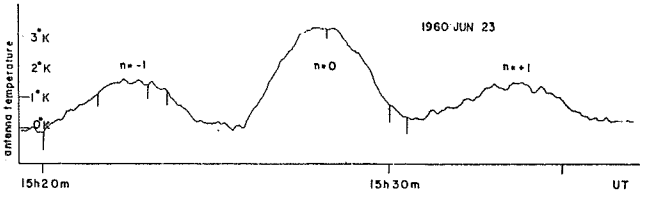

Fig. 8—Record made by D. Cudaback of a lunar passage through the fan beam. The antennas were stationary and a wide band used (300 Mc), so that the scans at $n = \pm 1$ are reduced and dispersed.

the pencil beam scans and a fan beam scan taken after the map was completed. The extent to which the 9 cm emission is dominated by the active centers is much clearer from the maps than from fan beam scans. Sequences of these maps are being studied to obtain physical data on the emissive regions at the levels from which the 9 cm radiation comes.

A record of the moon passing through the fan beam, taken with a bandwidth of 300 Mc, is shown in Fig. 8. Sequences of such scans are being studied for evidence of monthly variation by D. Cudaback. Cudaback has also examined the moon under conditions of microwave illumination by a radar transmitter.

VII. Discussion

The instrument described in the preceding pages is significant both for astronomy, to be discussed elsewhere, and for antenna practice, with which we are concerned here. The fierce demand for resolving power, exerted from the beginning by the challenge of radio astronomy, and the competitive international atmosphere in which it flourishes, has called forth tremendous advances in antenna technique, so that at the present time the most refined antennas are those in the hands of radioastronomers. The development has followed several lines. In the category of pencil beam interferometers, to which our instrument belongs, the resolving power is unmatched in other branches of radio science and technology where antennas are used. Even higher resolving power is indeed attainable for special purposes by the techniques of variable-spacing two-element interferometry; but among pencil beam antennas of all kinds, both fixed and steerable, and including millimeter-wave paraboloids, the finest beams are those furnished by pencil beam interferometers.

The demands of astronomy for resolving power are not satisfied, however. A fruitful approach to the question of resolving fine detail is to contemplate the radiation field on the ground and to ask how the information about the source that produced the field is spread over the ground [27]. Fundamental to the problem are the concepts of *complex coherence* and *principal solution*. If F_1 and F_2 are the field phasors at two points, the complex coherence Γ is defined as the normalized time average of the product $F_1F_2^*$; *i.e.*, $\Gamma = \langle F_1F_2^* \rangle / \langle F_1F_1^* \rangle$, and it depends only on the vector spacing of the two points. One can show [7], [28] that Γ, as a two-dimensional function of vector spacing, is the two-dimensional Fourier transform of the brightness distribution over the source. However, the vector spacings represented within a given antenna system, or accessible by variable-spacing interferometry, cover only a finite area; and the Fourier transform of the part of Γ within this area represents the best approximation to the actual brightness distribution (in the absence of outside information). This distribution, which is encountered in the antenna smoothing problem, is known as the principal solution [7], [25]. (In the presence of errors such that the signal-to-error ratio varies with spacing, as happens when redundant spacings are embraced, there is a modification to be allowed for [29]).

Two-element interferometry, or aperture synthesis, in which the accessible vector spacings are occupied sequentially, can be seen from this standpoint in its

relationship to pencil beam scanning, where the full range of spacings is embraced simultaneously, with much redundancy. The pencil beam interferometer, which is intermediate in character, avoids the slowness of sequential occupation of stations, and is economical as regards redundancy. It profits by the discrete interval theorem for discrete sources [28], in that many spacings may be left unoccupied.

These properties fit pencil beam interferometry, incorporating steerable multi-element arrays, for future progress to higher resolving power; we look forward confidently to the appearance of giant arrays composed of antenna units that are today considered large in themselves. The basic difficulty of coherence measurement, preservation of relative phase over great spacings, is under control by a technique that is not yet strained.

Acknowledgment

Financial support was provided by the Office of Scientific Research of the United States Air Force through the Physics Section under Dr. W. J. Otting. Day to day contact, initially with R. Heer, has been with Paul Johnson; the project has greatly benefited from Johnson's appreciation of the problems and his wise advice. While detailed design was in progress, but before the negotiation of the contract, a welcome grant was furnished by the Research Corporation through the kind offices of W. A. Woods. A good deal has been contributed to the project by Stanford University to whom we owe the land, buildings, roads, fences, earthmoving, maintenance and innumerable operations. The manifold services of the Stanford Electronics Laboratories have been indispensable; above all, administrative matters have been well cared for by the Associate Director, Dr. D. Bacon. A great number of students from the department of electrical engineering have contributed from time to time, major contributions having been made by R. Colvin, D. Cudaback, and K.-S. Yang. C. Sphar did the mechanical design, construction and surveying, and competently supervised a wide variety of technical tasks essential to the success of the project; C. C. Lee has ably maintained and operated the instrument. The project found its home at Stanford through the initiative of Prof. O. G. Villard, Jr., director of the Radioscience Laboratory, whose friendly interest throughout the whole project is here warmly acknowledged.

Bibliography

[1] W. N. Christiansen and J. A. Warburton, "The distribution of radio brightness over the solar disk at a wavelength of 21 centimetres, I," *Australian J. Phys.*, vol. 6, pp. 190–202; June, 1953.
[2] J. L. Pawsey and R. N. Bracewell, "Radio Astronomy," Oxford University Press, New York, N. Y.; 1955.
[3] B. Y. Mills and A. G. Little, "A high resolution aerial system of a new type," *Australian J. Phys.*, vol. 6, pp. 272–278; September, 1953.
[4] B. Y. Mills, A. G. Little, K. V. Sheridan, and O. B. Slee, "A high resolution radio telescope for use at 3.5 m," Proc. IRE, vol. 46, pp. 67–84; January, 1958.
[5] R. N. Bracewell, "A new instrument in radio astronomy," *Observatory*, vol. 73, pp. 200–201; October, 1953.
[6] R. N. Bracewell, "A Proposal for a Microwave Spectroheliograph," Radio Propagation Lab., Stanford University, Stanford, Calif., September 15, 1955.
[7] R. N. Bracewell, "Radio astronomy techniques," in "Handbuch der Physik," S. Flügge, Ed., vol. 54, Springer-Verlag, Berlin, Ger., to be published.
[8] R. N. Bracewell, "Interferometry and the spectral sensitivity island diagram," this issue, pp. 59–67.
[9] R. N. Bracewell, "Antenna tolerance theory," *Proc. Symp. on Statistical Methods in Radio Wave Propagation*, W. C. Hoffman, Ed., Pergamon Press, London, Eng., pp. 179–183; 1960.
[10] R. N. Bracewell, "Tolerance theory of large antennas," this issue, pp. 49–58.
[11] W. N. Christiansen, D. S. Mathewson, and J. L. Pawsey, "Radio pictures of the sun," *Nature*, vol. 180, pp. 944–946; November, 1957.
[12] W. N. Christiansen and D. S. Mathewson, "Scanning the sun with a highly directional array," Proc. IRE, vol. 46, pp. 127–131; January, 1958.
[13] W. N. Christiansen and D. S. Mathewson, "The origin of the slowly varying component," *Paris Symp. on Radio Astronomy*, R. N. Bracewell, Ed., Stanford University Press, Stanford, Calif., pp. 108–117; 1959.
[14] M. Gutmann and J. L. Steinberg, "Résultats préliminaires obtenus avec l'interféromètre à 8 antennes sur 3 cm de longueur d'onde," *Paris Symp. on Radio Astronomy*, R. N. Bracewell, Ed., Stanford University Press, Stanford, Calif., pp. 123–124; 1959.
[15] H. Tanaka, "An 8-element interferometer at 9,400 Mc," *Proc. Res. Inst. Atmosph.*, vol. 6, p. 67, 1959; vol. 8, to be submitted.
[16] H. Tanaka and T. Kakinuma, "Multiple element interferometer for locating sources of solar noise at 4000 Mc," *Proc. Res. Inst. Atmosph.*, vol. 2, pp. 53–76, 1954; pp. 102–109, 1955.
[17] A. E. Covington and N. W. Broten, "An interferometer for radio astronomy with a single-lobed radiation pattern," IRE Trans. on Antennas and Propagation, vol. AP-5, pp. 247–255; July, 1957.
[18] A. E. Covington, "Solar emission at 10-cm wavelength," *Paris Symp. on Radio Astronomy*, R. N. Bracewell, Ed., Stanford University Press, Stanford, Calif., pp. 159–165; 1959; "A compound interferometer," *J. Roy. Astron. Soc. Canada*, vol. 54, pp. 17–28, 58–68; February and April, 1960.
[19] J. Firor, "Solar radio bright spots at 88-cm wavelength," *Symp. on Radio Astronomy*, Paris, France, R. N. Bracewell, Ed., Stanford University Press, Stanford, Calif., pp. 136–139; 1959.
[20] E. J. Blum, J. F. Denisse, and J. L. Steinberg, "Radio astronomy at the Meudon Observatory," Proc. IRE, vol. 46, pp. 39–43; January, 1958; E. J. Blum, A. Boischot, and M. Ginat, "Le grand interféromètre de Nançay," *Ann. d'Astrophysique*, vol. 20, pp. 155–163; 1957.
[21] A. M. Malinge, E. J. Blum, M. Ginat, and M. Parise, "La branche Nord-Sud du grand interféromètre de la station de Nançay," *Comptes Rendus*, vol. 249, pp. 2009–2011; November, 1959.
[22] G. Swarup and K.-S. Yang, "Interferometer phasing problems at microwave frequencies," 1959 IRE WESCON Convention Record, pt. 1, pp. 17–24; 1959.
[23] G. Swarup and K.-S. Yang, "Phase adjustment of large antennas," this issue, pp. 75–81.
[24] G. Swarup and K.-S. Yang, "Monitoring paraboloidal antennas," Proc. IRE, vol. 48, pp. 1918–1919; November, 1960.
[25] R. N. Bracewell and J. A. Roberts, "Aerial smoothing in radio astronomy," *Australian J. Phys.*, vol. 7, pp. 615–640; December, 1954.
[26] R. N. Bracewell, "Two-dimensional aerial smoothing in radio astronomy," *Australian J. Phys.*, vol. 9, pp. 297–314; September, 1956.
[27] R. N. Bracewell, "Aerials and data processing," to be submitted for publication.
[28] R. N. Bracewell, "Radio interferometry of discrete sources," Proc. IRE, vol. 46, pp. 97–105; January, 1958.
[29] R. N. Bracewell, "Restoration in the presence of errors," Proc. IRE, vol. 46, pp. 106–111; January, 1958.
[30] S. E. Khaikin and N. L. Kaidanovskii, "A new radio telescope of high resolving power," *Paris Symp. on Radio Astronomy*, R. N. Bracewell, Ed., Stanford University Press, Stanford, Calif., pp. 166–170; 1959.

APPENDIX B

Map explanation from the *Descriptive Text, Solar-Geophysical Data*, February 1973.

9.1 cm Spectroheliograms -- Microwave spectroheliograms are made daily at the Radio Astronomy Institute, Stanford University, Stanford, California (37°23.9'N, 122°11.3'W) under the direction of Professor R. N. Bracewell. This program is supported by The Air Force Office of Scientific Research.

These spectroheliograms show the distribution of microwave emission over the sun's disk as observed with a pencil beam whose East-West width to half power is 3.1', and whose North-South width varies from 3.1' in summer to nearly 6' in mid-winter (actual value 3.1' sec (38.2° - $\delta_\odot$) at a declination $\delta_\odot$ on the meridian). For a full description of the instrument and its response see "The Stanford Microwave Spectroheliograph Antenna, a Microsteradian Pencil Beam Interferometer", IRE Transactions on Antennas and Propagation, AP-9, 22-30, 1961, by R. N. Bracewell and G. Swarup.

Since 1 January 1964 the maps have had 21 rows, each containing 25 temperature readings. The original maps, prior to reproduction, have 10 characters per inch horizontally and 3 lines per inch vertically, as on a typewriter; the radius of the solar disk agrees with the international standard of 7.5 cm (2.95 inches). Two + signs at the bottom of the map are 15 cm apart on the original. The center of the map, as fixed by absolute timing, is in the eleventh row, between the units and tens digits of the thirteenth reading.

Each reading of microwave emission occupies three spaces, and refers to a point on the sun centrally between the units and tens digits. The horizontal spacing of adjacent readings is about 1.63', and the vertical spacing is about 1.81'. Since the angular diameter of the sun varies with the season by about 1.7 percent, more precise values are 0.3R/2.95 and 1/3 R/2.95, where R is the sun's semi-diameter in minutes of arc taken from The American Ephemeris and Nautical Almanac. Each reading thus refers to a solid angle of about 1.63 x 1.81 square minutes of arc, or 2.50×10^{-7} steradians. We attempt to time our readings to better than 2^S absolute accuracy, or within about 0.5' at the worst in the horizontal direction. The precision with which the rows of the map are positioned on the sun's disk is a certain fraction of the North-South beamwidth, ranging from about 0.5' in summer to 1.0' in winter.

The reading printed on the map in the ith column and jth row is y_{ij} and the corresponding brightness temperature in degrees Kelvin, to the resolution allowed by the instrument, is Cy_{ij}. The unit C is currently 5000° K. (Before 1 July 1965, the unit C varied from day to day around a value of 2000° K which was stated on the map.) The readings are normalized so that the flux density S of the whole sun is equal to the absolute measurement obtained the same day on 10.7 cm by A. E. Covington at the National Research Council, Ottawa. No adjustment is made for the difference in wavelength. The formula used is

$$S = \frac{2k}{\lambda 2} C \sum y_{ij} \, (2.50 \times 10^{-7}) \left(\frac{R}{16.02}\right)^2$$

$$= 8.31 \times 10^{-28} \quad C \sum y_{ij} \left(\frac{R}{16.02}\right)^2 \quad Wm^{-2}Hz^{-1},$$

where S is the flux density of the whole sun, k is Boltzmann's constant (1.38×10^{-23} joules per Kelvin), λ(= 9.107 cm) is the operating wavelength, and R/16.02 is the ratio of the sun's semi-diameter in minutes of arc to its mean. Active regions are emphasized by simplified contours; intended as a visual aid to interpretation, the contours refer to the 50,000 and 100,000 K levels on a smoothed map in which each reading is replaced by the mean of the nine values centered on it. Negative readings which occur do so because of the sharp cutoff in the sensitivity of the instrument to the spatial Fourier components of the source. The two-dimensional response pattern of the instrument to a point source is

$$\operatorname{sinc} \frac{16dx}{\lambda} \operatorname{sinc} \frac{16d \cos (38.2^\circ - \delta_\odot) y}{\lambda} ,$$

where $\operatorname{sinc} x = (\sin \pi x)/\pi x$.

Flux densities of active regions may be calculated as follows. A point source on the sun produces a peak excess brightness temperature T_p (relative to the background temperature of the adjacent quiet areas) from which the flux density S_1 of the source can be calculated using the expression

$$S_1 = \frac{2kT_p}{\lambda^2} \Omega ,$$

where Ω is the effective solid angle of the antenna beam.

Now $\Omega = (\lambda/16d)^2 \sec (38.2^\circ - \delta_\odot)$, where d(= 25.00 feet) is the antenna spacing. Hence

$$S_1 = \frac{kT_p \sec (38.2^\circ - \delta_\odot)}{128d^2}$$

$$= 1.85 \times 10^{-27} T_p \sec (38.2^\circ - \delta_\odot).$$

Standardized spectroheliograms for the years 1964 through 1972 are available at Stanford Radio Astronomy Institute, with virtually no gaps, in digital form on magnetic tape, or as numerical printout. The contour charts in 15 cm diameter are also available from World Data Center A for Solar-Terrestrial Physics.

UAG Series of Reports

Prepared by World Data Center A for Solar-Terrestrial Physics, NOAA, Boulder, Colorado, U.S.A.

These reports are for sale through the National Climatic Center, Federal Building, Asheville, NC 28801, Attn: Publications. Subscription price: $25.20 a year; $12.00 additional for foreign mailing; single copy price varies. These reports are issued on an irregular basis with 6 to 12 reports being issued each year. Therefore, in some years the single copy rate will be less than the subscription price, and in some years the single copy rate will be more than the subscription price. Make check or money order payable to: Department of Commerce, NOAA.

Some issues are now out of print and are available only on microfiche as indicated. Requests for microfiche should be sent to World Data Center A for Solar-Terrestrial Physics, NOAA, Boulder, Co 80302, with check or money order made payable to Department of Commerce, NOAA.

UAG-1 "IQSY Night Airglow Data", price $1.75.
UAG-2 "A Reevaluation of Solar Flares, 1964-1966", price 30 cents.
UAG-3 "Observations of Jupiter's Sporadic Radio Emission in the Range 7.6-41 MHz, 6 July 1966 through 8 September 1968", microfiche only, price 45 cents.
UAG-4 "Abbreviated Calendar Record 1966-1967", price $1.25.
UAG-5 "Data on Solar Event of May 23, 1967 and its Geophysical Effects", price 65 cents.

UAG-6 "International Geophysical Calendars 1957-1969", price 30 cents.
UAG-7 "Observations of the Solar Electron Corona: February 1964-January 1968", price 15 cents.
UAG-8 "Data on Solar-Geophysical Activity October 24-November 6, 1968", price (includes Parts 1 and 2) $1.75.
UAG-9 "Data on Cosmic Ray Event of November 18, 1968 and Associated Phenomena", price 55 cents.
UAG-10 "Atlas of Ionograms", price $1.50.

UAG-11 "Catalogue of Data on Solar-Terrestrial Physics" (now obsolete).
UAG-12 "Solar-Geophysical Activity Associated with the Major Geomagnetic Storm of March 8, 1970", price (includes Parts 1-3) $3.00.
UAG-13 "Data on the Solar Proton Event of November 2, 1969 through the Geomagnetic Storm of November 8-10, 1969", price 50 cents.
UAG-14 "An Experimental, Comprehensive Flare Index and Its Derivation for 'Major' Flares, 1955-1969", price 30 cents.
UAG-15 "Catalogue of Data on Solar-Terrestrial Physics" (now obsolete).

UAG-16 "Temporal Development of the Geographical Distribution of Auroral Absorption for 30 Substorm Events in each of IQSY (1964-65) and IASY (1969)", price 70 cents.
UAG-17 "Ionospheric Drift Velocity Measurements at Jicamarca, Peru (July 1967-March 1970)", microfiche only, price 45 cents.
UAG-18 "A Study of Polar Cap and Auroral Zone Magnetic Variations", price 20 cents.
UAG-19 "Reevaluation of Solar Flares 1967", price 15 cents.
UAG-20 "Catalogue of Data on Solar-Terrestrial Physics" (now obsolete).

UAG-21 "Preliminary Compilation of Data for Retrospective World Interval July 26 - August 14, 1972", price 70 cents.
UAG-22 "Auroral Electrojet Magnetic Activity Indices (AE) for 1970", price 75 cents.
UAG-23 "U.R.S.I. Handbook of Ionogram Interpretation and Reduction", price $1.75.
UAG-24 "Data on Solar-Geophysical Activity Associated with the Major Ground Level Cosmic Ray Events of 24 January and 1 September 1971", price (includes Parts 1 and 2) $2.00.
UAG-25 "Observations of Jupiter's Sporadic Radio Emission in the Range 7.6-41 MHz, 9 September 1968 through 9 December 1971", price 35 cents.

UAG-26 "Data Compilation for the Magnetospherically Quiet Periods February 19-23 and November 29 - December 3, 1970", price 70 cents.
UAG-27 "High Speed Streams in the Solar Wind", price 15 cents.
UAG-28 "Collected Data Reports on August 1972 Solar-Terrestrial Events", price (includes Parts 1-3) $4.50.
UAG-29 "Auroral Electrojet Magnetic Activity Indices AE (11) for 1968", price 75 cents.
UAG-30 "Catalogue of Data on Solar-Terrestrial Physics", price $1.75.

UAG-31 "Auroral Electrojet Magnetic Activity Indices AE (11) for 1969", by Joe Haskell Allen, Carl C. Abston and Leslie D. Morris, National Geophysical and Solar-Terrestrial Data Center, Environmental Data Service, February 1974, 142 pages, price 75 cents.

UAG-32 "Synoptic Radio Maps of the Sun at 3.3 mm for the Years 1967-1969", by Earle B. Mayfield and Kennon P. White III, San Fernando Observatory, Space Physics Laboratory and Fred I. Shimabukuro, Electronics Research Laboratory, Laboratory Operations, The Aerospace Corporation, El Segundo, California, 90245, April 1974, 26 pages, price 35 cents.

UAG-33 "Auroral Electrojet Magnetic Activity Indices AE(10) for 1967", by Joe Haskell Allen, Carl C. Abston and Leslie D. Morris, National Geophysical and Solar-Terrestrial Data Center, Environmental Data Service, May 1974, 142 pages, price 75 cents.

UAG-34 "Absorption Data for the IGY/IGC and IQSY", compiled and edited by A. H. Shapley, National Geophysical and Solar-Terrestrial Data Center, NOAA, Boulder, Colorado, U.S.A., W. R. Piggott, Science Research Council, Slough, U.K., and K. Rawer, Arbeitsgruppe für Physikalische Weltraumforschung, Freiburg, G.F.R., June 1974, 381 pages, price $2.00.

UAG-35 "Catalogue of Digital Geomagnetic Variation Data at World Data Center A for Solar-Terrestrial Physics", prepared by Environmental Data Service, NOAA, Boulder, Colorado, July 1974, 20 pages, price 20 cents.

UAG-36 "An Atlas of Extreme Ultraviolet Flashes of Solar Flares Observed Via Sudden Frequency Deviations During the ATM-SKYLAB Missions", by R. F. Donnelly and E. L. Berger, NOAA Space Environment Laboratory, Lt. J. D. Busman, NOAA Commissioned Corps, B. Henson, NASA Marshall Space Flight Center, T. B. Jones, University of Leicester, UK, G. M. Lerfald, NOAA Wave Propagation Laboratory, K. Najita, University of Hawaii, W. M. Retallack, NOAA Space Environment Laboratory, and W. J. Wagner, Sacramento Peak Observatory, October 1974, 95 pages, price 55 cents.

UAG-37 "Auroral Electrojet Magnetic Activity Indices AE(10) for 1966", by Joe Haskell Allen, Carl C. Abston and Leslie D. Morris, National Geophysical and Solar-Terrestrial Data Center, Environmental Data Service, December 1974, 142 pages, price 75 cents.

UAG-38 "Master Station List for Solar-Terrestrial Physics Data at WDC-A for Solar-Terrestrial Physics", by R. W. Buhmann, World Data Center A for Solar-Terrestrial Physics, Juan D. Roederer, University of Denver, Denver, Colorado, M. A. Shea and D. F. Smart, A.F.C.R.L., Hanscom AFB, Massachusetts, December 1974, 110 pages, price $1.60.

UAG-39 "Auroral Electrojet Magnetic Activity Indices AE(11) for 1971", by Joe Haskell Allen, Carl C. Abston and Leslie D. Morris, National Geophysical and Solar-Terrestrial Data Center, Environmental Data Service, February 1975, 144 pages, price $2.05.

UAG-40 "H-Alpha Synoptic Charts of Solar Activity For the Period of Skylab Observations, May, 1973-March, 1974", by Patrick S. McIntosh, NOAA Environmental Research Laboratory, February 1975, 32 pages, price 56 cents.

UAG-41 "H-Alpha Synoptic Charts of Solar Activity During the First Year of Solar Cycle 20 October, 1964 - August, 1965", by Patrick S. McIntosh, NOAA Environmental Research Laboratory, and Jerome T. Nolte, American Science and Engineering, Cambridge, Massachusetts, March 1975, 25 pages, price 48 cents.

UAG-42 "Observations of Jupiter's Sporadic Radio Emission in the Range 7.6-80 MHz 10 December 1971 through 21 March 1975", by James W. Warwick, George A. Dulk, and Anthony C. Riddle, Department of Astro-Geophysics, University of Colorado, Boulder, Colorado 80302, April 1975, 49 pages, price $1.15.

UAG-43 "Catalog of Observation Times of Ground-Based Skylab-Coordinated Solar Observing Programs", compiled by Helen E. Coffey, World Data Center A for Solar-Terrestrial Physics, May 1975, 159 pages.

USCOMM-NOAA-ASHEVILLE--6-10-75--950